Renal allograft rejection in chemokine receptor Ccr1$^{-/-}$, Ccr5$^{-/-}$ and Ccr1$^{-/-}$/Ccr5$^{-/-}$ mice

and

Impact of Ccr5 deficiency on macrophage polarization

Von der Fakultät für Energie-, Verfahrens- und Biotechnik
der Universität Stuttgart zur Erlangung der Würde des
Doktors der Naturwissenschaften (Dr. rer. nat.) genehmigte Abhandlung

vorgelegt von

Stefan Dehmel

geboren in Altötting

Hauptberichter: Prof. Dr. Klaus Pfizenmaier
Mitberichter: Privatdozent Dr. Bruno Luckow

Tag der mündlichen Prüfung: 13. Juli 2009

Institut für Zellbiologie und Immunologie der Universität Stuttgart

2009

To a hammer every problem looks like a nail;

to an immune system every problem looks like an infection.

Rot and von Andrian,
Annu. Rev. Immunol.
2004. 22:891–928.

for Melanie

Acknowledgements

The time of my PhD thesis in the research group of Dr. Bruno Luckow brought me great scientific knowledge as well as new friendships. The people who work there have created an inspiring atmosphere and it was a pleasure to work with them.

I wish to thank PD Dr. Bruno Luckow for giving me the opportunity to be a member of his research group, for his excellent supervision, valuable time, suggestions and constructive criticisms. I'm also very thankful to my PhD supervisor Prof. Peter Scheurich and Prof. Klaus Pfizenmaier for their advice, valuable time and reviewing of my thesis.

Furthermore, I wish to thank all members of my group and the whole institute for their help and advice. I'm grateful to Silvia Chilla who was always helpful in everyday laboratory work and to Robert Löwe for critical discussions and the design of countless primer pairs used in this study. Moreover, I'd like to thank Stefanie Maier for useful advice at the flow cytometer.

Especially I'd like to thank Prof. Gerhild Wildner and Prof. Stefan Thurau for believing in me and support of my work. I thank Prof. Detlef Schlöndorff for his advice.

Since this work was accomplished in close collaboration with Prof. Hermann-Josef Gröne's group at the DKFZ Heidelberg (Dept. of Cellular and Molecular Pathology) I'd like to thank the members of his research group, especially Shijun Wang for the microsurgery of renal transplants, Dr. Eva Kiss for staining and evaluation of renal allografts and Claudia Schmidt for determination of BUN and Creatinine levels in plasma of transplanted mice.

My innermost gratefulness is with my family who always supported me during the years of my studies and was a constant source of strength to go on.

Declaration

I herewith declare that this thesis comprises only my own original research towards the degree of Doctor rerum naturalium (Dr. rer. net.) except as indicated under 'External Contribution' (see appendix 7.1) and that due acknowledgement has been made in the text to all other materials used. This thesis has not been submitted previously for a degree or any other qualification at this University or any other institution.

_____

Stefan Dehmel

München, _____

Table of Contents

Abbreviations

2-ME	2-Mercaptoethanol
7-AAD	7-Actino-aminomycin D
Ab	antibody
AAM	alternatively activated macrophages
AIDS	acquired immunodeficiency syndrome
AMA	alternative macrophage activation
APC	allophycocyanine or antigen-presenting cell
α-SMA	alpha-smooth muscle actin
bp	base pair/s
BMDM	bone-marrow derived macrophages
BSA	bovine serum albumin
BUN	blood urea nitrogen
c-Ets	cellular erythroblastosis virus E26 oncogene homolog (avian)
Ca^{2+}	calcium ions, double positive-charged
CAM	classically activated macrophages
cAMP	cyclic adenosine monophosphate
CCL	chemokine (CC-motif) ligand
CCR	chemokine (CC)-motif receptor
cM	centi Morgan
CREB	cAMP response element binding protein
CXCL	chemokine (CXC-motif) ligand
CXCR	chemokine (CXC-motif) receptor
CNS	central nervous system
Da	Dalton, unified atomic mass unit; 1 Da = 1 u = $1.660538782\times10^{-24}$ g. 1 Da is the equivalent of 1/12 of the mass of an unbound atom of carbon-12 (^{12}C) at rest in its ground state [10].
DAG	diacylglycerol
DARC	duffy blood group, chemokine receptor
DEPC-H_2O	diethylpyrocarbonate-treated H_2O
DMEM	Dublecco's modified Eagle medium
DMSO	dimethylsulfoxide
DNP	dinitrophenol
dNTP	desoxyribonucleotide triphosphate
DTH	delayed-type hypersensitivity
DTT	dithiothreitol
E. coli	*Escherichia coli*
EDTA	ethylenediaminetetraacetic acid
EtOH	ethanol
ER	endoplasmatic reticulum
FACS	fluorescence activated cell sorter
FCS	fetal calf serum
FcR	Fc (fragment, crystallizable) receptor

FDA	U.S. Food and Drug Administration
FITC	fluorescein isothiocyanat
FL	fluorescence
GAGs	glycosaminoglycans
GAP	GTPase activating protein
GDP	guanosine diphosphate
GM-CSF	granulocyte/macrophage-colony stimulating factor (= CSF2)
GTP	guanosine triphosphate
GTPase	GTP hydrolyzing enzyme
Glc	glucose
GPCRs	G protein-coupled transmembrane receptors
GRKs	G protein-coupled receptor kinases
HBSS	Hank's buffered salt solution
HMCV	human cytomegalovirus
HSP	heat shock protein
HIV	human immunodeficiency virus
IFNγ	interferon gamma
Ig	immunoglobulin
IL	interleukin
iNOS	inducible nitric oxide synthase
IP_3	inositol triphosphate
IRF	interferon regulatory factor
ITC	isotype- and concentration-matched antibody control
JAK	Janus kinase
K^+	potassium ion, single positive-charged
ko	knock-out
LPS	lipopolysaccharide
LTA	lymphotoxin α
MΦ	macrophage
M-CSF	macrophage colony stimulating factor (= CSF1)
mAb	monoclonal antibody
MAPK	mitogen-activated protein kinase
MCP	monocyte chemotactic protein
MDSCs	myeloid-derived suppressor cells
MFI	mean fluorescence intensity
MHC	major histocompatibility complex
MIP	macrophage inflammatory protein
MNP	MIP-1α nuclear protein
MMPs	matrix metalloproteinases
MOPS	3-N-(morpholino)-propanesulfonic acid
MPS	mononuclear phagocyte system
NK cells	natural killer cells
N-terminal	amino-terminal, NH_2-terminal
NADPH	nicotinamide adenine dinucleotide phosphate
NCBI	National center for biotechnology information

NF-IL6	nuclear protein Il6
NFκB	nuclear factor kappaB
NO	nitric oxide
NOD	nucleotide oligomerization domain
NOX system	NADPH oxidase system
ORF	open reading frame
PAS	periodic acid-Schiff stain
PBMCs	peripheral blood mononuclear cells
PBS	phosphate buffered saline
PCR	polymerase chain reaction
PE	phycoerythrin
pH	power of hydrogen; pH is defined as the negative decimal logarithm of the hydrogen ion activity in an aqueous solution at RT, $pH = -\log_{10}[H_3O^+_{aq}]$, [11]
$PI(4,5)P_2$	phosphatidylinositol 4,5-bisphosphate
PI3K	phosphoinositide 3-kinase
PKC	protein kinase C
PLA_2	phospholipase A_2
PLC	peritoneal lavage cells or phospholipase C
qPCR	quantitative PCR
RANTES	regulated upon activation, normal T-cell expressed, and secreted; new designation CCL5 (actually named after the alien protagonist in the movie *Man Facing Southwest*; [12])
REL	relative expression level
ROS	reactive oxygen species
RT	room temperature
SD	standard deviation
SLOs	secondary lymphoid organs
STAT	signal transducers and activators of transcription
TAM	tumor-associated macrophages
TBE	tris-borate-EDTA
TC	tissue culture
TGF-β	transforming growth factor beta
TNF	tumor necrosis factor
TNP-KHL	Trinitrophenol keyhole limpet hemocyanin
Tris	Tris-(hydroxymethyl-)aminomethane
TLR	Toll-like receptor
wt	wildtype
Xcr	chemokine (XC-motif) receptor

Nomenclature

According to the recommendations of the Mouse Genomic Nomenclature Committee (MGNC), mouse gene symbols used in this study begin with an uppercase letter followed by all lowercase letters (*e.g.* Ccr5), whereas protein symbols use all uppercase letters (*e.g.* CCR5) (see http://www.informatics.jax.org/nomen and [13]).

For symbols of human genes and proteins the recommendations of the HUGO Gene Nomenclature Committee (HGNC) are followed (http://www.genenames.org). Thus, symbols for human genes are all uppercase and italicized (*e.g. CCR5*), whereas human protein names are non-italicized and all uppercase (*e.g.* CCR5).

Abstract

Previous studies showed that loss of the chemokine receptor Ccr1 or Ccr5 has a beneficial effect on survival of cardiac, carotid, corneal and islet allografts in mice. Additionally, human renal allograft recipients homozygous for a null allele of *CCR5* (*CCR5Δ32*) experience significantly prolonged allograft survival. To analyze the mechanisms underlying reduced allograft rejection in $Ccr1^{-/-}$ and $Ccr5^{-/-}$ recipient mice, a renal transplantation model was utilized, that allowed the study of the acute (7d) and the clinically more important phase of chronic (42d) allograft rejection. $Ccr1^{-/-}/Ccr5^{-/-}$ mice were included to analyze whether loss of both receptors is accompanied by additional improvements. Reduced graft fibrosis, leukocyte infiltration and improved histopathology were observed in all knock-out groups, but additional improvements in $Ccr1^{-/-}/Ccr5^{-/-}$ recipients were limited to certain aspects at 42d. $Ccr1^{-/-}$ and $Ccr5^{-/-}$ recipients showed significantly diminished mRNA levels of Th1-associated cytokines and chemokines at 7d. Expression of these genes was restored to wildtype levels in $Ccr1^{-/-}/Ccr5^{-/-}$ recipients at 7d explaining the few additional improvements in $Ccr1^{-/-}/Ccr5^{-/-}$ recipients. $Ccr1^{-/-}$ recipients showed Th17-shifted immune responses, while $Ccr5^{-/-}$ recipients exhibited dramatically increased alternative macrophage (MΦ) activation (AMA) at 42d which might explain the beneficial effects observed in $CCR5^{\Delta 32/\Delta 32}$ human transplant recipients. AMA was also observed in unchallenged spleens and elicited peritoneal MΦ of $Ccr5^{-/-}$ mice indicating a general role for CCR5 in MΦ polarization. Results of bone marrow-derived MΦ suggest that strain differences influence MΦ polarization and that BALB/c allografts favor the induction of AMA in $Ccr5^{-/-}$ MΦ. Ccr1 or Ccr5 deficiency in recipients has beneficial effects on renal allograft rejection though the underlying mechanisms may be different and might lead to the observed ambiguous effects in $Ccr1^{-/-}/Ccr5^{-/-}$ recipients. Furthermore, no indication for redundant functions of CCR1 and CCR5 was found during renal allograft rejection.

1 INTRODUCTION

1.1 Chemokines and chemokine receptors

The members of the chemokine family are small, mostly basic, heparin-binding secreted proteins with a molecular weight between 8 and 14 kDa. Chemokines are *chemo*tactically active cyto*kines* that induce directed migration (chemotaxis) of leukocytes and other cells to sites of inflammation or injury. During chemotaxis cells follow a concentration gradient of a chemotactically active substance. The direction of migration depends on the nature of the substance: toxic substances will defer cells whereas nutrients and chemokines attract cells.

Chemokine structure is largely determined by the formation of intramolecular disulfide bonds between the thiol (-SH) groups of cysteine residues in the N-terminal and central regions of the amino acid backbone. Therefore, the presence and arrangement of the N-terminal cysteine residues has been used as a criterion to classify chemokines into four major subfamilies: XC- (only one N-terminal cysteine, γ-chemokines), CC- (two adjacent N-terminal cysteines, β-chemokines), CXC- (two N-terminal cysteines separated by one amino acid, α-chemokines), CX_3C- (two N-terminal cysteines with three amino acids in between, δ- chemokines – whose sole member is called Fractalkine/CX_3CL1). CC-, CXC- and CX_3C-chemokines all have 4 conserved cysteine residues forming two disulfide bonds, whereas C-chemokines lack the first and third cysteine of the other chemokine subfamily members resulting in only one intramolecular disulfide bond [9]. The rapid progress in the field of chemokine biology at the end of the 1990s resulted in considerable confusion when different groups reported the same molecule under different names. Therefore, a systematic nomenclature of chemokines and chemokine receptors was introduced in 2000. Since chemokine receptors usually bind chemokines of a specific subfamily, this nomenclature is based on the N-terminal cysteine motif determining subfamily membership [9, 14]. For instance, CCR5 binds members of the CC-chemokine

subfamily, whereas CXCR4 binds several members of the CXC-subfamily. Thus, CCR5 stands for chemokine (CC-motif) receptor 5 [9]. Accordingly, chemokines are designated by their respective N-terminal cysteine motif, *e.g.* the chemokine RANTES (regulated upon activation, normal T-cell expressed, and secreted) is now called CCL5, due to the presence of a CC-motif in the N-terminal region. However, to refer to the historical denomination, the previous designation is sometimes set in brackets behind the systematic name.

Chemokines are involved in diverse biological processes such as wound healing, lymphoid trafficking, organ development, Th1/Th2 development, angiogenesis/angiostasis, inflammation, cell recruitment and metastasis [15]. Functionally, chemokines come in two different flavors: homeostatic and inflammatory. Homeostatic chemokines are constitutively expressed and regulate homing of leukocytes within and between lymphoid organs as well as the development of lymphoid organs [16]. Additionally, homeostatic chemokines guide T and B lymphocytes to localize antigen-presenting cells (APCs) within lymphatic organs [15]. On the other hand, inflammatory chemokines are produced at a site of infection or tissue injury and induce the migration of leukocytes towards such sites where they contribute to leukocyte activation and wound healing [17]. However, the division of chemokines into homeostatic and inflammatory is not an absolute one. Some homeostatic chemokines are up-regulated during inflammation and there are inflammatory chemokines that are constitutively produced and secreted into *e.g.* milk, saliva, tears or sweat. Notably, homeostatic chemokines (*e.g.* CCL20 and CCL22) bind to only one receptor – but, one receptor may bind more than one homeostatic chemokine (compare **Figure 1**), whereas inflammatory chemokines (*e.g.* CCL5 and CCL8) appear to bind to more than one chemokine receptor [6].

Chemokines of both groups mediate their function via binding to a subfamily of seven-transmembrane, G protein-coupled receptors (GPCRs) expressed at the plasma membrane surface of leukocytes. These so-called chemokine receptors are peptide-binding members of

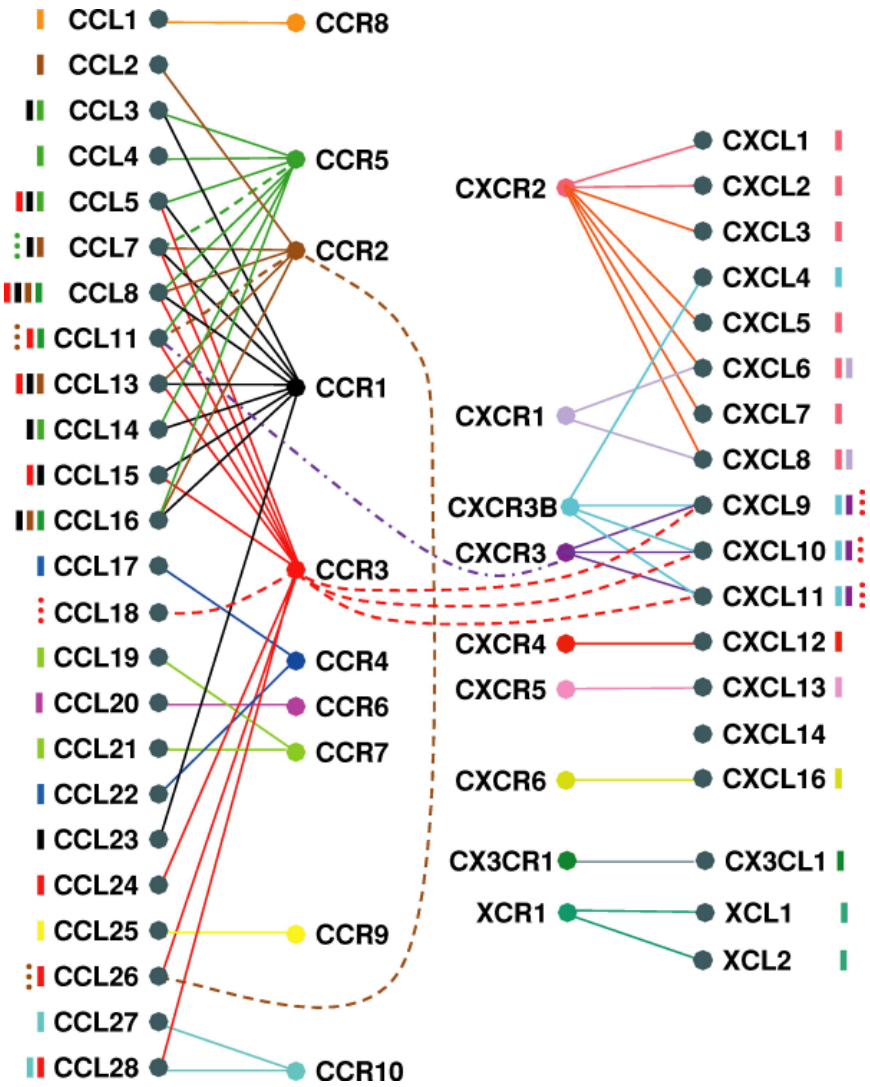

Figure 1. Overview of human chemokines and their receptors (adapted from Rot and von Andrian 2004, [6]). Solid and dashed lines connect receptors with their agonists and antagonists, respectively, and are color coded to correspond with the colors of individual receptor hubs. The bars next to individual chemokine numbers reflect the colors assigned to their apposite receptors. CXCR7, which binds to CXCL11 and CXCL12 [8], is not shown because it was unknown at the time of publication of this review. Furthermore, the so called "interceptors" DARC, D6 and CCX-CKR – chemokine receptors that bind chemokines without further signaling [6] – are excluded from the official nomenclature [9] and were therefore omitted here.

the class A Rhodopsin-like superfamily of GPCRs. They range in size from 340 to 370 amino acids and exhibit common structural features [3]. Some of these structural features are exampled in **Figure 2** by an illustration of the human CCR5 receptor protein. Chemokine receptors display the same classification already mentioned for chemokines. Some chemokine

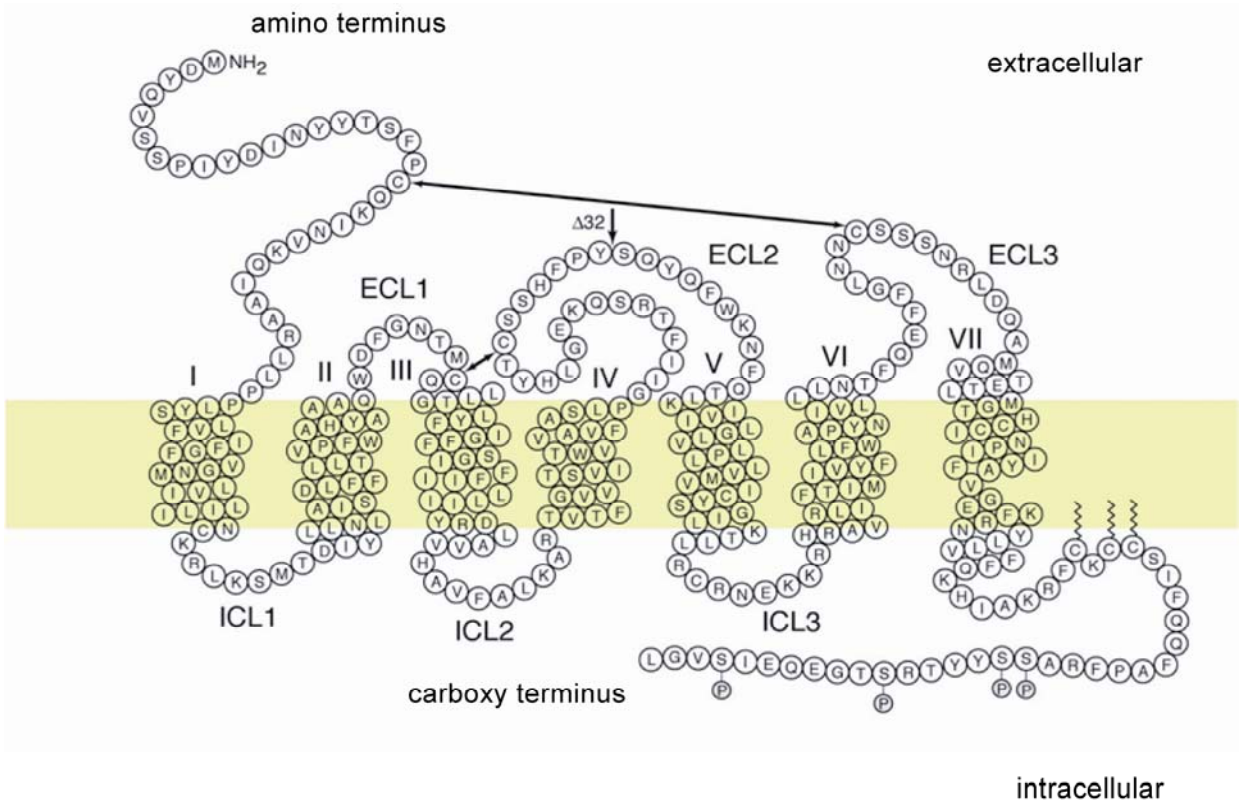

Figure 2. Proposed membrane topology of the human chemokine receptor CCR5 (adapted from Blanpain *et al.* 2002, [4]). Amino acids are indicated in one-letter code and the shaded area specifies the plasma membrane. The seven transmembrane regions of CCR5 are designated by roman numerals (I to VII). The intra- and extracellular loops between the seven transmembrane regions are indicated as ICL1-3 and ECL1-3, respectively. Two disulfide bonds link the extracellular domains of the receptor together (indicated by arrows). Δ32 indicates the location of a 32 bp deletion found at a frequency of about 1% in populations of European origin. This mutation results in a truncated, non-functional receptor that is not expressed at the surface of natural leukocytes or transfected cells but is retained in the endoplasmatic reticulum. The carboxy-terminal domain features a cluster of three palmitoylated cysteine residues anchoring this region to the plasma membrane and four phosphorylation sites for G protein–coupled receptor kinases (GRKs).

receptors – such as CCR1 and CCR5 – are up-regulated upon inflammatory stimuli or during infection, while others (*e.g.* CCR6 and CXCR4) are constitutively expressed (*i.e.* homoeostatic chemokine receptors) [6].

Chemokine receptors function as allosteric transmitters by communicating chemokine binding through modification of the tertiary structure into the inside of the cell. Ligand binding to chemokine receptors results in conformational changes and allows receptor dimerization upon

which complex signaling cascades are initiated (**Figure 3**). Receptor dimerization induces rapid phosphorylation of intracellular tyrosines residues by associated of Janus kinases (JAK) as well as subsequent recruitment and activation of STAT molecules (signal transducers and activators of transcription) [3]. Another major effect of chemokine triggering is the dissociation of receptor-associated heterotrimeric $G_{\alpha\beta\gamma}$ proteins into G_{α} and $G_{\beta\gamma}$ subunits upon exchange of G_{α}-bound GDP *vs.* GTP. Both subunits thereby acquire an activated state and are able to regulate the activity of plasma membrane-bound enzymes like adenylyl cyclase or phospholipase C (PLC). Chemokine receptors are usually coupled to G proteins with an $G_{\alpha i}$ subunit that exerts an inhibitory effect on adenylyl cyclase resulting in reduced intracellular cAMP (cyclic adenosine monophosphate) amounts, decreased cAMP-dependent protein kinase A activity and inhibition of CREB (cAMP response element binding protein)-mediated transcription. Besides these $G_{\alpha i}$-triggered effects, $G_{\beta\gamma}$ mediates the activation of phospholipase C. PLC catalyzes the hydrolytic cleavage of phosphatidylinositol 4,5-bisphosphate [$PI(4,5)P_2$] to inositol 1,4,5-trisphosphate [IP_3] and diacylglycerol (DAG) – two important secondary lipid messenger molecules. In turn, IP_3 opens Ca^{2+} channels in the membrane of the endoplasmatic reticulum thus activating calmodulin and other Ca^{2+} dependent cytoplasmic proteins. Increasing Ca^{2+} levels also induce the translocation of protein kinase C (PKC) isoforms from the cytoplasm to the plasma membrane where it is activated by Ca^{2+}, DAG and phosphatidylserine. PKC then phosphorylates downstream target proteins and initiates nuclear signal transduction events [3]. Furthermore, the finding that chemokine-induced MAPK (mitogen-induced protein kinases) and PI3K (phosphoinositide 3-kinase) cascades are inhibited by Pertussis toxin or PI3K inhibitors, respectively, indicated that both pathways are involved in chemokine signaling. Chemokine induced PI3K activity results in production of 3-phosphorylated lipids and subsequent initiation of PKC, Akt and Ras signaling. These pathways promote NADPH oxidase activity, polarization of adhesion molecules and re-organization of actin cytoskeleton. Arrestin proteins have been

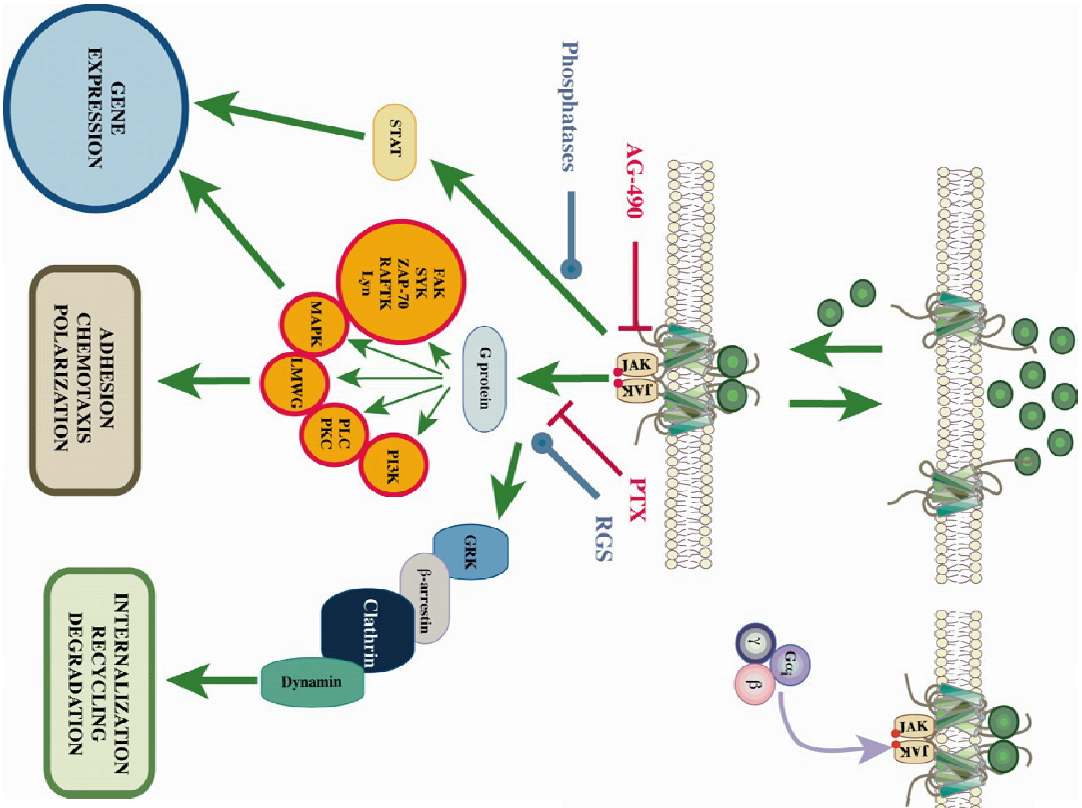

Figure 3. Schematic model showing chemokine-induced receptor dimerization, signaling pathways, receptor desensitization and internalization (adapted from Mellado *et al.* 2001, [3]). The figure shows some of the molecules involved in these pathways and the effects they promote. Selected regulatory molecules and the steps they affect are depicted. Chemokines induce receptor desensitization and internalization. Chemokine receptor desensitization is initiated by ligand binding and includes association of GRK molecules, receptor phosphorylation and association of β-arrestin. Internalization of chemokine receptors occurs in clathrin vesicles, which require the GTPase activity of dynamin. See text for further details.

shown to work as scaffold proteins mediating MAPK cascade initiation at activated chemokine receptors. Activation of phospholipase A_2 (PLA_2) through MAPK-mediated pathways results in the release of arachidonic acid which is important for the production of leukotrienes that promote actin polymerization. In addition, MAPK regulate several different protein kinases and transcription factors [3].

Chemokine receptor desensitization is thought to be an essential process that preserves the ability of cells to detect minute differences in chemokine gradients (**Figure 3**). Activated GPCRs induce their own shutdown by two processes. First, the slow intrinsic GTPase activity of activated G_α subunits leads to the re-association of $G_{\beta\gamma}$ with GDP-G_α subunits yielding an inactive heterotrimeric $G_{\alpha\beta\gamma}$ protein. GTPase-activating proteins (GAPs) accelerate this process and are therefore known as RGS proteins (regulators of G protein signaling). Second, $G_{\beta\gamma}$ subunits provide an interface for the docking of GRK proteins (G protein-coupled receptor kinases) at the receptor. The GRK protein sterically hinders G protein activation and induces phosphorylation of Ser/Thr residues at the intracellular regions of the receptor. These phosphorylation events recruit β-arrestin and adaptin molecules which uncouple receptors from G protein signaling and lead to receptor sequestering and down-regulation by internalization into clathrin-coated pits or caveolae. Receptor containing vesicles are then transported to perinuclear endosomes where the receptor is either degraded or recycled and brought back to the plasma membrane in a dephosphorylated from [3, 6, 18]. These complex regulatory pathways and signaling cascades amplify chemokine signals and result in modified gene expression patterns, cytoskeletal re-organization, increased integrin adhesiveness (a prerequisite for leukocyte transmigration), cell polarization and activation as well as directed migration towards a chemotactic source.

Chemokines and their receptors represent an extremely complex network. The human genome contains at least 53 genes encoding chemokines and 21 chemokine receptor genes (**Figure 1**).

To date, 39 chemokine genes and 20 chemokine receptor genes (Ccr1 – Ccr10, Ccr1l1, Cxcr1 – Cxcr7, Cx3cr1 and Xcr1) were identified in the genome of the mouse (Kumamoto Cytokine Database, http://cytokine.medic.kumamoto-u.ac.jp/CFC/CK/Chemokine.html).

Many chemokines bind to more than one receptor and many chemokine receptors are able to bind multiple chemokines (**Figure 1**). An agonist for one receptor might exhibit an antagonistic behavior on another receptor [19, 20]. Depending on the extracellular environment specific proteases truncate amino acids from the N-terminal domain thereby dramatically influencing receptor affinity or even specificity of chemokines [21, 22]. Receptor heterodimerization adds another layer of complexity, although the exact consequences of these interactions are unclear at present [23-26]. Furthermore, non-chemokines have been found to bind to chemokine receptors. For instance, human β-defensin 2 interacts with CCR6 [27, 28]. But it also works the other way round: chemokines bind to non-chemokine receptors: CCL16 binds to the histamine H4 receptor [29]. Cross-desensitization further complicates deciphering chemokine interactions, *e.g.* activation of CCR5 desensitizes μ-opioid receptors and vice versa [30]. Some chemokine receptors were shown to have overlapping ligand specificity and mouse models employing chemokine receptor deficient mice often show only mild effects between wildtype and knock out animals. Redundancy in the chemokine receptor network is therefore thought to be another factor contributing to this complexity. Additionally, heterodimerization of GPCR receptors – as proposed for CCR5 and CXCR4 as well as CCR5 and CCR2 - was also reported to influence signaling properties of chemokines [31-33].

1.2 Chemokine receptors Ccr1 and Ccr5

Chemokine receptor CCR1

CCR1 was identified in 1993 as the first CC-motif chemokine receptor [34]. The murine gene encoding Ccr1 has a two-exon structure with the complete ORF on exon 2 and is located on the

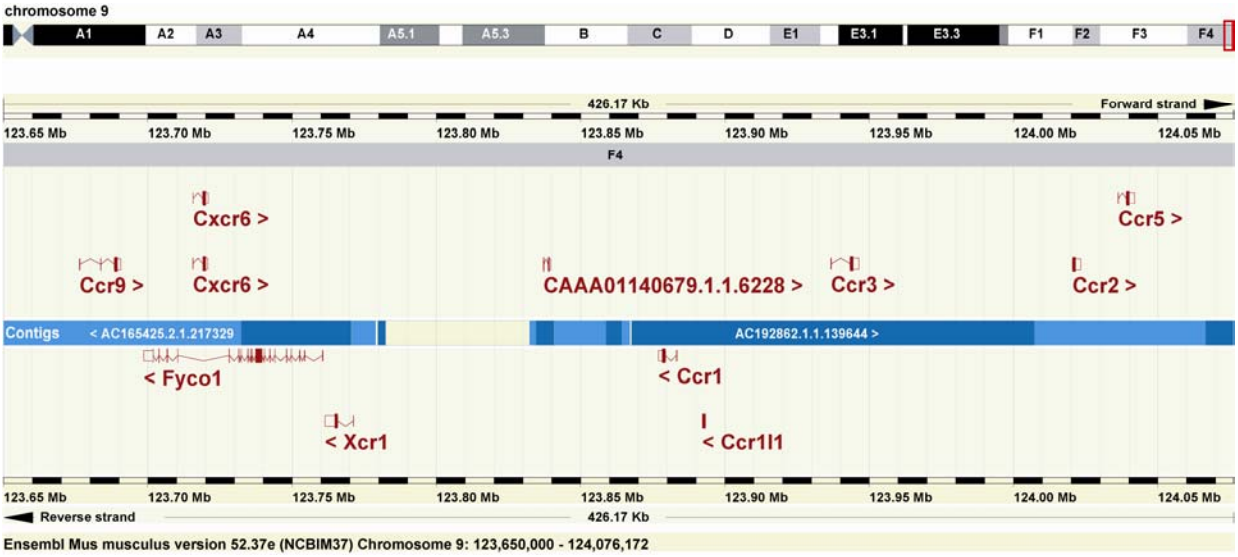

Figure 4. Map of the murine chemokine receptor cluster at the distal end of chromosome 9. The top panel shows the banding structure of chromosome 9. The lower panel represents an enlargement of the highlighted region (red box) at the end of band F4. Gene exon-intron structure and annotation is based on the Ensembl/Havana projects. Filled boxes are exons and lines connecting boxes are introns. Open boxes are untranslated regions. Annotations above the contig bar are in forward strand direction, while annotations below the contig bar are in reverse strand direction (Source: http://www.ensembl.org/; Mus musculus version 52.37e).

distal part of chromosome 9 in a cluster with seven other chemokine receptor genes: Ccr9, Cxcr6, Xcr1, Ccr1l1, Ccr3, Ccr2 and Ccr5 (**Figure 4**). Interestingly, the human cytomegalovirus encodes a functional homolog of CCR1 called US28 thereby manipulating cellular chemokine responses [35, 36]. The overall structure of the G protein-coupled chemokine receptor CCR1 resembles the structure of CCR5 (**Figure 2**) having seven transmembrane domains and two disulfide bonds that link the extracellular domains. However, some features distinguish the molecular structures of both receptors. CCR1 has a comparatively short intracellular C-terminal domain and palmitoylated cysteines which would connect the C-terminus to the plasma membrane are absent [37]. The murine as well as the human CCR1 protein has a size of 355 amino acids and CCL3 (MIP-1α), CCL5 (RANTES) and CCL7 (MCP-3) are high affinity ligands for CCR1 [9, 38]. Ccr1 expression has been reported on neutrophils, eosinophils, monocytes, T and B lymphocytes [39], basophils [40], mast cells [41], NK cells [42, 43], tissue macrophages [44,

45], immature dendritic cells [46-49], as well as erythroid progenitor cells [50] and platelets [51].

Due to its association with inflammatory and autoimmune diseases CCR1 is an interesting pharmaceutical target and several candidate antagonists are currently tested in clinical trials [52, 53]. Several studies using Ccr1-deficient mice suggest a role for this receptor in mobilization of neutrophils and hematopoietic progenitor cells [39, 54, 55]. Other studies showed a tendency towards decreased Th1 functions and/or increased Th2 immune responses in mice lacking functional CCR1 [39, 43, 56]. But these effects appear to depend on the particular disease model since other models showed increased Th1 responses in Ccr1-deficient mice [57, 58]. In a pathogen-free environment Ccr1-deficient mice develop normally but display opposite immune responses depending on the disease context.

Chemokine receptor CCR5

CCR5 shares many features with CCR1. The murine Ccr5 gene has a two-exon structure with the complete ORF on exon 2 and is located in the same gene cluster as CCR1 at the distal part of chromosome 9 (**Figure 4**). Murine CCR5 has a length of 354 amino acids, *O*-glycosylation sites, sulfated tyrosine residues and the intracellular C-terminal domain is plasma membrane-anchored via palmitoylated cysteines creating a fourth intracellular loop (compare topology of human CCR5 depicted in **Figure 2**) [18]. Human CCR5 shares about 82% amino acid identity with its murine ortholog [59]. Ccr5 expression was reported in progenitor as well as $CD4^+$ and $CD8^+$ thymocytes [9], NK cells [60], memory and effector T cells with a preferential Th1 polarization [4, 61, 62] and low levels of CCR5 were detected in circulating monocytes, whereas differentiated tissue macrophages express CCR5 at high levels [4, 45]. Furthermore, dendritic cells in the peripheral blood and immature dendritic cells as well as epidermal Langerhans cells [4], but CCR5 was absent from follicular dendritic cells in lymph nodes [9]. In addition, several

non-immune cells, such as neurons, astrocytes, endothelial and epithelial cells, smooth muscle cells and fibroblasts can express CCR5, but the functional role o this receptor in these cells remains to be determined [4, 9]. Interestingly, CCR5 expression was also found on sperm cells suggesting a role during fertilization [63, 64] and a potential way of transmitting HIV-1 by spermatozoa [65].

Pro-inflammatory stimuli (*e.g.* TNF, IL-12, LPS and ROS), Th1 cytokines like IFN-γ and IL-2 and growth factors (GM-CSF and M-CSF) were shown to up-regulate CCR5 expression on peripheral blood mononuclear cells (PBMCs), macrophages and lymphocytes [4]. Surprisingly, anti-inflammatory cytokines such as IL-10 and TGF-β can also induce CCR5 expression on monocytes, macrophages and dendritic cells [66-68].

High affinity agonists for CCR5 are CCL3 (MIP-1α), CCL4 (MIP-1β), CCL5 (RANTES) and CCL8 (MCP-2), whereas CCL7 (MCP-3) acts a natural antagonist [9]. Ligand binding to CCR5 was reported to initiate heterotrimeric $G_{\alpha\beta\gamma}$ protein signaling and triggers tyrosine kinase initiated pathways and several different kinase cascades such as JAK/STAT, MAP and PI3 kinase pathways. These pathways result in inhibition of adenylyl cyclase, release of intracellular Ca^{2+}, opening of K^+ ion channels, chemotaxis and activation of leukocytes. However, none of these effects is specific for CCR5 owing to the redundancy and overlap of chemokine specificities in the chemokine receptor system. Agonist ligation finally leads to phosphorylation, internalization and receptor recycling [4, 18].

Mice with a Ccr5 deficiency appear healthy and display no developmental abnormalities. Moreover, humans homozygous for a null allele of CCR5 (*CCR5Δ32*, see below) do not show any overt phenotype; suggesting that pharmacological blockade of this receptor should result in little side-effects. CCR5 has been implicated in several important pathologic conditions like rheumatoid arthritis, multiple sclerosis, organ transplant rejection, asthma, AIDS and atherosclerosis [53]. About ~30% of all prescription drugs on the market such as beta blockers,

neuroleptics and antihistamines target GPCRs [69]. Due to these reasons CCR5 has become a promising target for pharmaceutical industry. A first CCR5 antagonist (Maraviroc, Pfizer) has already been approved for the therapy of antiviral treatment-experienced HIV patients by the FDA in 2007 [70, 71]. Several other antagonists are currently tested in clinical trials against autoimmune and inflammatory diseases [72].

Ccr5-deficient mice were used to study the effects of Ccr5 deficiency on the outcome of parasitic [60, 73-76] or viral [77, 78] infections. These studies reported significant reductions in the numbers of infiltrating macrophages, NK cells, $CD4^+$ and $CD8^+$ T cells as well as reduced numbers of regulatory T cells at the site of inflammation in animals that lacked functional CCR5. Interestingly, Glass *et al.* reported that CCR5 represents a critical antiviral and survival determinant in a model of cerebral West Nile virus infection [79]. In an Influenza infection model, Tyner *et al.* showed that CCL5 (RANTES) signaling through CCR5 generates an anti-apoptotic signal, supporting macrophage survival and virus elimination [80]. Other studies reported reduced IFN-γ production [81] and attenuated Th1 responses [58] in $Ccr5^{-/-}$ mice.

In 1996, five groups simultaneously reported that CCR5 is the major co-receptor for macrophage-tropic HIV-1 strains (**Figure 5**) [82-86]. Besides CCR5, other chemokine receptors were proposed to act as co-receptors for different HIV isolates: CXCR4 (T cell-tropic HIV-1 [87]), CXCR6 (HIV-1 and HIV-2 isolates [88, 89]), CCR2b and CCR3 (dual-tropic HIV-1 89.6 [83, 85]), the HMCV-encoded US28 receptor (HIV-1 and HIV-2 isolates [90]) and the orphan receptor GPR15 (HIV-1 and HIV-2 isolates [88]). Weissman and colleagues reported in 1997 that the envelope protein gp120 of CCR5 tropic (R5) HIV strains induces calcium flux and chemotaxis in $CD4^+$ T cells through CCR5 in a CD4-dependent manner [91]. Subsequently, it was shown that CCR5 - as well as CXCR4 - associates physically with CD4 [92] - which is the natural receptor of IL-16. Interestingly, allosteric cross-talk between CD4 and CCR5 seems to promote signaling of IL-16 as well as CCL4 and results in the preferential recruitment of Th1 polarized $CD4^+$ T cells to sites

of inflammation [93, 94]. Despite the high amino acid identity between human and murine CCR5, the murine ortholog does not confer HIV-1 entry capabilities [59]. However, some monoclonal anti-CCR5 antibodies, the chemokines CCL3, CCL4, CCL5 and several CCL5 derivatives were shown to act as HIV entry inhibitors [9, 95] (**Figure 5**). Furthermore, a 32 bp deletion allele of CCR5 (designated *CCR5Δ32*) confers resistance to infection by R5 HIV strains in homozygous carriers. However, the *CCR5Δ32* allele might have a dual effect on AIDS progression, since individuals heterozygous for *CCR5Δ32* exhibit increased AIDS-free survival time, but, upon onset of AIDS, those patients have an accelerated decrease of $CD4^+$ T cell counts and reduced survival time [96]. Interestingly, apart from their resistance to HIV-1 infection and reduced risk for asthma [97], carriers of a homozygous *CCR5Δ32* genotype - ~1% of individuals of the northern European population - do not display an obvious phenotype [9]. The 32 bp deletion leads to a truncated, non-functional receptor protein that lacks the last three transmembrane domains and is retained in the endoplasmatic reticulum [4] (compare **Figure 2**). The *CCR5Δ32* allele is frequently found in populations of Caucasian origin showing a north-south gradient in Europe.

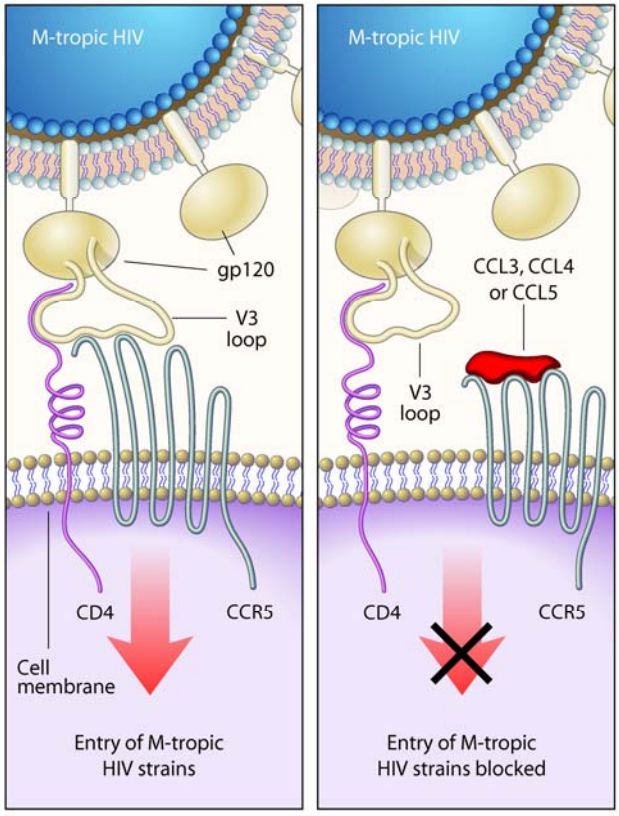

Figure 5. CCR5 mediates HIV entry and ligands of CCR5 block inhibition of HIV entry (adapted from Luster *et al.* 1998, [5]). HIV gp120 binds to CD4, inducing a conformational change that exposes the V3 loop and permits subsequent interaction with a chemokine receptor. To gain entry into cells, M-tropic HIV-1 uses CCR5 predominantly. Chemokine ligands for CCR5 (CCL3, CCL4 or CCL5) block M-tropic HIV-1 from entering cells.

Populations of northern Russia, Finland and Sweden have the highest allele frequencies (~15%) while residents in western and central European countries have allele frequencies of about 10% and around 1% homozygous carriers [98]. In southern countries such as Portugal, Greece and Turkey allele frequencies of 4-6% have been observed, and frequencies of *CCR5Δ32* drop to ~2% in northern Africa. Low allele frequencies are also found in the Middle East and India. *CCR5Δ32* does not occur in indigenous populations of other regions such as central and western Africa, China and Japan [4]. The relatively restricted distribution and the high incidence of the *CCR5Δ32* allele were attributed to a selection advantage associated with homo- or heterozygosity. Nevertheless, the driving force for such a positive selective pressure favoring the enrichment of *CCR5Δ32* remains unclear. Advantages in the resistance to pathogens like *Yersinia pestis* (plague) and *Variola* (smallpox) as well as to diseases such as rheumatoid arthritis, multiple sclerosis and asthma were postulated but not confirmed so far [4, 9]. Notably, recent studies suggested that the deletion first occurred about 7000 years ago. Thus, the observed allele frequencies might be the result of neutral evolution and genetic drift, though a possible influence of positive selection cannot be ruled out by these findings [99, 100].

1.3 Mechanisms of allograft rejection

An allograft is defined as transplanted cells, tissues or organs from a genetically different member of the same species as the recipient. Rejection of an allograft is mediated by cellular as well as humoral components of the immune system [1].

The main inductor of rapid rejection responses are allogeneic graft MHC (major histocompatibility complex) molecules. These proteins are recognized by recipient T cells by two possible pathways. In the direct pathway, intact MHC molecules of donor APCs present self- or allo-antigen either to naïve recipient T cells in the draining lymph node of the graft or to circulating memory T cells of the recipient generated during previous exposure to *e.g.* microbial

antigens. The recognition of self- or allo-antigen on foreign MHC molecules activates $CD4^+$ or $CD8^+$ T cells with reactivity towards allogeneic MHC. These T cells are self-restricted but recognize either the allogeneic MHC molecule itself or in combination with a bound peptide as a foreign structure. In a second, more indirect pathway, host dendritic cells process alloantigen within the graft or alloantigen that reached the lymph node. The alloantigen is usually presented on MHCII molecules by host APCs but presentation on MHCI molecules due to cross-priming has also been observed. Naïve T cells recognizing these alloantigens are activated and differentiate into $CD4^+$ or $CD8^+$ T cells. However, $CD8^+$ cytotoxic T cells generated by the indirect pathway are self-restricted and cannot directly kill the allograft cells [1].

Once activated by the direct or indirect pathway, alloreactive host T cells migrate into the graft and trigger graft rejection. Alloreactive $CD8^+$ cytotoxic T cells generated by the direct pathway kill graft cells which express allogeneic MHCI molecules. This reaction was suggested to be important during the acute phase of rejection. In contrast, alloreactive $CD4^+$ T helper cells might have a stronger relevance for the chronic phase of rejection by the production of cytokines which subsequently cause graft damage by inducing macrophage activation and inflammation in a manner resembling delayed type hypersensitivity (DTH) responses [1].

Polymorphic antigens other than MHC molecules induce weaker, more gradual rejection reactions, are usually presented via the indirect pathway and comprise the group of minor histocompatibility antigens. Besides these primary signals, activation of alloreactive T cells by co-stimulatory B7 molecules on APCs plays an important role during acute allograft rejection [1].

Humoral allograft rejection is initiated by preexisting host antibodies (generated during previous blood transfusion, transplantation or pregnancy) that bind to endothelial graft antigens and trigger complement activation. In turn, endothelial cell injury and exposure of the subendothelial basement membrane initiate platelet adhesion, thrombosis and vascular

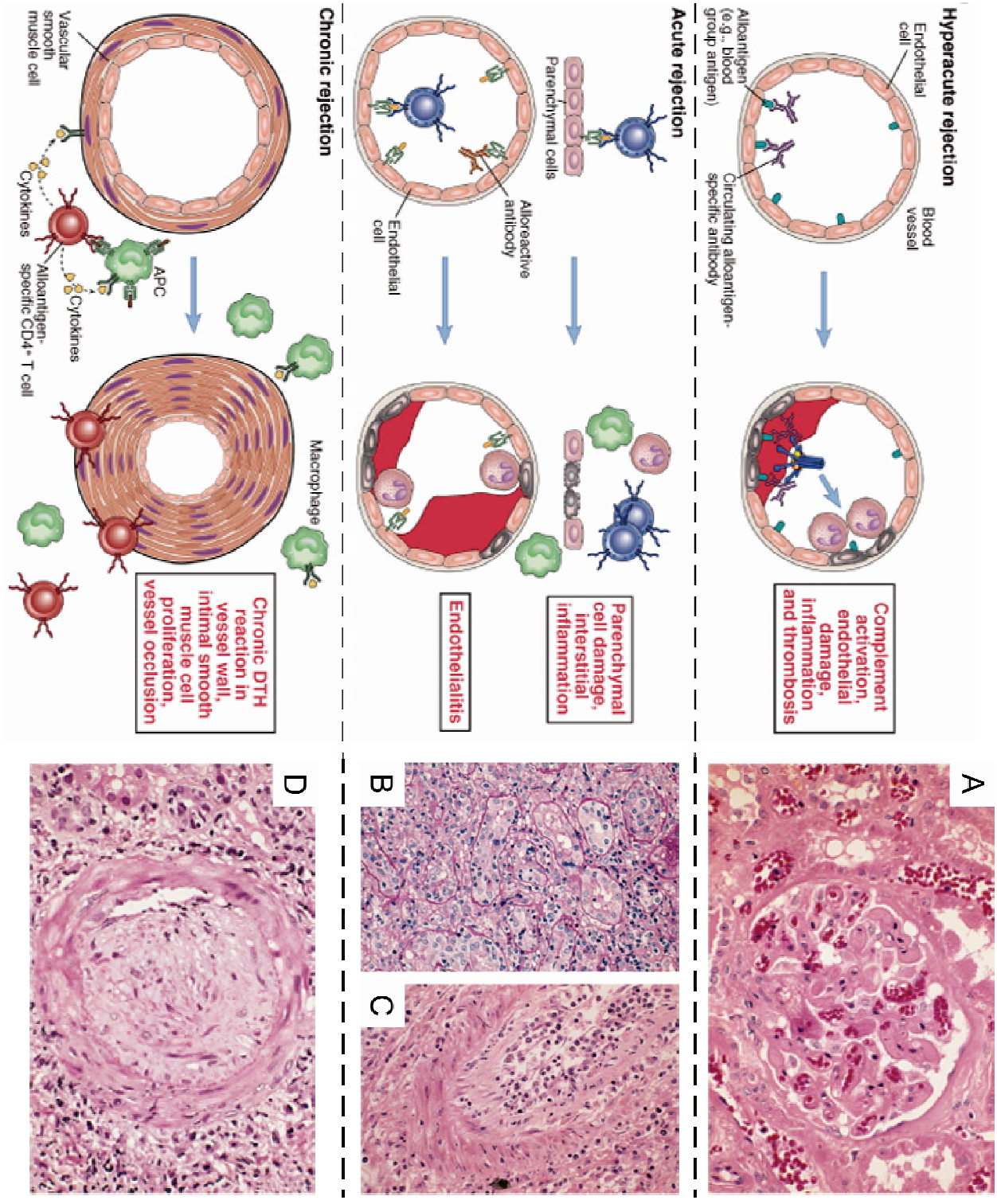

Figure 6. Immune mechanisms and histopathology of different forms of graft rejection (adapted from Abbas *et al.* 2007, [1]). In **hyperacute rejection**, preformed antibodies reactive with vascular endothelium activate complement and trigger rapid intravascular thrombosis and necrosis of the vessel wall. In acute rejection, $CD8^+$ T lymphocytes reactive with alloantigens on endothelial cells and parenchymal cells mediate damage to these cell types. (continued)

occlusion. This kind of rejection occurs right after anastomosis of host and donor vessels and is termed hyperacute rejection phase (**Figure 6A**). However, due to low levels of alloreactive antibody, hyperacute rejection may progress slowly over several years [1].

Acute rejection begins a few days after transplantation and is mediated by effector T cells and antibodies reactive to donor antigens present on endothelial and vascular cells (**Figure 6B+C**). T cells initiate direct killing of graft cells and produce cytokines that recruit and activate inflammatory cells thereby increasing graft damage (**Figure 6B** and **6C**). Antibodies against vessel wall antigens contribute to acute rejection by activating complement inducing vessel wall necrosis and acute inflammation; a histologic pattern different from hyperacute rejection [1].

Graft vasculopathy is characterized by proliferation of intimal smooth muscle cells, arterial occlusion and finally ischemic damage (**Figure 6D**). Graft vasculopathy is the consequence of a combination of processes, including damage by perioperative ischemia, acute rejection episodes and chronic DTH-like reactions. Proliferation of arterial smooth muscle cells is a result of growth factors and chemokines secreted by endothelial cells, smooth muscle cells and macrophages in response to cytokines produced by alloreactive T cells. Graft vasculopathy finally leads to chronic rejection due to the slow replacement of parenchymal cells by non-functioning fibrous tissue in response to the progress of arterial lesions and acute rejection episodes [1].

(**Figure 6** continued) Alloreactive antibodies formed after engraftment may also contribute to vascular injury. In chronic rejection with graft arteriosclerosis, injury to the vessel wall leads to intimal smooth muscle cell proliferation and luminal occlusion. This lesion may be caused by a chronic DTH reaction to alloantigens in the vessel wall. Photomicrographs on the right side of figure 6 show the **histopathology of rejecting renal allografts: 6A. Hyperacute rejection** of a kidney allograft with endothelial damage, platelet and thrombin thrombi and early neutrophil infiltration in a glomerulus. **6B. Acute rejection** of a kidney with inflammatory cells in the connective tissue around the tubules and between epithelial cells of the tubules. **6C. Acute rejection** of a kidney allograft with destructive inflammatory reaction destroying the endothelial layer of an artery. **6D. Chronic rejection** in a kidney allograft with graft arteriosclerosis. The vascular lumen is replaced by an accumulation of smooth muscle cells and connective tissue in the vessel intima.

1.4 Chemokine receptors CCR1 and CCR5 in allograft rejection

1.4.1 Role of Ccr1 and Ccr5 in rodent allograft models

Migration of leukocytes from the circulation into the graft as well as dendritic cell traffic from the graft to secondary lymphoid organs are crucial steps during the induction of allograft rejection and chemokines as well as their receptors have been implicated in both processes [101]. Moreover, several models of allograft rejection show that loss or blockade of the chemokine receptors Ccr1 or Ccr5 has a beneficial effect on allograft rejection and survival. In the year 2000, Gao *et al.* reported that loss of Ccr1 results in suppression of acute and chronic rejection and prolonged cardiac allograft survival in a murine transplantation model [102]. Another group showed that Ccr1-deficiency prolongs corneal allograft survival in a mouse model [103]. Bedke *et al.* used a Fischer to Lewis rat renal allograft model and observed a significant inhibition of chronic allograft damage by blocking CCR1 with the non-peptide antagonist BX 471 [104]. In addition, BX 471 was shown to be similar to cyclosporine in its ability to prevent extensive infarction of renal allografts and to prolong allograft survival in a rabbit model [105]. Furuichi *et al.* reported that CCR1 deficiency as well as application of BX 471 results in reduced infiltration by neutrophils and macrophages in a renal ischemia-reperfusion injury model [44]. Yun *et al.* utilized the potent chemokine receptor antagonist Met-RANTES (N-terminally methionylated RANTES (CCL5) [106]), for a combined blockade of the chemokine receptors CCR1, CCR3 and CCR5 in a murine model of chronic cardiac allograft rejection [107]. They found that application of Met-RANTES decreased chronic allograft vasculopathy and attributed this effect to reduced graft infiltration by macrophages and T cells as well as less intimal cell proliferation [107]. Met-RANTES blocked adhesion of monocytes to microvascular endothelium and decreased vascular and tubular damage during renal allograft rejection in rats [108]. Furthermore, TAK-779 – a small-molecule inhibitor of CCR5 and CXCR3 – was reported to enhance allograft survival and morphology in two allograft rejection models: TAK-779

prevented acute and chronic rejection of murine cardiac and islet allografts [109] and reduced numbers of infiltrating T cells in a rat model of small intestine transplantation [110].

Several groups observed that the rejection of cardiac and islet allografts is attenuated and accompanied by prolonged allograft survival in Ccr5-deficient mice. Gao and colleagues reported in 2001 that mice lacking Ccr5 or treated with a monoclonal antibody against CCR5 show prolonged cardiac allograft survival [111]. However, the mice used in this study were not backcrossed and displayed therefore a mixed genetic background. In 2004, our group investigated heart and carotid rejection in allografts transplanted to wildtype and $CCR5^{-/-}$ mice of fully MHC-mismatched genetic background [112]. Six days after transplantation, heart allografts of $Ccr5^{-/-}$ mice exhibited significantly diminished mRNA levels of four metalloproteinase genes (Mmp3, Mmp12, Mmp13 and Adam8), less tissue remodeling, better preservation of the myocardial architecture and prolonged cardiac allograft survival compared with wildtype allografts. At day 35 carotid allografts of $Ccr5^{-/-}$ recipients showed significant reduction of neointima formation and $CD3^{+}$ T cell infiltration, suggesting that CCR5 plays an important role in transplant-associated arteriosclerosis and MMP-mediated vessel wall remodeling during the acute and chronic rejection [112]. Fairchild and colleagues suggested that acute cardiac and renal allograft rejection in $Ccr5^{-/-}$ recipients is mainly mediated by increased intragraft complement deposition and alloreactive antibody serum levels [113, 114]. Schnickel *et al.* demonstrated that combined blockade of CXCR3 and CCR5 in a mouse model of cardiac allograft rejection prolongs graft survival [115]. Furthermore, two groups showed that Ccr5-deficiency prolongs islet allograft survival in a murine rejection model [116, 117]. Interestingly, enhanced islet graft survival in Ccr5-deficient recipients was also found in a xenograft model using transfer of porcine pancreatic cell clusters under the capsules of murine kidneys [118]. Moreover, CCR5 plays a complex role in graft-versus-host disease (GvHD). While CCR5 blockade prevented GvHD [119], loss of donor CCR5 led to accelerated GvHD in a murine

model [120, 121]. Notably, a study from Wysocki *et al.* suggests that CCR5 might be important for immunosuppressive function of regulatory T cells during GvHD [122]. The finding that CCR5 expressing regulatory T cells are important suppressors of graft rejection is supported by results from Kallikourdis *et al.* showing accumulation of highly suppressive $CCR5^+$ regulatory T cells in the uterus of pregnant mice [123].

1.4.2 Chemokine and chemokine receptor expression in rejecting human renal allografts

In 1953 Jones wrote: "In the injured glomerulus increased capillary permeability is associated, as in other examples of inflammation, with a so-called increased stickiness of the endothelial cells. Circulating polymorphonuclear neutrophils adhere to these sticky walls and thus accumulate in the glomerulus" [124]. Today, infiltration of renal allografts by leukocytes is recognized as a hallmark of acute graft rejection [125]. The migration of inflammatory cells to sites of renal injury is mediated by chemokines and their receptors in concert with adhesion molecules such as integrins and selectins. Since different subsets of leukocytes express different chemokine receptors, chemokines are able to selectively control the migration of these subsets [101, 126, 127]. Yun *et al.* found an early/late pattern of chemokine expression in a murine model of chronic allograft vasculopathy [128]. In this regard, Shimizu and Mitchell summarized: "Chemokines likely affect all phases of transplantation injury by regulating intragraft leukocyte recruitment and inflammatory responses, as well as through modulation of APC homing to secondary lymphoid organs and clonal expansion or tolerance induction of alloantigen-specific T cells" [129]. They conclude that chemokines selectively and temporally control leukocyte immigration to the allograft.

In 1994, Pattison *et. al* were the first to show that CCL5 is abundantly expressed in human kidney allografts with ongoing acute cellular rejection [130]. CCL5 mRNA was detected in infiltrating mononuclear cells and tubular epithelial cells. CCL5 protein was found on

mononuclear cells and tubular epithelium. Additionally, CCL5 protein localized to endothelial cells at the surface of peritubular capillaries, although CCL5 mRNA was absent from these cells as shown by *in situ* hybridization. This finding suggested that CCL5 protein was deposited on the surface of endothelial cells to promote migration of monocytes and T cells into the graft. Moreover, Pattison *et al.* claim that CCR5 is expressed on graft infiltrating cells which are predominantly macrophages, T cells and to a lesser extent eosinophils [130].

Segerer *et al.* reported up-regulation of the chemokines CCL3, CCL4 and CCL5 as well as enhanced expression of their corresponding chemokine receptors CCR1, CCR2 and CCR5 during acute rejection of human renal allografts [125]. Furthermore, this group demonstrated absence of Th2-associated chemokine receptors (CCR3 and CCR8) and increased Th1 cytokine expression (Cxcl10 (IP-10)) during acute rejection, thereby confirming earlier results showing that acute renal allograft rejection in humans has characteristics of a Th1-type immune response [131-133].

In 2004, Rüster and colleagues analyzed chemokine receptor expression in human renal allografts undergoing acute or chronic rejection [134]. They observed that chemokine and chemokine receptor expression was localized to infiltrating mononuclear cells. In addition, they report that biopsies from patients with chronic allograft rejection display significantly lower expression of CCL2, CCL5, CCR1, CCR2 and CCR5 in addition to reduced numbers of infiltrating monocytes/macrophages as compared with biopsies from patients with acute allograft rejection. These findings are in accordance with observations by Oliveira *et al.* demonstrating that acute rejection is dominated by Th1 responses, while chronic rejection is associated with increased expression of Th2 cytokines [133].

Mayer *et al.* characterized $CCR1^+$ cells in rejecting human renal allografts and found that CCR1 protein localized to monocytes, B cells and dendritic cells [135]. Furthermore, CCR1, CCL3 and CCL5 mRNA were increased in biopsies with acute and chronic allograft rejection compared to

pre-transplant controls. Mayer *et al.* suggested that absence of CCR1 on macrophages might be the result of down-regulation after migration into the graft.

1.4.3 Renal allograft long-term survival correlates with CCR5 genotype in humans

In 2001, Fischereder and Luckow *et al.* conducted a retrospective study correlating the renal allograft survival with the CCR5 genotype of 1227 patients with a renal transplant [8]. These patients were recruited from six European transplantation centers (München, Berlin, Erlangen, Regensburg, Hamburg and Zürich) between January, 1998, and March, 2000. 958 patients (=78.0%) were homozygous for the wildtype allele of CCR5, whereas 248 (=20.2%) were heterozygous and 21 (=1.7%) of these patients were homozygous for the *CCR5Δ32* allele. The effect of *CCR5Δ32* homozygosity on allograft survival was analyzed in 576 patients with available demographic and clinical follow-up data (**Figure 7**). No obvious demographic or clinical

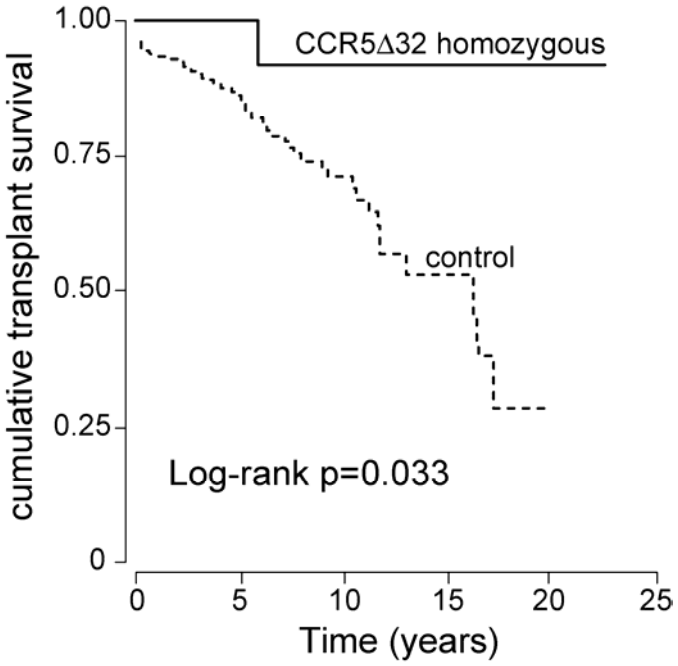

Figure 7. Kaplan-Meier plot showing renal allograft survival in patients with control (*CCR5* wildtype and *CCR5Δ32* heterozygous) or *CCR5Δ32* homozygous genotype (adapted from Fischereder and Luckow *et al.* 2001, [8]).

differences were found between the group of *CCR5Δ32* homozygous carriers and the control

group (wildtype plus *CCR5Δ32* heterozygous). Only one of the 21 patients with a homozygous *CCR5Δ32* genotype lost graft function and one patient died with a functioning graft. The other 19 patients were alive with functioning grafts in April, 2000. By contrast, in the control group graft failures occurred in 78 patients. Hence, 5 and 10 years after the transplantation significantly more patients of the control group lost graft function as compared with the group of *CCR5Δ32* homozygous transplant recipients (**Figure 7**. p=0.0108 after 5 years and p=0.0062 after 10 years, Fisher's exact test). Due to these results the authors suggested that homozygosity for the *CCR5Δ32* allele is associated with long-term graft survival representing an advantage in renal transplantation [8].

1.5 Macrophage biology

The investigation of renal allograft rejection in chemokine receptor deficient mice surprisingly showed that Ccr5 is involved in macrophage polarization. Therefore, the next two chapters are intended to give some background information on macrophage biology and activation phenotypes of macrophages.

The word "macrophage" stems from the Greek words for 'large' (*macros*) and 'to eat' (*phagein*) and means "big eater". This term was coined by the famous Russian zoologist Elie Metchnikoff (*1845-†1916) during his comparative studies of phagocytosis and the recruitment of phagocytes in different organisms in 1893 [136]. Metchnikoff was the first to fully recognize the significance of phagocytic cells for the host resistance against infectious agents and is therefore regarded today as the "Father of natural immunity" [137]. Two categories of phagocytic cells were already distinguished by Metchnikoff: small polymorphonuclear "microphages" (*i.e.* granulocytes, 10-15 µm in diameter) and larger sized "macrophages" (mononuclear phagocytes, 20-25 µm in diameter). Macrophages, monocytes and their precursors have been grouped into the mononuclear phagocyte system (MPS) due to common functional criteria:

they show avid phagocytosis and pinocytosis as well as the ability to attach firmly to glass surfaces [138]. Therefore, the cells of the MPS are separated from T and B lymphocytes, granulocytes and endothelial cells. The cells of the MPS derive from a common hematopoietic stem cell in the bone marrow (**Figure 8**). These precursor cells generate monoblasts which in turn give rise to promonocytes and these differentiate into monocytes [139]. Monocytes are incompletely differentiated non-dividing cells with irregular cell shape, bean-shaped nuclei, a high cytoplasm-to-nucleus ratio and a granular cytoplasm containing lysosomes and phagocytic vacuoles [1, 140]. Monocytes emigrate from the bone marrow into the circulation and the peripheral blood from where they transmigrate through the vascular endothelial cell layer into the tissues of the body – a process called diapedesis. Upon entry into the tissue the monocytes mature and become macrophages. In general, macrophages are large cells (20-25 µm in diameter) with an oval, bean-shaped or indented nucleus and distinct Golgi apparatus. They have a cytoplasm rich in lysosomes and endocytic vesicles as well as a plasma membrane covered by ruffles or microvilli [138]. However, macrophage morphology and expression of surface markers varies strongly depending on the anatomic site of tissue entry and different tissue macrophage populations have therefore been given different names. For example, in the CNS, tissue macrophages are called microglia cells, Kupffer cells line the vascular sinusoids of the liver, alveolar macrophages are found in pulmonary airways and multinucleated phagocytes in the bone are called osteoclasts. Macrophages in the spleen are even subdivided into at least 4 populations: red and white pulp macrophages, marginal zone and metallophilic macrophages [141]. Whether peripheral blood monocytes have the capacity to replenish each of these macrophage pools or if different monocyte subsets exist is currently a matter of debate. Besides replenishment by monocytes studies have also shown that local proliferation of tissue macrophages also plays a significant role for the maintenance of macrophage populations

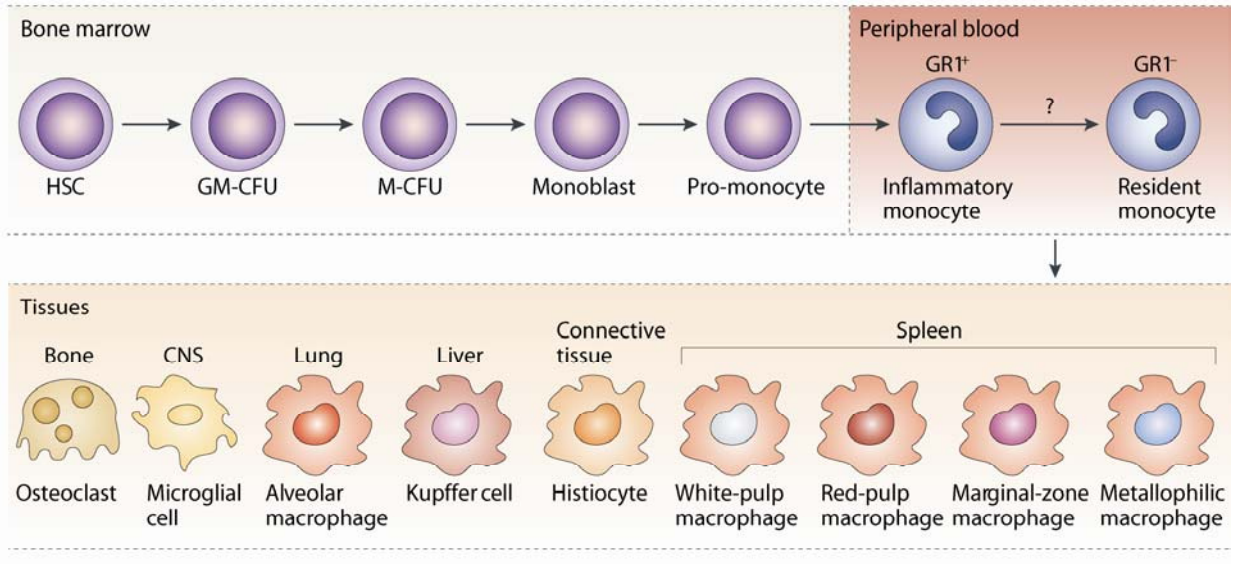

Figure 8. Heterogeneity of the mononuclear phagocyte system (adapted from Mosser *et al.* 2008, [2]). Monocytes originate in the bone marrow from a common haemopoietic stem cell (HSC). They undergo differentiation steps during which they commit to the myeloid and then to a monocyte lineage. In response to macrophage colony-stimulating factor, they divide and differentiate into monoblasts and then pro-monocytes before becoming monocytes, which exit the bone marrow and enter the bloodstream. Monocytes migrate to different tissues, where they replenish tissue-specific macrophages. CNS, central nervous system; GM-CFU, granulocyte/macrophage colony-forming unit; M-CFU, macrophage colony-forming unit.

under steady state conditions, whereas tissue injury and inflammation lead to recruitment of precursor cells from the blood [142, 143].

However, monocytes generate not only the various forms of tissue macrophages but give also rise to dendritic cells (DCs) raising the question if DCs can be placed in the system of mononuclear cells. In favor of this view, Hume summarized several lines of evidence and commented that “dendritic cells are a part of the mononuclear phagocyte system and are derived from a common precursor, responsive to the same growth factors (including CSF-1), express the same surface markers (including CD11c), and have no unique adaptation for antigen presentation that is not shared by other macrophages” [144]. From the point of this view, dendritic cells and macrophages are two sides of the same coin – the professional antigen presenting cell on the one side vs. the professional phagocyte on the other. So far, the best

feature to distinguish DCs from macrophages is by function: DCs are able to stimulate naïve T cells [143].

Macrophages, monocytes and polymorphonuclear cells have been called professional phagocytes due to the efficiency and rate with which they internalize particles [145]. Phagocytosis is a process whereby certain cells engulf relatively large particles (>0.5 μm) into intracellular vacuoles called phagosomes. This process is usually independent of clathrin but requires the polymerization of actin filaments thereby distinguishing classical phagocytosis from other endocytic mechanisms like pinocytosis (uptake of fluid and solutes) and receptor-mediated endocytosis (uptake of macromolecules, viruses and small particles) [146]. However, besides professional phagocytes some epithelial cell types are also capable of phagocytosis but to a lesser extent. Interestingly, transfection of fibroblasts with Fcγ receptors was found to confer phagocytic abilities to these cells. Thus, it was proposed that the phagocytic capacity depends on the range of phagocytic receptors expressed by a given cell type [146, 147]. Janeway named these receptors "pattern-recognition receptors" (PRRs). The targets of these receptors are conserved molecular patterns of foreign organisms like viruses, bacteria, fungi and parasites which are not normally found on host cells. Hence, these microbial structures were termed as "pathogen-associated molecular patterns" (PAMPs) [148]. Macrophages are able to express a variety of different PRRs. These can be categorized into opsonin receptors (*i.e.* receptors recognizing the Fc region of antibodies and receptors binding to complement proteins) and non-opsonic receptors (*i.e.* scavenger and lectin-like receptors as well as Toll-like receptors). PRRs are not only localized at the plasma membrane, they are also found in endosomal compartments (*e.g.* TLR3, TLR9) and in the cytosol (*e.g.* NOD-like receptors) thereby allowing the sensing of danger signals in phagocytosed material as well as in the cytoplasm in addition to sensing pathogens in the surrounding environment of the cell [149]. Upon ligand binding to these receptors signaling cascades are initiated leading to cytoskeletal

reorganization, activation of transcriptional programs, antimicrobial and secretory responses as well as phagocytosis [150].

1.6 Plasticity of macrophage activation and polarization

The cells of the mononuclear phagocyte system display a wide array of diverse functions. This is reflected by their heterogeneity and flexibility of transcriptional programs [151]. Resting tissue macrophages can be activated to provoke pro- or anti-inflammatory responses by appropriate stimuli. These stimuli trigger changes in macrophage phenotype and physiology resulting in different macrophage effector functions: host defense, wound healing or regulatory function (**Figure 9**) [2]. Initially, macrophage classification followed the scheme developed by Mosmann *et al.* for the division of Th1 and Th2 cells on the basis of mutually exclusive cytokine production leading to different functional states [152, 153]. Type 1 T helper cells (Th1) develop mainly in response to intracellular bacteria and viruses. Th1 cells produce pro-inflammatory cytokines like IFNγ, IL-2 and TNF, which trigger antimicrobial activity of macrophages and induce cell-mediated immunity. By contrast, type 2 T helper cells (Th2) are generated upon infection by extracellular parasites and induce the production of cytokines (*e.g.* IL-4, IL-5, IL-10 and IL-13) that initiate antibody production (mainly IgE), activation of eosinophils and mast cells as well as down-regulation of Th1 responses [1, 154]. Macrophages have been shown to produce either IL-12 or IL-10 in response to Th1 or Th2 stimuli, respectively. This finding set the basis for the M1/M2 paradigm of macrophage activation [155].

Classically activated macrophages (CAMs)

During a type 1 immune response, M1 macrophages are activated in reaction to bacterial stimuli (*e.g.* LPS) and pro-inflammatory cytokines such as IFN-γ, IL-12 and TNF that are generated by NK cells, APCs, activated $CD8^+$ cytotoxic T cells and $CD4^+$ Th1 cells (**Figure 9**).

These cytokines have several important effects on macrophages. They induce a program of enhanced phagocytotic activity and lysosomal enzyme synthesis, increased respiratory burst (by enhancement ROS and NO production) and increased expression of MHCII and co-stimulatory molecules. Furthermore, these macrophages show increased production of pro-inflammatory cytokines like IL-1, IL-6, IL-12 and TNF [156]. Moreover, M1 macrophages typically produce and secrete chemokine ligands for CCR5 and CXCR3 [157]. A hallmark of M1 macrophages is increased expression and activity of the enzyme 'nitric oxide synthase' (NOS2) which converts L-arginine to nitric oxide and citrulline, resulting in pronounced killing of pathogens by NO intermediates (**Figure 10**). Therefore, macrophages activated by IFN-γ and TLR ligands are potent killers of bacteria and intracellular pathogens and have tumoricidal capacity [158]. However, the M1 response is potentially dangerous for the host, due to production of radicals and substances not only toxic to bacteria but also to surrounding tissue. M1 macrophages have also been termed as classically activated macrophages or "*killer macrophages*".

Alternatively activated macrophages (AAMs)

In 1992 Gordon and colleagues introduced the concept of alternatively macrophage activation (AMA) by IL-4 to distinguish this process from the mechanism of classical activation by IFN-γ [159]. IL-4-activated macrophages acquire several functions distinct from classically activated macrophages (CAMs). IL-4 inhibits the respiratory burst by reduction of NOS2 activity and concomitant stimulation of arginase activity, thereby further reducing NO production since arginase as well as nitric oxide synthase use L-arginine as a substrate (**Figure 10**). The increase in arginase activity leads to enhanced production of proline and polyamines – both are important precursors for collagen synthesis. Furthermore, IL-4 induces up-regulation of mannose-receptor (MRC1) expression, MRC1-mediated endocytosis and stimulates MHCII expression and antigen presentation. IL-4 induces expression of mediators of tissue remodeling,

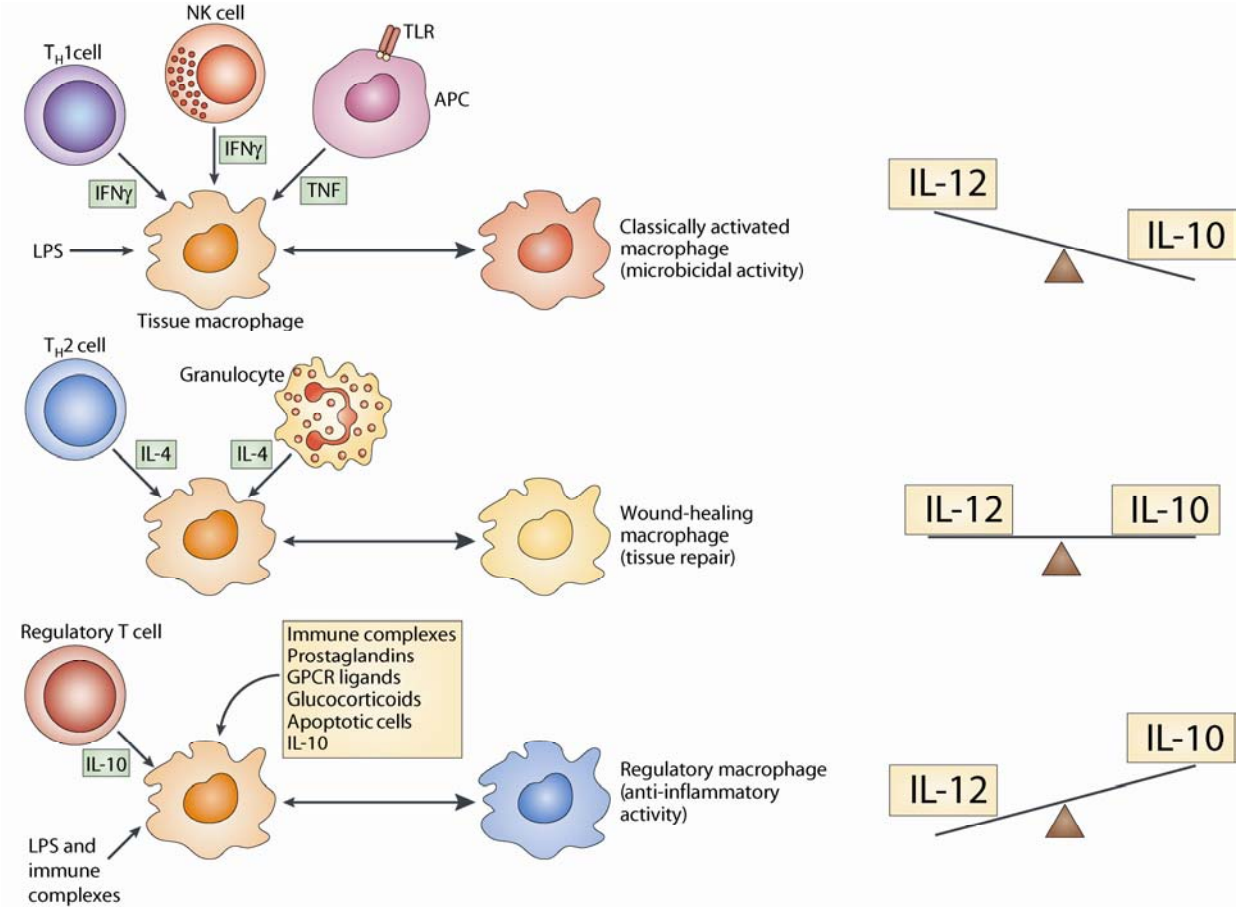

Figure 9. Plasticity of activated macrophages (adapted from Mosser *et al.* 2008, [2]). Classically activated macrophages (CAMs) arise in response to IFN-γ, which can be produced by T_h1 cells or $CD8^+$ T cells (not shown) or by natural killer (NK) cells and TNF, which is produced by antigen-presenting cells (APCs). CAMs produce high levels of IL-12 and modest levels of IL-10. Wound-healing macrophages which are similar in phenotype to alternatively activated macrophages (AAM) arise in response to IL-4, which can be produced by T_h2 cells or by granulocytes. AAMs produce only low levels of IL-10 and IL-12, but express resistin-like molecule α (Retnla) intracellularly, a marker that is not expressed by the other macrophage populations. Regulatory macrophages are generated in response to various stimuli, including immune complexes, prostaglandins, G-protein coupled receptor (GPCR) ligands, glucocorticoids, apoptotic cells or IL-10 and these macrophages produce high levels of IL-10 and low levels of IL-12. Each of these three populations has a distinct physiology. CAMs have microbicidal activity, whereas regulatory macrophages produce high levels of IL-10 to suppress immune responses. Wound-healing macrophages have a role in tissue repair.

promotes fibroblast proliferation as well as collagen synthesis (**Figure 10**). AAM preferentially produce chemokine ligands that bind to CCR3, CCR4 and CCR8 [157]. Interestingly, IL-13 – the nearest chromosomal neighbor of IL-4 – shares many overlapping effects with IL-4; for instance

inhibition of respiratory burst, tissue remodeling and autophagy [160]. Due to their promotion of tissue repair, production of extracellular matrix and return to homeostasis IL-4/Il-13 activated macrophages have been called "*wound healing*" macrophages [2]. IL-4 is mainly produced by activated $CD4^+$ Th2 cells, but also $CD8^+$ cytotoxic T cells, NK T cells, mast cells, basophils, eosinophils as well as human neutrophils have been reported to synthesize IL-4 suggesting that alternative macrophage activation is a feature of innate as well as adaptive immunity [160-162]. In accordance with the role of IL-4 in Th2-driven immune responses, alternative activation of macrophages occurs during host defense against extracellular parasites and enhanced expression of marker genes associated with AAMs were found in mouse models of asthma. Referring to the Th1/Th2 paradigm, AAMs have also been termed M2 macrophages [160].

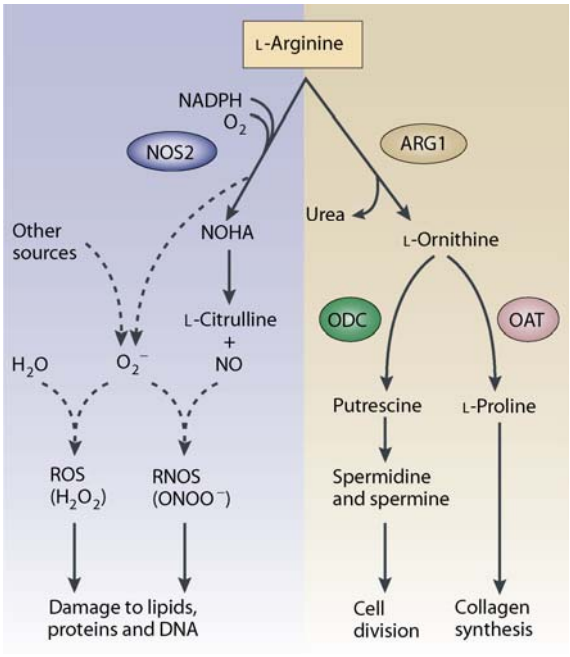

Figure 10. Schematic representation of arginase 1- and nitric-oxide synthase 2-dependent metabolic pathways (adapted from Bronte *et al.* 2005, [7]). The activities of the enzymes arginase 1 (ARG1) and nitric oxide synthase 2 (NOS2) are illustrated, together with the downstream pathways that are activated by L-arginine metabolites. Solid lines indicate the main enzymatic activity, whereas dashed lines indicate alternative metabolic pathways. NOHA, *N*G-hydroxy-L-arginine; OAT, ornithine amino-transferase; ODC, ornithine decarboxylase; RNOS, reactive nitrogen-oxide species.

Regulatory macrophages

A third group of activated macrophages has been emerging recently showing an additional flavor: regulatory macrophages [2]. This population of macrophages has an immunosuppressive

phenotype that is characterized by high expression of IL-10 and down-regulation of IL-12 synthesis. Their phenotype resembles that of myeloid-derived suppressor cells found in solid tumors. Among the various stimuli that have been identified to induce regulatory macrophages are glucocorticoids, TLR agonists in presence of IgG complexes, apoptotic cells, adenosine and histamine [2].

Originally sub-grouped as M2c macrophages [157] regulatory macrophages have recently been proposed to represent an own division [2]. Although, the M1/M2 annotation reflects that the primary Th1 cytokine IFN-γ induces M1 activation (and IL-12 synthesis in macrophages) whereas IL-4 – the prototypic Th2 cytokine – induces M2 activation (and IL-10 synthesis in macrophages), this scheme underscores that M1 and M2 phenotypes are endpoints in a wide spectrum of activation states found in macrophages [163]. Moreover, the finding that other stimuli like glucocorticoids, TGF-β and IL-10 or Fc receptor ligation and TLR ligands are also able to activate macrophages with similar activation phenotypes like IL-4/IL-13 additionally complicates such classification attempts [2]. Furthermore, several studies have demonstrated that macrophage activation states are fully reversible [164-166]. Therefore, Mosser *et al.* suggested a new classification system based on macrophage function: host defense, wound healing or regulatory (**Figure 9**) [2]. In summary, the cells of the mononuclear phagocyte system exhibit a unique plasticity that confers flexibility to the innate immune system and assists the immune system in adaptive immune responses.

1.7 Rationale and aim of this study

Kidney is the most frequently transplanted organ in human patients [167]. However, most immunosuppressive drugs available on the market to date, target the effects of acute allograft rejection and there are no real treatment options for chronic rejection [168]. This situation is reflected by excellent first-year survival rates and only moderate improvements in long-term

graft survival [169]. At best, prolonging allograft survival could supersede follow-up transplantations, help to alleviate the shortage of accessible organs and decrease waiting time for transplantation.

The murine model of renal allograft transplantation provides a useful method to study acute and chronic rejection. In this experimental setting antigen-independent factors such as donor age, graft size and time of cold ischemia can be controlled. Long-term survival of renal allografts in certain murine donor-recipient strain combinations allows studying chronic phase of rejection without the need for immunosuppression. Hence, chronic alloimmune responses can be studied without interfering effects of drug toxicity on chronic injury [170]. In contrast to heterotopic heart transplantation (*i.e.* transplantation into the abdominal cavity and vascularization of the graft via the aorta and vena cava below the renal vessels [171]), the orthotopic (*i.e.* in place of the recipient organ) renal allograft model used in this study is a more physiologic model, provides longer allograft survival times and graft failure ultimately leads to death of the animal defining an endpoint of rejection [172]. There is already a considerable amount of data available for the role of several chemokine receptors in cardiac allograft rejection. However, due to the underlying disease, different organs behave differently during transplant rejection [167] and it is still unclear if the beneficial effects of chemokine receptor deficiency are limited to certain organs or can be assigned to all transplanted organs [173-175]. The chemokine receptors CCR1 and CCR5 appear to play an important role in various processes during allograft rejection. Key findings from previous experiments (see section 1.4) are:

1. Mouse models of allograft rejection showed enhanced allograft function and survival upon blockade or deletion of Ccr1 or Ccr5.
2. Human renal allografts undergoing rejection show increased expression of the chemokines CCL3 and CCL5. Additionally, graft infiltrating cells express the corresponding chemokine receptors CCR1 and CCR5.

3. Long-time renal allograft survival in humans has been correlated with a lack of functional CCR5 protein.

To date, improved allograft outcome in mice lacking functional chemokine receptors due to blockade or genetic deletion has mostly been accounted to reduced graft infiltration by inflammatory leukocytes. However, the function of chemokines and their receptors is not limited to chemotaxis of leukocytes and other cells. Chemokines and chemokine receptors were shown to initiate distinct transcriptional programs leading to activation and/or differentiation of different target cell types [157, 176-178]. Therefore, it was tempting to speculate whether loss of Ccr1 or Ccr5 results in altered immune response phenotypes and whether those changes might contribute to reduced allograft rejection. On the other hand, the finding that loss of either Ccr1 or Ccr5 has a beneficial effect on allograft survival in several mouse models (see 1.4.1), prompted us to generate $Ccr1^{-/-}/Ccr5^{-/-}$ double-deficient mice and analyze whether loss of both chemokine receptors has additional or synergistic effects on allograft rejection leading to prolonged allograft survival times. Furthermore, these mice serve as an important tool to answer the question whether CCR1 and CCR5 have redundant function during allograft rejections.

2 MATERIALS AND METHODS

As outlined under “External contribution” (see 7.1), the group of Prof. Gröne at the DKFZ in Heidelberg (Dept. of Cellular and Molecular pathology) contributed to this work by performing orthotopic kidney transplantation (see 2.15), determination of plasma urea and creatinine (2.16), histopathology (2.17) and immunohistochemistry (2.18) of renal allograft sections. These methods are described to give complete insight into the sample preparation and analysis process. Methods and results supplied by Prof. Gröne’s group are indicated in section headlines by DKFZ in brackets to unambiguously indicate the origin of contribution.

2.1 Mice

C57BL/6NCrl (C57BL/6) and BALB/cAnNCrl (BALB/c) mice were obtained from Charles River (Sulzfeld, Germany). All mice were subsequently maintained as a breeding colony in our animal facility. Mice were fed fortified rodent chow and water *ad libitum*. Mice were raised under specific pathogen-free housing conditions in individually ventilated cages lined with sawdust.

Ccr1-deficient mice ($Ccr1^{tm1Gao}$) have been generated by Gao *et al.* [179]. Ccr5-deficient mice ($Ccr5^{tm1Blck}$) have been generated in our laboratory as described elsewhere [112]. Ccr5-deficient BALB/c mice were generated by back crossing of Ccr5-deficient C57BL/6 mice against the BALB/c background for at least 10 generations. C57BL/6 mice double-deficient for Ccr1 and Ccr5 were generated by crossing of fully backcrossed Ccr1- and Ccr5-deficient mice. The distance between both loci was large enough (~ 160 kbp) to allow this approach. The theoretical recombination frequency was 1 in 625 events (0.16 cM). Heterozygous ($Ccr1^{+/-}$/$Ccr5^{+/-}$) mice obtained from these matings were crossed with $Ccr1^{+/+}$/$Ccr5^{-/-}$ mice and recombination events between Ccr1 and the Ccr5 locus were analyzed by multiplex PCR with 4 different primer pairs (see Methods section 2.14, genotyping) in the resulting offspring mice. Two female mice out of 477 live pups showed the desired $Ccr1^{+/-}$/$Ccr5^{-/-}$ genotype and were

crossed with wildtype mice to produce male $Ccr1^{+/-}/Ccr5^{+/-}$ mice for intercrossing. Mating of these mice with their $Ccr1^{+/-}/Ccr5^{-/-}$ mothers finally yielded $Ccr1^{-/-}/Ccr5^{-/-}$ mice. Deletion of Ccr1 and/or Ccr5 was confirmed by repeated genotyping using multiplex PCR analysis of genomic DNA prepared from tail snips. Transplantation experiments were performed exclusively with male mice at least 8 to 10 weeks old with a weight between 20 and 25 g. All mice used in this thesis were backcrossed for at least 10 generations to the genetic backgrounds indicated in the individual experiments. All animal experiments were performed in compliance with governmental and institutional guidelines.

2.2 Murine cell lines

J558L, plasmacytoma cell line, BALB/c	Dr. T. Kammertoens, MDC Berlin, Germany
L929s, fibrosarcoma cell line, C3H/An, male	Dr. M. Freudenberg, MPI for Immunobiology, Freiburg, Germany

2.3 Chemicals and reagents

2-Mercapthoethanol	Carl Roth, Karlsruhe, Germany
7-Amino-actionomycin D (7-AAD)	BD Biosciences, Heidelberg, Germany
Acrylamide, linear	Applied Biosystems, Darmstadt, Germany
Agarose, Ultrapure	Invitrogen, Karlsruhe, Germany
Aqua ad injectabilia	Braun, Melsungen, Germany
BD Cytofix solution	BD Biosciences, Heidelberg, Germany
Brewer's thioglycollate medium	DIFCO, Lawrence, Kansas, USA
BSA (Fraction V)	Roche Diagnostics, Mannheim, Germany
BSA, PCR grade (50x)	Fermentas, St. Leon-Rot, Germany
Diethylpyrocarbonate (DEPC)	Fluka/Sigma-Aldrich, Schnelldorf, Germany

DMSO	Merck, Darmstadt, Germany
dNTP set (ATP, CTP, GTP and TTP; each 100 mM)	GE Healthcare, München, Germany
EDTA (EDTA-Na_2, Titriplex III, molecular biology)	Merck, Darmstadt, Germany
Ethidium bromide, aqueous solution, 1.0%	Merck, Darmstadt, Germany
Formaldehyde, p.a., ≥37%	Merck, Darmstadt, Germany
Formamide, p.a.	Fluka/Sigma-Aldrich, Schnelldorf, Germany
Gelatin	Sigma-Aldrich, Schnelldorf, Germany
Griess' reagent for nitrite	Fluka/Sigma-Aldrich, Schnelldorf, Germany
Hydrochloric acid, 37%	Merck, Darmstadt, Germany
$MgCl_2$ (25 mM)	Fermentas, St. Leon-Rot, Germany
MOPS PUFFERAN	Carl Roth, Karlsruhe, Germany
Sodium acetate	Merck, Darmstadt, Germany
Sodium hydroxide pellets, p.a.	Merck, Darmstadt, Germany
Nonidet P40 (Igepal CA 630)	Fluka/Sigma-Aldrich, Schnelldorf, Germany
PCR Optimizer (2.5x)	Bitop, Witten, Germany
Rox reference dye (25x)	Invitrogen, Karlsruhe, Germany
SYBRgreen I (250x)	Fluka/Sigma-Aldrich, Schnelldorf, Germany
Taq buffer without detergent (10x)	Fermentas, St. Leon-Rot, Germany
Tris base (PUFFERAN), p.a.	Carl Roth, Karlsruhe, Germany
Triton X-100	Fluka/Sigma-Aldrich, Schnelldorf, Germany
Tween 20	Fluka/Sigma-Aldrich, Schnelldorf, Germany

2.4 Antibodies

Table 1 summarizes all antibodies used in this study. Antibodies were purchased from Sigma (Taufkirchen, Germany), BD Biosciences (Heidelberg, Germany), Abd Serotec (Düsseldorf, Germany), Biogenesis (Poole, UK), eBiosciences (San Diego, California, USA) and R&D Systems (Minneapolis, Minnesota, USA). The anti-Chi3l3 antibody was a kind gift of Dr. Kimura (NCI, Bethesda, Maryland, USA).

Table 1. Monoclonal and polyclonal antibodies used in this study. (continued)

Antibodies for immunohistochemistry

murine antigen	isotype	clone	µg/µl	final dilution	label	manufacturer
α-smooth muscle actin (α-SMA)	mouse IgG2a, mouse ascites fluid	1A4	unknown	1:200	none (*	Sigma
Arginase 1	mouse IgG1, crossreacts with mouse	19	0.25	1:20	none (*	BD Biosiences
CD4	rat IgG2a, kappa	H129.19	unknown	1:20	none (*	BD Biosiences
CD8a	rat IgG2a, kappa	53-6.7	unknown	1:50	none (*	BD Biosiences
CD11c	hamster IgG1, lambda2	HL3	0.125	1:20	none (*	BD Biosiences
CD206 (MRC1)	rat IgG2a	MR5D3	1.00	1:100	none (*	Abd Serotec
Chi3l3 (Ym1/2)	rabbit IgG	polyclonal	unknown	1:60	none (*	Dr. Kimura
Collagen I/III	rabbit IgG	polyclonal	0.10	1:20	none (*	Biogenesis
F4/80	rat IgG2b, kappa	CI:A3-1	1.00	1:2000	none (*	Abd Serotec

*) Antibody binding was detected using the ABC detection system (Vector Laboratories).

Antibodies for determination of alloreactive antibody levels

murine antigen	isotype	clone	µg/µl	final dilution	label	manufacturer
IgG + IgM	goat anti-mouse Ig	polyclonal	0.50	1:20	FITC	BD Biosciences

Antibodies for flow cytometry

murine antigen	isotype	clone	µg/µl	final dilution for		label	manufacturer
				splenocytes	BMDM		
CCR6	rat IgG2a	140706	0.10	1:50	not used	FITC	R&D Systems
CD3ε	hamster IgG1, kappa	145-2C11	0.20	1:400	1:400	Alexa488	BD Biosciences
CD11b (Integrin αM, Mac-1)	rat IgG2b, kappa	M1/70.15	0.10	1:200	1:100	FITC	Abd Serotec
CD11b (Integrin αM, Mac-1)	rat IgG2b, kappa	M1/70	0.20	1:400	1:200	PE	BD Biosciences
CD11c (Integrin αX)	hamster IgG1, lambda2	HL3	0.20	1:400	1:200	PE	BD Biosciences
CD19	rat IgG2a, kappa	1D3	0.20	1:100	1:100	Alexa647	BD Biosciences
CD45	rat IgG2b, kappa	30-F11	0.50	1:100	1:100	FITC	BD Biosciences
CD115 (CSF1-R1, c-fms)	rat IgG1	604B5 2E11	0.01	1:600	1:100	PE	Abd Serotec
CD124 (IL4Ra)	rat IgG2a, kappa	mIL4R-M1	0.20	1:400	1:100	PE	BD Biosciences
CD169 (MOMA-1, Siglec1)	rat IgG2a	Moma-1	0.10	1:500	1:100	FITC	Abd Serotec
CD204 (MSR1/2)	rat IgG2b	2F8	0.05	1:1000	1:400	Alexa647	Abd Serotec
CD206 (MRC1)	rat IgG2a	MR5D3	0.05	1:400	1:100	Alexa647	Abd Serotec
CD206 (MRC1)	rat IgG2a	MR5D3	0.10	1:400	1:100	PE	Abd Serotec
CD206 (MRC1), intracellular	rat IgG2a	MR5D3	0.05	1:1000	1:100	Alexa647	Abd Serotec
CD206 (MRC1), intracellular	rat IgG2a	MR5D3	0.10	1:1000	1:100	PE	Abd Serotec
CD209b (SIGN-R1, Er-tr9)	rat IgM	Er-tr9	0.05	1:400	1:100	Alexa488	Abd Serotec
F4/80	rat IgG2a, kappa	BM8	0.20	1:800	1:400	PE	eBioscience
F4/80	rat IgG2b, kappa	CI:A3-1	0.01	1:200	1:100	APC	Abd Serotec
Gr-1 (Ly-6C/6G)	rat IgG2b, kappa	RB6-8C5	0.20	1:500	1:100	PE	BD Biosciences
MARCO	rat IgG1	ED31	0.10	1:600	1:100	PE	Abd Serotec
MOMA-2	rat IgG2b	Moma-2	0.01	1:800	1:200	PE	Abd Serotec
MOMA-2, intracellular	rat IgG2b	Moma-2	0.01	1:1000	1:200	PE	Abd Serotec
NK-1.1 (NK cells)	rat IgG2a, kappa	PK136	0.20	1:100	1:100	PE	BD Biosciences
CD16/32 (FcR Seroblock)	rat IgG2b	FCR4G8	1.00	1:200	1:100	none	Abd Serotec

Table 1 (continued)**. Monoclonal and polyclonal antibodies used in this study.**

Isotype-matched control antibodies for flow cytometry

murine antigen	isotype	clone	µg/µl	final dilution	label	manufacturer
TNP-KHL	hamster IgG1, kappa	A19-3	0.20	matched with test Ab	Alexa488	BD Biosciences
TNP-KHL	hamster IgG1, lambda1	G235-2356	0.20	matched with test Ab	PE	BD Biosciences
mouse Ig	rat IgG1, kappa	R3-34	0.20	matched with test Ab	PE	BD Biosciences
unspecific	rat IgG2a, kappa	R35-95	0.20	matched with test Ab	Alexa647	BD Biosciences
human lymphocytes	rat IgG2a	YTH71.3	0.10	matched with test Ab	FITC	Abd Serotec
human lymphocytes	rat IgG2a	YTH71.3	0.10	matched with test Ab	PE	Abd Serotec
TNP-KHL	rat IgG2b, kappa	A95-1	0.50	matched with test Ab	FITC	BD Biosciences
TNP-KHL	rat IgG2b, kappa	A95-1	0.20	matched with test Ab	PE	BD Biosciences
DNP	rat IgG2b	?	0.05	matched with test Ab	Alexa647	Abd Serotec
TNP-KHL	rat IgG2b, kappa	A95-1	0.20	matched with test Ab	APC	BD Biosciences

2.5 Recombinant proteins and reagents used for *in vitro* cell stimulation

Interferon gamma (IFNg), murine recombinant	Peprotech, Rocky Hill, USA
Interleukin-4 (IL-4), murine recombinant	Peprotech, Rocky Hill, USA
LPS from *E. coli* 0111:B4, cell culture tested, γ-irradiated	Sigma-Aldrich, Schnelldorf, Germany
M-CSF (CSF1), murine recombinant	Peprotech, Rocky Hill, USA
RNasin, recombinant Ribonuclease inhibitor, 40 u/µl	Promega, Mannheim, Germany

2.6 Enzymes

Taq DNA polymerase (recombinant, 5u/µl)	New England Biolabs, Frankfurt, Germany
AmpliTaq DNA polymerase (recombinant, 5u/µl)	Applied Biosystems, Foster City, CA, USA
Reverse transcriptase, SuperScript I	Invitrogen, Karlsruhe, Germany
Reverse transcriptase, SuperScript II	Invitrogen, Karlsruhe, Germany

2.7 Oligonucleotides

Pre-designed assays as well as custom-made primer/probes sets for TaqMan-PCR were ordered from Applied Biosystems (ABI, Foster City, California, USA). Custom primer pairs for SYBRgreen qPCR assays or mouse genotyping were obtained desalted in a 10-100 nmol scale from Invitrogen (Karlsruhe, Germany). Primers (**Table 2 and 3**) were designed using either the computer program 'Primer' provided by the software package HUSAR [180], the online portal of Primer3 [181] or the online database qPrimerDepot (http://mouseprimerdepot.nci.nih.gov/, [182]). To exclude amplification of unspecific products, custom-made primer pairs were subjected to melting curve analysis using the ABI PRISM 7000 Sequence Detection System. Random hexanucleotides for reverse transcription reactions were ordered from Roche Diagnostics (Mannheim, Germany). Oligonucleotides for mouse genotyping are summarized in **Table 2**. Pre- and self-designed oligonucleotides for real-time qPCR are listed in **Tables 3A** and **3B**, respectively.

Table 2. Oligonucleotides used for mouse genotyping by PCR.

allele	assay design	primer sequence	amplicon sizes [bp]
Ccr1 wildtype	HUSAR	forward: 5'-GAGTTCACTCACCGTACCTGTAGC-3' reverse: 5'-TGACCTTCTTCTCACTGGGTCTTC-3'	180
Ccr1 knock-out	HUSAR	forward: 5'-GCTGTCTCTGATCTGGTCTTCCTT-3' reverse: 5'-TGGGTGGAGAGGCTTTTTGCTTCCTCTTGC-3'	155
Ccr5 wildtype	HUSAR	forward: 5'-CGCTTCTTGCTGTCTATGGATG-3' reverse: 5'-CGGTGTGGTAGGATTTAGGTCTG-3'	277
Ccr5 knock-out	HUSAR	forward: 5'-TGGATTTTCAAGGGTCAGTTCC-3' reverse: 5'-TGTGCTGCAAGGCGATTAAG-3'	223

Table 3A. Oligonucleotides used for real-time quantitative RT-PCR.

gene	oligonucleotide supplier	assay type	assay order number
18S	Applied Biosystems (ABI)	pre-designed	4310893E (eukaryotic 18S rRNA, VIC-labeled probe)
Arg1	Applied Biosystems (ABI)	pre-designed	Mm00475988_m1 (FAM-labeled probe)
Ccl2	Applied Biosystems (ABI)	pre-designed	Mm00441242_m1 (FAM-labeled probe)
Ccl3	Applied Biosystems (ABI)	pre-designed	Mm00441258_m1 (FAM-labeled probe)
Ccl4	Applied Biosystems (ABI)	pre-designed	Mm00443111_m1 (FAM-labeled probe)
Ccl5	Applied Biosystems (ABI)	pre-designed	Mm01302428_m1 (FAM-labeled probe)
Ccl20	Applied Biosystems (ABI)	pre-designed	Mm00444228_m1 (FAM-labeled probe)
Ccr2	Applied Biosystems (ABI)	pre-designed	Mm00445551_m1 (FAM-labeled probe)
Ccr4	Applied Biosystems (ABI)	pre-designed	Mm00438271_m1 (FAM-labeled probe)
Ccr6	Applied Biosystems (ABI)	pre-designed	Mm01700299_m1 (FAM-labeled probe)
Chi3l3	Applied Biosystems (ABI)	pre-designed	Mm00657889_mH (FAM-labeled probe)
Cxcl10	Applied Biosystems (ABI)	pre-designed	Mm00445235_m1 (FAM-labeled probe)
Fcer2a	Applied Biosystems (ABI)	pre-designed	Mm00442792_m1 (FAM-labeled probe)
Foxp3	Applied Biosystems (ABI)	pre-designed	Mm00475156_m1 (FAM-labeled probe)
Gata3	Applied Biosystems (ABI)	pre-designed	Mm00484683_m1 (FAM-labeled probe)
Ifng	Applied Biosystems (ABI)	pre-designed	Mm00801778_m1 (FAM-labeled probe)
Il4	Applied Biosystems (ABI)	pre-designed	Mm00445259_m1 (FAM-labeled probe)
Il6	Applied Biosystems (ABI)	pre-designed	Mm00446190_m1 (FAM-labeled probe)
Il10	Applied Biosystems (ABI)	pre-designed	Mm00439616_m1 (FAM-labeled probe)
Il12a	Applied Biosystems (ABI)	pre-designed	Mm00434165_m1 (FAM-labeled probe)
Il13	Applied Biosystems (ABI)	pre-designed	Mm00434204_m1 (FAM-labeled probe)
Il17a	Applied Biosystems (ABI)	pre-designed	Mm00439619_m1 (FAM-labeled probe)
Mmp12	Applied Biosystems (ABI)	pre-designed	Mm00500554_m1 (FAM-labeled probe)
Mrc1	Applied Biosystems (ABI)	pre-designed	Mm00485148_m1 (FAM-labeled probe)
Nos2	Applied Biosystems (ABI)	pre-designed	Mm00440485_m1 (FAM-labeled probe)
Retnla	Applied Biosystems (ABI)	pre-designed	Mm00445109_m1 (FAM-labeled probe)
Rorc	Applied Biosystems (ABI)	pre-designed	Mm00441139_m1 (FAM-labeled probe)
Stat6	Applied Biosystems (ABI)	pre-designed	Mm01160477_m1 (FAM-labeled probe)
Tbx21	Applied Biosystems (ABI)	pre-designed	Mm00450960_m1 (FAM-labeled probe)
Tnf	Applied Biosystems (ABI)	pre-designed	Mm00443258_m1 (FAM-labeled probe)
gene	**oligonucleotide supplier**	**assay design**	**primer and probe (FAM-labeled) sequences**
Ccr7	Applied Biosystems (ABI)	HUSAR	FP: 5'-TCCTTGTCATTTTCCAGGTGTG-3' RP: 5'-CGTGGTATTCTCGCCGATGTA-3' probe: 5-'TTCTGCCAAGATGAGGTCACCGATGA-3'
Il2	Applied Biosystems (ABI)	HUSAR	FP: 5'-GTTGTAAAACTAAAGGGCTCTGACAA-3' RP: 5'-TGTTGAGATGATGCTTTGACAGAAG-3' probe: 5-'TGAGTGCCAATTCGATGATGAGTCAGC-3'
Tfgb1	Applied Biosystems (ABI)	HUSAR	FP: 5'-CACAGTACAGCAAGGTCCTTGC-3' RP: 5'-AGTAGACGATGGGCAGTGGCT-3' probe: 5-'CGCTTCGGCGTCACCGTGCT-3'

Table 3B. Oligonucleotides used for real-time quantitative RT-PCR.

gene	assay design	forward primer sequence	reverse primer sequence
18S rRNA	Primer3	5'-GCAATTATTCCCCATGAACG-3'	5'-AGGGCCTCACTAAACCATCC-3'
Arg1	Primer depot	5'-AGAGATTATCGGAGCGCCTT-3'	5'-TTTTTCCAGCAGACCAGCTT-3'
Ccl3	Primer depot	5'-ACCATGACACTCTGCAACCA-3'	5'-GTGGAATCTTCCGGCTGTAG-3'
Ccl4	Primer depot	5'-CATGAAGCTCTGCGTGTCTG-3'	5'-GAAACAGCAGGAAGTGGGAG-3'
Ccl5	Primer depot	5'-GTGCCCACGTCAAGGAGTAT-3'	5'-CCACTTCTTCTCTGGGTTGG-3'
Ccl20	Primer depot	5'-CTTGCTTTGGCATGGGTACT-3'	5'-TGTACGAGAGGCAACAGTCG-3'
Ccr6	Primer depot	5'-GGAGCCTGGATAACCACTGA-3'	5'-TTGAATGGCAGACACTCACAG-3'
Cd68	Primer depot	5'-ATCCCCACCTGTCTCTCTCA-3'	5'-ACCGCCATGTAGTCCAGGTA-3'
Chi3l3	Primer depot	5'-TCTGGGTACAAGATCCCTGAA-3'	5'-TTTCTCCAGTGTAGCCATCCTT-3'
Csf1	Primer3	5'-AAGGTCCTGCAGCAGTTGAT-3'	5'-CATCCAGCTGTTCCTGGTCTA-3'
Csf1r	Primer depot	5'-CTCTGCTGGTGCTACTGCTG-3'	5'-TTGCCTTCGTATCTCTCGATG-3'
Emr1	Primer depot	5'-GGATGTACAGATGGGGGATG-3'	5'-CATAAGCTGGGCAAGTGGTA-3'
Fcer2a	Primer3	5'-ATCCCTGGGCTTGAATGAG-3'	5'-TGCAGTTCCCTTTGAAATCAG-3'
Gata3	Primer depot	5'-GCCTGCGGACTCTACCATAA-3'	5'-AGGATGTCCCTGCTCTCCTT-3'
Ifng	Primer depot	5'-ACAGCAAGGCGAAAAAGGAT-3'	5'-TGAGCTCATTGAATGCTTGG-3'
Il4	Primer depot	5'-TGAACGAGGTCACAGGAGAA-3'	5'-CGAGCTCACTCTCTGTGGTG-3'
Il4ra	Primer3	5'-TGGATCTGGGAGCATCAAG-3'	5'-GGGATGCATGTGAGGTTTTC-3'
Il10	Primer depot	5'-ATCGATTTCTCCCCTGTGAA-3'	5'-TGTCAAATTCATTCATGGCCT-3'
Il12a	Primer3	5'-CTATGGTCAGCGTTCCAACA-3'	5'-GGCCAAAAAGAGGAGGTAGC-3'
Itgam	Primer depot	5'-ATTCGGTGATCCCTTGGATT-3'	5'-GTTTGTTGAAGGCATTTCCC-3'
Itgax	Primer3	5'-GAGAAGACCAGTGTGGTCGAA-3'	5'-ATTGGGTGAGTGGGTTCTGA-3'
Lamp1	Primer depot	5'-GTGGCAACTTCAGCAAGGA-3'	5'-GATACAGTGGGGTTTGTGGG-3'
Marco	Primer depot	5'-GAAGACTTCTTGGGCAGCAC-3'	5'-CCATTTCTCTTCTTGGGCAC-3'
Mmp12	Primer3	5'-GCACATTTTGATGAGGCAGA-3'	5'-TGAACAGCAACAAGGAAGAGG-3'
Mrc1	Primer3	5'-ATATATAAACAAGAATGGTGGGCAGT-3'	5'-TCCATCCAAATGAATTTCTTATCC-3'
Mrc2	Primer3	5'-GCAAAACCTGCAGAAGCTGT-3'	5'-ACCATCTGTCCACCTGAAGC-3'
Ms4a2	Primer3	5'-AATCCTCCAGTGCACCTGAC-3'	5'-TTTGTGTTGCTCCCAGGAA-3'
Msr1	Primer3	5'-TGACAAAAGAGATGACAGAGAATCA-3'	5'-TAGTGCTGTGAGGAAGGGATG-3'
Msr2	Primer3	5'-GCTCCTATTCCTGTAAGGCAGAT-3'	5'-TGGAAACAGCTCTTGGACATT-3'
Nos2	Primer depot	5'-TGAAGAAAACCCCTTGTGCT-3'	5'-TTCTGTGCTGTCCCAGTGAG-3'
Retnla	Primer depot	5'-CCCTTCTCATCTGCATCTCC-3'	5'-CTGGATTGGCAAGAAGTTCC-3'
Siglec1	Primer3	5'-AGCAACCGCTGGTTAGATGT-3'	5'-AGTTCCTCTCCATGCCTTCA-3'
Stat6	Primer3	5'-AACTCAGCTCAGATATGGGGTATC-3'	5'-CAGGTGAGGCTCCTGAAAAG-3'
Tnf	Primer depot	5'-CCACCACGCTCTTCTGTCTAC-3'	5'-AGGGTCTGGGCCATAGAACT-3'

2.8 Buffers and solutions

Unless noted otherwise in the text, all buffers and solutions were prepared using ultrapure water generated by a Millipore water purification system.

Acid mix for arginase enzyme assays	70 ml H_2O, 30 ml H_3PO_4 (85%) and 10 ml H_2SO_4 (96%) were mixed (7/3/1, v/v/v) and used immediately.
Brewer's thioglycollate solution, 4%	4.0 g Brewer's thioglycollate were dissolved in 100 ml H_2O and autoclaved.
BSA stock solution, 10 mg/ml	100 mg BSA (Fraction V) were dissolved in 10 ml protein lysis buffer and used immediately for arginase enzyme activity assays.
DEPC-H_2O	1.0 ml DEPC was added to 1.0 l of H_2O, stirred over night and autoclaved.
EDTA, 0.5 M, pH7.5, 100 ml	18.61 g EDTA-Na_2 (Triplex III) were dissolved in H_2O, pH was adjusted to 7.5 using sodium hydroxide pellets (~4 g) and volume was adjusted to 100 ml using H_2O. EDTA solution was autoclaved before use.
(α)-Isonitrosopropiofenon, 6%	600 mg α-ISPF were dissolved in 10 ml 100% EtOH and used immediately.
L-arginine, 0.5 M, pH 9.7, 50 ml	4.36 g L-arginine were dissolved in 40 ml H_2O, adjusted to pH 9.7 using 6 N HCl and filled up to 50 ml using H_2O.
$MnCl_2$, 1 M, 10 ml	1.26 g $MnCl_2$ were dissolved in 10 ml H_2O and autoclaved.
$MnCl_2$ solution, 10 mM, 100 ml	1 ml 1 M $MnCl_2$ was added to 99 ml 50 mM Tris-HCl (pH 7.5) and autoclaved.
MOPS buffer pH 7.0, 10x	200 mM MOPS, 50 mM sodium acetate, 10 mM EDTA in H_2O. pH was adjusted to 7.0 using 1 M sodium hydroxide. MOPS buffer was protected from light and stored at RT.
$NaNO_2$ stock solution, 25 µg/ml	125 mg $NaNO_2$ were dissolved in 5.0 ml medium, diluted 1:1000 in medium and used immediately for nitrite determination.

PBND buffer, 1x	50 mM KCl, 10 mM Tris-HCl pH 8.3, 2.5 mM MgCl2, 0.1 mg/ml gelatin, 0.45% (v/v) Nonidet P40, 0.45% (v/v) Tween 20, mixed in H_2O and sterilized by filtration.
Protease inhibitor cocktail, 25x	1 tablet (Roche Complete without EDTA) was dissolved in 2 ml D-PBS and stored in 200 µl aliquots at -20°C.
Protein lysis buffer	50 mM Tris-HCl pH 7.5, 0.5% Triton X-100, 40 µl/ml 25x protease inhibitor cocktail (Roche Complete without EDTA) were added just before use.
Proteinase K solution	20 mg/ml Proteinase K (lyophilized powder; Merck, Darmstadt, Germany) dissolved in millipore H_2O.
RNA isolation lysis buffer	Lysis buffer from respective RNA isolation kit containing 10 µl of 2-ME per milliliter.
RNA loading buffer	5 ml contain: 2950 µl Formamide 1180 µl Formaldehyde (≥37%) 855.5 µl 10x MOPS pH 7.0 29.5 µl Ethidium bromide (10mg/ml) RNA loading buffer was stored in 1 ml aliquots at -20°C.
Staining buffer for flow cytometry	2% heat-inactivated FCS in D-PBS.
SYBRgreen buffer for TaqMan, 2x	5 ml contain: 1000 µl 10x Taq Buffer (w/o deterg.) 75 µl 25 mM dNTPs 200 µl Rox reference dye (25x) 2000 µl PCR optimizer (2.5x) 100 µl BSA, PCR grade (50x) 20 µl SYBRgreen I (250x) 1200 µl 25 mM $MgCl_2$ 405 µl Aqua ad injectabilia SYBRgreen buffer was stored in 1.20 ml aliquots at 4°C.
TAC erythrocyte lysis buffer, 1x	TAC buffer was freshly prepared before use by mixing 90% solution A and 10% solution B. Solution A (170 mM NH_4Cl in H_2O) and B (240 mM Tris-HCl pH 7.5 in H_2O) were filter-sterilized and stored at 4°C until use.
TBE buffer, 10x	25 mM EDTA-Na_2 (Titriplex III), 900 mM Tris base and 889 mM boric acid were dissolved in H_2O.

TE buffer, 1x	10 mM Tris-HCl pH7.5, 1 mM EDTA, in H_2O, autoclaved.
Tris-HCl, 50 mM, pH 7.5, 500 ml	3,03 g Tris was dissolved in ~400 ml H_2O, adjusted to pH 7.5 using 6 N HCl, filled up to 500 ml with H_2O and autoclaved.
Urea stock solution, 1 mg/ml	1.0 g urea was dissolved in 10 ml 50 mM Tris-HCl pH7.5, diluted 1:100 in 50 mM Tris-HCl pH7.5 and used immediately for arginase enzyme activity assays.

2.9 Cell culture reagents and media

Cell culture reagents

2-Mercapthoethanol, 50 mM (1000x)	Invitrogen, Karlsruhe, Germany
Amino acid solution, 50x, liquid	Invitrogen, Karlsruhe, Germany
DMEM+Glutamax I, 4.5 g/l Glc	Invitrogen, Karlsruhe, Germany
D-PBS, Dulbecco's PBS without Ca/Mg (1x)	PAN Biotech GmbH, Aidenbach, Germany
Fetal calf serum (FCS): FBS superior	Biochrom, Berlin, Germany
FCS (heat-inactivated)	FCS was heat-inactivated before use by incubation at 56°C in a water bath for 30 minutes.
Harvest medium	RPMI1640 with Glutamax I, 10% heat-inactivated FCS, 1% PenStrep
Hank's balanced salt solution (HBSS)	Sigma-Aldrich, Schnelldorf, Germany
Non-essential amino acids, 100x, liquid	Invitrogen, Karlsruhe, Germany
Penicillin/Streptomycin 10 ku/ml Penicillin, 10 mg/ml Streptomycin	PAA Laboratories, Vienna, Austria
RPMI1640+Glutamax I	Invitrogen, Karlsruhe, Germany
Trypan blue, 0.4%	Sigma-Aldrich, Schnelldorf, Germany
Trypsin-EDTA, 1x 0.5 g/l Trypsin, 0.22 g/l EDTA in D-PBS.	PAA Laboratories, Pasching, Austria

Cell culture media

PM medium

Composition: RPMI1640+Glutamax I, 10% heat-inactivated FCS and 1% Penicillin/Streptomycin
Application: Cultivation of peritoneal macrophages

HS medium

Composition: DMEM+Glutamax I (4.5 g/l Glc), 10% heat-inactivated FCS and 1% Penicillin/Streptomycin
Application: Harvesting of splenocytes

SSB medium

Composition: DMEM+Glutamax I (4.5 g/l Glc), 10% heat-inactivated FCS, 1% Penicillin/Streptomycin, 1x non-essential amino acid solution, 1x amino acid solution and 50 µM 2-ME
Application: Stimulation of splenocytes and BMDM

BBM medium

Composition: DMEM+Glutamax I (4.5 g/l Glc), 10% heat-inactivated FCS, 1% Penicillin/Streptomycin and 50 µM 2-ME
Application: Harvesting of bone marrow cells
Removal of stromal cells and mature macrophages from bone marrow cells
Differentiation of bone marrow cells in Petri dishes (= BBM medium + 20 ng/ml murine recombinant M-CSF)
Stimulation of BMDM

DBM medium

Composition: DMEM+Glutamax I (4.5 g/l Glc), 15% L929s-conditioned medium, 10% heat-inactivated FCS, 5% heat-inactivated horse serum, 1% Penicillin/Streptomycin and 50 µM 2-ME
Application: Differentiation of bone marrow cells in Teflon bags

L929 medium

Composition: DMEM+Glutamax I (4.5 g/l Glc), 10% heat-inactivated FCS, 1% Penicillin/Streptomycin
Application: Cultivation of L929 cells

CC medium

Composition: DMEM+Glutamax I (4.5 g/l Glc)/50% heat-inactivated FCS/10% DMSO
Application: Cryoconservation medium for BMDM

2.10 Consumables

6 well plates for bacteriology	Greiner Bio-One, Frickenhausen, Germany
6 well plates for tissue culture	Corning Costar, Lowell, Massachusetts, USA
10 cm plastic dish for bacteriology	Greiner Bio-One, Frickenhausen, Germany
10 cm plastic dish for tissue culture	TPP, Trasadingen, Switzerland
12 well plates for tissue culture	Corning Costar, Lowell, Massachusetts, USA
15 cm plastic dish for tissue culture	TPP, Trasadingen, Switzerland
Cell strainer, 100 µm	BD Biosciences, Heidelberg, Germany
Centrifugation tubes, 15 ml, polyprop.	BD Falcon, Heidelberg, Germany
Centrifugation tubes, 50 ml, polyprop.	BD Falcon, Heidelberg, Germany
Cryovials, 2.0 ml, free standing	Alpha Laboratories, Eastleigh, UK
FACS tubes, round bottom, 5 ml	BD Biosciences, Heidelberg, Germany
Forceps, sterile and disposable	Seidel Medizin, Gauting-Buchendorf, Germany
Gauge needle, 20Gx1½″, BD Microlance 3	BD Biosciences, Heidelberg, Germany
Gauge needle, 26Gx½″, BD Microlance 3	BD Biosciences, Heidelberg, Germany
lumox™ film fluorocarbon foil, 25 µm	In Vitro Systems & Services, Göttingen, Germany
MagNA Lyser Green Bead tubes	Roche Diagnostics, Mannheim, Germany
Microscope slides, SuperFrost, grinded	Menzel, Braunschweig, Germany
Microtiter plates, 96 well, flat bottom	Greiner Bio-One, Frickenhausen, Germany
Paper pad cards for cytospin	Shandon Inc., Pittsburgh, Pennsylvania, USA
PCR tubes, 0.5 ml, DNase/RNase-free	Trefflab, Degersheim, Switzerland
Reaction tubes, PCR clean, 1.5 ml	Eppendorf AG, Hamburg, Germany
Scalpels, sterile and disposable, No. 11	Feather, Osaka, Japan
Scalpels, sterile and disposable, No. 20	Feather, Osaka, Japan
Sterile filter, PES, 0.22 µm, 250 ml	TPP, Trasadingen, Switzerland

Syringes, BD Plastipak, 1 ml	BD Biosciences, Heidelberg, Germany
Syringes, BD Discardit II, 10 ml	BD Biosciences, Heidelberg, Germany
Syringe filter, 0.45 µm pore size	Nalgene, Roskilde, Denmark
TissueTek	Leica Microsystems, Nussloch, Germany

2.11 Kits

ABC detection system	Vector Laboratories, Burlingame, USA
BD Fix & Perm kit	BD Biosciences, Heidelberg, Germany
DC protein assay, detergent compatible	Bio-Rad, München, Germany
DiffQuick staining kit	Dade Behring, Marburg, Germany
PureLink RNA Mini Kit	Invitrogen, Karlsruhe, Germany
RNase-free DNase set	Qiagen, Hilden, Germany
RNeasy Mini Kit	Qiagen, Hilden, Germany
RiboGreen (20x)	Invitrogen, Karlsruhe, Germany
Superscript I kit	Invitrogen, Karlsruhe, Germany
Superscript II kit	Invitrogen, Karlsruhe, Germany

2.12 Devices

ABI Prism 7000 Sequence Detection System	Applied Biosystems, Weiterstadt, Germany
ABI Prism 7700 Sequence Detection System	Applied Biosystems, Weiterstadt, Germany
Bag sealer Polystar 100 GE and tongs 30D	Rische & Herfurth, Hamburg, Germany
Camera for Leica DMIL, Jenoptic ProgRes CF	Jenoptic, Jena, Germany
Camera for Leica DMRBE, DC300F	Leica Microsystems, Nussloch, Germany
Centrifuge, bench top, Rotanta 460R	Hettich, Tuttlingen, Germany
Centrifuge, bench top, Universal 16	Hettich, Tuttlingen, Germany

Centrifuge, refrigerated, model 5417R	Eppendorf, Hamburg, Germany
Centrifuge, Cytospin	Shandon Southern, Runcorn, UK
CO_2 incubator	Heraeus, Hanau, Germany
Cryo freezing container	Nalgene, Roskilde, Denmark
FACSCalibur flow cytometer	BD Biosciences, Heidelberg, Germany
Electrophoresis chamber	MBT Brand, Gießen, Germany
Hemocytometer, Neubauer improved, 0.1mm	Marienfeld, Lauda-Königshofen, Germany
Hitachi 9-17E autoanalyzer	Hitachi, Frankfurt, Germany
Hot air oven	Heraeus, Hanau, Germany
Image documentation system CS1	Cybertech, Berlin, Germany
Image capture computer ICC/4	Cybertech, Berlin, Germany
MagNA Lyser	Roche Diagnostics, Mannheim, Germany
Microplate reader, GENios plus	TECAN, Crailsheim, Germany
Microscope, Leica DMIL	Leica Microsystems, Nussloch, Germany
Microscope, Leica DMRBE	Leica Microsystems, Nussloch, Germany
Power supply, PowerPack 300	Bio-Rad, München, Germany
Pipettes, Pipetman 2/20/200/1000 µl	Gilson, Middleton, Wisconsin, USA
Pipettor, accu-jet pro	Brand, Wertheim, Germany
Qubit fluorometer	Invitrogen, Karlsruhe, Germany
Spectrophotometer UV/Vis, DU 530	Beckman Coulter, Fullerton, California, USA
Thermocycler, RoboCycler Gradient 96	Stratagene, La Jolla, California, USA
Thermo mixer, Thermomixer comfort	Eppendorf, Hamburg, Germany
Thermo mixer, Thermomixer 5436	Eppendorf, Hamburg, Germany
UV transilluminator, (254 nm)	Bachofer, Reutlingen, Germany
Vortex mixer, Vortex-Genie 2	Scientific Industries, New York, USA

2.13 Software

CellQuest 3.3 for Mac	BD Biosciences, Heidelberg, Germany
Endnote X for Mac	Thomson Reuters, Carlsbad, California, USA
FlowJo 6.4.7 for Mac	Tree Star, Ashland, Oregon, USA
HUSAR software package (version 5)	Genetics computer group, University of Wisconsin, Madison, USA [180, 181]
Illustrator 10.0.3 for Mac	Adobe, Dublin, Ireland
Office 2004 for Mac	Microsoft, Redmond, Washington, USA
Photoshop 7.0 for Mac	Adobe, Dublin, Ireland
Primer3	Steve Rozen, Helen Skaletsky, Whitehead Institute for Biomedical Research, Cambridge, USA [181]
Prism 4.0c for Mac	GraphPad, La Jolla, California, USA

2.14 Mouse genotyping

1-2 mm of sample material were cut off the end of a mouse tail using sterile surgical scissors and placed in 1.5 ml reaction tubes on ice. To each sample 200 µl of PBND buffer containing 1 µl Proteinase K solution (20 mg/ml) were added and incubated in a thermo mixer for 4 h at 56°C and 1000 rpm to degrade tissue material. Afterwards, indigestible material was pelleted by centrifugation at 20,000xg for 1 minute and 150 µl of the supernatant were transferred to new 1.5 ml reaction tubes and stored at -20°C until analysis. 1 µl of the obtained lysates was used in PCR reactions. The PCR reaction mix was prepared on ice and contained:

2.50 µl	10x PCR buffer (ThermoPol)
4.00 µl	1.25 mM dNTPs
1.00 µl	10 pmol/µl forward primer
1.00 µl	10 pmol/µl reverse primer
1.00 µl	tail DNA lysate
0.20 µl	5 u/µl AmpliTaq polymerase
15.30 µl	H_2O (Aqua ad injectabilia)
25.00 µl	

For multiplex reactions (up to 4 primer pairs) the amount of H_2O added was adjusted accordingly. PCR reactions were carried out in a RoboCycler using the following program for the detection of Ccr1 and Ccr5 wildtype and knock-out alleles:

1 cycle	3 minutes at 94°C
30 cycles	30 seconds at 94°C, 30 seconds at 60°C and 30 seconds at 72°C
1 cycle	5 minutes at 72°C

10 µl of the PCR reaction were separated on 2 % agarose gels prepared with 0.5x TBE. The running buffer and the gel contained ethidium bromide at a concentration of 0.1 µg/ml. Expected amplicon sizes are listed in **Table 2** (see Materials section 2.7).

2.15 Orthotopic kidney transplantation (DKFZ)

Wildtype, $Ccr1^{-/-}$, $Ccr5^{-/-}$ and $Ccr1^{-/-}/Ccr5^{-/-}$ C57BL/6 (H-2^b) mice were used as recipients of fully MHC-mismatched BALB/c (H-2^d) renal allografts (n≥10 per group). For isograft controls C57BL/6 donor kidneys were transplanted into C57BL/6 recipient mice (n=5). Orthotopic kidney transplantation was performed as described elsewhere [183]. Briefly, the left kidney attached to a segment of the aorta and the renal vein along with the ureter was removed from the donor animal *en bloc*. The donor aorta and inferior vena cava were then anastomosed end to side to the recipient abdominal aorta and inferior vena cava below the level of the native renal vessels, respectively. The native left kidney was removed before revascularization. Donor and recipient ureter were anastomosed end to end at the border of the renal pelvis. The native right kidney was immediately removed after grafting. The animals did not receive any immunosuppressive therapy throughout the experiment. Grafts were explanted and further processed either on post-transplantation day 7 or on day 42. For histology, graft samples were fixed in buffered 4% formaldehyde or zinc fixative and embedded in paraffin. For immunohistochemistry the samples were embedded in TissueTek and for RNA analysis the samples were snap-frozen in liquid nitrogen.

2.16 Determination of blood urea nitrogen and creatinine (DKFZ)

Blood was obtained either 7 or 42 days after transplantation from the heart of anesthetized mice using heparinized glass capillaries. After centrifugation plasma was collected and stored at -20°C. Blood urea nitrogen (BUN) and plasma creatinine levels were measured using a Hitachi 9-17 E autoanalyzer.

2.17 Histopathology and lesion scores (DKFZ)

Light microscopy was performed on 3 µm sections stained by PAS. A person trained in nephropathology performed the histopathologic analysis in a blinded manner. Histopathologic inspection of sections from allo- and isografts included counting of mononuclear infiltrates and assessment of graft injury in three compartments of renal grafts: endothelia covering the inner surface of blood vessels as well as the glomerular and the tubulointerstitial compartment. While scores for vascular rejection, tubulointerstitial inflammation and acute glomerular damage are a composition of scored infiltration by mononuclear cells and tissue damage, the scores for tubulointerstitial damage and transplant glomerulopathy do not include infiltration by mononuclear cells (see below for details). Different lesion scores were calculated as described in the following ([184, 185] and personal communication with Dr. Eva Kiss, nephropathologist, DKFZ Heidelberg).

Acute and chronic vascular rejection score

The vascular rejection was evaluated in whole kidney sections including cortex and outer stripe of outer medulla. Acute vascular rejection was assessed as no injury (0), sticking of the mononuclear cells to the endothelium (0.5), subendothelial location of the mononuclear cells (1), inflammation of the media, including transmural infiltration (2), fibrinoid necrosis of the vessel wall and/or thrombosis of the vessel in addition to the inflammatory reaction (3).

Chronic vascular rejection was evaluated as negative (-) or positive (+), determined as narrowing of the luminal area by fibrointimal thickening with or without presence of foam cells and expressed as the percentage of (+) vessels. The vascular rejection index was defined as the percentage of vessels with respective degree of the rejection encountered in a whole kidney section. The vascular rejection score was calculated as the sum of all specific vascular rejection indices, whereby the index of vessels with degree 0.5 was multiplied by 0.5, that of degree 1 by 1, that of degree 2, by 2, that of degree 3 by 3.

Acute tubulointerstitial damage score

Acute tubulointerstitial damage was evaluated as nonexistent (0), as thinning of the brush border with or without interstitial edema (0.5), thinning of the tubular epithelia with or without interstitial edema (1), denudation of the tubular basement membrane with or without interstitial edema (2), and tubular necrosis with or without interstitial edema (3). Tubulointerstitial damage was judged in 20 high-power fields of cortex (objective 40x), and the tubulointerstitial damage score was calculated in the same way as described for the vascular rejection score.

Chronic tubulointerstitial damage score

Chronic tubulointerstitial damage was defined as broadening of the basement membrane of the tubuli with flattened epithelium, tubular atrophy, and interstitial matrix increase. It was evaluated as 0.5, focal chronic damage and 1, diffuse chronic damage. Tubulointerstitial damage was judged in 20 high-power fields of cortex (objective x40), and the tubulointerstitial damage score was calculated as described for the transplant glomerulopathy score.

Tubulointerstitial inflammation score

The interstitial inflammation score was described by degree: no mononuclear cells in the interstitium or tubuli (0), focal mononuclear cell infiltration in the interstitium (0.5), focal mononuclear infiltration in the interstitium with tubulitis (1), diffuse mononuclear infiltration of the interstitium (2), and diffuse mononuclear infiltration in the interstitium with tubulitis (3). Tubulitis was defined as one or more mononuclear cells per tubular cross-section. The tubulointerstitial inflammation was judged in 10 fields (objective 20x) of cortex; the total tubulointerstitial inflammation score was calculated as described for the total vascular rejection score.

Acute glomerular damage score

Acute glomerular damage was described as no injury (0), sticking of mononuclear cells to the capillary endothelium in less than 50% of the convolute (0.5), sticking of the mononuclear cells to the capillary endothelium in more than 50% of the convolute (1), mesangiolysis with or without sticking of the mononuclear cells (2), aneurysm, thrombosis, or necrosis of the capillary loops (3). The acute glomerular damage score was calculated as described for the total vascular rejection score.

Transplant glomerulopathy score (=glomerulosclerosis score)

Transplant glomerulopathy was defined as 0, no sclerosis; 0.5, sclerosis of less than 25% of capillary loops; 1, sclerosis of 26 to 50% of the capillary loops; 2, sclerosis of 51 to 75% of the capillary loops; 3, sclerosis of more than 75% of the capillary loops. The transplant glomerulopathy score was calculated as the sum of all specific injury indices, whereby the index of glomeruli with degree 0.5 was multiplied by 0.5, that of degree 1 x 1, that of degree 2 x 2, that of degree 3 x 3.

2.18 Immunohistochemistry (DKFZ)

Immunohistochemical staining was performed on 5 µm sections of frozen- or zinc-fixed tissue. Antibodies and antibody concentrations used are listed in the Materials chapter (see 2.5, Table 1). The rabbit polyclonal antiserum against murine Chi3l3 peptides [186] was kindly provided by Dr. Kimura (NCI, Bethesda, MD). An ABC detection system was applied for visualization. Controls, omitting the first antibody or replacing the first antibody by a nonimmune IgG, were negative for each section tested. The number of cells staining positive for the above markers were counted for all glomeruli and in 10 high power fields (HPF, 40x) of the tubulointerstitium.

2.19 Isolation and purification of total RNA

RNA extraction from different sources

For the preparation of total RNA from tissues (spleen or renal allografts) snap frozen organs or parts thereof were transferred into prechilled 2 ml screw tubes filled with 1.4 mm ceramic beads (MagNA Lyser, Green Bead tubes, Roche) and 1 ml of lysis buffer containing 2-ME. Tubes were loaded into the rotor of a MagNA Lyser instrument (Roche) and tissue was disrupted by two runs at 6500 rpm for 1 minute separated by 2 minutes on ice. Lysates were transferred into new tubes and the volume was increased by the addition of lysis buffer (*e.g.* for RNA extraction from a complete spleen or renal allograft, volume was adjusted to 4 ml lysate). Lysates were stored at -20°C and cleared by centrifugation at 4300rpm and 4°C for 10 minutes before RNA purification.

Lysates from in vitro cultured cells (*e.g.* bone marrow-derived and peritoneal macrophages) were prepared by completely removing supernatant and adding an appropriate amount of lysis buffer containing 2-ME to the cell culture vessel (*e.g.* $1.5x10^6$ BMDM were lysed in 1.0 ml of lysis buffer per well of a 6 well plate). After incubation for 2-3 minutes at RT lysates were mixed by pipetting, transferred into prechilled tubes and stored at -20°C until RNA extraction.

For the generation of lysates from splenocytes growing adherently and in suspension the suspension cells were centrifuged (500xg, 4°C, 5 minutes) and during this time, adherent cells were lysed by adding 1.0 ml lysis buffer containing 2-ME to each well of a 6 well plate, incubation for 2-3 minutes at RT and pipetting. This lysate was transferred into the tube containing the corresponding pellet of suspension cells and pelleted cells were disrupted by pipetting. Lysates prepared in this manner were stored at -20°C until RNA extraction.

Total RNA was extracted from lysates using commercial kits either from Qiagen (RNeasy Mini Kit) or Invitrogen (PureLink Mini RNA kit) according to manufacturer´s instructions. Briefly, lysates were loaded onto columns containing ion exchange material and washed once with buffer included in the respective kit. Contaminating genomic DNA was removed by on column-digestion with RNase-free DNase (Qiagen) for 20 minutes and RNA was eluted in 60-100 µl RNase-free H2O after several washing steps.

RNA quantification

Determination of RNA concentrations was done spectrophotometrically. RNA samples were appropriately diluted in RNase-free H_2O and absorbance was measured at 260 nm using a spectrophotometer (Beckman Coulter, model DU530). The RNA concentration was calculated by using the Beer-Lambert law and consideration of the dilution factor:

$A_{260} = \varepsilon \times C \times L$

A: absorbance at 260 nm

ε: extinction coefficient (for RNA: 0.025 $(mg/ml)^{-1}cm^{-1}$)

C: concentration of nucleic acid

L: path length of the spectrophotometer cuvette

Since an A_{260} of 0.1 corresponds to ~4 µg/ml RNA this method is often not practical for RNA samples with low concentrations. In such cases a fluorescent dye called RiboGreen (Invitrogen) was used in combination with the Qubit fluorometer (Invitrogen). Upon binding to nucleic acids

RiboGreen exhibits a large fluorescence enhancement and RiboGreen is relatively insensitive to contaminants of nucleic acid preparations (manufacturer's data). To determine the RNA concentration of a sample using the RiboGreen assay 10 µl of appropriately diluted RNA sample (1:200 – 1:2000 according to the expected yield) were added to 190 µl of working solution in RNase-free 0.5 ml PCR tubes. The working solution consisted of 5 µl RiboGreen (1x) and 185 µl 1x TE buffer. The sample was vortexed shortly and incubated for 5 minutes in the dark. The Qubit fluorometer was calibrated by using RNA standards with 0 and 10 ng/µl in high sensitivity (HS) mode. Samples were measured and the indicated RNA concentration (ng/ml) was multiplied with the total dilution factor and converted to µg/µl.

RNA quality control

Integrity of isolated RNA was verified by analytical agarose gel electrophoresis. A 1% agarose 1x MOPS gel was prepared and 0.5-1 µg of RNA sample (in a maximum volume of 10 µl) was added to 17 µl RNA loading buffer. After incubation at 65°C for 15 minutes to remove secondary structures the denatured RNA was chilled on ice and centrifuged. RNA samples were electrophoretically separated at 90 V for 30-45 minutes and RNA quality was assessed by visualization using an UV transilluminator and a digital camera system.

Optimal RNA quality is indicated if (1st) the upper 28S ribosomal RNA band is about double the intensitiy of the lower 18S ribosomal RNA band and only a weak or no smear is visible in each lane (signs of RNA degradation) and (2nd) if no further bands above the 28S ribosomal are visible that would indicate contamination with genomic DNA.

2.20 Reverse transcription of total RNA

Renal allograft RNA samples

To obtain cDNA from renal allograft RNAs the Superscript I kit from Invitrogen was used according to the manufacturer's instructions with the following modifications. The reaction mix for reverse transcription was prepared on ice and contained:

8.00 µl	5x first strand buffer
0.80 µl	25 mM dNTPs
2.00 µl	100 mM DTT
0.50 µl	15 µg/ml linear acrylamid
0.43 µl	1.56 µg/µl hexanucleotide mix
1.00 µl	40 u/µl RNasin
0.87 µl	200 u/µl Superscript I
13.60 µl	

2 µg of total RNA were added and the final volume was adjusted to 40 µl using DEPC-H_2O. RNA was reverse transcribed at 42°C for 60 minutes. The samples were centrifuged and stored at -20°C until analysis.

RNA Samples from spleen and in vitro cultured cells

During the course of this thesis, Superscript I became unavailable by the manufacturer. Therefore, Superscript II (Invitrogen) was used instead and the procedure of reverse transcription was altered in a way to obtain comparable results as with Superscript I. 1-2 µg of RNA were adjusted to a volume of 26.4 µl with DEPC-H_2O and RNA was incubated for 5 minutes at 65°C to remove secondary structures. The RNA samples were transferred to ice, spun down and 13.6 µl of reaction mix (as used for renal allograft RNA samples) containing Superscript II instead of Superscript I were added. The samples were vortexed for 2-3 seconds, centrifuged and put into a heating block set to 42°C for 90 minutes. Afterwards the samples were incubated

at 85°C for 5 minutes to inactivate the Superscript II enzyme. The samples were centrifuged and stored at -20°C until analysis.

2.21 Real-time RT-PCR

The mRNA expression levels of selected genes were quantified by real-time RT-PCR using an ABI Prism 7700 Sequence Detection System (Applied Biosystems). Pre-designed cDNA-specific TaqMan Gene Expression Assays (Applied Biosystems) were applied in combination with the TaqMan Universal PCR master mix (Applied Biosystems) according to manufacturer's instructions in a final volume of 20 µl. Thermal conditions were set according to the specifications of the manufacturer. Self-designed cDNA-specific primers were used in combination with a SYBRgreen buffer (see buffers and solutions). For this approach one reaction mix contained:

10.00 µl	2x SYBRgreen buffer for TaqMan
0.60 µl	10 pmol/µl forward primer
0.60 µl	10 pmol/µl reverse primer
0.12 µl	5 u/µl Taq polymerase
2.00 µl	cDNA sample
6.68 µl	H_2O (Aqua ad injectabilia)
20.00 µl	

Depending on the expression level of the target gene cDNA samples were used either undiluted or diluted 1:10 in TE buffer. The following thermal conditions were used for self-designed primers at the ABI Prism 7700 Sequence Detection System:

1 cycle	5 seconds at 50°C
1 cycle	5 minutes at 95°C
40x cycles	15 seconds at 95°C, 1 minute at 60°C

Usually, mRNA expression in each sample was determined in duplicates and expression of target genes was normalized to 18S ribosomal RNA using the comparative CT method in all

cases [187]. The resulting relative expression levels (REL) were multiplied by a factor of 10^5 to avoid very small numbers.

2.22 Determination of alloreactive antibody levels

Flow cytometry was used to determine alloreactive antibody levels in plasma samples from C57BL/6 wildtype (n=3) and $Ccr5^{-/-}$ mice (n= 3), which had been immunized on day -21 and -14 by i.p. injection of $4x10^7$ BALB/c splenocytes. In parallel, plasma samples from wildtype (n=5) and $Ccr5^{-/-}$ (n=3) renal allograft recipients 42d post transplantation were analyzed using a modification of published methods [113, 188]. Aliquots containing $4.5x10^5$ J558L BALB/c plasmacytoma cells ($H\text{-}2^d$) [189] in 150 µl HBSS were mixed with 150 µl HBSS diluted plasma samples from wildtype (1:4) or $Ccr5^{-/-}$ (1:4, 1:16, 1:64, 1:256) C57BL/6 recipients ($H\text{-}2^b$) and this mixture was incubated for 1 h on ice. After 3 washing steps with D-PBS/2% FCS, the cells were stained for 30 min on ice with a 1:20 dilution of a FITC-conjugated goat anti-mouse IgG and IgM specific antiserum (BD Biosciences) in 200 µl D-PBS/2% FCS. The cells were washed twice, fixed using Cytofix (BD Biosciences), and analyzed by flow cytometry using a FACSCalibur instrument (BD Biosciences). Plasma from naive C57BL/6 mice served as a control. For each sample the mean channel fluorescence was determined. Flow cytometry data were collected using CellQuest and analyzed using FlowJo software. Antibodies used in these experiments are listed in **Table 1** in the Materials section (see 2.4).

2.23 Preparation of protein lysates from cultured cells

Culture medium was removed completely and cells were washed once with D-PBS. Protein lysates for the determination of arginase enzyme activity were generated by adding 300 µl protein lysis buffer to each well of a 6 well plate containing $2x10^6$ cells and incubation for 30

minutes at 4°C on a horizontal shaker. Lysates were either directly quantified for protein content or snap frozen in liquid nitrogen and stored at -80°C.

2.24 Protein quantitation

Protein concentrations of cell lysates were determined using the detergent compatible (DC) protein assay (Bio-Rad) in a microplate scale according to the manufacturer's instructions.
25 µl of solution A' (consisting of 1 ml solution A plus 20 µl solution S) were prefilled in the wells of a 96 well microtiter plate. A standard curve was prepared in protein lysis buffer using triplicates of ten BSA standards in concentrations ranging from 0 to 2.0 µg/µl. 5 µl BSA standard or sample and 200 µl solution B were added per well and mixed by pipetting up and down. The plate was incubated at RT in the dark for 15 minutes and absorbance was determined at 690 nm using a microplate reader.

2.25 Determination of arginase enzyme activity

Arginase enzyme activity was determined as previously described with slight modifications [190-192]. Determination of arginase activity is based on the measurement of urea production rates. For each sample protein content was determined and duplicates of each sample were used to determine arginase enzyme activity. Arginase enzyme was activated by adding 20 µl 10 mM $MnCl_2$ solution to 100 µl protein sample (containing 3.0 µg protein in protein lysis buffer) and incubation for 8 minutes at 56°C. Afterwards 100 µl 0.5 M L-arginine (pH 9.7) were added and the sample was incubated at 37°C for 1h to allow conversion of L-arginine to urea and ornithine by arginase. During this time ten urea standards were prepared in duplicates at a concentration ranging from 0 to 10 mM urea. Urea production was stopped by adding 780 µl acid mix to protein samples and 900 µl acid mix were added to 100 µl of each urea standard. By addition of 40 µl 6% α-ISPF and two incubation steps (45 minutes at 95°C followed by 30

minutes at 4°C in the dark) a colorimetric reaction was induced that changed sample color from clear/transparent to pink-violet depending on the urea concentration. 200 µl of standard or sample were transferred into the wells of a 96 well microtiter plate and absorption was measured at 540 nm in a microplate reader. Arginase enzyme activity was calculated as nM urea per µg protein per hour (nM µg protein^{-1} h^{-1}).

2.26 Determination of NO production

Griess' reagent was used to determine nitrite concentrations in cell culture supernatants. Nine nitrite standards ranging from 0 to 6.4 ng/µl were prepared in duplicates from a fresh 25 µg/ml $NaNO_2$ stock solution in DMEM medium. The wells of a 96 well microtiter plate were prefilled with 100 µl of Griess' reagent and mixed with 100 µl nitrite standard or cell culture supernatant by pipetting up and down. After incubation for 10 minutes in the dark the absorbance was measured at 540 nm using a microplate reader. Nitrite production was calculated as nmol nitrite per mg protein per 48 h (nmol NO_2^- mg protein^{-1} 48h^{-1}).

2.27 Cytospin and differential leukocyte staining

For cytospins cell suspensions were prepared containing 2.0x10^5 cells/ml in a buffer consisting of 90% FCS and 10% D-PBS. 200 µl cell suspension was spun down onto clean, degreased microscope slides mounted with paper pad cards for 2 minutes at 500 rpm in a cytospin centrifuge and air dried. For differential staining the DiffQuick kit from DADE Behring was used. The samples were stained by dipping the slide 5x for 1 second into fixative solution, holding the slide 8 seconds into solution 1 and 3 seconds in solution 2. The slides were rinsed in distilled water and air dried before microscopic inspection.

2.28 Experimental peritonitis and cultivation of elicited peritoneal macrophages

Mice were injected i.p. with 2.5 ml of 4% Brewer's thioglycollate medium and euthanized by CO_2 asphyxiation at 1.5, 5.0 and/or 96h after injection. The abdomen was sterilized by wetting with 70% ethanol and a small midline incision was made with sterile scissors. The abdominal skin was carefully retracted leaving the abdominal wall intact. Avoiding perforation of intestines 10 ml ice cold harvest medium was injected using a syringe with 26G needle. The needle was retracted from the peritoneum and the slat with the pinned down mouse was put on a vortex mixer for 30 seconds to increase the amount of cells in suspension. To collect the harvest medium containing the detached cells a syringe with a 20G needle was inserted into the peritoneal cavity and the peritoneal fluid was carefully withdrawn. The cell suspension was transferred into 50 ml polypropylene centrifugation tubes on ice. Numbers of viable cells were determined using the dye exclusion method with trypan blue and a hemocytometer. The cells were pelleted by centrifugation at 250xg for 4 minutes and resuspended in PM medium at an appropriate concentration for the respective experiment. In some experiments harvested peritoneal lavage cells were lysed directly using 1 ml of RNA isolation lysis buffer for $4x10^6$ cells. Peritoneal lavage cells harvested after thioglycollate-induced peritonitis were cultivated in tissue culture 6 well plates at a density of $10x10^6$ per well in 3 ml PM medium. Cells were incubated at 37°C and 5% CO_2 in a humidified atmosphere for the times indicated in each experiment.

2.29 Preparation of splenocyte suspensions and cultivation of splenocytes

For the generation of single cell suspensions from spleens mice were euthanized by CO_2 asphyxiation and the spleen was explanted under aseptic conditions. The spleen was transferred into a 10 cm bacteriological plastic dish filled with 5 ml ice cold HS medium and was minced on ice using two disposable sterile forceps. The suspension was sieved through a 100

µm cell strainer into a 50 ml polypropylene tube and remaining material was forced through the strainer using the plunger of a syringe. The strainer was then rinsed with medium and the cells were centrifuged (10 minutes, 75xg, RT). Afterwards the splenocytes were resuspended in SSB medium, seeded in duplicates into the wells of a tissue culture 6 well plate at a concentration of $5x10^6$ cells per well and incubated at 37°C and 5% CO_2 in a humidified atmosphere (3 ml medium per well) for 24 h. In case of low RNA yields, RNA lysates were prepared by combining lysates from duplicate wells. Therefore, the supernatants of duplicate wells were combined and the suspension cells were pelleted (5 minutes, 250xg, RT). Adherent cells were lysed by adding 1 ml of RNA isolation lysis buffer to one of the duplicate wells and then transferring to the second well. This lysate was then combined with the pelleted suspension cells of both wells. In this way 1 ml RNA lysate was generated from the total splenocytes (adherent and non-adherent cells) of duplicate wells from one mouse. RNA isolation and reverse transcription was carried out as described above.

2.30 Preparation of splenocyte suspensions for FACS analysis

Single cell suspensions of splenocytes were prepared as described in 2.29 with the distinction that medium was replaced by staining buffer. After centrifugation (10 minutes, 75xg, RT) erythrocytes were lysed by resuspending the cell pellet in 5 ml TAC erythrocyte lysis buffer for 4 minutes at RT. After this time 25 ml staining buffer were added and the suspension was filtered through a 100 µm cell strainer. The cells were pelleted again (5 minutes, 400xg, 4°C) and resuspended in staining buffer. After determining the number of viable cells using a hemocytometer and the dye exclusion method the cell concentration was adjusted to $20.0x10^6$ cells/ml. This cell suspension was used for extra- and intracellular staining procedures as outlined in flow cytometry.

2.31 Generation of bone marrow-derived macrophages (BMDM)

Harvesting of bone marrow cells

Mice were euthanized by cervical dislocation and skin was removed from hind legs using disposable sterile scalpels and forceps. Femur and tibia were explanted, muscle tissue removed from the bones and the articular capsules were cut off at both ends. A syringe with a 26G needle was inserted into the bone cavity and bone marrow was flushed out with BBM medium until the bone cavity appeared white. Wash medium from one mouse was collected in a 50 ml polypropylene centrifugation tube on ice and cell aggregates were separated by pipetting up and down. Bone marrow cells were pelleted by centrifugation (10 minutes, 200xg, 4°C) and used to generate bone marrow-derived macrophages as described below.

Differentiation of bone marrow cells in Petri dishes

To remove stromal cells and mature macrophages the bone marrow cell suspension of one mouse was first resuspended in 10 ml BBM medium and then seeded in 10 cm tissue culture dishes and incubated at 37°C and 5% CO_2 in a humidified atmosphere for 4h. After this time non-adherent cells were centrifuged (10 minutes, 200xg, RT) and resuspended in 30 ml BBM medium containing 20 ng/ml murine recombinant M-CSF. The cell suspension was seeded on a 15 cm tissue culture dish and incubated at 37°C and 5% CO_2 in a humidified atmosphere for 7 days. During this time non-adherent cells were removed every 24h and half of the medium was replaced by 15 ml fresh medium containing 40 ng/ml murine recombinant M-CSF. Cells grown in a confluent monolayer (**Figure 11**) were harvested by washing once with 10 ml D-PBS and incubation with 5 ml 5 mM EDTA for 10 minutes at RT. After detachment EDTA was inactivated with medium and cells were pelleted (5 minutes, 200xg, RT) to remove EDTA before seeding the cells for stimulation experiments or FACS analysis. This method yielded 10-15x10^6 bone

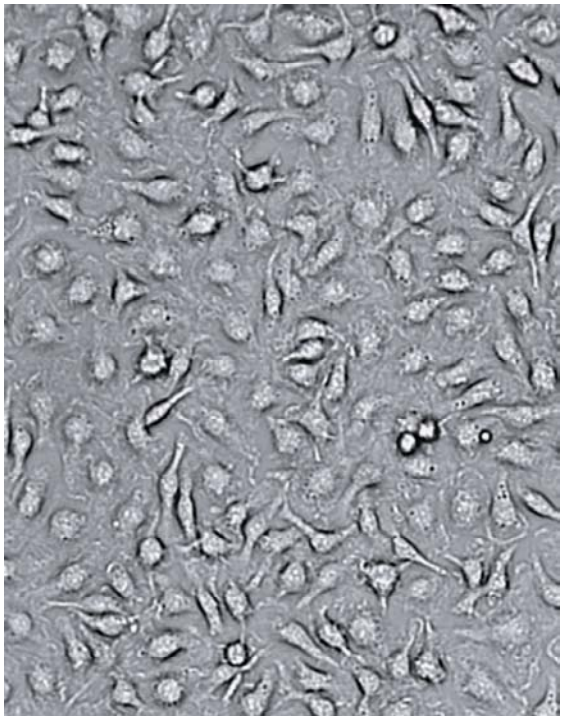

Figure 11. Micrograph showing morphology of BMDM 7 days after seeding of bone marrow cells onto tissue culture plastic dishes (200x). Bone marrow cells were harvested and cultivated as outlined in the text (see 2.31).

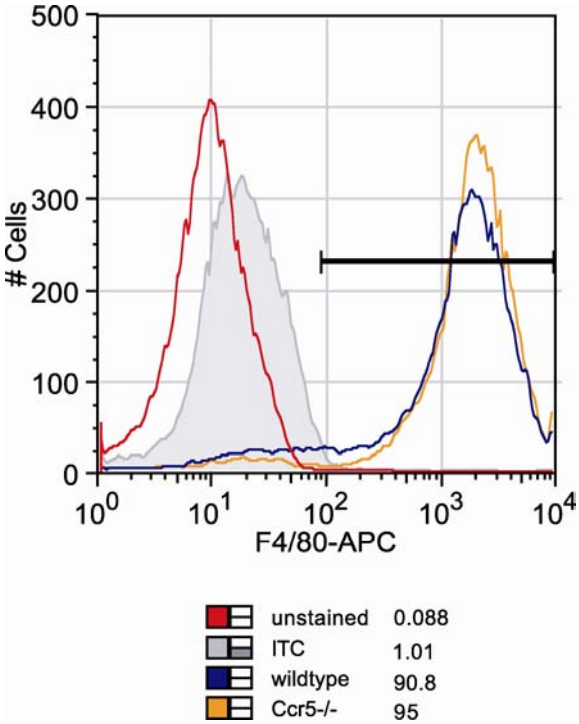

Figure 12. Flow cytometric analysis of F4/80 surface expression on BMDM generated in Petri dishes. Numbers below the histogram indicate percentages of cells within the plotted region.

marrow-derived macrophages per mouse and ≥90% of these cells stained positive for the macrophage marker F4/80 (**Figure 12**).

Differentiation of bone marrow cells in Teflon bags

Numbers of viable bone marrow cells were determined using the dye exclusion method with trypan blue and a hemocytometer. Cell concentrations were adjusted to $5x10^6$ cells/ml in DBM medium. Teflon bags were filled with 50 ml differentiation medium, 2 ml of bone marrow cell suspension were added and bags were sealed by heat using a bag sealer. The Teflon bags were placed on plastic racks to allow gas exchange from both sides (**Figure 13**) and incubated at 37°C and 10% CO_2 in a humidified atmosphere for 10 days. After this time bone marrow-derived macrophages were detached by incubating the Teflon bags for 30 minutes on ice and gentle

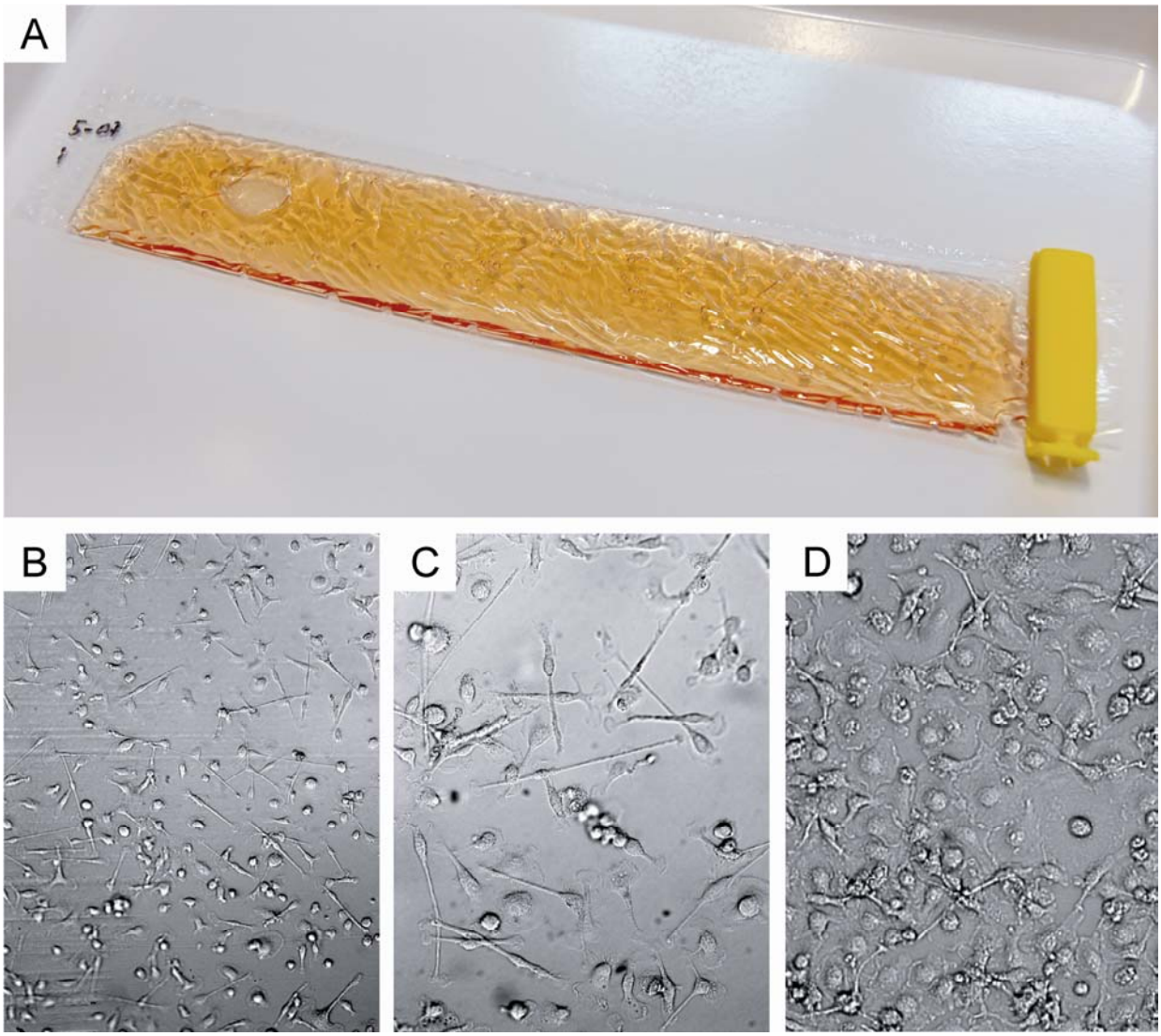

Figure 13. Cultivation and morphology of BMDM generated in Teflon bags. Teflon bag **(A)** and microscopic images of BMDM 1 day after re-seeding into Teflon bags (**(B)** 200x, **(C)** 400x). **(D)** BMDM cultivated 24h on tissue culture plastic dish (400x). Bone marrow cells were harvested and cultivated as outlined in the text (see 2.31).

massage and stretching of the bags. The bags were opened using sterile scissors and the suspension of BMDM was transferred into 50 ml polypropylene centrifugation tubes for further use in stimulation experiments or FACS analysis. In this manner, up to $30x10^6$ BMDM were harvested from one Teflon bag. Excess BMDM not used immediately for experiments were either seeded into fresh Teflon bags and further cultivated or cryopreserved (see 2.32) and stored frozen in liquid nitrogen.

Preparation of Teflon bags

Lumox™ film fluorocarbon foil (In Vitro Systems & Services) was cut into strips of 25x10 cm size and put onto a glass plate with the hydrophobic side facing upward. The stripe was folded at the long side and sealed by heat. In the next step the open long side was sealed. To facilitate opening of the bag after hot air sterilization a small stripe of aluminum foil was inserted into the upper part of the bag before wrapping it into aluminum foil as a container for sterilization. Sterilization was done in a hot air oven at 180°C for 1.5 h.

Long-term storage of BMDM in liquid nitrogen

Excess BMDM were pelleted (5 minutes, 200xg, RT) and resuspended in CC medium at a concentration of 10-20x10^6 cells per aliquot. Aliquots of 1.5 ml were filled into cryovials, stored in an isopropyl alcohol-filled cryo freezing container at -80°C over night and transferred to liquid nitrogen.

Preparation of L929s-conditioned medium

L929s fibroblast cells are known to produce high amounts of chemokines and growth factors like CCL2 (MCP-1) and CSF1 (M-CSF) that promote macrophage differentiation and survival [193, 194]. Therefore L929s-conditioned medium has been extensively used as a source for these factors and to generate bone marrow-derived macrophages [195]. For the generation of L929s-conditioned medium 0.25x10^6 L929s cells were seeded into 15 cm tissue culture dishes containing 25 ml of L929 medium. The cells were incubated at 37°C and 10% CO_2 in a humidified atmosphere until the cells formed a confluent monolayer (8-10 days). The supernatant (=L929s-conditioned medium) was sterilized using 0.22 µm sterile filters (TPP) and aliquots of 45 ml were stored at -80°C. The remaining cells were washed once with D-PBS and detached by adding 5 ml Trypsin-EDTA (1x) per dish for 10 minutes at RT. After detachment

Trypsin-EDTA was inactivated by addition of fresh medium and the cell concentration was determined using a hemocytometer. After pelleting (5 minutes, 200xg, RT) the cells were either seeded again as outlined above or resuspended in medium containing 7% DMSO at a concentration of $2.0x10^6$cells/ml for long term storage in liquid nitrogen.

2.32 Cultivation and stimulation of bone marrow-derived macrophages (BMDM)

BMDM were generated as described above and used for stimulation experiments at a concentration of $2.0x10^6$ cells per well of a tissue culture 6 well plate. Cells were rested over night in 3 ml medium per well (3) without M-CSF or L929s-conditioned medium before stimulation with reagents indicated in the respective experiment. Unstimulated cells served as controls. After the stimulation period medium was removed and BMDM cells were lysed using RNA isolation lysis buffer. For arginase enzyme activity assays $0.75x10^6$ BMDM cells were seeded in the wells of a tissue culture 12 well plate in a volume of 1.5 ml medium.

2.33 Flow cytometry

Dead cell discrimination

For the exclusion of non-viable cells the G-C base-specific DNA intercalating reagent 7-AAD (7-Amino-Actinomycin D, BD Biosciences) was used [196]. Like propidium iodide (PI) 7-AAD diffuses into dead and dying cells due to loss of membrane integrity, whereas living cells exclude these fluorescent DNA dyes. However, in contrast to PI 7-AAD has minimal spectral overlap with FITC and PE fluorescence emissions and is therefore ideally suited for use in conjunction with FITC- and PE-labeled antibodies in multicolor analysis. For the detection of 7-AAD fluorescence a 650 nm long-pass filter (FL3) in the far red spectrum was used. By using 7-AAD dead cells are excluded on the basis of their forward scatter (FSC) and FL3 properties. Dead cells have high 7-AAD intensities (FL3) and medium to low forward scatter intensities

[197]. Dead cell discrimination was done as the last step before analysis and after labeling cells with monoclonal antibodies. Therefore 1.0-3.0x10^6 cells were resuspended in 100 µl staining buffer containing 5 µl of 7-AAD. Cells were incubated for 10 minutes at RT in the dark and immediately analyzed at the flow cytometer without further washing steps. Cells fixed for intracellular staining were not stained with 7-AAD.

Fc receptor (FcR) blocking

Almost all immune cells express receptors that bind immunoglobulin molecules. During the adaptive immune response these receptors bind to sites located on the constant region of immunoglobulin (Ig) molecules [198]. Therefore it is important to block these receptors before staining with fluorescently labeled antibodies since binding to Fc receptors would lead to increased non-specific binding of test antibodies and hence high background staining. Blocking of Fc receptors was achieved by incubating the cells in staining buffer containing a non-labeled monoclonal antibody recognizing CD16 and CD32 (FcR gamma 3 and 2b, respectively). Cell suspensions were incubated with Fc blocking antibody (Abd Serotec, Mouse Seroblock FcR) at 4°C for 30 minutes before addition of the fluorescently labeled monoclonal antibodies. Depending on the origin of cells, Fc block was applied at a final dilution of 1:200 for BMDM or 1:400 for splenocytes. Fc block was not removed before addition of the fluorescently labeled monoclonal antibodies. Optimal dilutions of Fc block were determined by titration in halving steps (1:50 – 1:1600) against F4/80-APC antibody.

Determination of optimal staining concentrations of antibodies by titration

Using the optimal concentration of antibody is important in flow cytometric analysis. Factors that determine antibody binding rates (*i.e.* the affinity constant) are temperature, pH, buffer composition, antibody concentration and amount of available antigen. Very high antibody

concentrations can lead to diminished signal intensities due to self-quenching and cause increased non-specific binding ("high background") of test and isotype-matched control antibody [199]. Low antibody concentrations underestimate the presence of antigen thereby masking differences between samples of different origin (*e.g.* genotype, stimulation, etc.). To find optimal antibody concentrations test and isotype-matched control antibodies were titrated at equal concentrations and mean fluorescence intensities (MFI) were determined. The antibody concentration giving the best signal-to-noise ratio (i.e. MFI (test Ab) vs. MFI (control Ab)) was used as the optimal antibody concentration. Since antigen amounts vary depending on experimental conditions, titrations were performed for each experimental set individually.

Staining of extracellular antigens

Staining of cell surface antigens was done by incubating 1.0-3.0x10^6 cells in 100 µl staining buffer containing monoclonal antibodies for 30 minutes at RT or 1 h at 4°C in 5 ml round bottom tubes (BD Falcon) in the dark. Optimal antibody concentrations were determined by titration as outlined above. After incubation the cells were washed once in 3 ml ice cold staining buffer (5 minutes, 440xg, 4°C), resuspended in 200 µl staining buffer and stored on ice until flow cytometric analysis.

2.34 Statistical analysis

Values are presented as means ± SD. Pairwise statistical comparisons were performed either by two-tailed unpaired Student´s t test (parametric data) or Mann-Whitney U test (nonparametric data). $P < 0.05$ was considered significant.

3 RESULTS

As outlined under ”External contributions” (see appendix 7.1), the group of Prof. Gröne at the DKFZ in Heidelberg (Dept. of Cellular and Molecular pathology) contributed to this work by performing orthotopic kidney transplantation (see 2.15), determination of plasma urea and creatinine (3.1.1), histopathology (3.1.2) and immunohistochemistry (3.1.3) of renal allograft sections. The results of these investigations are described to provide comprehensive insight to this complex project. Results supplied by Prof. Gröne’s group are indicated in section headlines by DKFZ in brackets to unambiguously indicate the origin of contribution.

3.1 Analysis of renal allograft rejection in chemokine receptor-deficient mice

3.1.1 Functional analysis of renal allografts (DKFZ)

In order to assess renal allograft function creatinine and urea levels were determined in plasma samples collected at days 7 (acute rejection phase) and 42 (chronic rejection phase) after transplantation of a single kidney into bilaterally nephrectomized wildtype, $Ccr1^{-/-}$, $Ccr5^{-/-}$ and $Ccr1^{-/-}/Ccr5^{-/-}$ recipients.

While the organism catabolizes carbohydrates and lipids almost entirely to CO_2 and H_2O, nitrogen from amino acid, protein and nucleotide catabolism is excreted in the form of urea and to a minor extent as creatinine and other nitrogen compounds. During the urea cycle amino groups from ammonia and L-aspartate are converted to urea, using L-ornithine, citrulline, L-argininosuccinate and L-arginine as intermediates. Although the production of urea is an energy dependent anabolic process it is necessary to detoxify ammonia which would raise intracellular pH to toxic levels. Creatinine is a metabolic waste product of muscular tissues and its plasma concentrations are relatively constant in healthy individuals. Creatinine as well as urea is excreted by the kidney as components of the urine. Increased concentrations of creatinine and urea in the blood indicate defective glomerular filtration and renal dysfunction

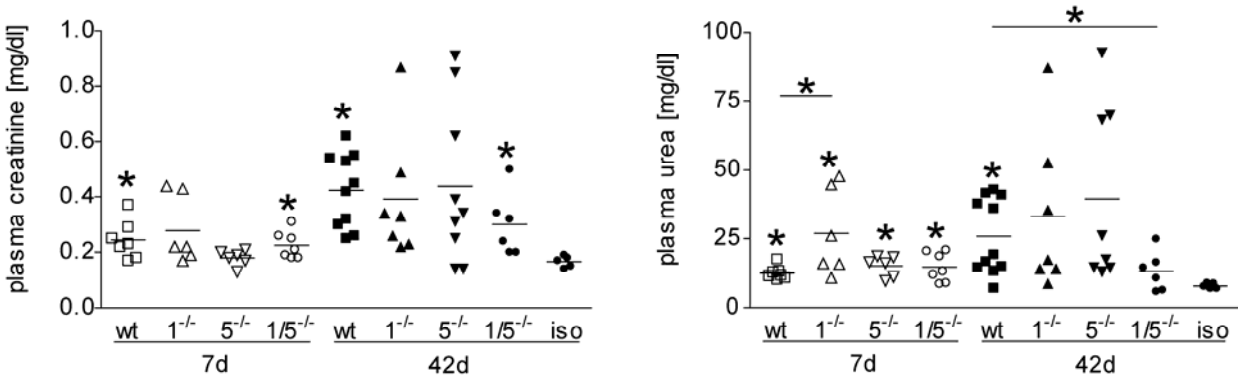

Figure 14. Effect of chemokine receptor deficiency on renal allograft function. Plasma from wildtype, $Ccr1^{-/-}$, $Ccr5^{-/-}$ and $Ccr1^{-/-}/Ccr5^{-/-}$ renal allograft recipients was collected 7 and 42 days after transplantation and used to assess allograft function by determining creatinine and urea levels. Each symbol represents the corresponding value from an individual mouse. Mean values for each group are indicated by a horizontal line. The levels in isografts at 42d are also shown. Asterisks above individual columns indicate significance against isograft whereas asterisks on horizontal lines indicate significance between groups of recipients. * $p<0.05$.

[200]. Creatinine and urea levels increased moderately between 7 and 42 days in all recipient groups (**Figure 14** and **Table 4**) demonstrating deterioration of renal allograft function over time. At 42 days after transplantation recipients of fully MHC-mismatched allografts showed higher creatinine and urea levels as recipients in the isograft group indicating ongoing allograft rejection. No differences were found for creatinine levels between the individual recipient groups at both investigated time points. However, plasma urea levels were significantly increased in $Ccr1^{-/-}$ recipients at 7 days post transplantation, but this increase disappeared at 42 days. Remarkably, $Ccr1^{-/-}/Ccr5^{-/-}$ recipients showed significantly decreased plasma urea concentrations at this time point whereas single deficient recipients had moderately increased mean plasma urea levels.

3.1.2 Histopathologic analysis of renal allografts (DKFZ)

To assess allograft damage periodic acid-Schiff (PAS)-stained sections from renal allografts of all recipient genotypes (wildtype, $Ccr1^{-/-}$, $Ccr5^{-/-}$ and $Ccr1^{-/-}/Ccr5^{-/-}$) and both time points (7d, 42d) were evaluated by light microscopy using lesion scores as defined in Materials and Methods.

Representative micrographs are shown in **Figure 15**. In general, all acute damage scores as well as the score for tubulointerstitial inflammation increased between 7 and 42 days after transplantation (**Table 4**) indicating ongoing rejection.

The lesion score for acute vascular rejection was significantly reduced in allografts from $Ccr1^{-/-}$ and $Ccr5^{-/-}$ recipients at day 7. Although, double-deficient recipients showed significantly reduced acute vascular rejection compared to wildtype recipients there was no additional decrease compared to single-deficient recipients at this time point. During the chronic rejection phase (42d postTX) a significant reduction of acute vascular rejection was observed only in $Ccr5^{-/-}$ recipients and remained above isograft level in all recipient groups. A chronic vascular rejection score was calculated for allografts at day 42 and significant reductions were observed in $Ccr1^{-/-}$, $Ccr5^{-/-}$ and $Ccr1^{-/-}/Ccr5^{-/-}$ recipients. Notably, the chronic vascular rejection score was reduced to the level of isograft recipients in double-deficient recipients.

Acute and chronic tubulointerstitial damage scores showed reductions in all analyzed chemokine receptor-deficient recipients but these differences did not reach statistical significance at both time points. At 7 days post transplantation tubulointerstitial inflammation was significantly reduced only in $Ccr1^{-/-}$ recipients whereas all recipient groups showed reduced tubulointerstitial inflammation compared to wildtype recipients at 42 days post transplantation. No additional reduction was found for double-deficient recipients and all recipient groups displayed tubulointerstitial inflammation above isograft level at 42 days.

Similar to acute vascular rejection at 7 days the lesion score for acute glomerular damage was significantly reduced for allografts from $Ccr1^{-/-}$, $Ccr5^{-/-}$ and $Ccr1^{-/-}/Ccr5^{-/-}$ recipients during acute rejection. At 42 days after transplantation the score for acute glomerular damage was significantly reduced in $Ccr1^{-/-}$ and $Ccr5^{-/-}$ recipients. Again, no additional reduction was found for double-deficient recipients and all recipient groups displayed acute glomerular damage scores above isograft level at 42 days. The lesion score for transplant glomerulopathy was

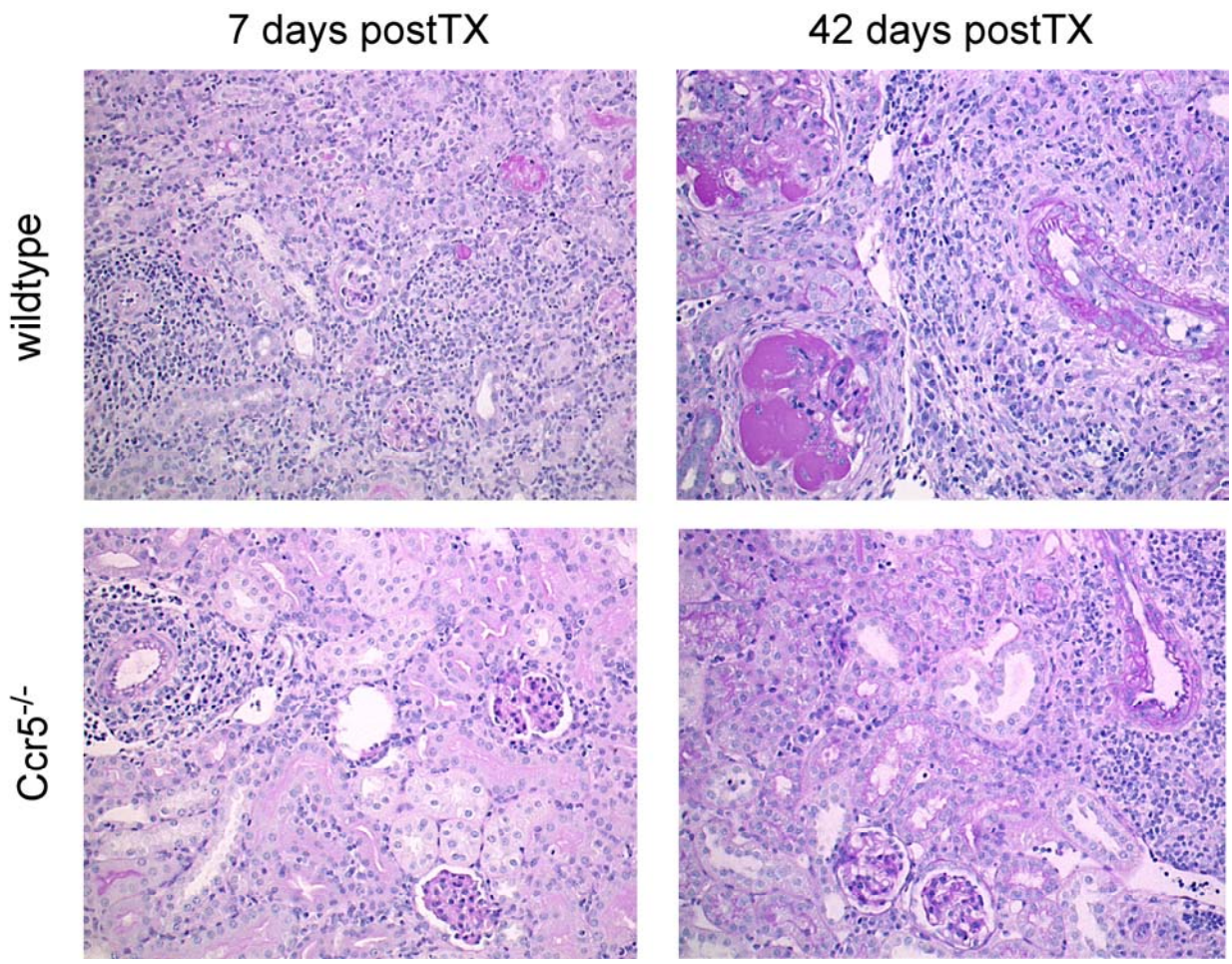

Figure 15. Effects of chemokine receptor deficiency on the histology of renal allografts. Representative micrographs of PAS-stained sections of renal allografts from wildtype and $Ccr5^{-/-}$ recipients from 7d and 42d post transplantation are shown (200x). Due to the exemplary character of these illustrations only wildtype and $Ccr5^{-/-}$ micrographs are shown here.

reduced in all analyzed chemokine receptor-deficient recipients at 42 days after transplantation but reached statistical significance only in double-deficient recipients.

Graft fibrosis was analyzed to assess transplant damage. Fibrosis is the formation of excess fibrous connective tissue. This process is either due to a healing process during the restoration of injured tissue by scar tissue or an abnormal condition where normal tissue is replaced by fibrous tissue. During allograft rejection fibrosis is induced by acute immune responses directed against the transplant that lead to cellular necrosis. Infiltrating lymphocytes within the vessel wall of the allograft are activated by antigen and stimulate macrophages to produce smooth muscle growth factors. Eventually, proliferation of smooth muscle cells results in thickening,

Table 4. Compilation of functional and histopathologic data from renal allograft recipients. Pairwise comparisons between wt and $Ccr1^{-/-}$, $Ccr5^{-/-}$ or $Ccr1^{-/-}/Ccr5^{-/-}$ at either 7d or 42d using Student's T-test or Mann-Whitney-U test were appropriate. Significant improvements are highlighted in light grey. Fields in dark grey highlight additional improvements in $Ccr1^{-/-}/Ccr5^{-/-}$ recipients (mean±SD; *: p<0.05; **: p<0.01; ***: p<0.001).

	acute rejection (7d postTX)				chronic rejection (42d postTX)				
	wildtype	$Ccr1^{-/-}$	$Ccr5^{-/-}$	$Ccr1/5^{-/-}$	wildtype	$Ccr1^{-/-}$	$Ccr5^{-/-}$	$Ccr1/5^{-/-}$	isograft
functional data									
plasma creatinine [mg/dl]	0.24 ± 0.07	0.28 ± 0.12	0.18 ± 0.03	0.23 ± 0.05	0.4 ± 0.16	0.39 ± 0.23	0.44 ± 0.29	0.3 ± 0.11	0.17 ± 0.01
plasma urea [mg/dl]	12.6 ± 2.4	26.9 ± 15.8	15.1 ± 3.7	14.7 ± 5.2	25.8 ± 13.7	32.8 ± 28.5	39.5 ± 32	*** 13.2 ± 7.1**	7.92 ± 0.43
lesion scores									
acute vascular rejection	29.8 ± 9.2	**** 11 ± 6.9**	*** 16 ± 3**	**** 12.6 ± 6**	42 ± 25	30 ± 29	**** 16 ± 9**	25 ± 7	1.40 ± 0.91
chronic vascular rejection	-	-	-	-	18.8 ± 12.9	**** 3.4 ± 6.4**	**** 1.7 ± 3.4**	**0 ± 0**	0 ± 0
acute tubulointerstitial damage	3.2 ± 2.4	2.5 ± 4.2	3.8 ± 3.8	1.7 ± 1.3	12 ± 8	6.8 ± 4.9	6.4 ± 5	7.5 ± 6.7	-
chronic tubulointerstitial damage	-	-	-	-	5.3 ± 2.3	3.4 ± 3.3	4 ± 3.4	2.9 ± 2.7	-
tubulointerstitial inflammation	187 ± 47	*** 109 ± 40**	129 ± 33	126 ± 50	241 ± 43	*** 166 ± 58**	*** 166 ± 84**	*** 173 ± 56**	6.00 ± 2.92
acute glomerular damage	19.5 ± 4.1	**** 7.3 ± 3.4**	**** 8.1 ± 3.5**	***** 7.3 ± 2.9**	86 ± 66	*** 26 ± 11**	*** 28 ± 26**	27 ± 15	3.58 ± 0.74
transplant glomerulopathy	-	-	-	-	51 ± 37	37 ± 22	20 ± 11	**** 8 ± 8**	0 ± 0
matrix deposition									
α-SMA	-	-	-	-	34 ± 16.6	**** 12.5 ± 5**	**** 11.6 ± 2.4**	*** 17.3 ± 7.3**	-
Coll I/III	-	-	-	-	125 ± 19	*** 103 ± 19**	107 ± 15	**** 85 ± 22**	-

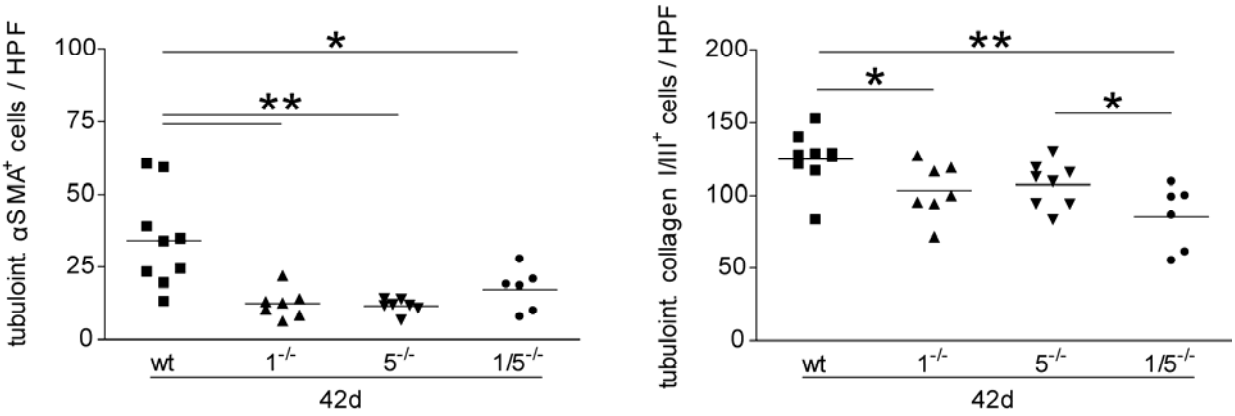

Figure 16. Effects of chemokine receptor deficiency on matrix deposition. αSMA$^+$ and collagen I/III$^+$ cells were counted in sections of renal allograft recipients at day 42 after transplantation. Each symbol represents the corresponding value from an individual mouse. Mean values for each group are indicated by a horizontal line. Asterisks on horizontal lines indicate significance between groups of recipients (*: p<0.05; **: p<0.01).

hardening and loss of elasticity of graft vessels – a process also seen in arteriosclerosis.

Graft fibrosis was determined at day 42 after transplantation in the tubulointerstitial compartment by immunohistochemical staining for alpha-smooth muscle actin (α-SMA) and collagen I/III (**Figure 16** and **Table 4**). The number of α-SMA$^+$ cells was significantly reduced in allografts from Ccr1$^{-/-}$, Ccr5$^{-/-}$ and Ccr1$^{-/-}$/Ccr5$^{-/-}$ recipients compared to wildtype recipients but no additional reduction was found in double-deficient recipient mice. Ccr1$^{-/-}$ and Ccr1$^{-/-}$/Ccr5$^{-/-}$ recipients showed a significant decrease of collagen I/III deposition in comparison to wildtype recipients. The staining for collagen I/III in Ccr5$^{-/-}$ recipients tended to decrease in comparison to wildtype recipients but did not reach statistical significance.

In summary, pathological analysis revealed significantly reduced lesion scores in Ccr1$^{-/-}$ and Ccr5$^{-/-}$ recipients (glomerular damage, vascular rejection and tubulointerstitial inflammation) at the investigated time points but additional improvements due to double deficiency were limited to certain parameters during the chronic phase of rejection (transplant glomerulopathy and chronic vascular damage).

3.1.3 Analysis of leukocyte infiltration in renal allografts (DKFZ)

Immunohistochemical staining for CD4, CD8, CD11c and F4/80 was performed on renal allograft sections to determine the number of infiltrating leukocytes (T cells, dendritic cells and macrophages) in the glomerular and tubulointerstitial compartment. Statistical evaluation of immunohistologic results is shown in **Figures 17 and 18.** An overview of these results is shown in **Table 5**. Representative micrographs are shown in **Figure 34-37** (see appendix 7.2).

In all recipient groups the number of tubulointerstitial $CD4^+$ and $CD8^+$ cells declined between 7 and 42 days after transplantation and glomerular $CD8^+$ cells showed a similar trend. Interestingly, $CD4^+$ cells in the glomerular compartment showed a different behavior (**Figure 17**). Wildtype, $Ccr1^{-/-}$ and $Ccr1^{-/-}/Ccr5^{-/-}$ recipients displayed higher numbers of glomerular $CD4^+$ cells at day 42 compared to day 7 after transplantation, whereas the number of glomerular $CD4^+$ cells in $Ccr5^{-/-}$ recipients remained constant over time. The number of glomerular and tubulointerstitial $CD4^+$ cells was significantly reduced in the $Ccr1^{-/-}$ group at day 7 after transplantation and $Ccr5^{-/-}$ recipients showed reduced numbers of glomerular $CD4^+$ cells at day 42. $CD8^+$ cells in both compartments were reduced during acute phase in $Ccr1^{-/-}$ recipients while $Ccr5^{-/-}$ recipients again showed a significant reduction during chronic phase of rejection. Double-deficient recipients had reduced numbers of glomerular $CD8^+$ at days 7 and 42 as well as a reduction of tubulointerstitial $CD8^+$ cells at day 42. However, the observed reductions showed no additional effect in double-deficient recipients when compared to single-deficient recipients. There was no clear trend for a reduction of $CD11c^+$ infiltrating leukocytes between 7 and 42 days after transplantation. While tubulointerstitial $CD11c^+$ cells from wildtype recipients decreased from 7 to 42 days, the number of glomerular $CD11c^+$ cells was constant over time in recipients with wildtype genotype (**Figure 17**).

Numbers of glomerular $CD11c^+$ cells increased over time in $Ccr1^{-/-}$ recipients while tubulointerstitial $CD11c^+$ cells in $Ccr1^{-/-}$ recipients and $CD11c^+$ cells of $Ccr5^{-/-}$ and $Ccr1^{-/-}/Ccr5^{-/-}$

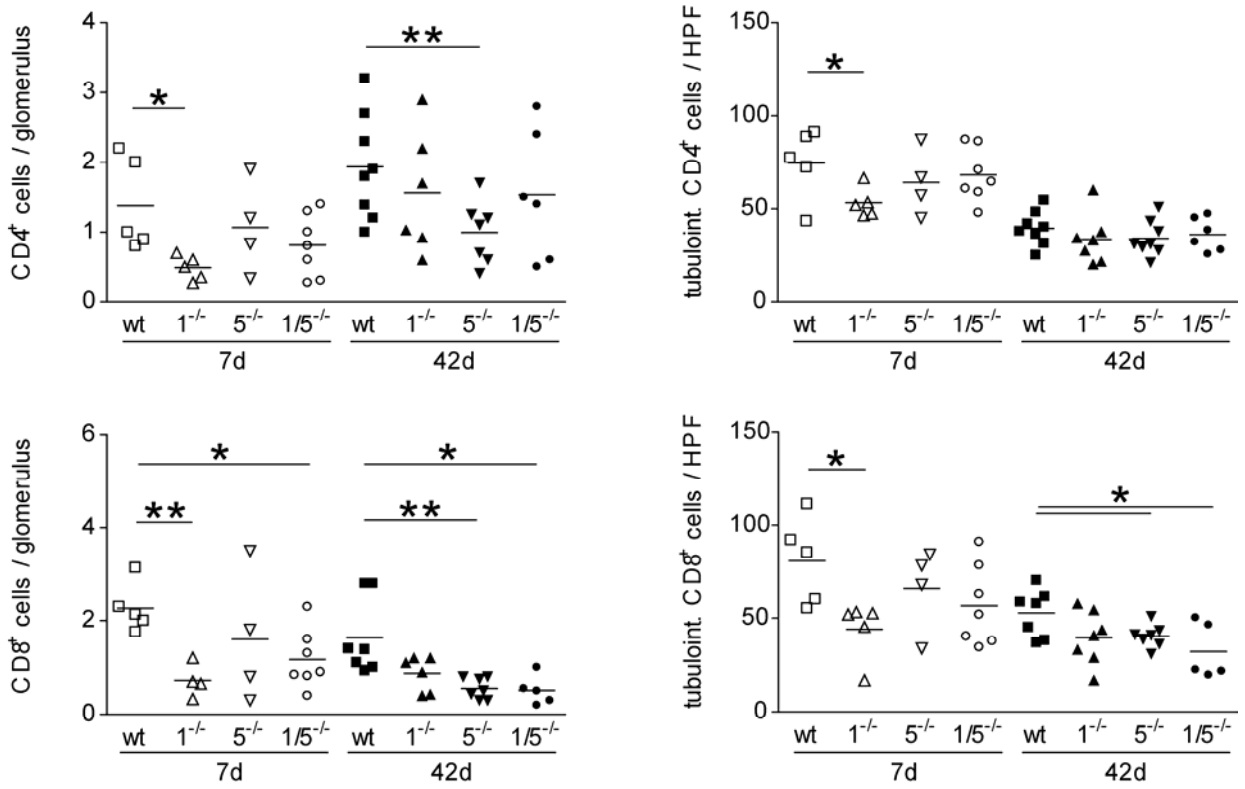

Figure 17. Quantitative evaluation of allograft infiltration by CD4$^+$ and CD8$^+$ cells. Cells stained for either CD4 or CD8 were counted in sections of renal allografts at day 42 after transplantation. Glomerular and tubulointerstitial (tubint.) infiltration are depicted in spate diagrams. Each symbol represents the corresponding value from an individual mouse. Mean values for each group are indicated by a horizontal line. Asterisks on horizontal lines indicate significance between groups of recipients (*: p<0.05; **: p<0.01). HPF: high power field.

recipients showed only moderate reductions in both compartments (**Figure 18**). Compared to wildtype recipients CD11c$^+$ cells were decreased in Ccr1$^{-/-}$ recipients in both compartments and in Ccr5$^{-/-}$ recipients in the tubulointerstitium at 7 days. At the later time point this pattern was inverted and significant reductions were only observed for glomerular CD11c$^+$ cells in Ccr5$^{-/-}$ recipients. Although Ccr1$^{-/-}$/Ccr5$^{-/-}$ recipients had reduced glomerular CD11c$^+$ cells in chronic phase and a reduction in tubulointerstitial CD11c$^+$ cells in acute and chronic phase, only the reduction of tubulointerstitial CD11c$^+$ cells at 42 days was attributable to an additional effect of double deficiency. However, this additional effect was only moderately pronounced. While infiltration by F4/80$^+$ cells in the glomerular compartment increased from 7 to 42 days in all

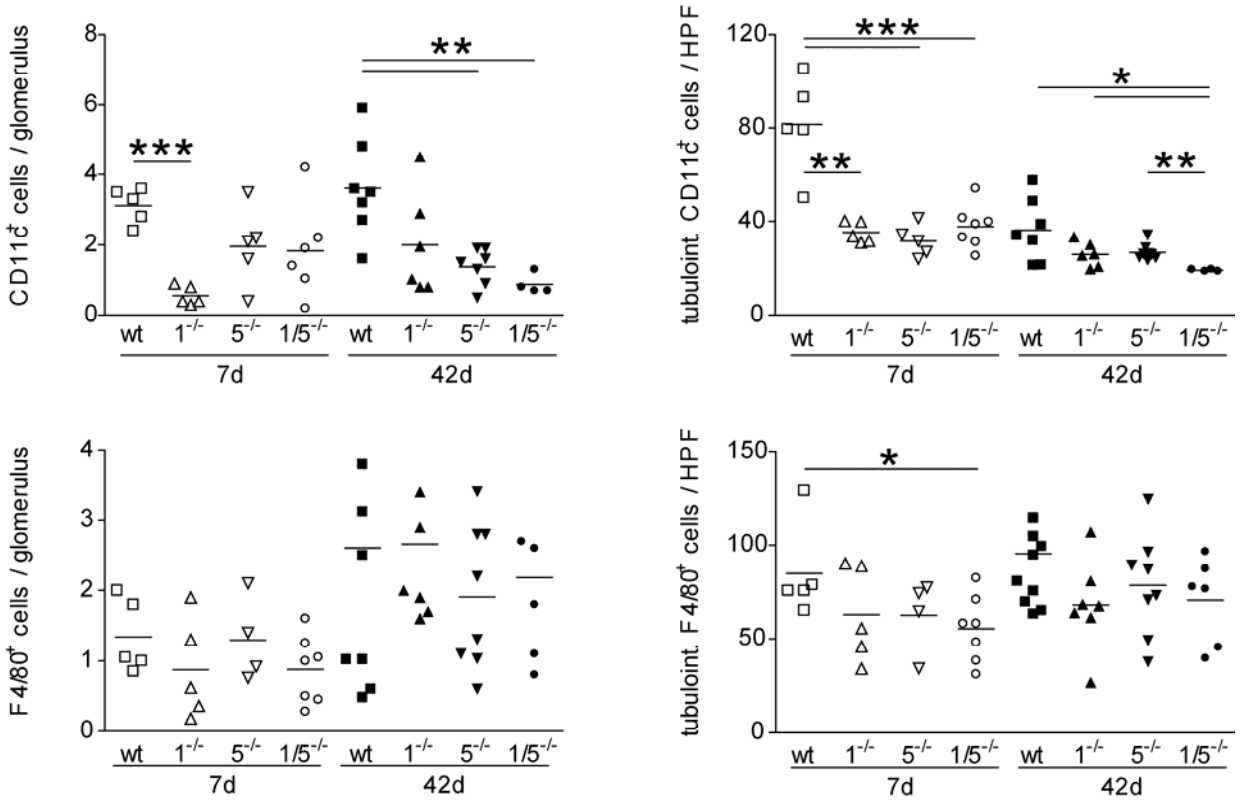

Figure 18. Quantitative evaluation of allograft infiltration by CD11c$^+$ and F4/80$^+$ cells. Cells stained for either CD11c or F4/80 were counted in sections of renal allografts at day 42 after transplantation. Glomerular and tubulointerstitial (tubint.) infiltration are depicted in spate diagrams. Each symbol represents the corresponding value from an individual mouse. Mean values for each group are indicated by a horizontal line. Asterisks on horizontal lines indicate significance between groups of recipients (*: p<0.05; **: p<0.01; ***: p<0.001). HPF: high power field.

recipient groups, numbers of tubulointerstitial F4/80$^+$ cells were more or less unchanged within this period. Remarkably, the only significant reduction found for infiltration by F4/80$^+$ cells was observed in Ccr1$^{-/-}$/Ccr5$^{-/-}$ recipients in the tubulointerstitium during the acute phase of rejection (**Figure 18**).

In summary, deficiency in Ccr1 caused reduced leukocyte infiltration during acute phase (less CD4$^+$, CD8$^+$ and CD11c$^+$ cells in both compartments), while Ccr5 deficiency resulted in reduced numbers of infiltrating leukocytes in the chronic phase of rejection (less glomerular CD4$^+$, CD8$^+$ and CD11c$^+$ cells as well as decreased tubulointerstitial CD8$^+$ cells) (**Table 5**). Surprisingly, infiltration by F4/80$^+$ cells in Ccr1$^{-/-}$ and Ccr5$^{-/-}$ recipient allografts (both compartments and time

Table 5. Summary of immunohistologic results from renal allograft recipients. Pairwise comparisons between wildtype and Ccr1$^{-/-}$, Ccr5$^{-/-}$ or Ccr1$^{-/-}$/Ccr5$^{-/-}$ at either 7d or 42d post transplantation using Student's T-test. Significant improvements against wildtype recipients are highlighted in light grey. Fields in dark grey highlight additional improvements in Ccr1$^{-/-}$/Ccr5$^{-/-}$ recipients (mean ± SD; *: p<0.05; **: p<0.01; ***: p<0.001).

	acute rejection (7d postTX)				chronic rejection (42d postTX)			
	wildtype	Ccr1$^{-/-}$	Ccr5$^{-/-}$	Ccr1/5$^{-/-}$	wildtype	Ccr1$^{-/-}$	Ccr5$^{-/-}$	Ccr1/5$^{-/-}$
glomerular								
CD4+	1.4 ± 0.7	*** 0.5 ± 0.2**	1.1 ± 0.7	0.8 ± 0.5	1.9 ± 0.8	1.6 ± 0.9	*** 1.0 ± 0.4**	1.5 ± 0.9
CD8+	2.3 ± 0.5	**** 0.7 ± 0.4**	1.6 ± 1.4	**** 1.2 ± 0.6**	1.6 ± 0.8	0.9 ± 0.4	*** 0.6 ± 0.2**	*** 0.5 ± 0.3**
CD11c+	3.1 ± 0.5	***** 0.6 ± 0.3**	2 ± 1.1	1.8 ± 1.4	3.6 ± 1.4	2 ± 1.5	**** 1.4 ± 0.5**	**** 0.9 ± 0.3**
F4/80+	1.3 ± 0.5	0.9 ± 0.7	1.3 ± 0.6	0.9 ± 0.5	2.6 ± 2	2.7 ± 1.3	1.9 ± 1	2.2 ± 1.2
tubulointerstitial								
CD4+	75 ± 19	*** 53 ± 8**	64 ± 18	68 ± 15	39 ± 9	34 ± 13	34 ± 10	36 ± 9
CD8+	81 ± 23	*** 44 ± 16**	66 ± 23	57 ± 22	53 ± 13	39 ± 14	*** 40 ± 6**	*** 32 ± 15**
CD11c+	82 ± 21	**** 35 ± 4**	**** 32 ± 7**	**** 38 ± 9**	36 ± 13	26 ± 5	27 ± 3	*** 19 ± 0.4**
F4/80+	85 ± 25	63 ± 25	63 ± 20	*** 55 ± 18**	95 ± 37	68 ± 24	78 ± 27	71 ± 23

points) did not show genotype specific differences and a further reduction of allograft infiltration due to double deficiency was restricted to CD11c^{+} cells in the tubulointerstitium at 42d post transplantation. Representative micrographs are shown in **Figures 34-37** (see appendix 7.2).

3.1.4 Analysis of alloreactive antibody titers in renal allograft recipients

Two recent publications suggested that Ccr5 deficiency in allograft recipients is leading to increased humoral rejection [113, 114]. Therefore, the levels of alloreactive IgG and IgM antibodies were measured in plasma samples from C57BL/6 wildtype and Ccr5$^{-/-}$ mice, which had either been immunized by intraperitoneal injection with BALB/c splenocytes or which had received a BALB/c renal allograft 42 days ago. Plasma from naive mice was used to determine baseline levels. Immunization with splenocytes as well as allografting induced a significant increase in alloreactive antibody levels, which was unaffected by the presence or absence of Ccr5 (**Figure 19**). At least for renal allografting experiments with the strain combination BALB/c

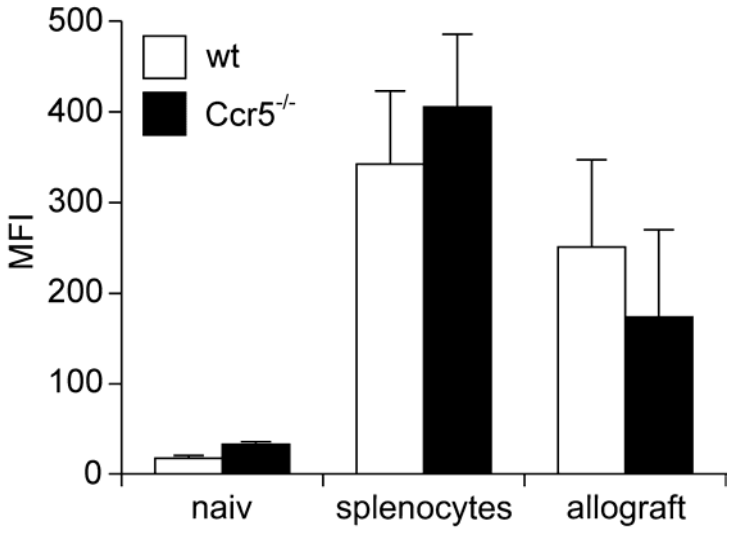

Figure 19. Effect of Ccr5 deficiency on alloreactive antibody titers. Plasma from C57BL/6 wt (n=3) and $Ccr5^{-/-}$ (n=3) mice immunized with BALB/c splenocytes or plasma from C57BL/6 wt (n=5) and $Ccr5^{-/-}$ (n=3) renal allograft recipients 42 days after transplantation was used to determine alloreactive antibody levels by flow cytometry as described in Materials and Methods. Plasma from naive mice was used as control. MFI, mean fluorescence intensity.

donors and C57BL/6 recipients no evidence was found for increased humoral rejection in Ccr5-deficient recipients at 42 days after transplantation.

3.1.5 Gene expression analysis in renal allografts

To further investigate the role of Ccr1 and Ccr5 in renal allograft rejection, mRNA levels of selected marker genes were determined by real-time RT-PCR in grafts from wildtype, $Ccr1^{-/-}$, $Ccr5^{-/-}$ and $Ccr1^{-/-}$/$Ccr5^{-/-}$ recipients at 7d and 42d after transplantation (**Figures 20-23**). A first set of markers analyzed included the cytokines Ifng and Tnf, the chemokine Cxcl10 (interferon-inducible protein 10, IP-10), the Th1-specific transcription factor Tbx21 (T-bet) and the interleukin Il12a (encoding the p35 subunit of IL-12). These genes have been implicated in proinflammatory and Th1-driven immune responses (**Figure 20**). The observed expression profiles – except for Il12a – reflected this common feature: a high expression during the acute phase was followed by a considerable lower level of expression during the chronic phase of rejection. In contrast, Il12a showed relatively low expression levels and increased moderately between 7 and 42 days. These changes demonstrate an overall reduction of the proinflammatory/Th1-type milieu within the allografts from acute to chronic phase of rejection. In addition, acute phase mRNA levels of Ifng, Tnf and Cxcl10 were significantly decreased in

Ccr1$^{-/-}$ and Ccr5$^{-/-}$ recipients compared to wildtype recipients indicating a further attenuation of Th1-type immune responses in acute phase allografts from single-deficient recipients. Surprisingly, mRNA levels of Ifng, Tnf and Cxcl10 were similar in wildtype and Ccr1$^{-/-}$/Ccr5$^{-/-}$ recipients during acute phase. In chronic phase of rejection a significant rise in the amounts of Tnf and Cxl10 mRNA above wildtype level was detected, suggesting ongoing acute phase or delayed Th1-type immune responses in double-deficient recipients. No significant differences were observed for the expression of the Th1-specific transcription factor Tbx21 and Il12a between the individual recipient groups at both time points.

The next panel of markers analyzed consisted of genes with established proinflammatory functions: the chemokines Ccl3 (MIP-1α), Ccl4 (MIP-1β) and Ccl5 (RANTES) [201]. CCL3 and CCL5 are ligands of the chemokine receptors CCR1 and CCR5 while CCL4 only binds to CCR5. Ccr2 and its main ligand Ccl2 (MCP-1) were included in this panel because of their importance for the recruitment of monocytes to sites of inflammation [202]. Furthermore, Il2 mRNA expression was analyzed due to its central role as an immune regulator [203]. IL-2 is an autocrine growth factor for T cells and promotes the proliferation of B cells in the presence of additional factors like IL-4. Furthermore, IL-2 shows Th1-associated functions by stimulating the synthesis of IFNγ and inducing of TNFα secretion. Expression of the IL-2 receptor was also proposed to be diagnostic for acute renal allograft rejection in human patients [204]. In accordance with these data, the expression profile observed for Il2 was similar to those found for Ifng and Tnf (**Figure 20**). Moreover, there was a significant reduction during acute phase in single-deficient recipients whereas mRNA levels at 42 days were considerably lower than at 7 days without any differences between the individual recipient groups.

The mRNA levels for Ccl2 were decreased in renal allografts from Ccr1$^{-/-}$ and Ccr5$^{-/-}$ recipients compared to wildtype recipients at 7 days after transplantation suggesting reduced infiltration by monocytes in allografts of single-deficient recipients during the acute phase of rejection

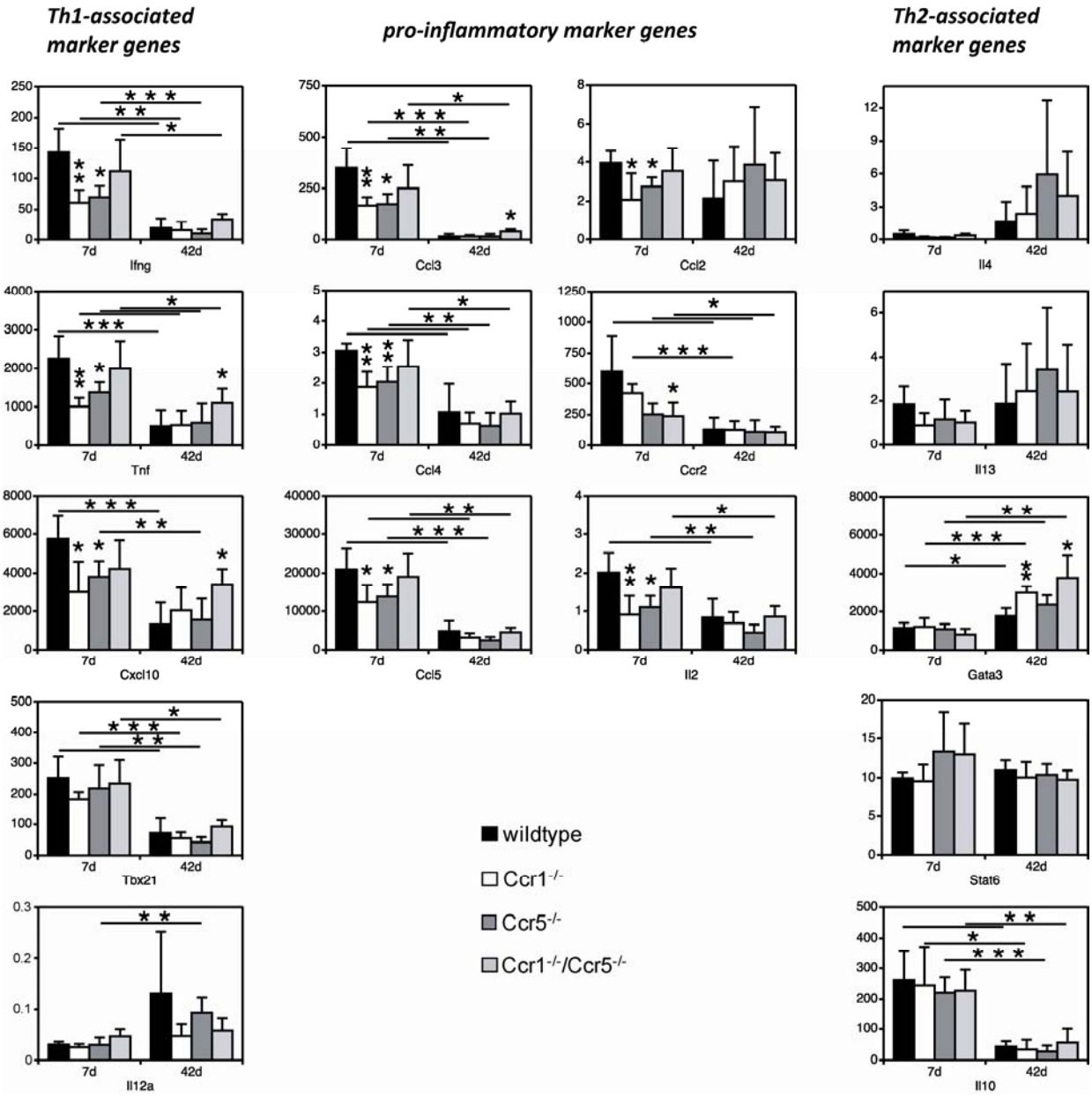

Figure 20. Effect of chemokine receptor deficiency on mRNA levels of selected Th1 (Ifng, Tnf, Cxcl10, Tbx21 and Il12a), pro-inflammatory (Il2, Ccl3, Ccl4, Ccl5, Ccl2 and Ccr2) and Th2 (IL-4, Il10, Il13, Gata3, Stat6) marker gene sets in renal allografts. Real-time RT-PCR was used to quantify intragraft mRNA levels for marker genes. Bar diagrams show mean values ± SD of 18S rRNA normalized expression for allografts from wildtype, $Ccr1^{-/-}$, $Ccr5^{-/-}$ and $Ccr1^{-/-}/Ccr5^{-/-}$ recipients at 7 and 42 days after transplantation. Asterisks on top of a horizontal line indicate statistically significant differences between the acute and the chronic phase for animals with the same genotype, whereas asterisks on top of an error bar indicate statistically significant differences between animals with different genotypes at the same time point (either 7d or 42d). * $p<0.05$, ** $p<0.01$, *** $p<0.001$.

(**Figure 20**). Additionally, a trend towards decreased Ccr2 mRNA was observed at this early time point in $Ccr1^{-/-}$ and $Ccr5^{-/-}$ recipients, supporting the idea of reduced monocyte infiltration.

While Ccl2 levels in allografts of $Ccr1^{-/-}/Ccr5^{-/-}$ recipients were comparable to wildtype levels at 7 days, expression of Ccr2 mRNA was significantly reduced in double-deficient recipient allografts at this time point. At 42 days post transplantation the levels of Ccr2 were noticeably lower in all recipient groups than at 7 days and differences in the mRNA expression of Ccr2 and Ccl2 disappeared between the recipient groups.

Ccl3 and Ccl5 are ligands of both CCR1 and CCR5 and have been implicated in Th1-type immune responses [205]. Expression profiles for these two genes resembled those found for the Th1-type immune response associated genes Ifng and Tnf: high expression during acute phase with decreased levels in $Ccr1^{-/-}$ and $Ccr5^{-/-}$ recipients, comparable levels between wildtype and double-deficient recipients and drastically reduced expression in chronic phase without differences amongst the individual recipient groups except for case of Ccl3 where double-deficient recipients expressed significantly higher levels than wildtype recipients. Interestingly, Ccl4, a ligand of CCR5, displayed the same expression profile as Ccl3 and Ccl5 suggesting Ccl4 to be a Th1-type immune response gene – at least in the setting of renal allograft rejection (**Figure 20**).

The marker panel for Th2-type immune response-associated genes included the cytokines IL-4, Il10 and Il13 which are primarily produced by Th2 cells, the Th2 cell-specific transcription factor Gata3 and also Stat6, a transcription factor mediating of IL-4 and IL13 signaling [206, 207]. IL-4 and Il13 mRNAs had comparable expression profiles. While both genes showed only low mRNA expression during acute phase without any differences between individual recipient groups, expression increased during chronic phase with the highest levels in the group of $Ccr5^{-/-}$ recipients. However, none of these differences reached statistical significance due to large intragroup variations. Gata3 mRNA showed a significant increase in all recipient groups from 7 to 42 days and was significantly increased in $Ccr1^{-/-}$ and $Ccr1^{-/-}/Ccr5^{-/-}$ recipients at 42 days post transplantation. In contrast to the aforementioned Th2-type markers mRNA expression of the

transcription factor Stat6 remained constant over time and differences between the recipient groups were not observed. Interestingly, the mRNA expression profile of Il10 resembled those observed for Th1-type marker genes and did not show differences among individual recipient groups (**Figure 20**).

In summary, the acute phase of rejection is characterized by an increased Th1-type gene expression pattern, whereas Th2-type marker genes are increased during the chronic phase of rejection but did not reach the levels of Th1-type genes during acute rejection. While single-deficient recipients showed decreased Th1-type marker expression during acute phase (Ifng, Tnf, Cxcl10, Il2, Ccl3 and Ccl5), significant differences in double-deficient recipients were limited to decreased expression of Ccr2 in acute phase and increased expression of Tnf, Cxcl10 and Ccl3 during chronic phase. In contrast to single-deficient recipients, double-deficient recipients often showed expression levels for Th1-marker genes (Ifng, Tnf, Cxcl10, Il2, Ccl3 and Ccl5) that were comparable to wildtype recipients during acute phase. During chronic phase a trend towards Th2-type immune responses was observed for $Ccr5^{-/-}$ recipients by increased expression of IL-4 and Il13 (**Figure 20**).

Skewing of immune responses to Th17-type has been implicated in the development of acute transplant rejection in humans [208, 209]. Therefore, the effect of Ccr1-, Ccr5- and double deficiency on Th17-type immune response-associated marker gene expression was determined in our murine renal allograft model (**Figure 21**). The marker gene set for this purpose consisted of the cytokine Il17a (produced by Th17 cells), the Th17-specific transcription factor Rorc, the cytokines Tgfb1, Il6 and Il23 which induce Th17 cell proliferation and the chemokine Ccl20 along with its corresponding receptor Ccr6 that is expressed by the majority of IL17 producing cells [210, 211]. The expression of Il17a mRNA was remarkably reduced in $Ccr1^{-/-}$, $Ccr5^{-/-}$ and $Ccr1^{-/-}$/$Ccr5^{-/-}$ recipients at 7 days after transplantation but did not reach statistical significance (**Figure 21**). Furthermore, at 42 days Il17a expression levels in $Ccr1^{-/-}$ recipients exceeded those

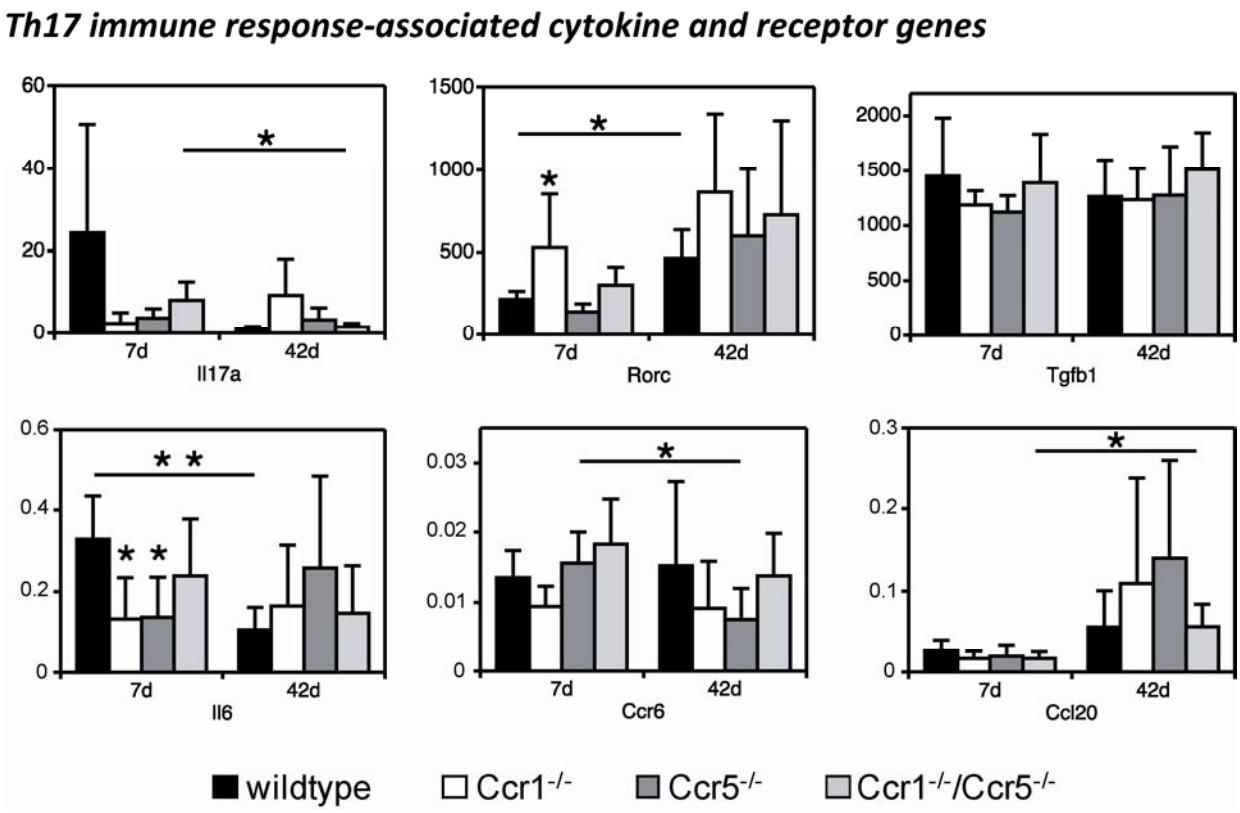

Figure 21. Effects of chemokine receptor deficiency on mRNA levels of selected Th17 (Il17a, Rorc, Tgfb1, Il6, Ccr6 and Ccl20) marker genes in renal allografts. Real-time RT-PCR was used to quantify intragraft mRNA levels for marker genes. Bar diagrams show mean values ± SD of 18S rRNA normalized expression for allografts from wildtype, $Ccr1^{-/-}$, $Ccr5^{-/-}$ and $Ccr1^{-/-}/Ccr5^{-/-}$ recipients at 7 and 42 days after transplantation. Asterisks on top of a horizontal line indicate statistically significant differences between the acute and the chronic phase for animals with the same genotype, whereas asterisks on top of an error bar indicate statistically significant differences between animals with different genotypes at the same time point (either 7d or 42d). * $p<0.05$, ** $p<0.01$.

of the other analyzed recipient groups. Interestingly, the increase of Il17a at 42d was associated with a significant elevation of Rorc in $Ccr1^{-/-}$ recipients during the acute phase of rejection. These findings suggest a Th17 skewing of immune responses in allografts of $Ccr1^{-/-}$ recipients. However, the expression profile of Tgfb1 remained constant over time and did not show changes between recipient groups. In addition, Il6 mRNA expression was relatively low, decreased in $Ccr1^{-/-}$ and $Ccr5^{-/-}$ at 7 days and potential differences among recipient groups at 42 days were washed by considerable variability. Ccr6 mRNA expression was also quite low and remained constant over time with the exception of $Ccr5^{-/-}$ recipients which showed a decrease

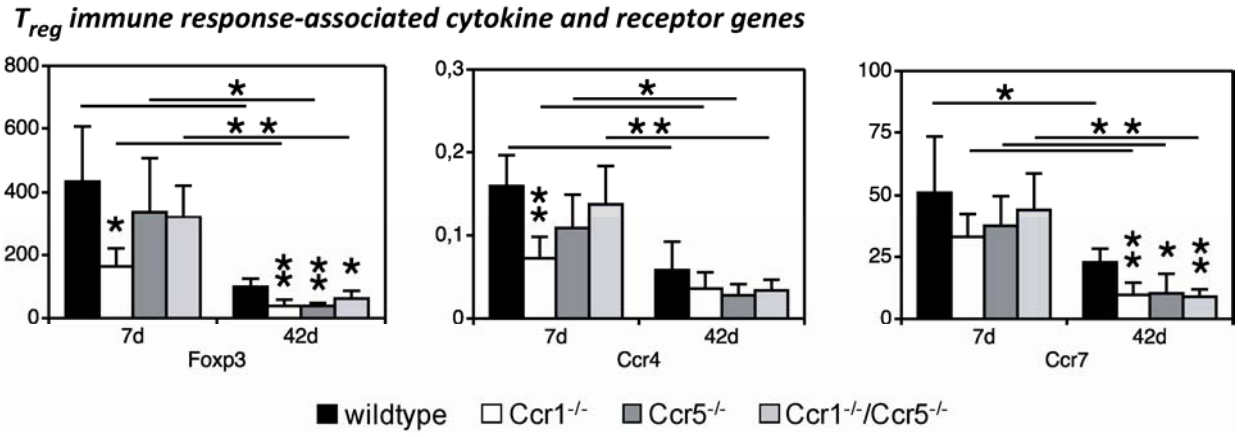

Figure 22. Effects of chemokine receptor deficiency on mRNA levels of selected Treg (Foxp3, Ccr4 and Ccr7) marker genes in renal allografts. Real-time RT-PCR was used to quantify intragraft mRNA levels for marker genes. Bar diagrams show mean values ± SD of 18S rRNA normalized expression for allografts from wildtype, $Ccr1^{-/-}$, $Ccr5^{-/-}$ and $Ccr1^{-/-}/Ccr5^{-/-}$ recipients at 7 and 42 days after transplantation. Asterisks on top of a horizontal line indicate statistically significant differences between the acute and the chronic phase for animals with the same genotype, whereas asterisks on top of an error bar indicate statistically significant differences between animals with different genotypes at the same time point (either 7d or 42d). * $p<0.05$, ** $p<0.01$.

in Ccr6 mRNA levels at 42 days compared to 7 days. Moreover, no significant differences were found for Ccr6 mRNA expression within the recipient groups. Ccl20 mRNA expression did not show differences between recipient groups at both time points, but an increase from 7 to 42 days in $Ccr1^{-/-}/Ccr5^{-/-}$ recipients. However, increased mRNA expression of the chemokine Ccl20 was not accompanied by an increase in Ccr6 mRNA levels (**Figure 21**).

Regulatory T cells exert immunosuppressive roles and were suggested to prolong allograft function [212]. Therefore, the influence of chemokine receptor Ccr1-, Ccr5- and double deficiency on expression of marker genes for regulatory T cells was analyzed (**Figure 22**). Regulatory T cells specifically express the transcription factor Foxp3 and Treg precursors express the chemokine receptor Ccr7 which is involved in homing of naive and regulatory T cells to secondary lymphoid organs as well as migration of dendritic cells into lymph nodes via afferent lymphatic vessels [213]. Recently, it has been shown by Lee *et al.* that the chemokine receptor Ccr4 is required for recruitment of tolerance mediating regulatory T cells to cardiac allografts [214]. Expression levels of these markers decreased over time in all recipient groups

and Foxp3 as well as Ccr4 mRNA levels were considerably lower in $Ccr1^{-/-}$ recipients at 7 days (**Figure 22**). Additionally, expression of Ccr7 and Foxp3 was significantly reduced in allografts from $Ccr1^{-/-}$, $Ccr5^{-/-}$ and $Ccr1^{-/-}/Ccr5^{-/-}$ recipients at day 42. These results indicate reduced suppression of immune responses in the analyzed chemokine receptor deficient recipients during chronic phase of rejection and in $Ccr1^{-/-}$ recipients already during acute phase. Reduced suppression could lead to enhanced effects of Th1- or Th2-skewed immune responses.

Besides T cells, macrophages constitute a major fraction of infiltrating leukocytes within the allograft. For that reason, the effect of chemokine receptor deficiency on the expression of certain macrophage marker genes in renal allografts was tested. Numbers of $F4/80^{+}$ cells (mostly macrophages) remained constant in single-deficient recipients compared to wildtype recipients. Therefore, mRNA expression of macrophage phenotype associated marker genes was analyzed to determine, whether loss of Ccr1 and/or Ccr5 influences macrophage polarization.

Genes induced in classically activated macrophages (CAMs) are Tnf, Ifng and the chemokines Ccl3, Ccl4, Ccl5 along with Cxcl10 (**Figure 20**). Interestingly, all of these genes were significantly reduced in renal allografts from $Ccr1^{-/-}$ as well as $Ccr5^{-/-}$ recipients at 7 days and showed lower expression at 42 days than at 7 days while Nos2, another marker for CAMs, remained constant over time showing no differences between recipient groups (**Figure 23**).

A strong increase for IL-4 and Il13 was observed between 7 and 42 days, which was paralleled by a decrease of marker expression for Th1-type immune responses and classical macrophage activation, respectively. Since IL-4 and IL-13 are known to induce alternatively activated macrophages (AAM) it was tempting to speculate whether intragraft macrophages might be skewed towards such a phenotype. Therefore, the intragraft mRNA expression of several signature genes for AAM including Arg1, Chi3l3, Retnla, Mrc1, Mrc2 and Fcer2a was tested.

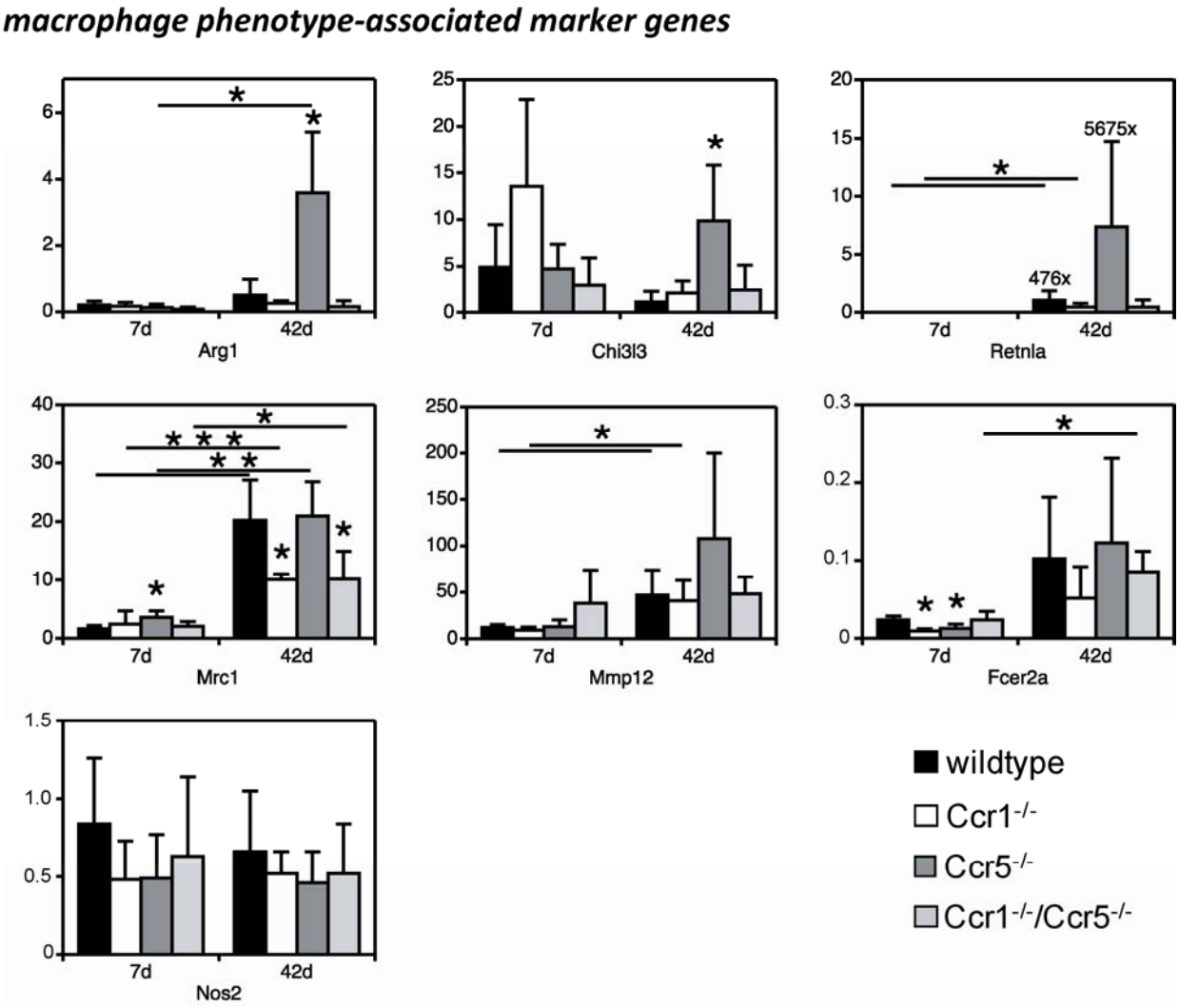

Figure 23. Effects of chemokine receptor deficiency on mRNA expression of macrophage phenotype-associated marker genes (Arg1, Chi3l3, Retnla, Mrc1, Mmp12, Fcer2a and Nos2) in renal allografts. Real-time RT-PCR was used to quantify intragraft mRNA levels for marker genes. Bar diagrams show mean values ± SD of 18S rRNA normalized expression for allografts from wildtype, $Ccr1^{-/-}$, $Ccr5^{-/-}$ and $Ccr1^{-/-}/Ccr5^{-/-}$ recipients at 7 and 42 days after transplantation. Asterisks on top of a horizontal line indicate statistically significant differences between the acute and the chronic phase for animals with the same genotype, whereas asterisks on top of an error bar indicate statistically significant differences between animals with different genotypes at the same time point (either 7d or 42d). * $p<0.05$, ** $p<0.01$, *** $p<0.001$.

Surprisingly, allografts from $Ccr5^{-/-}$ recipients displayed considerably increased expression of Arg1, Chi3l3 and Retnla at 42 days while no statistically significant differences were observed at 7 days between the groups (**Figure 23**). Mannose receptor C type 1 (Mrc1) mRNA levels were

significantly increased in Ccr5$^{-/-}$ recipients at 7 days. During the chronic phase, however, Mrc1 mRNA levels in Ccr5$^{-/-}$ recipients remained at wildtype niveau, while significantly less Mrc1 expression was observed in Ccr1$^{-/-}$ and double-deficient recipients.

The mRNA expression profiles observed for Mmp12, a matrix metalloproteinase associated with alternatively activated macrophages [215], supported the findings for Arg1, Chi3l3 and Retnla in Ccr5$^{-/-}$ recipients (**Figure 23**). The levels of Mmp12 mRNA were low during acute phase and increased over time in all groups. Mmp12 mRNA expression was highest in the group of Ccr5-deficient recipients but did not reach statistical significance due to large intragroup variation.

The next gene analyzed was Fcer2a (CD23), which encodes the Fcε receptor 2a. Mantovani *et al.* [216] proposed Fcer2a to be a signature gene for macrophages with an alternative activation phenotype. The mRNA expression of Fcer2a was determined in our renal allograft samples. Ccr1 and Ccr5-deficient recipients demonstrated reduced Fcer2a mRNA levels at 7d post transplantation (**Figure 23**). Furthermore, Fcer2a mRNA expression was diminished in Ccr1- and Ccr1-/Ccr5-deficient recipients, but allografts from Ccr5$^{-/-}$ mice had Fcer2a levels comparable to animals of the wildtype group.

In summary, macrophages in renal allografts from Ccr5$^{-/-}$ recipients appear to be skewed towards an alternative activation phenotype – a finding which might explain the beneficial effects of Ccr5 deficiency on allograft rejection.

3.1.6 Protein expression of alternatively activated macrophage (AAM) markers in renal allografts

To confirm the mRNA data on alternative macrophage activation at the protein level immunohistochemical stainings for Arg1, Chi3l3 and Mrc1 were performed in allograft sections taken from wildtype and $Ccr5^{-/-}$ recipients at 42 days post transplantation. Representative micrographs are shown in **Figure 24A**. The quantitative evaluation of all 3 stainings is shown in **Figure 24B**. Significantly increased numbers of $Arg1^{+}$ and $Chi3l3^{+}$ cells were observed in the tubulointerstitium as well as an increase of $Mrc1^{+}$ and $Chi3l3^{+}$ cells in the glomerular

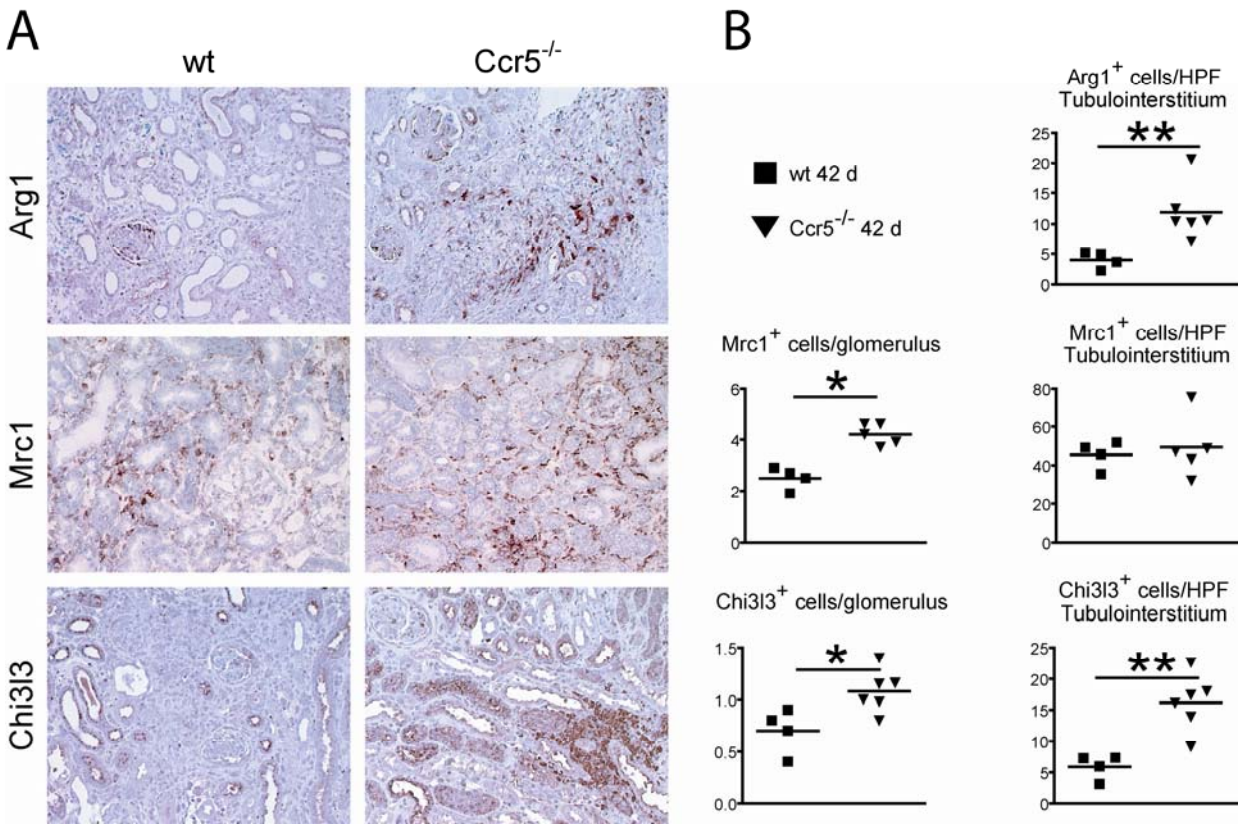

Figure 24A-B. Effect of Ccr5 deficiency on the expression of signature genes for alternatively activated macrophages in chronically rejecting renal allografts. Renal allografts from wildtype (wt) and $Ccr5^{-/-}$ recipients were collected 42 days after transplantation and sections were stained by immunohistochemistry for arginase 1 (Arg1), mannose receptor C type 1 (Mrc1) and chitinase 3-like 3 (Chi3l3). All 3 markers are associated with AAM. **A)** Representative micrographs of the immunohistochemical stainings. **B)** Quantitative evaluation of the immunohistochemical staining exemplified in A). Asterisks indicate significance between wildtype and $Ccr5^{-/-}$ groups (* $p<0.05$, ** $p<0.01$).

compartment of renal allografts from $Ccr5^{-/-}$ recipients at 42d. Due to the fact that podocytes residing within the glomerular compartment stained positive for Arg1 made it impossible to determine the number of $Arg1^{+}$ macrophages within this compartment. These protein data strongly support the hypothesis that Ccr5 deficiency leads to a change of macrophage phenotype during the chronic phase of renal allograft rejection.

3.2 Effects of Ccr5 deficiency on macrophage polarization

Loetscher *et al.* showed that the chemokine receptor CCR5 is highly abundant on $CD4^{+}$ Th1 cell clones [61]. Therefore a lack of CCR5 could lead to diminished Th1 immune responses by reduced chemotaxis or signaling in Th1 cells. This finding and the marked increase of signature gene expression indicative for alternatively activated macrophages (Arg1, Chi3l3, Retnla and Mrc1) in renal allografts from $Ccr5^{-/-}$ recipients at day 42 led to the hypothesis that Ccr5 deficiency might induce a shift in macrophage polarization already under basal conditions. To test this hypothesis, the expression of specific markers for the alternative activation pathway was tested by real-time RT-PCR and/or flow cytometry in wildtype and $Ccr5^{-/-}$ macrophages of different origins: spleen and cultivated splenocytes, elicited peritoneal macrophages and bone marrow-derived macrophages (BMDM). These cellular systems provide macrophage populations with different activation states and degrees of purity – allowing the study of effects due to other cell populations and inflammatory stimuli on macrophage polarization.

3.2.1 Spleens from $Ccr5^{-/-}$ mice show increased expression of AAM marker genes

Total RNA was isolated from spleens of C57BL/6 wildtype and $Ccr5^{-/-}$ mice ($n \geq 5$) and subjected to reverse transcription. The cDNA obtained by this procedure was then used as a template for real-time RT-PCR. Loss of Ccr5 was accompanied by significantly increased mRNA expression of the AAM signature genes Arg1, Mmp12, Mrc1 and Mrc2 (**Table 6**). In addition, mRNAs for the

Table 6. Effect of Ccr5 deficiency on AAM and Th2 marker gene expression in spleens of unchallenged mice. Real-time RT-PCR was used to quantify mRNA expression in spleens from wildtype and $Ccr5^{-/-}$ C57BL/6 mice (n≥5 per group, all female, all 20 weeks of age). Shown are means and corresponding standard deviations. Ratios are fold changes of $Ccr5^{-/-}$ to wt means. Significance values (p) were calculated using Student's t test and values reaching significance levels ($p < 0.05$) are highlighted in bold letters.

gene	marker type	wildtype		Ccr5-/-		ratio Ccr5-/- vs wt	p value
		mean relative expression	SD	mean relative expression	SD		
Arg1	AAM	0.0005	0.0002	0.0019	0.0011	**3.92**	**0.0041**
Chi3l3	AAM	0.64	0.20	1.43	1.19	2.25	0.2109
Retnla	AAM	0.44	0.16	0.72	0.45	1.64	0.2504
Mmp12	AAM	0.20	0.06	0.61	0.42	**3.02**	**0.0186**
Mrc1	AAM	11.30	1.09	36.57	16.37	**3.24**	**0.0161**
Mrc2	AAM	0.15	0.03	0.30	0.16	**1.97**	**0.0407**
Msr1	AAM	0.23	0.07	0.44	0.23	1.89	0.0772
Tgfb1	AAM / Th2	1.47	0.08	4.02	1.63	**2.73**	**0.0015**
Il10	AAM / Th2	0.010	0.004	0.067	0.068	**6.57**	**0.0354**
Gata3	Th2	0.11	0.04	0.25	0.08	**2.27**	**0.0010**
Stat6	Th2	12.37	1.57	34.64	18.44	**2.80**	**0.0067**
Itgam	macrophages	4.28	0.83	10.97	8.51	2.56	0.0608

cytokines Tgfb1 and Il10, which have been associated with regulatory macrophages [2, 155], were also markedly up-regulated (2.7 and 6.6 fold, respectively) in spleens from mice lacking Ccr5. mRNAs for the AAM marker genes Chi3l3, Retnla and Msr1 were increased in $Ccr5^{-/-}$ spleens but the differences did not reach statistical significance. To assess the effect of Ccr5 deficiency on Th2-polarization mRNA expression of the classical Th2 cytokine Il4 and the Th2-associated transcription factors Gata3 and Stat6 was analyzed. Expression of Il4 mRNA was below detection limit (data not shown) but both transcription factors were significantly increased in spleens of $Ccr5^{-/-}$ mice indicating Th2 skewing already under basal conditions in mice lacking Ccr5. Taken together, these findings suggest that macrophages are already polarized towards an alternative activation phenotype in spleens from unchallenged Ccr5-deficient mice.

3.2.2 In vitro cultivated Ccr5$^{-/-}$ splenocytes show enhanced expression of AAM marker genes

Due to the findings in spleens from unchallenged mice, splenocytes were used in a first attempt to obtain an *in vitro* system useable for the analysis of the mechanisms underlying alternative macrophage activation in Ccr5$^{-/-}$ mice. In a first pilot experiment, splenocytes from one wildtype and two Ccr5$^{-/-}$ mice were cultured in tissue culture 6 well plates for 24h at a density of 5x10^{6} per well and AAM signature gene expression was determined using real-time RT-PCR (**Table 7**). The mRNA expression of Chi3l3 and Retnla, two widely accepted markers for alternatively activated macrophages, showed a marked increase (23.1 and 29.9 fold, respectively) in cultivated Ccr5$^{-/-}$ compared to wildtype splenocytes. This increase was even more pronounced than in spleens from unchallenged mice (compare **Table 6**). Furthermore, Arg1 and Msr1 mRNAs showed up-regulation in Ccr5$^{-/-}$ splenocytes on a comparable level to direct lysates from

Table 7. Effect of Ccr5 deficiency on AAM marker gene expression in cultivated splenocytes. Real-time RT-PCR was used to quantify mRNA expression of splenocytes from wildtype (n=1) and Ccr5$^{-/-}$ (n=2) C57BL/6 (male, 16-19w) mice cultivated for 24h in 6 well plates with 3 ml SSB medium per well. Shown are means and ratios are fold changes of Ccr5$^{-/-}$ to wildtype means. Compare Table 6 for expression data in direct lysates of total spleens.

probe	marker type	wildtype mean relative expression	Ccr5-/- mean relative expression	ratio
Arg1	AAM	0.006	0.021	3.4
Chi3l3	AAM	0.06	1.49	23.2
Retnla	AAM	0.67	20.1	29.9
Mmp12	AAM	26.0	23.4	-1.1
Mrc1	AAM	1.04	1.37	1.3
Msr1	AAM	1.78	5.94	3.3
Il10	AAM / Th2	0.20	0.41	2.0
Stat6	Th2	6.71	7.03	1.0
Gata3	Th2	0.29	0.30	1.0
Itgam	macrophages	18.76	116.94	6.23

spleens while other AAM markers which showed up-regulation in Ccr5$^{-/-}$ direct lysates were not differentially regulated upon *in vitro* cultivation (Mmp12 and Mrc1). The difference in wildtype and Ccr5$^{-/-}$ splenocytes for Il10 mRNA expression was also less pronounced and the difference observed for mRNA expression of the Th2-associated transcription factors Gata3 and Stat6 was lost upon *in vitro* cultivation. Interestingly, mRNA for Itgam (protein name CD11b) showed an increase (6.2 fold) in Ccr5$^{-/-}$ spleen cells compared to wildtype splenocytes after cultivation.

3.2.3 In vitro cultivated Ccr5$^{-/-}$ splenocytes show increased frequencies of CD206^{+} cells

To confirm these findings on protein level, splenocytes were cultured for 24h in Teflon bags to allow easy detachment of adherent cells for subsequent flow cytometric analysis of AAM marker expression. In this experiment, antibodies directed against CD204 and CD206 were used to quantify the effect of Ccr5 deficiency on alternative macrophage activation. Both proteins are known to be up-regulated in alternatively activated macrophages and have a function as phagocytic receptors [160]. The antibody directed against CD204 recognizes an epitope present on macrophage scavenger receptors 1 and 2 (gene symbols Msr1 and Msr2) and the antibody directed against CD206 recognizes the mannose receptor C type 1 (gene symbol Mrc1).

Analysis of flow cytometry data revealed that Ccr5$^{-/-}$ splenocytes have higher frequencies of CD11b^{+} (4.2% *vs.* 2.6%) and CD206^{+} (5.9% *vs.* 3.8%) cells than splenocytes from wildtype mice (**Figure 25**, lower panel). Frequencies of CD204^{+} cells did not differ between wildtype and Ccr5$^{-/-}$ splenocytes (**Figure 25**, upper panel). Surprisingly, subpopulations with double-positive (CD11b^{+}/CD204^{+} or CD11b^{+}/CD206^{+}) staining could not be identified. This finding suggests that a subpopulation other than CD11b^{+} macrophages in the spleen expresses the alternative activation markers CD204 (Msr1/Msr2) and CD206 (Mrc1).

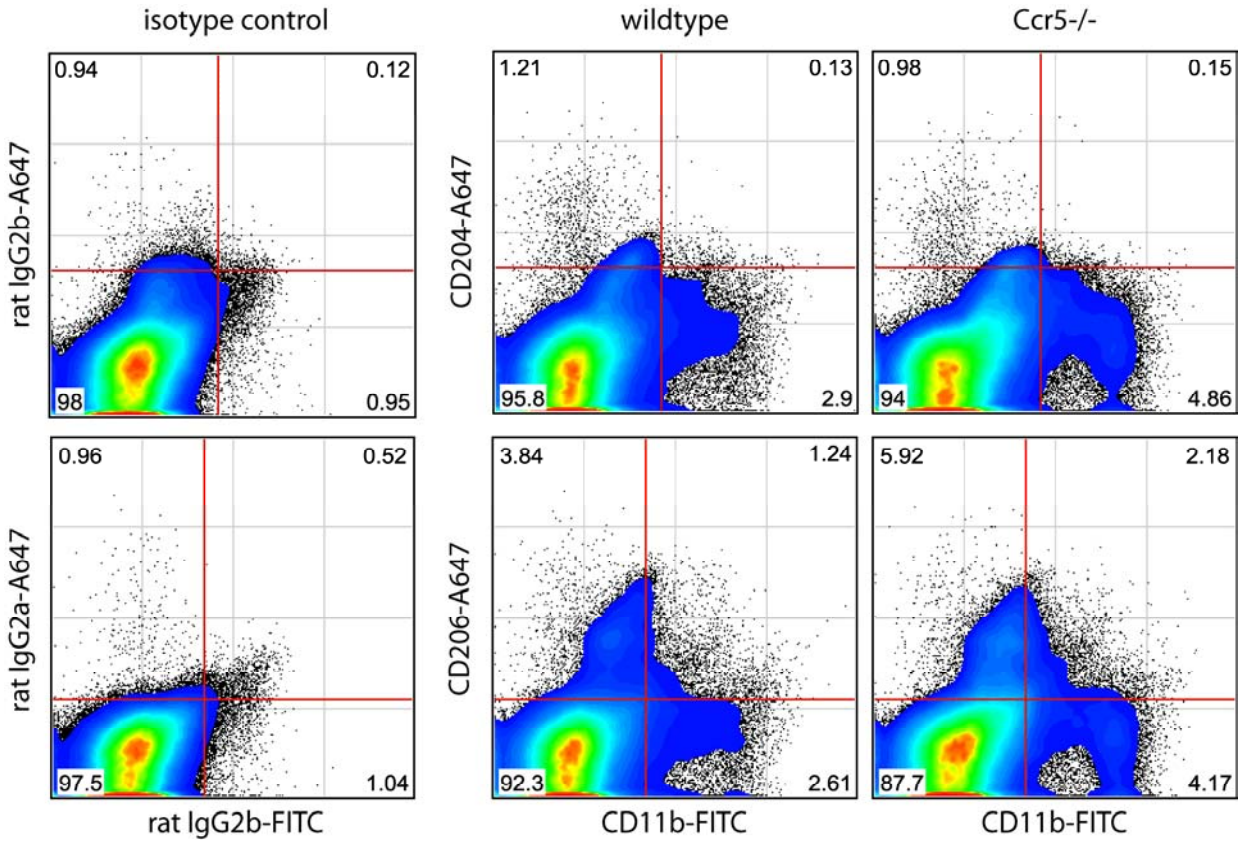

Figure 25. Effect of Ccr5-deficiency on surface expression of AAM markers CD204 (macrophage scavenger receptors 1 and 2) and CD206 (mannose receptor C type 1) on splenocytes from unchallenged mice. Splenocytes from unchallenged mice (C57BL/6, male, 18w, n=1) were harvested and cultivated in Teflon bags at a density of $1.0x10^6$ cells/ml in SSB medium. After resting for 24h at 37°C and 10% CO_2 the cells were harvested, remaining erythrocytes were lysed and surface staining of CD11b and CD204 (upper panel) or CD206 (lower panel) was performed using fluorochrome-conjugated antibodies as described in materials and methods. Isotype-matched control antibodies were used to check unspecific binding (plots on the left). 300,000 events were counted in every sample. For analysis a gate was set in an FSC-SSC plot to exclude debris and remaining erythrocytes and quadrant gates were set according to isotype control antibodies.

3.2.4 Polarization of cultivated peritoneal macrophages

Observations made in renal allograft rejection and in the spleen under basal conditions show that Ccr5 deficiency results in a shift towards alternative macrophage activation. To further explore the possibility that this effect might be a general phenomenon of Ccr5 deficiency, mRNA expression of macrophage activation marker genes was analyzed in an inflammatory

model of experimental peritonitis. Intraperitoneal injection of sterile thioglycollate solution causes the rapid influx of granulocytes, consisting primarily of neutrophils, in the first few hours after injection. Between day 3 and 5 after injection, peritoneal cells mainly consist of macrophages. Thus, harvesting peritoneal cells by lavage at this time point yields cell populations consisting predominantly of macrophages [217, 218].

In a first experiment, peritoneal lavage cells (PLCs) from 4 mice per genotype were harvested 4 days after thioglycollate-injection, pooled and cultured for 2 days. Non-adherent cells were removed 24h after plating by washing, while adherent cells (mostly macrophages) were further incubated. Subsequently, peritoneal macrophages were incubated for 24h with or without IL-4, which is the typical inductor of alternative macrophage activation. Already under unstimulated conditions, considerably increased AAM marker mRNA expression (Arg1) was observed in $Ccr5^{-/-}$ peritoneal macrophages compared to wildtype cells (**Figure 26A**). Upon IL-4 stimulation Arg1 mRNA levels increased dramatically, but the differences between wildtype and

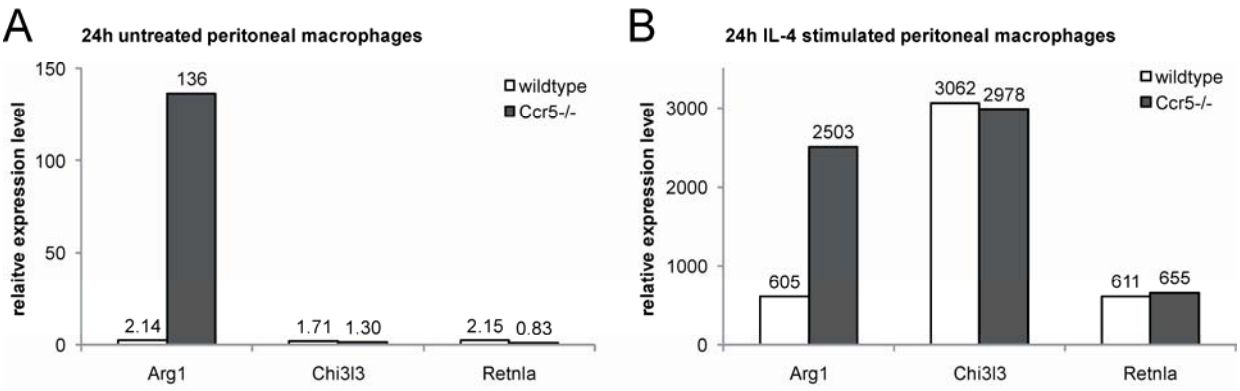

Figure 26A-B. Effect of Ccr5 deficiency on gene expression of macrophage polarization markers in thioglycollate-elicited peritoneal lavage cells (PLCs) after *in vitro* cultivation. PLCs were harvested from the peritoneal cavity 4 days after i.p. injection of 2.5 ml 4% thioglycollate solution. Cells from 4 mice (C57BL/6) were pooled, plated into the wells of 6 well plates ($10x10^6$ cells/well) and incubated in 3 ml PM medium/well for 24h at 37°C and 5% CO_2. After this time, non-adherent cells were removed, while adherent PLCs (mostly macrophages) were further incubated for 24h. Following this initial *in vitro* cultivation period, medium was replaced and cells were either left untreated (**A**) or stimulated with 100 ng/ml IL-4 (**B**) for 24h. Afterwards, total RNA was prepared and mRNA expression of marker genes for AAMs (Arg1, Chi3l3 and Retnla) was analyzed by real-time RT-PCR.

Ccr5-deficient cells were less pronounced as compared to the unstimulated situation (**Figure 26B**). Although, mRNA expression of the AAM marker genes Chi3l3 and Retnla increased dramatically upon IL-4 stimulation, no differential expression was observed between wildtype and $Ccr5^{-/-}$ PLCs.

Next, experiments were made to verify these findings on a single animal basis, but due to large intragroup variability – especially when using female mice – these results could not be replicated yet (data not shown).

3.2.5 Generation and phenotypic evaluation of BMDM

3.2.5.1 Phenotype of BMDM

Splenocytes and peritoneal lavage cells as well represent highly heterogeneous cell populations making it difficult to attribute specific effects to a certain cell population. Therefore, a system was established to generate large quantities of highly pure macrophages. Bone marrow cells were cultivated in petri dishes using medium with recombinant murine M-CSF (macrophage colony stimulating factor) to drive macrophage differentiation. The cells were differentiated for 8d and then incubated for 48h in medium without M-CSF to obtain a non-proliferative state receptive to stimulation. To assess the polarization state of these BMDM mRNA levels of AAM and CAM signature genes as well as Th1 and Th2 associated gene markers were determined (**Table 8**). The mRNAs for Chi3l3, Msr2 and Il4ra were moderately increased (1.6x) and Retnla mRNA showed a 5.9x increase in $Ccr5^{-/-}$ BMDM. The remainder of the investigated AAM signature genes (Arg1, Mrc1, Mrc2, Mmp12, Trem2, Il10 and Stat6) was not differentially expressed in $Ccr5^{-/-}$ BMDM compared to wildtype BMDM. Il4 mRNA expression was below detection limit (data not shown). On the other hand, the Th1-associated marker gene Ccl5 showed a moderate 1.7x fold decrease in $Ccr5^{-/-}$ BMDM (**Table 8**). The Th1-associated marker genes Tnf and Ccl3 did not show differential expression between wildtype and $Ccr5^{-/-}$ BMDM

Table 8. Effects of Ccr5 deficiency on mRNA expression in unstimulated BMDM. BMDM were generated from male C57BL/6 mice (wildtype: n=3, $Ccr5^{-/-}$: n=2) by plating bone marrow cells on tissue culture dishes and cultivation for 8 days in BBM medium in the presence of recombinant murine M-CSF (20 ng/ml). After this time BMDM were harvested and cultivated for 48h in tissue culture 6 well plates with BBM medium without M-CSF (3 ml/well). Total RNA was prepared and subjected to real-time RT-PCR analysis.

probe	marker type	wildtype mean relative expression	Ccr5-/- mean relative expression	ratio Ccr5-/- vs wt
Arg1	AAM	0.17	0.18	1.07
Chi3l3	AAM	0.81	1.32	1.63
Retnla	AAM	5.72	33.8	**5.92**
Mrc1	AAM	206	169	-1.22
Mrc2	AAM	39.3	49.2	1.25
Mmp12	AAM	881	788	-1.12
Msr2	AAM	57.3	92.4	1.61
Trem2	AAM	265.3	259	-1.03
Il10	Th2, AAM	14.0	13.9	-1.01
Il4ra	Th2, AAM	160	271	1.69
Stat6	Th2, AAM	86.0	80.4	-1.07
Tnf	Th1	26.1	21.8	-1.20
Ccl3	pro-inflammatory, Th1	2.48	2.36	-1.05
Ccl4	pro-inflammatory	51.9	59.4	1.14
Ccl5	pro-inflammatory, Th1	14.5	8.41	-1.72
Itgam	macrophages	46.8	47.5	1.02
Emr1	macrophages	61.7	68.6	1.11
Csf1	MΦ proliferation	389	364	-1.07
Csf1r	MΦ proliferation	2132	2637	1.24

and the Th1/CAM signature genes Ifng, Il12a and Nos2 were expressed below detection limit (data not shown). In summary, mRNA expression of AAM and Th2 signature genes is only moderately increased in unstimulated $Ccr5^{-/-}$ BMDM compared to wildtype BMDM. However, mRNA expression levels of CAM- and Th1-associated markers were either very weak or tended to decrease in $Ccr5^{-/-}$ BMDM compared to wildtype BMDM in most cases. In addition, BMDM generated in this way showed marked mRNA expression of macrophage markers Itgam (protein name CD11b) and Emr1 (protein name F4/80) (**Table 8**). Nevertheless, no differential expression was found for the investigated macrophage markers between wildtype and $Ccr5^{-/-}$ BMDM. Interestingly, the highest mRNA expression levels were observed for the M-CSF gene

(Csf1) and its associated receptor Csf1r (**Table 8**). The high abundance of Csf1r, Emr1 and Itgam mRNAs suggests that the generated cell population consists predominantly of macrophages.

Since BMDM showed no genotype-specific differences for AAM marker expression under unstimulated conditions macrophage polarization was analyzed after stimulation with IL-4, which is the classical inductor of AAMs. Arginase converts L-arginine to urea and ornithine whereas the competing enzyme nitric oxide synthase generates nitrite and citrulline from the same substrate [219]. Therefore, arginase enzyme activity and NO production assays were established to determine macrophage polarization on a functional level. Urea production was determined in protein lysates and nitrite concentrations in supernatants of wildtype and $Ccr5^{-/-}$ BMDM under vehicle- and IL-4 stimulated conditions (**Figure 27A-C**).

Under unstimulated conditions no significant differences were observed for mRNA expression of the AAM signature genes (**Figure 27A)** and for NO production between wildtype and $Ccr5^{-/-}$ BMDM. However, arginase enzyme activity showed a slight but significant increase in $Ccr5^{-/-}$ BMDM without IL-4 stimulation (**Figure 27B**). Upon IL-4 stimulation mRNA expression of the AAM signature genes Arg1, Chi3l3 and Retnla increased dramatically in both groups and surprisingly, mRNA expression of Chi3l3 and Retnla was significantly reduced in $Ccr5^{-/-}$ compared to wildtype BMDM (**Figure 27A**). On a functional level, the presence of IL-4 markedly stimulated arginase enzyme activity and reduced NO production in comparison to unstimulated samples but differences between wildtype and $Ccr5^{-/-}$ BMDM were not observed (**Figure 27B+C**). In summary, the results on the functional level reflect the findings on mRNA level showing only a mild trend towards an alternative activation phenotype of $Ccr5^{-/-}$ BMDM.

These findings fostered the idea, that BMDM might need an initial maturation or priming step in order to obtain an alternative activation phenotype. For that reason cells were primed with different stimuli before addition of IL-4 to induce alternative activation. Bacterial lipopolysaccharide (LPS) was used to trigger macrophage activation. LPS is a component of the

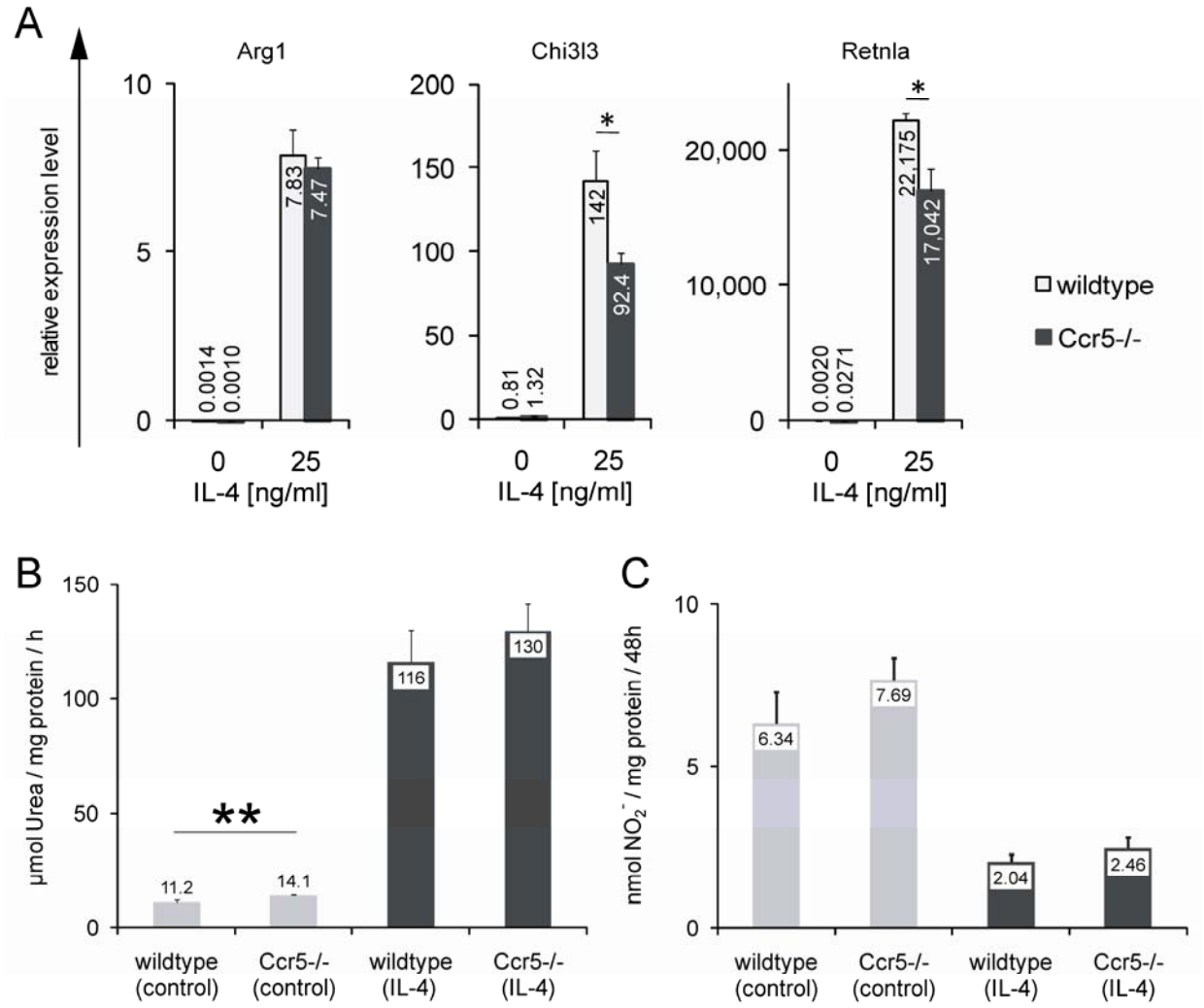

Figure 27A-C. Effect of Ccr5 deficiency on AAM marker expression, urea and NO production in BMDM. BMDM (C57BL/6, n=3, all male) were plated into the wells of 6 well plates for expression analysis **(A)** or 12 well plates for functional assays **(B+C)** at a density of $0.5x10^6$ cells/ml and cultivated with BBM medium alone or with murine recombinant IL-4 (25 ng/ml) for 48h. **(A)** Total RNA was subjected to real-time RT-PCR to determine mRNA levels of AAM signature genes Arg1, Chi3l3 and Retnla. Protein lysates were used to determine arginase enzyme activity **(B)** and supernatants were used to determine NO production **(C)**. *: $p < 0.05$.

cell wall of Gram-negative bacteria and induces classical activation of macrophages. Furthermore, interferon gamma (IFN-γ) was applied as a non-pathogen derived stimulus for macrophages. However, in this experiment no differences for the mRNA expression of AAM markers Arg1, Chi3l3 or Retnla were observed besides a slight increase of Arg1 mRNA after LPS/IL-4 stimulation (**Figure 28**). Furthermore, treatment with D-PBS, LPS or IFN-γ alone did not

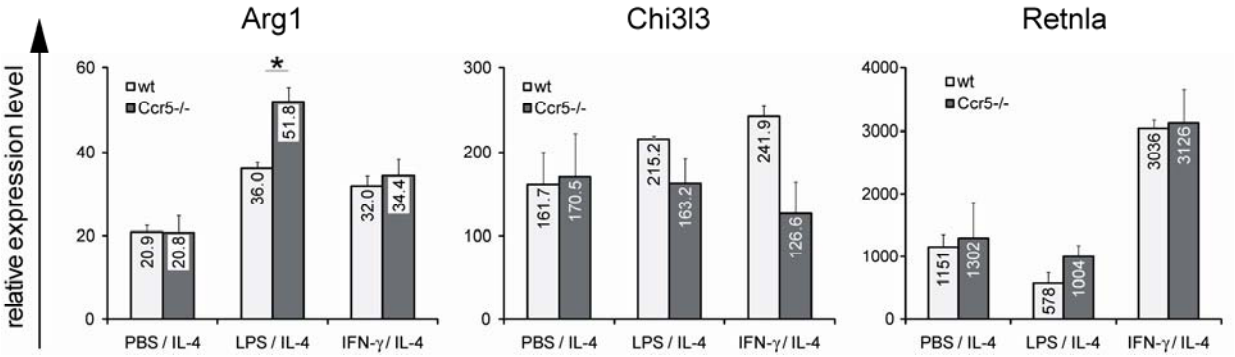

Figure 28. Effect of Ccr5 deficiency on AAM marker mRNA expression in pre-stimulated BMDM. $1.5x10^6$ BMDM (C57BL/6, n=2) were plated into each well of a 6 well plate with 3 ml BBM medium/well and allowed to adhere for 6h. After this time LPS (100 ng/ml), murine recombinant IFN-γ (10 ng/ml) or D-PBS (vehicle control) were added and the cells were incubated at 37°C and 5% CO_2. After 18h medium was replaced by IL-4 containing medium (25 ng/ml) and cells were incubated for 48h. Total RNA was prepared from these cells and subjected to real-time RT-PCR analysis. *: $p<0.05$.

induce any significant differences in Arg1, Chi3l3 and Retnla mRNA expression between wildtype and $Ccr5^{-/-}$ BMDM (data not shown).

The mRNA expression of AAM (Arg1, Chi3l3 and Retnla) and CAM (Nos2) signature genes might show time-dependent differences. Therefore, a time-course experiment was performed. Wildtype BMDM were stimulated with IL-4 and cells were harvested after 24, 48, 72 and 120h. While Arg1 mRNA decreased steadily over time, expression of Retnla mRNA peaked between 48 and 72h (**Figure 29**). Interestingly, expression levels of Chi3l3 mRNA were rather low from 24 to 72 h but increased drastically after 72h. In comparison to the AAM markers, expression of Nos2 mRNA was extremely low between 24 and 72h, but increased noticeably after 72h suggesting that IL-4 availability starts to decline at this time resulting in the release of Nos2 suppression. These results clearly show that the time courses of individual AAM signature genes are different.

It was unclear, whether the AAM observed in renal allografts from Ccr5-deficient recipients originated from the allograft (= BALB/c) or from the recipient (= C57BL/6). Therefore, an IL-4 dose-response experiment was performed with wildtype and Ccr5-/- BMDM generated from BALB/c mice (**Figure 30A-D**). In wildtype as well as $Ccr5^{-/-}$ BMDM from BALB/c mice expression

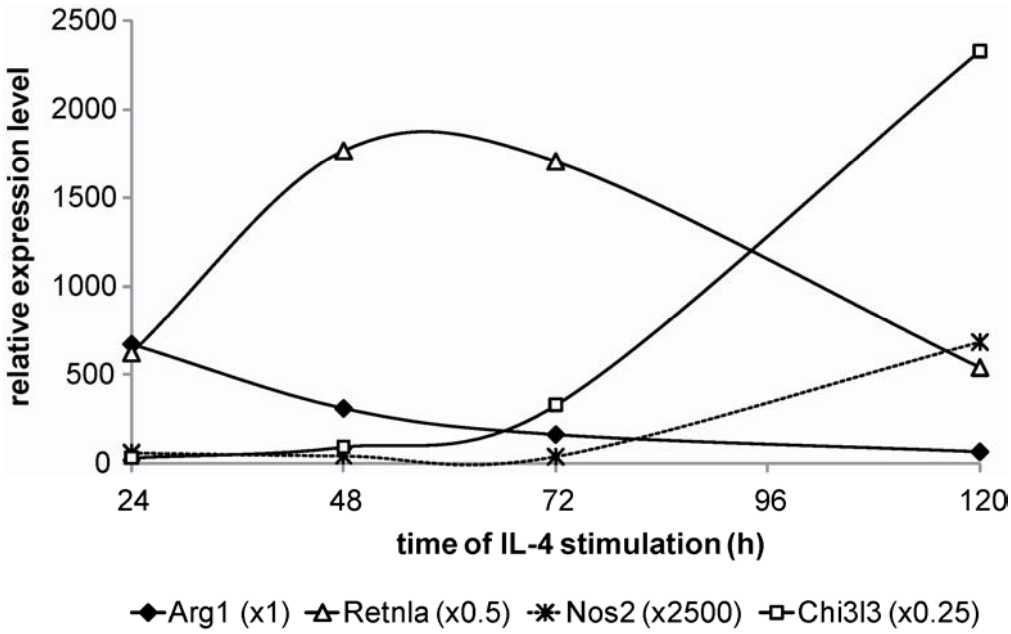

Figure 29. Time course of marker gene expression in IL-4 stimulated wildtype BMDM. Wildtype C57BL/6 BMDM were generated in Petri dishes and $1.5x10^6$ cells were plated into each well of a 6 well plate with 3 ml BBM medium per well and stimulated with murine recombinant IL-4 (10 ng/ml). Cells were lysed at the indicated time points and total RNA was prepared. Expression levels for each gene were adjusted with the indicated factors in brackets to allow side by side comparison on the same axis of ordinates.

of the AAM signature genes Arg1, Chi3l3 and Retnla increased in a dose-dependent manner. Without IL-4 (0 ng/ml), Arg1, Chi3l3 and Retnla mRNA was undetectable in wildtype and $Ccr5^{-/-}$ BALB/c BMDM (**Figure 30A**). At 0.4 ng/ml IL-4, mRNA expression of all three markers was slightly increased in wildtype BABL/c BMDM compared to $Ccr5^{-/-}$ BALB/c BMDM. Interestingly, at concentrations from 2 to 50 ng/ml IL-4 $Ccr5^{-/-}$ BALB/c BMDM showed consistently increased expression of Arg1 and Chi3l3 mRNA compared to wildtype BALB/c BMDM with the strongest differences at a concentration of 10 ng/ml IL-4. However, Retnla mRNA levels did not differ significantly in wildtype and $Ccr5^{-/-}$ BALB/c BMDM at any concentration of IL-4. The mRNA expression of the CAM marker gene Nos2 decreased in an IL-4-dependent manner in wildtype as well as $Ccr5^{-/-}$ BALB/c BMDM. However, at low concentrations of IL-4 (0 and 0.4 ng/ml) Ccr5-deficient BMDM from BALB/c mice showed considerably less Nos2 mRNA expression as wildtype BALB/c BMDM (**Figure 30A**). In contrast, BMDM from C57BL/6 mice showed mRNA

expression of Arg1, Chi3l3 and Retnla already under unstimulated conditions and the Retnla mRNA levels were considerably increased in Ccr5$^{-/-}$ compared to wildtype C57BL/6 BMDM but the differences did not reach statistical significance due to large inter-animal variability (**Figure 27A**). To further corroborate these findings on a functional level arginase enzyme activity and nitrite production were determined in BALB/c BMDM stimulated for 48h with different concentrations of IL-4 (**Figure 30B-D**). Nitrite production decreased already under unstimulated conditions in Ccr5$^{-/-}$ BMDM as compared to wildtype BMDM (**Figure 30B**). With increasing amounts of IL-4, NO production diminished in BMDM of both genotypes. However, at 25 ng/ml IL-4 nitrite production in Ccr5$^{-/-}$ BMDM slightly increased, resulting in comparable NO

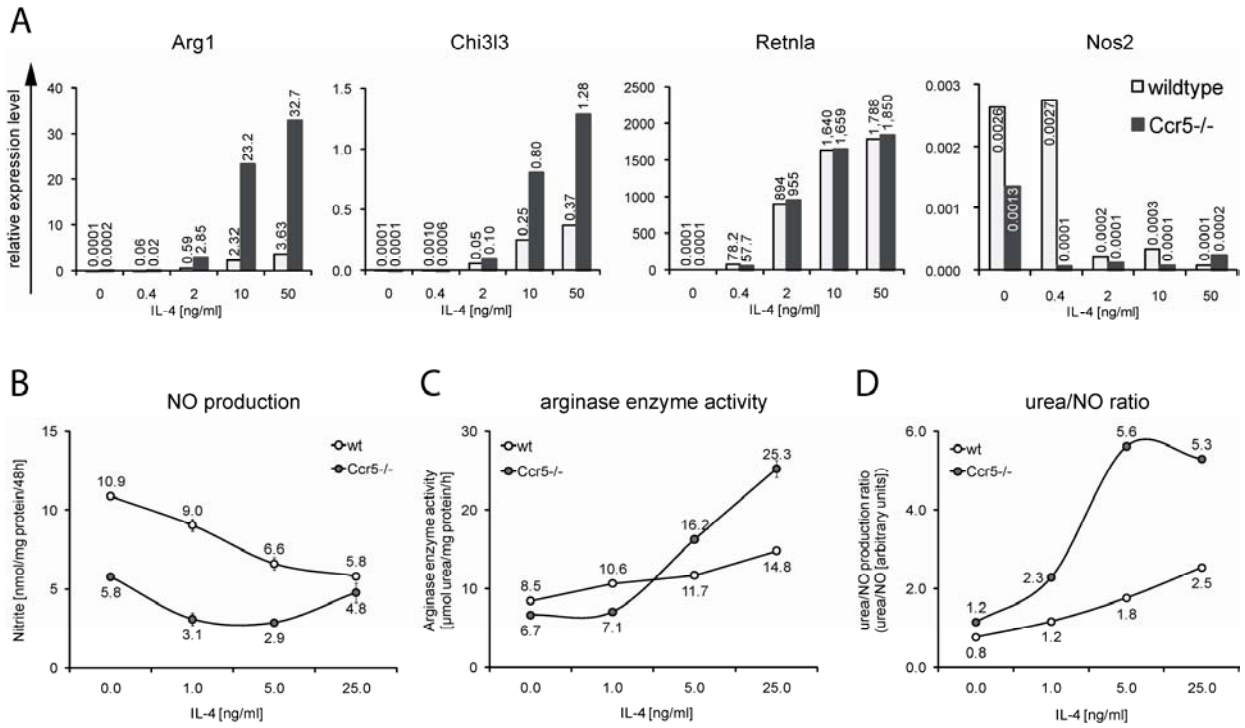

Figure 30A-D. Mouse strain contribution to macrophage polarization in wildtype and Ccr5$^{-/-}$ BMDM. **(A)** BMDM from wildtype and Ccr5$^{-/-}$ BALB/c mice (n=1) were plated into the wells of 6 well plates for expression analysis **(A)** or 24 well plates for functional assays **(B-D)** at a density of 0.5x10^6 cells/ml (BBM medium). The cells were cultivated for 24h before incubation with BBM medium alone or with varying concentrations of murine recombinant IL-4 for 48h. **(A)** Total RNA was subjected to real-time RT-PCR to determine mRNA levels of AAM signature genes (Arg1, Chi3l3 and Retnla) and the CAM marker gene Nos2. Protein lysates were used to determine arginase enzyme activity **(B)** and supernatants were used to determine NO production **(C)**. **(D)** shows urea/NO production ratios to indicate the general macrophage polarization status.

production levels in BMDM of both genotypes. Arginase enzyme activity increased in BMDM of both genotypes in a dose-dependent manner. While arginase enzyme activity was comparable in BMDM of both genotypes at 0 and 1.0 ng/ml IL-4, arginase enzyme activity was elevated in $Ccr5^{-/-}$ BMDM at IL-4 concentrations of 5.0 and 25.0 ng/ml compared to wildtype BMDM (**Figure 30C**).

Macrophage polarization is a continuous process showing also intermediate phenotypes between the (extreme) endpoints of alternative and classical activation [163]. Thus, the ratio of arginase enzyme activity to nitrite production was calculated to determine the general effect of Ccr5 deficiency on macrophage polarization (**Figure 30D**). This ratio showed a dose-dependent increase in BMDM of both genotypes, but ratios were higher at all tested concentrations in $Ccr5^{-/-}$ BMDM compared to wildtype BMDM. This result suggests that L-arginine is predominantly degraded by arginase and might be limited to nitric oxide synthase in Ccr5-deficient BMDM.

In summary, these findings suggest that BMDM from BALB/c mice are more easily skewed towards an alternative activation phenotype in the absence of Ccr5 than BMDM derived from C57BL/6 mice.

3.2.5.2 Phenotype of BMDM generated in Teflon bags

Teflon is the brand name coined by DuPont for the synthetic fluorocarbon polymer polytetrafluoroethylene (PTFE). Teflon foil is a transparent, biologically inert material that is gas permeable but impermeable to water and electrolytes. Consequently, for cells grown directly on Teflon foil the medium does not act as a diffusion barrier allowing optimal growth conditions. Due to the high electronegativity of fluorine and the strength of the carbon-fluorine bonds PTFE is not wetted by water- or oil-containing substances and is chemically non-reactive. The use of heat-sealed Teflon bags to generate highly pure populations of macrophages from

bone marrow precursor cells has already been described in the early 1970s [220-222]. Macrophages generated in Teflon bags offer several advantages over conventional BMDM generated in Petri dish plates. On the one hand, macrophages adhere only weakly to the hydrophobic Teflon bags allowing easy detachment of cells thereby minimizing cellular damage which would be induced by the use of proteases such as Trypsin. The Teflon bags are simply put on ice for 30 minutes resulting in quantitative detachment of the cells from the hydrophobic surface. On the other hand, Teflon bags provide means of generating high amounts of ≥95% pure macrophages (80-100x10^6 from a single mouse). The fact that no medium changes are required during the differentiation period reduces growth factor consumption and the risk of contamination. Additionally, macrophages obtained from Teflon bags can be passaged for several weeks allowing a constant source of cells for experiments.

Characterization of BMDM generated in Teflon bags

To investigate the changes in the composition of the bone marrow cells during the differentiation period DiffQuick stained cytospins were prepared from fresh bone marrow cells and from bone marrow cells that were cultivated in Teflon bags in the presence of L929s supernatant for 10 days (**Figure 31**). Fresh bone marrow was mainly composed of cells resembling polymorphonuclear leukocytes and to a lesser extent of cells with lymphocyte or monocyte morphology (**Figure 31A**). In striking contrast, cells generated by 10 days incubation of bone marrow in Teflon bags showed a highly uniform macrophage-like morphology (compare [223] and [195]) with extended and vesicle-rich cytoplasm (**Figure 31B**).

In the next step, expression analysis of certain cell-specific markers by flow cytometry was performed to confirm the impression that Teflon bag cultured bone marrow cells consist mainly of macrophages (**Figure 32**). To this end, fluorochrome-labeled antibodies directed against the typical macrophage markers CD11b and F4/80 were used. Antibodies directed against CD11c

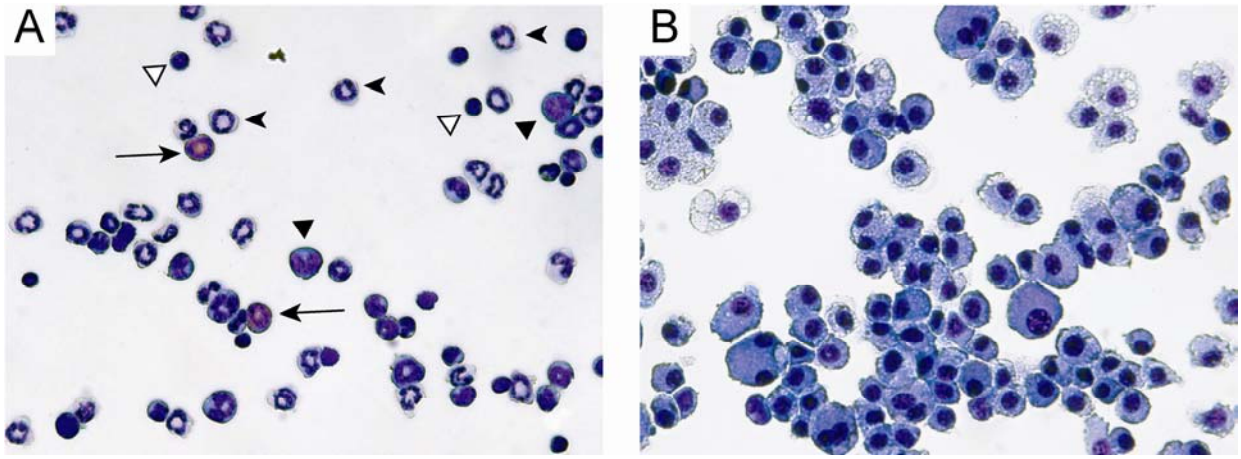

Figure 31. DiffQuick stained cytospins of fresh bone marrow cells (A) and BMDM generated by culture of unfractioned bone marrow in Teflon bags for 10 days (B). Arrows: eosinophils, arrowheads: neutrophils, white triangles: lymphocytes and black triangles: monocytes. Note the large vesicle-rich cytoplasm of cells in shown **(B)**. Both photomicrographs 400x.

(dendritic cells), Gr-1 (granulocytes), CD3ε (T cells), CD19 (B cells) and NK1.1 (natural killer cells) were used to exclude the presence of other cell types. Furthermore, an antibody against CD45 was applied to determine the percentage of leukocytes within the generated cell population. Isotype-matched antibodies without a relevant specificity were used as controls for unspecific binding (isotype controls). Non-viable cells were excluded from the analysis by staining with 7-AAD (7-amino-actinomycin D), a fluorescent chemical compound that intercalates with nucleic acids of dead and dying cells but is efficiently excluded from viable cells [197]. We speculated that Ccr5 deficiency might already have an effect at the level of macrophage differentiation and therefore included cells from Ccr5-deficient mice in this analysis. Nearly all BMDM were positive for CD11b and F4/80 (≥98.5%). No differences were observed for CD11b and F4/80 expression between wildtype and $Ccr5^{-/-}$ BMDM. BMDM were also highly positive for the common leukocyte antigen CD45 (wildtype: 79.2%, $Ccr5^{-/-}$: 87.9%) whereas expression of CD3ε (T cells), NK1.1 (NK cells) or Gr-1 (granulocytes) did not exceed isotype control antibody levels. Interestingly, BMDM showed moderate expression of CD19 and CD11c. Both of these markers were differentially regulated between wildtype and $Ccr5^{-/-}$ BMDM ($CD19^{+}$: wt: 20.7%, $Ccr5^{-/-}$: 12.3%; $CD11c^{+}$: wt: 8.20%, $Ccr5^{-/-}$: 20.6%) (**Figure 32**). However, additional experiments

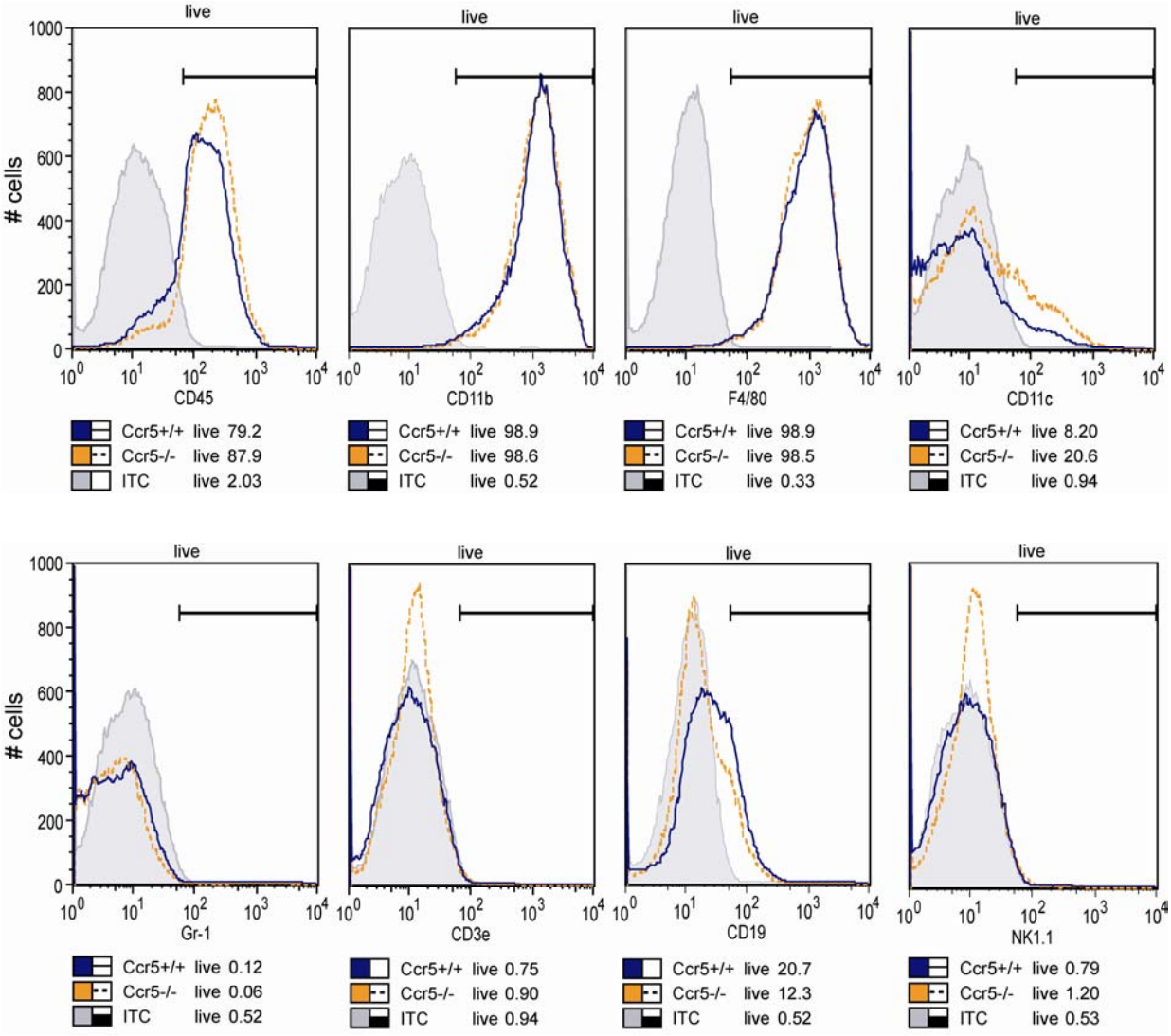

Figure 32. Flow cytometric characterization of wildtype and Ccr5$^{-/-}$ BMDM generated in Teflon bags. Bone marrow cells (n=1) were seeded into Teflon bags containing 50 ml differentiation DBM medium at a density of 10x10^6 per bag before flow cytometric analysis. BMDM were harvested after 10 days incubation at 37°C and 10%CO_2 and stained for the indicated surface markers. Live/dead cell discrimination was carried out using 7-AAD and an appropriate live cell gate was set (FL3 (7-AAD) *vs.* FSC). 50,000 events were counted for each sample. Results of analysis are shown as histograms: isotype control antibody (ITC, shaded areas), wildtype (Ccr5$^{+/+}$, blue lines) and Ccr5$^{-/-}$ BMDM (orange dotted lines). Markers used are: CD45 (common leukocyte antigen), CD11b (macrophages), F4/80 (macrophages), CD11c (dendritic cells), Gr-1 (granulocytes), CD3ε (T cells), CD19 (B cells) and NK1.1 (NK cells). Numbers below each histogram indicate percentages of positive live cells in plotted regions which were set according to isotype control antibodies.

with increased numbers of animals are required to confirm these differences. In conclusion, these data show that cell populations are highly pure macrophages on the basis of morphology and expression of the macrophage markers CD11b and F4/80.

Effect of Ccr5 deficiency on macrophage polarization of BMDM generated in Teflon bags

To study the effect of Ccr5 deficiency on macrophage polarization Teflon bag BMDM (C57BL/6) were stimulated with IFN-γ+LPS to induce classical activation and the combination of IL-4+IL13 was applied to provoke alternative activation. Unstimulated samples were carried along to investigate macrophage polarization under basal conditions (**Figure 33**).

In vehicle-treated BMDM from $Ccr5^{-/-}$ mice a slight and statistically not significant increase for Chi3l3 (5.6x) and Retnla (2.1x) mRNA expression was observed compared to wildtype BMDM, while Arg1 and Mmp12 mRNA levels were not influenced by loss of Ccr5. Combined stimulation of BMDM with IL-4+IL-13 (each 20 ng/ml, for 24h) induced a dramatic up-regulation of Arg1 (~140x), Chi3l3 (~680x) and Retnla (~7100x) and a moderate increase of Mmp12 (~1.8x) mRNA expression compared to vehicle-treated BMDM. However, these AAM marker genes were not differentially regulated in $Ccr5^{-/-}$ compared to wildtype BMDM upon IL-4+IL-13 stimulation. Interestingly, combined stimulation with IFN-γ+LPS – stimuli typically inducing classical macrophage activation – resulted in significantly increased mRNA expression of AAM markers Arg1 (1.9x) and Mmp12 (1.6x) in $Ccr5^{-/-}$ compared to wildtype BMDM (**Figure 33**). Furthermore, $Ccr5^{-/-}$ BMDM showed 5.1x up-regulation of Retnla mRNA in response to IFN-γ+LPS compared to wildtype BMDM. However, this difference did not reach statistical significance due to large inter-animal variability. The increased expression of AAM marker genes in $Ccr5^{-/-}$ BMDM upon IFN-γ+LPS stimulation suggests that CCR5 exerts a suppressive effect on alternative macrophage activation under conditions that normally lead to classical macrophage activation.

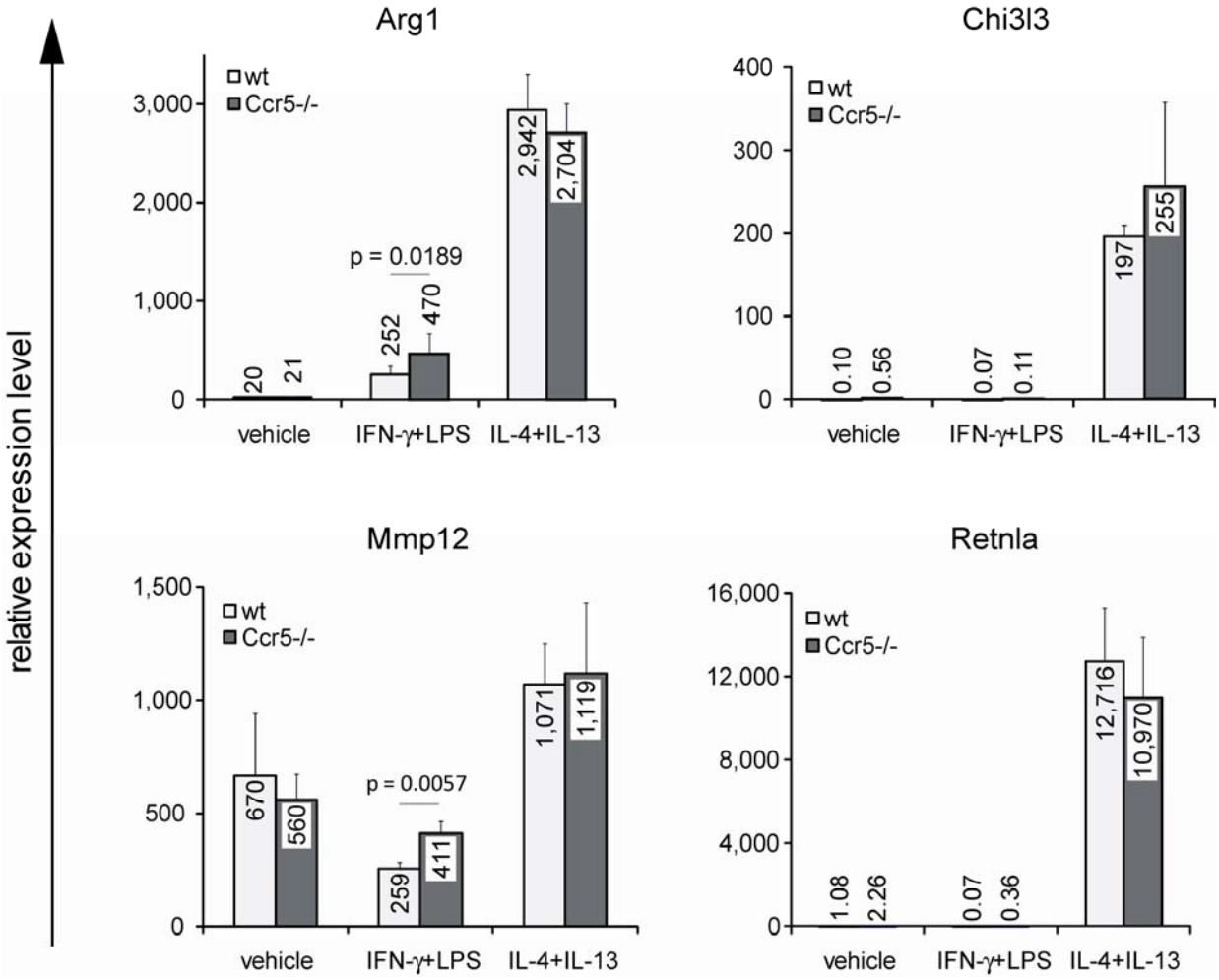

Figure 33. Effect of Ccr5 deficiency on mRNA expression AAM marker genes (Arg1, Chi3l3, Mmp12 and Retnla in stimulated BMDM generated in Teflon bags. Bone marrow cells (C57BL/6, male, 22-24w, n=4) were differentiated to BMDM in Teflon bags and plated in the wells of 6 well plates at a density of $2.5x10^6$ cells/well in 3 ml SSB medium/well. 3h after seeding (adherence period) stimuli were added in final concentrations of 20 ng/ml (IFN-γ, IL-4 and IL-13) or 100 ng/ml (LPS) and cells were further incubated for 24h at 37°C and 10% CO_2. After this time total RNA was prepared from the stimulated BMDM and subjected to real-time RT-PCR. Depicted are means ± SD of relative expression levels. Statistical significance (p) was calculated using Student's t test.

4 DISCUSSION

The mechanisms underlying improved allograft function and long-term consequences due to loss of Ccr1 or Ccr5 are not well understood. Therefore, a murine renal transplantation model was utilized, which allows the study of both the acute and the clinically more important phase of chronic allograft rejection without additional immunosuppression [224]. Wildtype BALB/c (H-2^d) mice served as donors of renal allografts, which were transplanted into bilaterally nephrectomized C57BL/6 (H-2^b) mice as recipients resulting in a full MHC-mismatch and a maximal severity of transplant rejection. Besides wildtype, $Ccr1^{-/-}$ and $Ccr5^{-/-}$ recipient mice, mice lacking both chemokine receptors ($Ccr1^{-/-}$/$Ccr5^{-/-}$) were included in this study to analyze potential additive or synergistic effects due to deficiency of both Ccr1 and Ccr5. Recipients of C57BL/6 isografts were used as a control. Effects of chemokine receptor deficiency on allograft function, histopathology, graft infiltration, expression of selected marker genes and humoral rejection were analyzed. $Ccr5^{-/-}$ recipients of renal allografts demonstrated massive alternative activation of intragraft macrophages as compared to wildtype recipients.

To answer the question, whether this phenomenon is specific for renal allograft rejection or if Ccr5 deficiency has a general impact on macrophage polarization the investigation was extended to macrophage populations in the spleen of unchallenged mice and to inflammatory macrophages elicited during experimental peritonitis.

Furthermore, methods to generate bone marrow-derived macrophages (BMDM) were established, which allowed analysis of highly pure macrophage populations.

The first two sections of the discussion (4.1 and 4.2) are intended to provide an overview to the marker genes used in this study and to the current knowledge of how the function of these genes might be related to allograft rejection.

4.1 Chemokines and chemokine receptors in allograft rejection

Chemokines and chemokine receptors play important roles during allograft rejection. In the first hours after transplantation, tissue injury caused by surgical trauma and ischemia-reperfusion triggers a series of events that finally induce the recruitment of leukocytes – mostly T cells and macrophages – from the peripheral blood into the allograft [101, 225]. Stressed allograft cells generate increased amounts of oxygen and nitric oxide radicals [226] which in turn leads to the release of inflammatory mediators such as platelet-activating factor and TNF. Furthermore, adhesion molecules are induced that enhance leukocyte rolling and firm adhesion to the endothelium [101]. In the next step, chemokines secreted by activated endothelial cells or platelets bind to the surface of activated endothelia in the allograft via glucosaminoglycans (GAGs) [227]. Rolling leukocytes that encounter chemokines presented on GAGs are activated resulting in surface expression of integrins and firm adhesion. In addition, chemokines also promote the following events of spreading, diapedesis and migration into the allograft [101, 127]. Interestingly, CCL5 was found to mediate CCR1-dependent firm adhesion, whereas CCR5 seems to be important for the process of leukocyte spreading [228]. During the process of extravasation T cells and monocytes express matrix metalloproteinases (MMPs), which degrade extracellular matrix components and promote leukocyte migration through basement membranes [101]. MMPs are also able to proteolytically cleave chemokines, thereby changing their receptor specificity, affinity or activity. Consequently, MMPs might alter or regulate chemokine signaling and contribute to differential cell recruitment [21, 101, 229].

Additionally, chemokines contribute to allograft rejection by mediating traffic of dendritic cells from the allograft to secondary lymphoid organs (SLOs) [101]. The finding that mice lacking SLOs accept cardiac allografts indefinitely highlights the importance of this mechanism during allograft rejection [230]. Immature dendritic cells express inflammatory chemokine receptors such as CCR1, CCR2, CCR5 and CXCR1 which promote the immigration of dendritic cells into

inflamed tissues [231]. During the maturation process, dendritic cells loose expression of the inflammatory receptors and up-regulate chemokine receptors like CCR4, CCR7 and CXCR4 which guide mature DCs into SLOs where they activate naïve T and B lymphocytes. Interestingly, T cells show a reciprocal chemokine receptor expression pattern. Upon activation by dendritic cells expression of inflammatory chemokine receptors (CCR3, CCR5, CCR8, and CXCR3) increases in naïve T cells, whereas receptors for homing to lymphoid organs (CCR7 and CXCR4) are down-regulated [231]. Thereby, activated T cells acquire the ability to migrate into inflamed tissue and sites of allograft rejection. Besides their role in promoting allograft rejection, dendritic cells have been implicated to play an important role during tolerance induction by several processes including induction of regulatory T cells, polarization of T helper cell populations, depletion of tryptophan needed for T cell activation as well as initiation of T cell anergy and deletion [232, 233]. Furthermore, chemokines are able to selectively control leukocyte influx. While Th1 cells preferentially express the chemokine receptor CCR5 and CXCR3, Th2 polarized cells favorably expresses CCR3 and CCR4 [234]. Additionally, CCR6 expression was recently demonstrated on the newly discovered Th17 cell population and Bromley *et al.* suggested that corresponding to each of these effector Th cell subsets a subset of regulatory T cells exists with a similar pattern of chemokine receptor expression [235].

Besides T cells, chemokines influence migration of circulating monocytes to sites of inflammation. In the mouse, monocytes can be divided into two subsets according to differential expression of chemokine receptors. The first set is characterized by high expression of CX_3CR1 and low expression of CCR1, CCR2, Gr-1 and L-selectin. These are long-lived ‘resident monocytes’ which home to non-inflamed sites and serve as precursors of resident tissue macrophages. A second set of short-lived ‘inflammatory monocytes’ displays low expression of CX_3CR1 and high expression of CCR2 and Gr-1 and is actively recruited to sites of inflammation

[157, 236]. Upon maturation into tissue macrophages expression of CCR1 and CCR5 increases whereas CCR2 expression is lost [45, 157, 237].

Little is known about chemokine receptor expression on activated macrophages. A study by Martinez *et al.* demonstrated that classically (IFN-γ+LPS) activated human macrophages have increased of *CCR7* and diminished *CCR1* mRNA expression, whereas alternative activation by IL-4 led to up-regulation of *CXCR4* [151]. Another study showed that IL-4 inhibits CCR5 expression, while growth factors (M-CSF and GM-CSF) induced CCR5 expression on human macrophages [238]. The immunosuppressive cytokine IL-10 was also shown to induce expression of CCR1, CCR2 and CCR5 in human monocytes [238, 239]. Classically activated macrophages produce chemokines that bind to pro-inflammatory chemokine receptors like CCR5 and CXCR3 expressed on Th1 cells, cytotoxic T cells and NK cells. By contrast, alternatively activated macrophages induce recruitment of basophils, eosinophils, Th2 cells, regulatory T cells and B cells by secretion of chemokines that bind to CCR3, CCR4 and CCR8 [151, 155, 157].

4.2 Role of T helper cells and regulatory T cells in allograft rejection and tolerance induction

Initially, Th1 cells (which produce IL-2, IFN-γ and TNF) – were thought to be the central mediators of rejection by supporting $CD8^+$ cytotoxic T cell development, delayed-type hypersensitivity (DTH) immune responses and macrophage activation as well as promotion of IgG2a isotype switching which facilitates complement activation and antibody-dependent cellular cytotoxicity [240-242]. In turn, activated $CD8^+$ cytotoxic T cells stimulate Th1 differentiation of naïve $CD4^+$ T cells by secretion of IFN-γ and the induction of IL-12 synthesis in alloreactive DCs [243]. On the other hand, Th2-type alloimmune responses have so far been associated with induction of tolerance and prolonged allograft survival due to suppressive effects of Th2 cytokines (IL-4, IL-5 and IL-13) on Th1 polarization and development of $CD8^+$

cytotoxic T cells [240, 242]. Furthermore, maternal tolerance of fetal tissues has been correlated with the presence of Th2 cells and deletion or anergy of $CD8^+$ cytotoxic T cells [242]. However, several lines of evidence suggest that Th2 cells are also able to promote allograft rejection. Neutralization of IFN-γ or IL-12 does not prolong allograft survival and even exacerbates rejection by an increase of eosinophil infiltration which has been associated with Th2-biased immune responses [241]. Additionally, depletion of $CD8^+$ T cells led to increased Th2 cytokine synthesis, eosinophil infiltration and Th2-promoted IgG1 production [244]. Another study showed that Th2 cytokines promote deposition of collagen and fibrous material within the graft thereby contributing to chronic rejection [242]. In contrast, neutralization of IL-4 or depletion of $CCR3^+$ cells (mainly Th2 cells and eosinophils) delays allograft rejection in models of CD4-restricted alloreactivity [241]. Interestingly, IFN-γ might have different functions during allograft rejection, since this cytokine is also required for tolerance induction by regulatory T cells [245-248]. In summary, these findings suggest that Th1 and Th2 cytokines play complex roles during allograft rejection and induction of tolerance [241].

The recent identification of a new pro-inflammatory $CD4^+$ T helper cell population that is distinct from Th1 and Th2 cells might help to explain discrepancies of the Th1/Th2 paradigm in the setting of allograft rejection. This new population is defined by the selective production of IL-17. Th17 cells specifically express the transcription factor RORγτ (gene symbol Rorc) which is induced by STAT3-mediated signaling in response to IL-6, IL-21 or IL-23. Antigen-presenting cells (APCs) produce IL-6 and IL-23 upon stimulation of pattern recognition receptors (*e.g.* TLRs) by "danger" signals. These signals include exogenous ligands (*i.e.* viral or bacterial molecular patterns) as well as endogenous ligands (*e.g.* hyaluronic acid, heparin sulfate, high mobility group box 1 HMGB1, *etc.*) that are released during infections or ischemia/reperfusion injury and transplant handling. Several studies report that TLR activation induces resistance to tolerance induction [241, 249-251]. Moreover, the nature of this signal determines the balance

between IL-12 and IL-23 production by APCs and therefore controls Th1 or Th17 differentiation, respectively [241]. IL-21 is produced by Th17 cells in an autocrine fashion, induces IL-23 receptor expression on Th17 cells and inhibits IFN-γ production by Th1 cells. Additionally, Th1 and Th2 cytokines were shown to suppress Th17 functions or antagonize TGF-β induced Th17 cell differentiation suggesting complex cross-regulation between these T helper cell populations [209]. IL-17 and IL-23 were suggested to induce neutrophil recruitment to sites of inflammation. Interestingly, cardiac allografts of $Ifng^{-/-}$ recipients exhibited increased IL-17 production and neutrophil infiltration indicating that Ifng-deficiency might lift inhibition of Th17 cell differentiation [209, 252]. During allograft rejection, IL-17 antagonism was shown to prolong allograft survival in a number of studies [253-255]. IL-17 blockade seems to prevent acute rejection more efficiently than chronic rejection indicating a role for IL-17 during early rejection [208]. Antonysamy *et al.* suggested that IL-17 promotes the maturation of alloreactive dendritic cells [254].

Besides their interaction with Th1 and Th2 cells, Th17 cells also show complex interactions with regulatory T cells. Treg cells specifically express the transcription factor Foxp3 and suppress Th1 and Th2 alloimmune responses. Foxp3 induces expression of molecules with an immunosuppressive function: CD39 generates adenosine from nucleotides which exerts suppressive effects on activated effector T (Teff) cells. Furthermore, Foxp3 up-regulates the immunosuppressive cytokine IL-35 and CTLA-4 (a negative co-stimulatory molecule) and represses production of cytokines such as IL-2, IL-4, IFN-γ and TNF [241]. Naïve $CD4^+$ T cells develop into Treg cells in the presence of TGF-β. However, in the presence of TGF-β and IL-6 naïve $CD4^+$ T cells develop into Th17 cells. Therefore, IL-6 was suggested to shift Treg differentiation towards Th17 development – a finding important for strategies targeting Treg cells for the induction of transplant tolerance, since IL-6 is induced during acute phase of

inflammation by ischemia/reperfusion injury [256] and has been associated with increased IL-17 levels in lung transplantation [209].

4.3 Effects of Ccr1 and Ccr5 deficiency on tolerance induction by regulatory T cells and inhibition of DTH reactions

Russell *et al.* already described in 1978 that certain donor-recipient combinations of H-2 incompatible mouse strains exhibit extended periods of renal graft survival (>60 days) without any further immunosuppression [224, 233, 257, 258]. Due to the finding, that cardiac allografts in the same donor-recipient strain combination and transplanted in the same location as renal allografts (*i.e.* in the peritoneal cavity) were rejected within 10 days, the authors suggested that renal allografts were accepted spontaneously. However, in this study lesion scores increased from 7 to 42d post transplantation and biochemical parameters (creatinine and BUN) indicate decreasing allograft function over time in all investigated groups compared to isograft recipients. Furthermore, the abundant leukocyte infiltrate, marked glomerulosclerosis and chronic vascular rejection at 42 days after transplantation show that in our experiments renal allografts were not accepted spontaneously in any of the analyzed groups. In summary, these findings indicate ongoing allograft rejection and demonstrate the validity of this model to study renal allograft rejection.

Regulatory T (Treg) cells have been implicated to play an important role during tolerance induction [208]. These cells are able to suppress allograft rejection by activated T cells. Thus, it was tempting to speculate whether Treg cells might be affected by loss of Ccr1 and/or Ccr5. Therefore, intragraft mRNA expression of genes previously associated with Treg cells was determined [235]. Lee *et al.* demonstrated that long-term engraftment of cardiac allografts by costimulatory blockade induces up-regulation of intragraft mRNA for the Treg-specific transcription factor Foxp3 and that the chemokine receptor CCR4 is required for recruitment of

immunosuppressive Treg cells into the graft [214]. Another chemokine receptor required for the *in vivo* function of Treg cells is CCR7. This chemokine receptor has been reported to be required for the homing of Treg cells [259] as well as dendritic cells [213] to SLOs. The immunosuppressive cytokines TGF-β and IL-10 have been shown to play a role in tolerance induction by inhibition of donor-reactive DTH immune responses [258].

Whereas Tgfb1 mRNA remained constantly high throughout the period of observation, intragraft mRNAs for Il10, Foxp3, Ccr4 and Ccr7 decreased over time in all analyzed recipient groups indicating decreased immunosuppression within the allografts itself and supporting the view that allografts were not spontaneously accepted. At 42 days post transplantation Foxp3 and Ccr7 mRNA levels were markedly reduced in all chemokine receptor-deficient compared to wildtype recipients indicating that loss of Ccr1 and/or Ccr5 induces additional reduction of Treg-mediated immunosuppression. Further analyses involving SLOs (*e.g.* spleens) of renal allograft recipients are required to gain a better understanding of the consequences of Ccr1 and Ccr5 deficiency on immune responses that rely on leukocyte traffic between the site of inflammation and SLOs.

DTH reactions contribute to chronic allograft rejection by T cell-dependent activation of macrophages. Although the intragraft mRNA levels of cytokines promoting DTH reactions (Ifng, Tnf and Il2) and Th1-associated chemokines (Ccl2, Ccl3, Ccl4, Ccl5 and Cxcl10) were down-regulated in acute phase $Ccr1^{-/-}$ and $Ccr5^{-/-}$ recipients, recruitment of $F4/80^{+}$ cells (macrophages) and mRNA levels of Nos2 were not differentially regulated in $Ccr1^{-/-}$ and $Ccr5^{-/-}$ recipients compared to wildtype recipients at both time points. Interestingly, decreased numbers of glomerular ($CD4^{+}$ and $CD8^{+}$) and tubulointerstitial ($CD8^{+}$) T cells in chronic phase $Ccr5^{-/-}$ recipients was accompanied by moderately increased expression of Th2 cytokines (Il4 and Il13) and a strong polarization of macrophages towards an alternative activation phenotype (see 4.6). In summary, while ongoing DTH reactions in $Ccr1^{-/-}$ recipients cannot be ruled out

completely on the basis of the underlying results, the findings in $Ccr5^{-/-}$ recipients suggest that the effects of DTH reactions are at least diminished in this recipient group.

4.4 Ccr1 and Ccr5 play different roles during allograft rejection

Histopathologic analysis revealed improvements for vascular and glomerular lesion scores in $Ccr1^{-/-}$ and $Ccr5^{-/-}$ recipients at day 7 after transplantation compared to wildtype recipients. These improvements continued to day 42 and were complemented by reduced tubulointerstitial inflammation and less matrix deposition in both recipient genotypes at the later time point. In spite of these histopathologic similarities found in $Ccr1^{-/-}$ and $Ccr5^{-/-}$ recipients, analysis of leukocyte infiltration and intragraft mRNA expression (see 4.3, 4.5 and 4.6) demonstrated significant differences between $Ccr1^{-/-}$ and $Ccr5^{-/-}$ recipients, suggesting that Ccr5-dependent rejection mechanisms are different from those involving on Ccr1.

Analysis of leukocyte infiltration further supported this view. $Ccr1^{-/-}$ recipients demonstrated reduced acute phase infiltration in glomerular and tubulointerstitial compartments by $CD4^+$, $CD8^+$ and $CD11c^+$ cells, whereas reduced infiltration by these cells in $Ccr5^{-/-}$ recipients was mostly limited to the glomerular compartment in the chronic phase of rejection. Reduced acute tubulointerstitial infiltration by $CD4^+$ and $CD8^+$ T cells observed only in $Ccr1^{-/-}$ recipients might also explain why tubulointerstitial inflammation improved only in $Ccr1^{-/-}$ recipients.

The finding that loss of either Ccr1 or Ccr5 resulted in only moderately reduced numbers of infiltrating $F4/80^+$ cells (monocytes/macrophages) was rather unexpected, since both receptors were reported to be involved in monocyte migration into the graft [101, 108]. However, there was a considerable decrease of acute phase $CD11c^+$ cells in all three analyzed chemokine receptor-deficient recipient groups suggesting that loss of Ccr1 or Ccr5 influences infiltration and/or maturation of dendritic cells ($CD11c^+$) in the graft.

Both single-deficient recipients demonstrated diminished intragraft mRNA expression of pro-inflammatory cytokines (Ifng, Tnf and Il2) and chemokines (Ccl2, Ccl3, Ccl4, Ccl5 and Cxcl10) during acute phase, which in turn might contribute to the observed reductions in leukocyte infiltration in acute phase $Ccr1^{-/-}$ recipients and chronic phase $Ccr5^{-/-}$ recipients. Furthermore, the decreased acute phase production of cytokines and chemokines suggests less activation of infiltrating leukocytes and might therefore also contribute to improvements in acute and chronic lesion scores and matrix deposition observed in mice lacking Ccr1 or Ccr5. Interestingly, certain signature genes for specific T helper cell populations were differentially expressed in $Ccr1^{-/-}$ and $Ccr5^{-/-}$ recipients and loss of Ccr5 induced alternative macrophage activation (detailed discussion in 4.5 and 4.6).

In summary, these findings suggest that Ccr1 and Ccr5 have stage and compartment-specific functions during allograft rejection and that both receptors are involved in different types of alloimmune responses.

4.5 $Ccr1^{-/-}$ recipients show Th17-skewed alloimmune responses and improved allograft outcome

$Ccr1^{-/-}$ recipients displayed gene expression patterns characteristic for Th17-skewed immune responses. Most importantly, $Ccr1^{-/-}$ recipients demonstrated significantly increased mRNA expression of the Th17-specific transcription factor Rorc during acute phase and increased expression of Il17a mRNA during chronic phase as compared to wildtype recipients. Furthermore, decreased acute phase mRNA levels of Th1 cytokines (Ifng, Tnf and Il2) and Th1-associated chemokines (Ccl3, Ccl5 and Cxcl10) might contribute to this shift by reducing the inhibitory signal on Th17 differentiation in $Ccr1^{-/-}$ recipients [260]. In the next step, mRNA expression of two cytokines promoting Th17 development was analyzed: TGF-β and IL-6. TGF-β

promotes differentiation of Treg cells, but in the presence of TGF-β and IL-6 differentiation is shifted towards Th17 development [256, 261, 262].

No genotype-specific differences for the mRNA expression of Tgfb1 were found, but in contrast to Th1 cytokines (Ifng, Tnf and Il2) and Th1-associated chemokines (Ccl3, Ccl5 and Cxcl10) which dropped significantly in all groups between the investigated time points, mRNA levels of Tgfb1 remained consistently high from acute to chronic stage and demonstrated the highest expression levels of all analyzed cytokines during the later phase. Furthermore, Il6 mRNA levels in $Ccr1^{-/-}$ recipients were significantly reduced in acute phase and expression of Ccr6 and Ccl20 – both genes were associated with Th17 cells – showed no differential regulation in the analyzed recipient groups at both time points. However, development of Treg and Th17 cells is a mutually exclusive process. Intriguingly, $Ccr1^{-/-}$ recipients displayed decreased expression of Foxp3 – a transcription factor specific for regulatory T cells – indicating either reduced Treg recruitment or increased differentiation of Treg cells into Th17 cells in allografts of $Ccr1^{-/-}$ recipients. Interestingly, increased Rorc mRNA expression during acute phase was accompanied by significantly reduced Ccr4 mRNA levels, indicating that Treg recruitment might be inhibited in the absence of Ccr1 since Ccr4 was found to be required for Treg recruitment and tolerance induction in cardiac allografts [214].

Possibly, the sustained expression of Tgfb1 outweighs the slightly reduced amount of Il6 mRNA observed during acute phase in $Ccr1^{-/-}$ recipients. Therefore, TGF-β/IL-6 promoted Th17 differentiation might dominate in $Ccr1^{-/-}$ recipients due to reduced Th1 polarization and Treg differentiation during acute phase of rejection. Expression analysis of additional Th17-associated genes such as Il21, Il23 and their corresponding receptors, could further corroborate these findings.

Several studies in human allograft recipients pointed to a detrimental effect of Th17-polarized immune responses and the IL-17/IL-23 axis has been associated with increased neutrophil

recruitment into transplants [209, 241]. In contrast to these findings, $Ccr1^{-/-}$ recipients demonstrated improved allograft histopathology and fibrosis. Interestingly, there is striking evidence that neutrophil recruitment into inflamed tissues is dependent – at least in part – on the presence of CCR1 [44, 263-265]. Therefore, loss of Ccr1 might shift Th1 alloimmune responses towards a Th17 response phenotype that is not accompanied by neutrophil-mediated tissue damage. However, additional immunohistologic stainings of neutrophils with appropriate antibodies in sections of renal allografts are required to confirm this idea and to clarify the functional role of CCR1 in Th17 alloimmune responses. These findings also suggest a role for CCR1 in the development of autoimmune diseases, since IL-17 producing T cells have been associated with several pathologic conditions including Crohn's disease, multiple sclerosis, autoimmune diabetes and rheumatoid arthritis [241].

4.6 $Ccr5^{-/-}$ recipients show decreased Th1 responses and increased alternative macrophage activation during chronic phase of rejection

$Ccr5^{-/-}$ recipients demonstrated improved chronic phase histopathology and less graft fibrosis compared to wildtype recipients at this time point. Moreover, Ccr5 deficiency resulted in improved histology as observed by reduced numbers of T cells in the glomerular ($CD4^+$ and $CD8^+$ cells) as well as in the tubulointerstitial ($CD8^+$ cells) compartment. Similar to $Ccr1^{-/-}$ recipients, $allograft^-$ recipients lacking Ccr5 displayed reduced acute phase intragraft mRNA levels of Th1 cytokines (Ifng, Tnf and Il2) and Th1-associated chemokines (Ccl3, Ccl5 and Cxcl10) as compared to wildtype recipients. Additionally, the mRNA levels of these Th1 marker genes and the Th1-specific transcription factor Tbx21 decreased significantly between acute and chronic phases, so that no significant differences remained between wildtype and $Ccr5^{-/-}$ at 42 days post transplantation. Interestingly, the immunosuppressive cytokine Il10 also decreased from acute to chronic phase in Ccr5-deficient recipients. Nevertheless, this finding is in full

agreement with recently published data showing that Th1 cells produce IL-10 under certain conditions to limit immune responses and prevent damage to the host [266].

Taken together, these observations suggest that the beneficial effect of Ccr5 deficiency on renal allograft rejection might be due to decreased Th1 immune responses including acute Th1 cytokine production and chronic infiltration by $CD4^+$ Th1 cells as well as cytotoxic $CD8^+$ T cells. These observations therefore suggest, that Th1-driven DTH reactions and cytotoxic T cell-mediated tissue injury are decreased by loss of Ccr5.

On the one hand, immunosuppression by Treg cells appears to be an unlikely explanation for the observed improvements, since Foxp3 mRNA levels decreased considerable over time in wildtype and $Ccr5^{-/-}$ recipients and were even significantly lower in chronic phase allografts from Ccr5-deficient recipients. Furthermore, Ccr7 mRNA was significantly down-regulated in $Ccr5^{-/-}$ recipients at 42 days post transplantation as compared to wildtype recipients. Schneider *et al.* reported that CCR7 is required for the *in vivo* function of Treg cells [259]. Therefore, this finding further supports the view, that improvements in Ccr5-deficient recipients are not mediated by Treg cells.

Alternatively, a shift in the immune response from a Th1-type to a Th2-type could potentially contribute to the improved allograft outcome observed in $Ccr5^{-/-}$ recipients. Expression of CCR5 on $CD4^+$ T lymphocytes has been associated with a Th1-type immune response [61]. Subsequently it was reported that Ccr5 deficiency results in a shift from a Th1- towards a Th2-type response in mice with dextran sodium sulfate-induced colitis [267]. In a murine islet transplantation model Abdi *et al.* demonstrated, that Ccr5 deficiency skews intragraft alloimmune responses towards the Th2-type [117]. They observed increased Il4 and Il5 as well as decreased Ifng mRNA levels in $Ccr5^{-/-}$ as compared to wildtype recipients. Interestingly, this Th2-shift was not only found within the allograft, but also in the periphery, when the response of splenocytes to donor cells was investigated.

The experiments of this these show that intragraft mRNA levels of Th1-associated marker genes such as Ifng and Tbx21 decreased over time, while expression of Th2-associated cytokines Il4, Il13 and the Th2-specific transcription factor Gata3 increased over time in all analyzed recipient groups. However, mRNA expression of Th2-associated cytokines Il4 and Il13 genes tended to be stronger in allografts from $Ccr5^{-/-}$ recipients. Hence, diminished Th1-driven DTH reactions in parallel with increased Th2 cytokine expression in $Ccr5^{-/-}$ allograft recipients, might generate a microenvironment that affects the polarization of intragraft macrophages and induces the alternative activation pathway in macrophages [160].

Alternatively activated macrophages (AAMs) characteristically show a strong expression of the signature gene Arg1 (arginase 1). Therefore, Arg1 mRNA expression was analyzed in renal allografts. Interestingly, Arg1 was only increased at 42d and only in Ccr5-deficient recipients. The notion that Ccr5 deficiency reprograms macrophages to the AAM phenotype was confirmed by analysis of intragraft expression of additional AAM marker genes including Chi3l3 (chitinase 3-like 3, also called Ym1), Retnla (resistin like alpha, also known as Fizz1 (Found in inflammatory zone 1)) and Mmp12 (matrix metallopeptidase 12) [160, 215, 268]. All three AAM marker genes showed a marked up-regulation in $Ccr5^{-/-}$ recipients at 42d. In addition, determination of the numbers of $Arg1^{+}$, $Mrc1^{+}$ and $Chi313^{+}$ cells within grafts during the chronic phase by immunohistological staining corroborated the findings on mRNA level.

Besides the Th2 cytokines IL-4 and IL-13, the immunosuppressive cytokines IL-10 and TGF-β have been implicated to play a role during alternative macrophage activation [155]. The mRNAs for Il10 and Tgfb1 were highly abundant in chronic allografts of all recipient groups, but AAMs were only observed in $Ccr5^{-/-}$ recipients, suggesting that signaling through CCR5 might inhibit alternative macrophage activation.

The data presented in this thesis provide a possible explanation for the mechanism underlying the beneficial effect of Ccr5 deficiency, which goes beyond a recruitment defect for

inflammatory cells. In the past most investigations have concentrated on quantitative effects that chemokine receptors have on the recruitment of specific leukocyte subpopulations. Qualitative phenotypic changes in leukocytes induced by loss of a specific chemokine receptor have been investigated much less. The number of infiltrating cells can be the same and still a profound effect may be observed when the phenotype of the infiltrating leukocytes has changed. The number of $F4/80^{+}$ cells (mostly macrophages) in the glomerular and the tubulointerstitial compartment did not differ significantly between grafts from wildtype and $Ccr5^{-/-}$ recipients at both time points. Interestingly, Abdi *et al.* made a similar observation in a murine islet transplantation model [117]. While immune responses where shifted towards Th2, numbers of infiltrating mononuclear cells ($CD4^{+}$ and $F4/80^{+}$ cells) remained unchanged between wildtype and $Ccr5^{-/-}$ recipients. Therefore, the authors concluded that immunosuppression due to loss of Ccr5 is not necessarily the result of altered leukocyte infiltration [117]. However, when analyzing numbers of intragraft macrophages one has to take into account that effects due to the presence of donor macrophages and local proliferation might obscure the true number of infiltrating recipient macrophages [269, 270]. In this context it would be interesting to determine intragraft levels of Csf1 (macrophage colony-stimulating factor) mRNA to get a first impression whether macrophage proliferation could be relevant in this model [271, 272].

However, the macrophages found in grafts from $Ccr5^{-/-}$ recipients at 42 days had been reprogrammed to AAMs, which clearly have a different phenotype than the macrophages found in grafts from wildtype recipients. In summary, these data indicate that loss of Ccr5 in the recipient is responsible for the accumulation of AAM and a Th2-type immune response during the chronic phase of transplantation, thereby favoring “repair” rather than progressive inflammation and destruction.

Eosinophil infiltrates have been associated with Th2-polarized alloimmune responses directed against skin grafts and antibody blockade of CCR3 was shown to inhibit graft infiltration by

eosinophils [273-275]. Therefore, intragraft Ccr3 mRNA expression was analyzed, but only very low levels of Ccr3 mRNA near or below detection limit were observed which did not allow accurate analysis (data not shown). Therefore it is conceivable, that eosinophil infiltration does not play a significant role in this experimental model. However, the possibility that small numbers of highly potent eosinophils might affect allograft rejection cannot be ruled out on the basis of these findings. Additional analyses of eosinophil-associated markers (*e.g.* IL-5, major basic protein (MBP) and eosinophil cationic protein (EBP) [276]) and Giemsa-stained sections are required to obtain an answer this question.

In 2004, our group demonstrated that Ccr5 has a role in carotid artery allograft rejection [277]. Ccr5-deficient recipients showed a significantly reduced infiltration with $CD3^+$ T cells and a marked reduction in neointima formation. Although transplant-associated arteriosclerosis represents a special case of vasculopathy caused by an activation of the immune system, these findings are compatible with the hypothesis that Ccr5 might also be involved in the pathogenesis of “classical” atherosclerosis. This disease is nowadays considered to represent a chronic inflammatory Th1-cell driven disease with macrophages playing a key role in the disease process [278]. In cooperation with the groups of François Mach from Geneva and Christian Weber from Aachen our group studied the role of Ccr5 in a high-fat diet induced atherosclerosis model. It was demonstrated, that deletion of Ccr5 in Apoe-deficient mice protected the animals from diet-induced atherosclerosis [279]. This phenotype was associated with decreased atherosclerotic lesion extent, reduced mononuclear cell infiltration and attenuated Th1 immune responses. Thus, the beneficial effect of Ccr5 deficiency on atherosclerosis might be caused by the presence of alternatively activated macrophages in the atherosclerotic lesions.

4.7 $Ccr5^{-/-}$ recipients do not show increased humoral rejection

Several transplantation studies in $Ccr5^{-/-}$ recipient mice including heart [111, 112], islet [116, 117] and carotid artery [112] allografts, demonstrated a beneficial effect of Ccr5 deficiency on allograft rejection leading to prolonged survival times. In contrast, two recent studies by Fairchild and colleagues using $Ccr5^{-/-}$ mice as recipients of cardiac [113] or renal [114] allografts showed, that loss of Ccr5 does not prolong cardiac allograft survival and results in accelerated rejection of renal allografts. In both studies, the authors explained these results by increased acute humoral rejection occurring in $Ccr5^{-/-}$ mice. This explanation was supported by increased deposition of the complement split product C3d and markedly elevated alloreactive antibody serum titers in $Ccr5^{-/-}$ recipients [113, 114]. In the renal transplantation experiments described in this thesis a comparable model of murine renal allograft rejection was performed, which resulted in long-term graft survival, though with evidence of chronic graft nephropathy. This was demonstrated by moderately increased serum creatinine and BUN levels as well as histopathologic changes consistent with mild to moderate chronic rejection. Furthermore, antibody levels did not increase in our fully backcrossed $Ccr5^{-/-}$ recipient mice and histopathologic analysis revealed significant improvements compared to wildtype recipients. A possible explanation for the differences obtained between our renal allograft model and the transplantation studies by Fairchild *et al.* could be the use of different donor-recipient strain combinations. In this thesis BALB/c ($H\text{-}2^{d}$) mice were utilized as donors of renal allografts, while Fairchild *et al.* used A/J mice ($H\text{-}2^{a}$) as donors of cardiac and renal allografts. Furthermore, different Ccr5-deficient recipient mouse lines were used ($Ccr5^{tm1Blck}$ (our group) *vs.* $Ccr5^{tm1Kuz}$ (Fairchild)) and our mice had acquired a true congenic status. For both studies, Fairchild *et al.* purchased Ccr5-deficient mice from The Jackson Laboratory. Fully backcrossed (N10) Ccr5-deficient mice in the C57BL/6 background are available from The Jackson Laboratory only since November 2005 (personal communication, Technical Service, The Jackson Laboratory). Thus, at

least the mice used for the cardiac transplantation study (received for publication in March 2004 [113]) were not appropriately backcrossed and therefore on a mixed genetic background at the time of the experiment. The backcrossing status of the mice used in the subsequent renal allograft study is not mentioned in their publication [114].

Another explanation for the differences between our study and the results of Fairchild *et al.* may be, that donor-reactive antibody levels are highly variable over time showing significant fluctuations above and below detection limits [280]. Cornell *et al.* suggested that this phenomenon is the result of a cycle of complement- and antibody-mediated injury, endothelial activation and repair [280].

4.8 $Ccr1^{-/-}/Ccr5^{-/-}$ recipients resemble wildtype recipients in certain aspects

Targeted deletion of a single inflammatory chemokine or chemokine receptor gene in mice often results in a mildly developed or no apparent phenotype. This phenomenon has been attributed to redundancy and promiscuity of the chemokine network [101, 281]. A single chemokine may bind to different receptors and a single chemokine receptor can bind different chemokines (see **Figure 1**). For instance, CCL3 and CCL5 bind to CCR1 and CCR5. As a result, it is thought that loss of one chemokine receptor can be compensated for by another receptor [282, 283], explaining the mild phenotypes often found in knockout mice. On the other hand, an agonist for one receptor might exhibit an antagonistic behavior on another receptor [19, 20]. These complex interactions confer a high degree of flexibility to the chemokine network and allow the fine-tuning of immune responses.

Previous studies showed that deficiency of the chemokine receptor Ccr1 or Ccr5 has beneficial effects on survival of cardiac, carotid, corneal and islet allograft in mice. Furthermore, it is known that both chemokine receptors are co-regulated, share ligands and are frequently expressed by the same cell types. These findings indicate potential redundant functions of CCR1

and CCR5 and suggest that loss of both receptors might be accompanied by additional or synergistic improvements in allograft recipients. Moreover, Ccr1/Ccr5 double-deficient mice serve as an important tool to answer the question whether redundant ligand-binding specificities observed *in vitro* are also present *in vivo*. Finally, small molecule antagonists used to block chemokine receptor function have come into the focus of the pharmaceutical industry to treat diseases that are currently beyond remedy. However, the potential redundancy of the chemokine system challenges the validity of chemokine receptors as therapeutic targets [284]. These important questions prompted us to generate Ccr1/Ccr5 double-deficient mice. To our best knowledge, these mice are only available in our laboratory to date. $Ccr1^{-/-}/Ccr5^{-/-}$ recipients were included in this study to answer the question whether redundancy exists between these receptors which might result in additive or synergistic effects in double-deficient recipients.

$Ccr1^{-/-}$ and $Ccr5^{-/-}$ single-deficient transplant recipients demonstrated significantly decreased allograft rejection compared to wildtype recipients during acute and chronic phase of rejection. Although $Ccr1^{-/-}/Ccr5^{-/-}$ double-deficient recipients showed improved graft histology and less leukocyte infiltration at both time points compared to wildtype recipients, additional improvements due to Ccr1/Ccr5 double deficiency were surprisingly limited to certain parameters during the chronic phase of allograft rejection. These effects were striking and nearly reached isograft levels, but were only observed in vascular (chronic vascular damage) and glomerular (transplant glomerulopathy) compartments. Double deficiency resulted in significantly reduced plasma urea levels and less collagen deposition – effects that were less pronounced in single-deficient recipients. Other improvements in double-deficient recipients were substantial, but did not excel the degree observed in single-deficient hosts. These improvements included acute vascular rejection and glomerular damage, chronic tubulointerstitial inflammation and actin (α-SMA) deposition.

Furthermore, numbers of infiltrating $CD8^+$, $CD11c^+$ and $F4/80^+$ cells were considerably diminished by loss of both chemokine receptors, but additional effects remained limited to chronic $CD11c^+$ cells in the tubulointerstitium and were only moderately pronounced. F4/80 and CD11c are markers typically expressed by cells of monocytic origin. Monocytes were shown to require the chemokine receptor CCR2 for emigration from the bone marrow [202]. Remarkably, intragraft Ccr2 mRNA levels were significantly reduced in acute phase double-deficient recipients, whereas levels of Ccl2 mRNA (encoding an important ligand of CCR2) were unchanged between wildtype and $Ccr1^{-/-}/Ccr5^{-/-}$ recipients. Thus, reduced infiltration by monocytic cells in allografts from double-deficient recipients might result in the decreased numbers of macrophages/dendritic cells observed in this study. CCR1 as well as CCR5 are known to play important roles during monocyte diapedesis. Weber and colleagues demonstrated that CCR1 is predominantly required for firm adhesion of monocytes and Th1-like T cells, while CCR5 mainly contributes to spreading in shear flow. Additionally, the authors showed that both receptors mediate transendothelial chemotaxis towards CCL5 [228]. However, reduced Ccr2 expression in monocytic bone marrow precursor cells from $Ccr1^{-/-}/Ccr5^{-/-}$ mice might also contribute to the observed reductions of graft infiltrating $F4/80^+$ and $CD11c^+$ cells – a possibility that requires further examination. Nevertheless, additional effects on chronic infiltration by $CD11^+$ cells were only marginal developed in double-deficient recipients and no additional effect on acute phase infiltration by $F4/80^+$ cells was observed. In summary, these data indicate that CCR1 and CCR5 may not share redundant functions during renal allograft rejection.

Interestingly, numbers of $CD4^+$ T cells were not affected by Ccr1/Ccr5 double deficiency in both renal compartments during acute and chronic phase, contrasting the findings from single-deficient recipients where loss of Ccr1 reduced the numbers of $CD4^+$ T cells during acute phase, while Ccr5 deficiency diminished chronic phase numbers of $CD4^+$ T cells. However, these results

correlate well with the observation that acute phase mRNA levels of Th1 cytokines (Ifng, Tnf and Il2) remained unchanged in double-deficient recipients compared to wildtype recipients. Thus, Th1 cytokine production by graft infiltrating $CD4^+$ T cells might not be affected in double-deficient recipients, while single deficiency had a marked impact on these parameters.

Acute phase Ccr1 and Ccr5 single-deficient recipients demonstrated reduced Th1 cytokine (Ifng, Tnf and Il2) mRNA expression that was paralleled by diminished mRNA levels of pro-inflammatory chemokines Ccl3, Ccl4 and Ccl5 compared to wildtype recipients. Remarkably, mRNA expression of these genes was restored to wildtype levels in acute phase $Ccr1^{-/-}/Ccr5^{-/-}$ recipients. Therefore, loss of both receptors might be compensated for by increased cytokine and chemokine production, in turn leading to increased leukocyte activation and/or infiltration compared to single-deficient recipients. On the other hand, double-deficient recipients showed ambiguous gene expression patterns in chronic phase of rejection: Th1-associated genes Tnf, Ccl3 and Cxcl10 showed significant up-regulation and the Th2-specific transcription factor Gata3 was also increased considerably. Therefore, it appears as if different immune response types reached a stalemate at this time point in double-deficient recipients. These findings could explain why additional effects due to double deficiency remained limited to certain parameters in chronic phase of rejection. Furthermore, a chemokine might function as an agonist for one receptor, while exhibiting antagonistic behavior on another receptor [19, 20]. Thus, it is conceivable that the observed restoration of wildtype chemokine levels (Ccl3-5) in double-deficient recipients induces contrary effects on immune responses mediated by chemokine receptors which share ligand binding specificity with CCR1 and CCR5 [9].

The observed phenomenon of restored cytokine and chemokine production might also be relevant for pharmaceutical approaches targeting chemokine receptors with small molecule antagonists directed against more than one receptor [53]. Use of such antagonists might affect

opposing immune responses. In this thesis, loss of Ccr1 induced a Th17-polarized immune response, while Ccr5 deficiency led to Th2-shifted immune responses and accumulation of AAM in the allograft. Therefore, a combined blockade of both receptors by antagonistic drugs might induce a phenotype similar to the observed phenotype of Ccr1/Ccr5 double-deficient recipients resembling wildtype recipients in many aspects.

In conclusion, no indication was found for redundant functions of CCR1 and CCR5 during renal allograft rejection. Moreover, effects of the different immune responses, which induced improved allograft outcome in single-deficient recipients, appear to neutralize each other in double-deficient recipients and might hinder the development of additive or synergistic effects in Ccr1/Ccr5 double-deficient recipients.

Although loss of Ccr1 or Ccr5 had beneficial effects on allograft rejection, different studies showed that loss of Ccr1 or Ccr5 is not necessarily accompanied by beneficial effects on disease outcome. Zernecke *et al.* showed that Ccr5 but not Ccr1 deficiency reduced neointima formation upon wire injury in atherosclerosis-prone mice [58]. In cooperation with the groups of François Mach from Geneva and Christian Weber from Aachen our group analyzed the effect of Ccr1 and Ccr5 deficiency in a high-fat diet induced atherosclerosis model [279]. Ccr5 deficiency was demonstrated to reduce diet-induced atherosclerosis, while loss of Ccr1 induced an opposing phenotype with increased plaque size and T cell infiltration. Moreover, our own unpublished results show that loss of Ccr1 aggravates lupus nephritis in MRL/lpr mice, while Ccr5 deficiency had a beneficial effect on the disease course compared to wildtype mice. On the other hand, Ccr1-deficient mice exhibited reduced numbers of infiltrating leukocytes and less fibrosis in a unilateral ureter obstruction model, while loss of Ccr5 had no effect on these parameters compared to wildtype mice [263]. Therefore, it appears that the effects due to the loss of one of these receptors are strongly dependent on the disease model analyzed. Frequently, loss of Ccr1 or Ccr5 induced contrary effects on disease outcome. Such contrary

effects might also explain why additional effects due to double deficiency remained limited and why Ccr1/Ccr5 double-deficient recipients resembled wildtype recipients in several aspects in the model of renal allograft rejection analyzed in this thesis.

4.9 Effects of Ccr5 deficiency on macrophage polarization are not limited to renal allograft rejection

The massive accumulation of AAM in grafts from $Ccr5^{-/-}$ recipients during the chronic phase of rejection raised the question, whether this change in macrophage phenotype was restricted to this particular disease model or whether Ccr5 deficiency has a general effect on macrophage polarization. In a first attempt to obtain an answer to this important question, macrophage polarization was analyzed in spleens and cultivated splenocytes from unchallenged wildtype and $Ccr5^{-/-}$ mice.

The increased expression of the AAM signature genes observed in spleens (Arg1, Mmp12, Mrc1 and Mrc2) and cultivated splenocytes (Arg1, Chi3l3, Msr1 and Retnla) from unchallenged $Ccr5^{-/-}$ mice suggested that Ccr5 deficiency indeed reprograms macrophages to an alternatively activated, anti-inflammatory phenotype already under basal conditions. These results are corroborated on protein level by increased frequencies of $CD206^{+}$ cells in $Ccr5^{-/-}$ splenocytes. However, additional experiments are required to identify the $CD206^{+}$ splenic macrophage subpopulation, since $CD206^{+}$ cells did not show surface expression of the common monocyte/macrophage marker CD11b. Interestingly, expression of CD11b (gene symbol Itgam) was up-regulated on mRNA level and frequencies of $CD11b^{+}$ cells were increased in cultivated $Ccr5^{-/-}$ splenocytes compared to wildtype splenocytes. Lloyd *et al.* suggested that $CD11b^{+}$ cells in spleens of unchallenged mice represent either neutrophils, monocytes or cells of monocytic origin [285]. Furthermore, it is conceivable that expression of the phagocytic mannose receptor C type 1 (CD206) occurs upon maturation of monocytes to tissue macrophages, explaining why

$CD206^+$ cells did not co-express CD11b. To date, at least four populations of splenic macrophages have been described based on different localization, function and expression of surface markers: white pulp macrophages (MOMA-2^+), red pulp macrophages ($F4/80^+$), marginal zone macrophages (SIGN-$R1^+$) and marginal metallophilic macrophages (MOMA-1^+) [286]. These markers could be used in additional experiments to identify the $CD206^+$ splenic macrophage population. Such an analysis might also provide new insights into the functional role of CCR5 in splenic macrophages.

Several subgroups have been defined for alternatively activated macrophages depending on the nature of the activating stimuli. While IL-4-activated AAM show a wound-healing phenotype, stimulation with various stimuli including IL-10, glucocorticoids or apoptotic cells, induces AAM with a regulatory phenotype. These so-called regulatory macrophages produce high levels of IL-10 and TGF-β and suppress immune functions [2, 155, 287]. Since IL-10 and TGF-β were shown to induce expression of CCR5 on human monocytes [67, 239] and human blood-derived DCs [68], CCR5 might as well have a function in regulatory macrophages.

Indeed, increased AAM marker expression (Arg1, Mmp12, Mrc1 and Mrc2) in spleens of $Ccr5^{-/-}$ mice was accompanied by augmented mRNA levels of Il10 and Tgfb1 supporting the view that macrophages in the spleen of $Ccr5^{-/-}$ mice might be shifted towards a regulatory phenotype compared to wildtype macrophages.

In addition to these findings in unchallenged mice, the effect of Ccr5 deficiency on cultivated macrophages obtained by thioglycollate-induced peritonitis was also analyzed. In this model, dramatically increased mRNA expression of Arg1 (~65x) was observed in untreated peritoneal macrophages from $Ccr5^{-/-}$ mice compared to wildtype mice. Two other AAM signature genes Chi3l3 and Retnla were not differentially regulated in untreated and IL-4-stimulated peritoneal macrophages while differences for Arg1 mRNA expression remained upon IL-4 stimulation. These results also contribute to the hypothesis that loss of Ccr5 induces an alternative

activation phenotype in macrophages. Several reasons might explain why the effect of Ccr5 deficiency was limited to Arg1 in this model. First, alternatively activated macrophages represent a highly heterogeneous cell population with different marker expression characteristics [163]. While IL-4-induced AAM express high amounts of Chi3l3 and Retnla mRNAs, AAMs activated by IL-10 did not express Chi3l3 or Retnla mRNA [288, 289]. Since the peritoneal macrophages used in the experiment shown in this thesis were harvested 4 days after thioglycollate-injection these cells might possibly be derived from a resolution phase micromillieu resembling more closely the phenotype of regulatory macrophages than the typical IL-4 induced alternatively activated macrophages.

Second, experiments performed in this study (see **Figure 29** and 4.10) showed that the time course of mRNA expression varies between different AAM marker genes - a result which is confirmed by the findings of Loke *et al.* [290]. Furthermore, it is unclear whether loss of Ccr5 delays or accelerates induction of these markers. Third, complex cytokine production by elicited peritoneal macrophages might also contribute to the modulation of AAM marker expression and result in altered macrophage activation compared to the situation found in renal allografts or cultivated splenocytes. Additional analyses on protein and functional level are required to confirm the findings from peritoneal macrophages and spleen cells. The established methods to determine arginase enzyme activity and measure NO production will be very useful to investigate differences on a functional level. Determining AAM marker protein expression by ELISA (cytokine expression in supernatants), Western blot and flow cytometric approaches offer additional methods to study the effect of Ccr5 deficiency on macrophage polarization.

In summary, the observations made in renal allografts, in spleens of unchallenged mice, in cultivated splenocytes and peritoneal macrophages reveal a novel phenotype in $Ccr5^{-/-}$ mice favoring alternative activation of macrophages. This finding may account for the improved transplant survival described in Ccr5-deficient mice [111, 112, 116, 117], in primates treated

with CCR5 antagonists [291], and in humans homozygous for the *CCR5Δ32* allele [8]. Furthermore, this observation may prove to be of considerable significance for the progression of chronic inflammatory and fibrosing disease processes.

4.10 Analysis of macrophage polarization in BMDM generated in Petri dishes

Due to the limitations and difficulties experienced with macrophages obtained by experimental peritonitis a method to generate pure macrophage populations was established. In a first approach, macrophages were generated by cultivation of bone marrow cells in Petri dishes using medium containing murine recombinant M-CSF. This method yielded 10-15x10^6 bone marrow-derived macrophages (BMDM) from a single mouse and ≥90% of these cells stained positive for the macrophage marker F4/80. Under basal conditions BMDM from C57BL/6 mice expressed high amounts of mRNAs typically expressed by macrophages (Csf1r and Mmp12) but did not display any genotype-specific differences for macrophage activation markers. Additionally, Nos2 and Ifng mRNA levels were below the detection limit (data not shown) in wildtype and Ccr5$^{-/-}$ BMDM. These results and the dramatic increase of AAM marker gene expression upon IL-4 stimulation suggest that wildtype and Ccr5$^{-/-}$ BMDM were unbiased regarding their phenotypic polarization under basal conditions. However, it is conceivable that Ccr5$^{-/-}$ BMDM show an altered time course of AAM marker expression compared to wildtype BMDM – a possibility which has not been analyzed in this study. The slightly decreased mRNA expression levels of Chi3l3 and Retnla in Ccr5$^{-/-}$ BMDM (C57BL/6) at 48h after IL-4 stimulation do therefore not exclude the possibility that Ccr5$^{-/-}$ BMDM show increased AAM marker expression at an earlier time point but might indicate an accelerated expression of Chi3l3 and Retnla in Ccr5$^{-/-}$ compared to wildtype BMDM. On a functional level, Ccr5$^{-/-}$ BMDM displayed significantly increased arginase enzyme activity compared to wildtype BMDM under unstimulated conditions. However, the increase under basal conditions was only moderate

(~1.27x) and disappeared upon IL-4 stimulation. On the other hand, the amount of NO produced under unstimulated or IL-4-stimulated conditions remained unchanged in wildtype and $Ccr5^{-/-}$ BMDM.

BMDM from wildtype and $Ccr5^{-/-}$ mice were pre-stimulated to analyze whether an activation/priming step might be necessary to obtain differential macrophage polarization. Interestingly, only pre-stimulation with LPS followed by IL-4 stimulation induced a significant difference in Arg1 mRNA expression while expression of other AAM marker genes (Chi3l3 and Retnla) remained unchanged.

It is known for years, that different mouse strains exhibit different or even opposite immunological responses to the same pathogen. For example upon infection with the intracellular pathogen *Leishmania major* C57BL/6 mice show Th1 responses whereas BALB/c mice show Th2 reactions. In case of *Leishmania* infection the Th1 response results in a resistant phenotype whereas BALB/c mice are rendered susceptible to this intracellular pathogen by induction of a Th2 response [292]. Interestingly, these strain differences occur already without priming through infection. Mills *et al.* found that macrophages from C57BL/6 and BALB/c strains differ in their capability to produce nitrite and ornithine in response to IFN-γ, LPS or both. While macrophages from Th1 responders (C57BL/6) predominantly produced nitrite and citrulline (products of classically activated macrophages [7]), Th2 macrophages (BALB/c) preferentially generated ornithine – an amino acid precursor that is predominantly produced by alternatively activated macrophages [7, 293]. In this thesis, a shift in macrophage polarization towards AAM was observed in renal BALB/c allografts transplanted in $Ccr5^{-/-}$ C57BL/6 recipients. Wyburn *et al.* showed that macrophages in the renal allograft are a mixed population consisting of infiltrating recipient macrophages and donor tissue macrophages which proliferate in response to inflammatory stimuli induced by ischemia/reperfusion injury of the transplanted kidney [270]. Therefore it is conceivable, that BALB/c donor macrophages are present at least during the

acute phase of rejection and might influence allograft rejection profoundly. Accordingly, the impact of Ccr5 deficiency on macrophage polarization in BMDM from BALB/c mice was analyzed. Upon stimulation with increasing amounts of IL-4 the dose-dependent increase of AAM marker gene expression (Arg1 and Chi3l3) was more pronounced in $Ccr5^{-/-}$ than in wildtype BMDM. In parallel, increased arginase enzyme activity and reduced NO production were observed in $Ccr5^{-/-}$ BMDM. In summary, while C57BL/6 $Ccr5^{-/-}$ BMDM did not show relevant differences under unstimulated and IL-4-stimulated conditions, BALB/c $Ccr5^{-/-}$ BMDM displayed increased alternative activation upon IL-4 stimulation compared to BALB/c wildtype BMDM. However, pre-stimulation by LPS induced a slight increase of AAM marker expression in $Ccr5^{-/-}$ compared to wildtype BMDM from C57BL/6 mice.

In conclusion, the Th2-polarized micromillieu of BALB/c allografts potentially supports alternative activation of C57BL/6 $Ccr5^{-/-}$ recipient macrophages and suggests complex strain dependent influences on macrophage polarization. Additionally, classical activation stimuli might induce AAMs in the absence of Ccr5 in C57BL/6 mice.

4.11 Analysis of macrophage polarization in BMDM generated in Teflon bags

BMDM generated in Teflon bags provide several advantages compared to conventional BMDM generated in Petri dishes. While the use of Petri dishes allowed the generation of $10\text{-}15x10^6$ BMDM/mouse, the Teflon bag method increased the amount of BMDM obtainable from a single mouse to $80\text{-}100x10^6$. Furthermore, use of proteases or scraping is not required to detach BMDM from the hydrophobic Teflon surface thereby reducing stress and damage to cells during harvesting. Additionally, generation of BMDM in Teflon bags is less time consuming and laborious, since it is not necessary to change medium during the differentiation period.

Morphologic and flow cytometric analysis revealed that the cell population generated by the Teflon bag culture method consists of highly pure macrophages. Over 98% of these cells

expressed the macrophage marker proteins CD11b and F4/80, while expression of granulocyte (Gr-1), T cell (CD3ε) and NK cell (NK1.1) markers was not detectable. BMDM from Teflon bags also showed weak expression of DC (CD11c) and B cell (CD19) marker proteins. Interestingly, CD11c as well as CD19 are subunits of the complement receptor complexes CR4 and CR2, respectively, which recognize cleavage products of C3b [1]. The presence of CD11c and CD19 on BMDM is in accordance with recent findings showing that both markers are also expressed by macrophage subsets. On the one hand, evidence is accumulating that CD11c – previously considered to be a specific marker of dendritic cells – is also expressed on macrophage subsets [285, 294] and the concept of dendritic cells and macrophages representing different cell types is being challenged [144]. On the other hand, a particular subset of $CD19^+$ myeloid progenitor cells ($CD45R^-CD19^+$) was demonstrated to generate either B cells or macrophages in mice [295]. The interesting observation that CD11c and CD19 were differentially expressed in BMDM from wildtype and $Ccr5^{-/-}$ mice requires additional experiments due to the low number of animals analyzed.

Next, the impact of Ccr5 deficiency on macrophage polarization was analyzed by stimulation of BMDM from Teflon bags with IFN-γ+LPS or IL-4+IL-13, thus inducing classical or alternative activation, respectively. While alternative activation drastically induced expression of AAM marker genes Arg1 (~138x), Chi3l3 (~1200x) and Retnla (~8300x) differential expression of these genes was not observed between wildtype and $Ccr5^{-/-}$ BMDM. However, IFN-γ+LPS-stimulated $Ccr5^{-/-}$ BMDM showed significantly increased expression of Arg1 and Mmp12 as well as a 5x increase of Retnla mRNA compared to wildtype BMDM. The increase of Arg1 mRNA upon IFN-γ+LPS stimulation compared to unstimulated BMDM is in accordance with earlier observations by Munder *et al.* showing that LPS induces Arginase 1 protein expression and enzyme activity in BMDM [191].

Together, these findings suggest that classical activation might induce a phenotype resembling alternative macrophage activation in $Ccr5^{-/-}$ BMDM from C57BL/6 mice. Further investigations including time course and dose/response analyses using classical activation stimuli are required to confirm these findings.

An interesting interpretation of the findings from BMDM generated in Petri dishes and Teflon bags is that Ccr5 deficiency reduces the capacity of macrophages to appropriately respond to Th1-associated stimuli. Instead, impaired signaling in $Ccr5^{-/-}$ macrophages may induce an alternative activation-like program under circumstances normally inducing classical macrophage activation. This notion is supported by the finding that CCR5 is generally expressed by Th1 lymphocytes [61] and might therefore be associated with classical rather than alternative macrophage activation.

The experiments provided in this thesis showed that renal allografts from $Cc5^{-/-}$ recipients, spleens and peritoneal lavage cells of $Ccr5^{-/-}$ mice exhibit a marked increase of AAM marker expression compared to their wildtype counterparts. However, pure macrophage populations derived from bone marrow cells of $Ccr5^{-/-}$ C57BL/6 mice showed only slight increases of AMM signature gene levels compared to wildtype BMDM. These results suggest that reproducing the effect of Ccr5 on macrophage polarization *in vitro* might be more complex than previously anticipated. Interestingly, Tiemessen *et al.* reported that Tregs induce alternative activation of co-cultivated human macrophages [296]. Thus, co-cultivation of Tregs and BMDM might be a promising approach to induce differential macrophage polarization in wildtype and $Ccr5^{-/-}$ BMDM.

5 OUTLOOK

The novel observation, that loss of Ccr5 induces alternative macrophage activation during renal allograft rejection in mice provides an explanation, why human transplant patients homozygous for a *CCR5Δ32* null allele show significantly prolonged survival of renal transplants. This hypothesis has not yet been tested. However, once optimal conditions have been found to induce differential macrophage polarization in BMDM from wildtype and $Ccr5^{-/-}$ mice these settings might be applied to macrophages derived from peripheral blood of human wildtype and $CCR5^{\Delta 32/\Delta 32}$ donors. This study established basic methods (generation of BMDM, functional assays for macrophage polarization and determination of AAM marker expression by flow cytometry) that could improve our understanding of the role of CCR5 during macrophage polarization. Nevertheless, species-specific differences might pose a serious hurdle when it comes to transfer the settings from the murine to the human system. For instance, while iNOS and ARG1 are readily inducible in murine macrophages upon stimulation with classical or alternative stimuli, respectively, detection of Nos2 expression in human macrophages is difficult *in vitro* [297] and ARG1 is expressed only in human granulocytes [298]. Moreover, the murine AAM signature genes Chi3l3 and Retnla lack human homologs, whereas Mrc1 expression indicates alternative activation in both species [160]. To date, most of our knowledge about gene expression in alternatively activated macrophages is derived from murine models, whereas studies using human macrophages remain scarce [160]. Although differences exist for macrophage polarization in mice and men, sufficient data should be available to distinguish between classical and alternative activation phenotypes on the basis of marker expression in human macrophages [160].

The role of Th17 immune responses in allograft rejection is not well understood, but it was shown that Il17 mRNA expression is increased in rejecting human transplants [299, 300] and

that IL-17 antagonism prolongs allograft survival in rats [208, 241, 253]. The experiments of this thesis show that loss of Ccr1 induces a shift away from Treg- and towards Th17-mediated immune responses. Paradoxically, $Ccr1^{-/-}$ recipients showed improved chronic phase lesion scores and less fibrosis as compared to wildtype recipients – a finding which is in accordance with previously reported results from other groups [102, 103]. The IL23/IL17 axis is known to induce neutrophil recruitment into the allograft [301] – a process that probably requires the presence of CCR1 [44, 263-265]. Hence, improvements in Ccr1-deficient recipients might – at least in part – be due to decreased neutrophil recruitment in a Th17-shifted microenvironment. To further corroborate these findings, expression of Th17 marker genes should be determined on the protein level which might be done by Western blot or flow cytometric analysis of allograft cell suspensions. Detection of IL-17 levels in urine might also be of interest. Additionally, investigation of allograft infiltration by neutrophils could be of importance.

Th17 immune responses have been implicated to play a role in several autoimmune pathologies. Thus, investigation of the impact of Ccr1 deficiency on autoimmune disease progression might shed new light into the function of CCR1 in this context. A first step into this direction might be the analysis of MRL/lpr $Ccr1^{-/-}$ mice which have already been generated in our laboratory.

6 ZUSAMMENFASSUNG

HINTERGRUND

Die Nierentransplantation ist die weltweit am häufigsten durchgeführte Art der Organtransplantation am Menschen [167]. Doch trotz der Fortschritte zur Behandlung der akuten Abstoßungsreaktion, werden immer noch mehr als 40% der transplantierten Organe durch chronische Abstoßungsreaktionen so stark geschädigt, dass sie schließlich durch ein neues Transplantat ersetzt werden müssen [168].

Vorangehende Studien legen eine Beteiligung des Chemokinrezeptors CCR5 bei der Abstoßung humaner Transplantate nahe. So ist bekannt, dass Nierentransplantate, die abgestoßen werden, eine erhöhte Expression des Chemokins CCL5/RANTES und des zugehörigen Rezeptors CCR5 aufweisen [125, 130]. In der kaukasischen Bevölkerung findet man relativ häufig ein Mutationsallel für *CCR5*, das *CCR5Δ32* genannt wird. Diese Mutation führt zur Expression eines verkürzten, nicht-funktionellen Rezeptorproteins, das im endoplasmatischen Retikulum verbleibt und nicht an die Zelloberfläche transportiert wird. Homozygote Träger dieses Allels stellen deshalb einen humanen „knockout“ für *CCR5* dar [4]. Unser Labor bestimmte im Jahr 2001 im Rahmen einer retrospektiven Studie den CCR5 Genotyp von Patienten mit Nierentransplantation und korrelierte den Genotyp mit dem Transplantatüberleben. Von 1227 untersuchten Patienten waren 21 homozygot für *CCR5Δ32* und diese Patientengruppe zeigte ein signifikant verlängertes Transplantatüberleben [8]. In einer Reihe von Tierversuchen mit gentechnisch veränderten Mäusen konnte außerdem gezeigt werden, dass der Verlust von Ccr5 oder des nahe verwandten Chemokinrezeptors Ccr1 in einer verminderten Abstoßungsreaktion von Herz-, Karotiden-, Kornea- und Inselzelltransplantaten resultiert [102, 103, 111, 112, 116, 117]. Die Chemokinrezeptoren CCR1 und CCR5 zeigen außerdem deutliche Überschneidungen in ihrer Ligandenspezifität, werden häufig gemeinsam reguliert und von den gleichen Zelltypen

exprimiert, was auf eine gewisse Redundanz in der Funktion dieser Rezeptoren hinzudeuten scheint [6, 45, 302].

ZIELE

Zum einen sollte geklärt werden, ob der Verlust von Ccr5 auch im Falle der Nierentransplantation in der Maus Verbesserungen mit sich bringt und welche Mechanismen für die beobachtete Verminderung der chronischen Transplantatabstossung in Patienten mit einem *CCR5*$^{\Delta 32/\Delta 32}$ Genotyp in Betracht gezogen werden können. Auf Grund der positiven Befunde aus Transplantationsversuchen mit CCR1-defizienten Mäusen, sollte zum anderen geklärt werden, ob sich der Verlust dieses nahe verwandten Rezeptors ebenso in einer Verminderung der Abstoßungsreaktion von transplantierten Nieren auswirkt und ob dabei ähnliche Mechanismen wie bei einem Verlust von Ccr5 beteiligt sind. In vorangegangenen Studien wurde beobachtet, dass der Verlust oder eine Blockade von CCR1 oder CCR5 im Empfängertier zu einer Verminderung der Abstoßungsreaktion führt [102, 103, 111, 112, 116, 117]. Außerdem sind beide Rezeptoren häufig koreguliert, besitzen ein überlappendes Ligandenspektrum und werden von den gleichen Zelltypen exprimiert. Diese Befunde veranlassten uns, Ccr1$^{-/-}$/Ccr5$^{-/-}$ doppelt-defiziente Mäuse zu generieren, um zu klären, ob CCR1 und CCR5 redundante Funktionen während der Transplantatabstoßung ausüben. Der Verlust beider Rezeptoren würde in diesem Fall additive oder synergistische Auswirkungen auf die Abstoßungsreaktion haben und könnte so das Transplantatüberleben zusätzlich begünstigen.

METHODEN

Um die Ursachen der verringerten Transplantatabstossung besser zu verstehen, wurde ein allogenes Nierentransplantationsmodell in der Maus genutzt, das sowohl die Analyse der akuten als auch der klinisch relevanteren chronischen Abstoßungsreaktion erlaubt, ohne dabei

immunsuppressive Medikamente einsetzen zu müssen, deren toxische Nebenwirkungen die zu untersuchenden Prozesse beeinflussen könnten.

Neben Wildtyp, $Ccr1^{-/-}$ und $Ccr5^{-/-}$ Mäusen dienten „doppelt-defiziente“ ($Ccr1^{-/-}$/$Ccr5^{-/-}$) C57BL/6 Mäuse als Empfänger von allogenen Wildtyp BALB/c Nierentransplantaten. Den Empfängertieren wurden zuvor beide Nieren mikrochirurgisch entfernt, so dass der eingesetzten Spenderniere eine lebenserhaltende Funktion zukam. Durch die Kombination von BALB/c (H-2^{d}) Spender- und C57BL/6 (H-2^{b}) Empfängertieren ergibt sich eine maximale MHC-Inkompatibilität und damit eine starke Abstoßungsintensität. Als Kontrollen dienten Wildtyp C57BL/6 Nieren, die in C57BL/6 Wildtypempfänger eingepflanzt wurden („Isograft“-Gruppe). Um mögliche Unterschiede in der akuten und chronischen Phase der Transplantatabstoßung analysieren zu können, wurden die Spendernieren 7 bzw. 42 Tage nach der Transplantation entnommen und mit verschiedenen Methoden untersucht. Außerdem wurden zu beiden Zeitpunkten Harnstoff- und Kreatininspiegel im Plasma bestimmt, um die Transplantatfunktion beurteilen zu können. An PAS-gefärbten Schnitten wurde die Transplantatschädigung mittels verschiedener Schädigungsindizes bewertet. Die Infiltration tubulointerstitieller und glomerulärer Kompartimente der Nierentransplantate durch verschiedene Leukozyten-Subpopulationen wurde mit Hilfe immunhistochemischer Färbungen ($CD4^{+}$, $CD8^{+}$, $CD11c^{+}$ und $F4/80^{+}$ Zellen) analysiert. Zur Bestimmung fibrotischer Prozesse wurden „smooth muscle actin (α-SMA)“ und Collagen I/III immunhistochemisch nachgewiesen. Die Expression ausgewählter Markergene in den Transplantaten wurde mittels quantitativer real-time RT-PCR bestimmt. Vorangehende Untersuchungen einer anderen Arbeitsgruppe deuteten darauf hin, dass sich der Verlust von Ccr5 auf die humorale Abstoßungsreaktion auswirken könnte [113, 114]. Daher wurden die Plasmaspiegel alloreaktiver Antikörper in Wildtyp und Ccr5-defizienten Mäusen bestimmt, die zuvor entweder mit BALB/c Milzzellen immunisiert wurden oder ein BALB/c Transplantat erhalten hatten.

Ccr5-defiziente Empfängertiere entwickelten im Verlauf der Abstoßungsreaktion erhebliche Unterschiede hinsichtlich des Aktivierungsphänotyps von Makrophagen im Transplantat. Um zu untersuchen, ob der Verlust von Ccr5 die Makrophagenpolarisierung allgemein beeinflusst, oder ob die beobachteten Effekte auf die Abstoßungsreaktion beschränkt sind, wurde der Aktivierungsphänotyp von Makrophagen aus Wildtyp und $Ccr5^{-/-}$ Mäusen bestimmt. Eine erste Versuchsreihe mit relativ heterogenen Zellpopulationen, die zum einen aus der Milz und zum anderen durch Thioglycolat-induzierte Peritonitis gewonnen wurden, wurde durch Versuche mit Knochenmark-abgeleiteten Makrophagen (BMDM) ergänzt. Neben der Expressionsanalyse von Signaturgenen mittels quantitativer real-time RT-PCR und Durchflusszytometrie, kamen dabei auch Methoden zur Bestimmung des Makrophagenphänotyps auf funktioneller Ebene (Bestimmung von Nitrat-Produktion und Arginaseenzymaktivität) zum Einsatz.

ERGEBNISSE

Die Funktion des Transplantats verschlechterte sich in allen Empfängergruppen, außer bei Ccr1/Ccr5 doppelt-defizienten Mäusen, deren Konzentrationen an Plasmaharnstoff zwischen 7 und 42 Tagen nach Transplantation konstant blieben. Die histopathologische Untersuchungen der Nierentransplantate ergaben bei $Ccr1^{-/-}$ und $Ccr5^{-/-}$ Empfängertieren signifikant verringerte Schädigungsindizes schon während der akuten Phase der Abstoßung und verringerte Fibrose während der chronischen Phase. Zusätzliche Effekte in doppelt-defizienten Empfängern waren auf verbesserte Schädigungsindizes (Transplantatglomerulpathie und chronisch-vaskulären Schäden) in der chronischen Phase beschränkt. $Ccr1^{-/-}$ Empfänger zeigten signifikant verringerte Infiltration durch $CD4^{+}$, $CD8^{+}$ und $CD11c^{+}$ Zellen nur während der akuten Abstoßungsphase, während die Infiltration des Transplantats mit diesen Zelltypen in $Ccr5^{-/-}$ Empfängertieren erst in der chronischen Phase und hauptsächlich im glomerulären Kompartiment der Niere signifikant reduziert war. Zusätzliche Effekte durch das Fehlen beider Rezeptoren waren

erstaunlicherweise auf die Infiltration mit F4/80^{+} Zellen bei 7 Tagen und auf CD11c^{+} Zellen bei 42 Tagen nach Transplantation beschränkt. Die Anzahl CD4^{+} T-Zellen in Transplantaten von doppelt-defizienten Empfängern wies im Gegensatz zu einfach-defizienten Empfängern keine Verringerung im Vergleich zu Wildtyp Empfängern auf. In vorangehenden Studien konnte gezeigt werden, dass CCR1 und CCR5 von Monozyten und Makrophagen exprimiert werden [45] und eine Rolle während der Diapedese von Monozyten spielen [101, 228]. Jedoch war die Anzahl F4/80^{+} Zellen in Transplantaten von Ccr1$^{-/-}$ und Ccr5$^{-/-}$ Empfängern gegenüber Wildtyp Empfängern erstaunlicherweise nicht verändert. Keine Unterschiede wurden für die Plasmaspiegel alloreaktiver Antikörper von Wildtyp und Ccr5$^{-/-}$ Mäusen gefunden, die mit BALB/c Milzzellen immunisiert wurden oder eine BALB/c Spenderniere erhalten hatten.

Die Expressionsanalyse ausgewählter Markergene zeigte, dass sowohl Transplantate von Ccr1$^{-/-}$ als auch Ccr5$^{-/-}$ Empfängertieren signifikant verringerte mRNA-Spiegel für Th1-Zytokine (Ifng und Tnf) sowie für Th1-assoziierte Chemokine (Ccl2-5 und Cxcl10) in der akuten Phase der Abstoßungsreaktion aufweisen. Überraschenderweise zeigten doppelt-defiziente Empfänger in der akuten Phase keine Veränderung der mRNA-Spiegel dieser Gene im Vergleich zu Wildtypempfängern. Allerdings war die mRNA Expression von Ccr2 nur in doppelt-defizienten Empfängern am Tag 7 nach Transplantation signifikant verringert. Die mRNA-Spiegel von Ccr7 waren am Tag 42 in allen knock-out Empfängergruppen signifikant reduziert.

Ccr1-defiziente Empfänger zeigten erhöhte Expression der Th17-assoziierten Gene Rorc und Il17a, während Gene, die mit der Funktion regulatorischer T-Zellen (Treg) in Verbindung gebracht werden (Foxp3 und Ccr4), eine signifikant verringerte Expression aufwiesen. Im Vergleich zu diesen Ergebnissen, zeigten Ccr5-defiziente Empfänger deutlich unterschiedliche Expressionsmuster. Der Verlust von Ccr5 führte zu einem Anstieg der mRNA Expression von Th2 Zytokinen (Il4 und Il13) in der chronischen Phase der Abstoßungsreaktion, der von einer dramatischen Erhöhung der mRNA-Spiegel von Signaturgenen (Arg1, Chi3l3 und Retnla) für

alternative aktivierte Makrophagen (AAM) begleitet war. Die Anreicherung von AAM in Transplantaten von $Ccr5^{-/-}$ Empfängern wurde auf Proteinebene durch immunhistologische Färbung von $Arg1^{+}$, $Chi3l3^{+}$ und $Mrc1^{+}$ Zellen bestätigt. Zusätzliche Experimente mit C57BL/6 Mäusen zeigten, dass der Verlust von Ccr5 auch in Milzen sowie *in vitro* kultivierten Milzzellen und Makrophagen, die durch Thioglycolat-induzierte Peritonitis gewonnen wurden, eine erhöhte Expression von AAM Signaturgenen bewirkt. Ein ähnlicher, wenn auch weniger ausgeprägter Effekt auf die Makrophagenpolarisierung durch den Verlust von Ccr5 konnte dagegen in einer einheitlicheren Makrophagen-Population, die aus Knochenmarkszellen von C57BL/6 Tieren hergestellt wurde, bisher nur nach Stimulation mit IFN-γ+LPS bzw. Vorstimulation mit LPS und nachfolgender Stimulation mit IL-4, nachgewiesen werden. Allerdings zeigten $Ccr5^{-/-}$ BALB/c BMDM verstärkte, dosisabhängige Expression von AAM Signaturgenen, erhöhte Arginaseenzymaktivität und verringerte NO-Produktion nach Stimulation mit IL-4 im Vergleich zu Wildtyp BALB/c BMDM.

SCHLUSSFOLGERUNGEN

Im Vergleich zu Wildtyp Empfängern zeigten Ccr1- und Ccr5-defiziente Empfängertiere Verbesserungen bei akuten sowie chronischen Schädigungsindizes, verringerte Fibrose und geringere mRNA Expression von Th1-assoziierten Zytokinen und Chemokinen in der akuten Phase.

Die beobachtete Verminderung der Transplantatabstoßung lässt sich nicht auf eine spontane Akzeptanz der Transplantate zurückführen, da sich zum einen die Transplantatfunktion (Plasmakreatinin- und Harnstoffkonzentration) und die meisten Schädigungsindizes in allen Empfängergruppen zwischen 7 und 42 Tagen nach der Transplantation verschlechterten. Zum anderen bestätigt die Anwesenheit eines ausgeprägten leukozytären Infiltrates während der chronischen Phase in allen Empfängergruppen das Andauern von Abstoßungsreaktionen und

unterstreicht somit die Gültigkeit dieses Modells für die Untersuchung von Abstoßungsreaktionen in der transplantierten Niere. Außerdem konnten die verminderten Abstoßungsreaktionen in keiner der Chemokinrezeptor-defizienten Gruppen mit einer verstärkten Immunsuppression durch regulatorische T Zellen (Treg) in Verbindung gebracht werden.

Obwohl die Abstoßungsreaktion in Ccr1- als auch in Ccr5-defizienten Empfängern vermindert war (reduzierte Fibrose, verringerte Leukozyteninfiltration und Verbesserung der Transplantathistopathologie), scheinen diese Effekte durch unterschiedliche Mechanismen vermittelt zu werden. So resultierte der Verlust von Ccr1 in einer verringerten glomerulären und tubulointerstiellen Einwanderung von $CD4^+$, $CD8^+$ und $CD11c^+$ Zellen in der akuten Phase, während Verringerungen in der Anzahl dieser infiltrierenden Leukozyten nach Verlust von CCR5 eher auf das glomeruläre Kompartiment und die chronische Phase beschränkt sind. Dieser Befund könnte auch Einfluss auf den zeitlichen Einsatz von Antagonisten am Menschen haben.

Desweiteren zeigten Ccr1- und Ccr5-defiziente Empfänger wesentliche Unterschiede bei der Art der ausgeprägten Immunantwort. Erstaunlicherweise zeigten Ccr1-defiziente Empfängertiere trotz einer Th17-polarisierten Immunantwort, die mit erniedrigter mRNA Expression Treg-assoziierter Gene einherging, verbesserte Transplantathistopathologie und weniger Fibrose. Dieser widersprüchliche Befund ist möglicherweise auf verringerte Infiltration durch neutrophile Granulozyten zurückzuführen, die eine Rolle bei Th17-vermittelten Pathologien spielen [209, 241] und deren Einwanderung an Entzündungsherde in vielen Fällen von CCR1 abhängt [44, 263-265]. Deshalb könnte der Verlust von Ccr1 die Abstoßungsreaktion in Richtung Th17 polarisieren, ohne dabei Schädigungen durch einwandernde Neutrophile auszulösen. Weitere Analysen sind notwendig, um diese Vermutung zu untermauern.

Die Ergebnisse der vorliegenden Arbeit deuten darauf hin, dass der Verlust von Ccr5 die alternative Aktivierung von Makrophagen (AAM) begünstigt. Dies konnte in

Nierentransplantaten Ccr5-defizienter Empfängertiere, in $Ccr5^{-/-}$ Milzen und kultivierten Milzzellen sowie in kultivierten Peritoneallavage-Makrophagen aus $Ccr5^{-/-}$ Mäusen gezeigt werden. Daher besteht die Möglichkeit, dass dieser Effekt nicht auf Prozesse während der Transplantatabstoßung begrenzt ist, sondern auch bei chronischen und entzündlichen Erkrankungen eine wichtige Rolle spielt. Im Gegensatz zu klassisch aktivierten Makrophagen (sog. „killer macrophages“) besitzen alternativ aktivierte Makrophagen einen „wound-healing“ Phänotyp, der sich positiv auf das Transplantatüberleben auswirken könnte. Interessanterweise unterschied sich die Anzahl infiltrierender $F4/80^{+}$ Zellen (hauptsächlich Makrophagen) nicht signifikant zwischen Wildtyp und $Ccr5^{-/-}$ Empfängern, aber der Verlust von Ccr5 führte zu einer dramatischen Veränderung des Aktivierungsphänotyps, der für die beobachteten Verbesserungen verantwortlich sein könnte und auch eine mögliche Erklärung für die beobachtete Verlängerung des Transplantatüberlebens in Patienten mit $CCR5^{\Delta 32/\Delta 32}$ Genotyp darstellt. Allerdings müssen weitere Analysen am Menschen zeigen, ob sich die in der Maus gewonnen Erkenntnisse auf den Menschen übertragen lassen. Interessanterweise, zeigten Experimente mit BMDM aus verschiedenen Mausstämmen, dass die Polarisierbarkeit von Makrophagen stark vom eingesetzten Mausstamm abhängig ist, und legen den Schluss nahe, dass das BALB/c Spenderorgan möglicherweise die alternative Aktivierung von Makrophagen begünstigt.

Obwohl der Verlust von CCR1 oder CCR5 in Transplantatempfängern zu einer Abschwächung der Abstoßungsreaktion führte, waren zusätzliche Effekte in Ccr1/Ccr5 doppelt-defizienten Empfängern auf einige wenige Parameter in der chronischen Phase beschränkt. Außerdem war die mRNA Expression Th1-assoziierter Zytokine und Chemokine in der akuten Phase mit Wildtyp Empfängern vergleichbar. Im Gegensatz zu Ccr1- und Ccr5-defizienten Empfängern blieb auch die Anzahl $CD4^{+}$ T-Zellen, in doppelt-defizienten Empfängern zu beiden Zeitpunkten im Vergleich zu Wildtyp Empfängern konstant, wodurch möglicherweise die unveränderte

Expression Th1-assoziierter Gene in der akuten Phase erklärt werden kann. Jedoch zeigten Transplantate doppelt-defizienter Empfänger verringerte Infiltration durch $F4/80^{+}$ Zellen (hauptsächlich Makrophagen) in der akuten und durch $CD11c^{+}$ Zellen (Dendritische Zellen) in der chronischen Phase. Ein Befund der sich auf mRNA-Ebene in einer verringerten Expression von Ccr2 (notwendig für die Auswanderung von Monozyten-Vorläuferzellen aus dem Knochenmark) und Ccr7 (notwendig für die Einwanderung Antigen-präsentierender Dendritischen Zellen in sekundäre lymphatische Organe) wiederspiegelt. Allerdings war das Ausmaß zusätzlicher Verbesserungen in Transplantaten doppelt-defizienter Empfänger relativ gering und auf wenige Parameter beschränkt. Daher legen diese Befunde die Vermutung nahe, dass CCR1 und CCR5 keine redundanten Funktionen während der Transplantatabstoßung ausüben. Die in den einfach-defizienten Empfängertieren beobachteten unterschiedlich polarisierten Immunantworten (Th17 bei $Ccr1^{-/-}$ *vs.* Th2/AAM bei $Ccr5^{-/-}$ Empfängern) heben sich in doppelt-defizienten Empfängern möglicherweise gegenseitig auf und führen so zu einem Phänotyp, der in vielen Aspekten dem der Wildtyp Empfänger entspricht.

7 APPENDIX

7.1 External contribution

This study started as a collaborative effort of our group and the group of Prof. Dr. Gröne at the DKFZ in Heidelberg (Dept. for Cellular and Molecular Pathology). The mice required for this study were bred and housed in our specified-pathogen free facility at the Poliklinik der LMU (Innenstadt) here in Munich. When the mice reached an appropriate age they were sent to the collaborating group of Prof. Dr. Gröne. There, Shijun Wang performed the transplantation microsurgery and animal materials (allografts, spleens and serum) were sent back to us for further analysis as described in this thesis. Claudia Schmidt (DKFZ) determined BUN and Creatinine levels of transplanted animals. Dr. Eva Kiss, a well-trained kidney pathologist and also a member of Prof. Gröne's group in Heidelberg, generated organ sections for histopathologic and immunohistologic stainings and conducted microscopic evaluation of those specimens. Accumulated data was sent to us for further analysis.

7.2 Figures of immunohistologic stainings of allograft sections

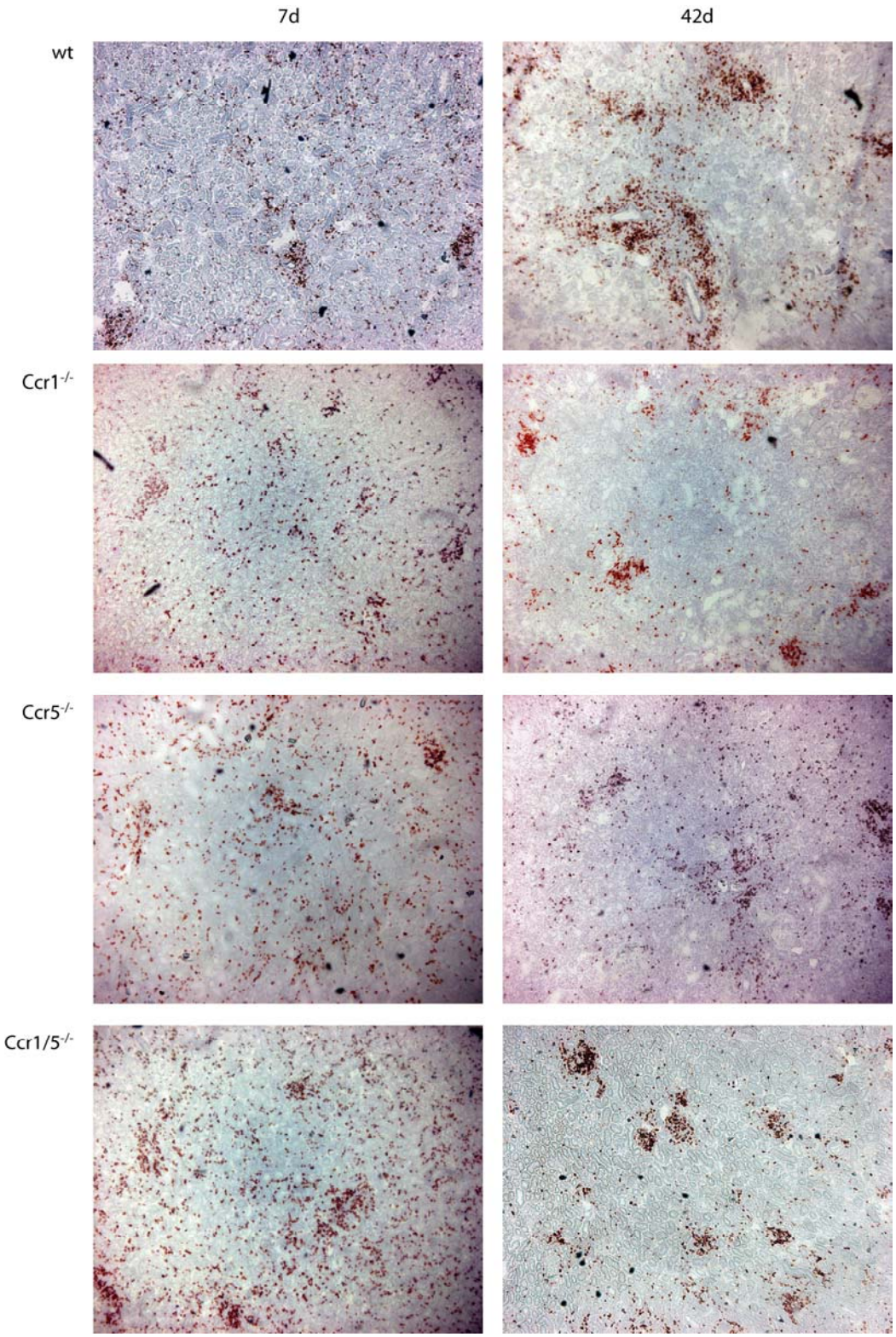

Figure 34. Effect of chemokine receptor deficiency on renal allograft infiltration with $CD4^+$ cells. Representative micrographs of sections from wt, $Ccr1^{-/-}$, $Ccr5^{-/-}$ and $Ccr1/Ccr5^{-/-}$ renal allograft recipients stained for $CD4^+$ cells after 7d and 42d post transplantation are shown (50x).

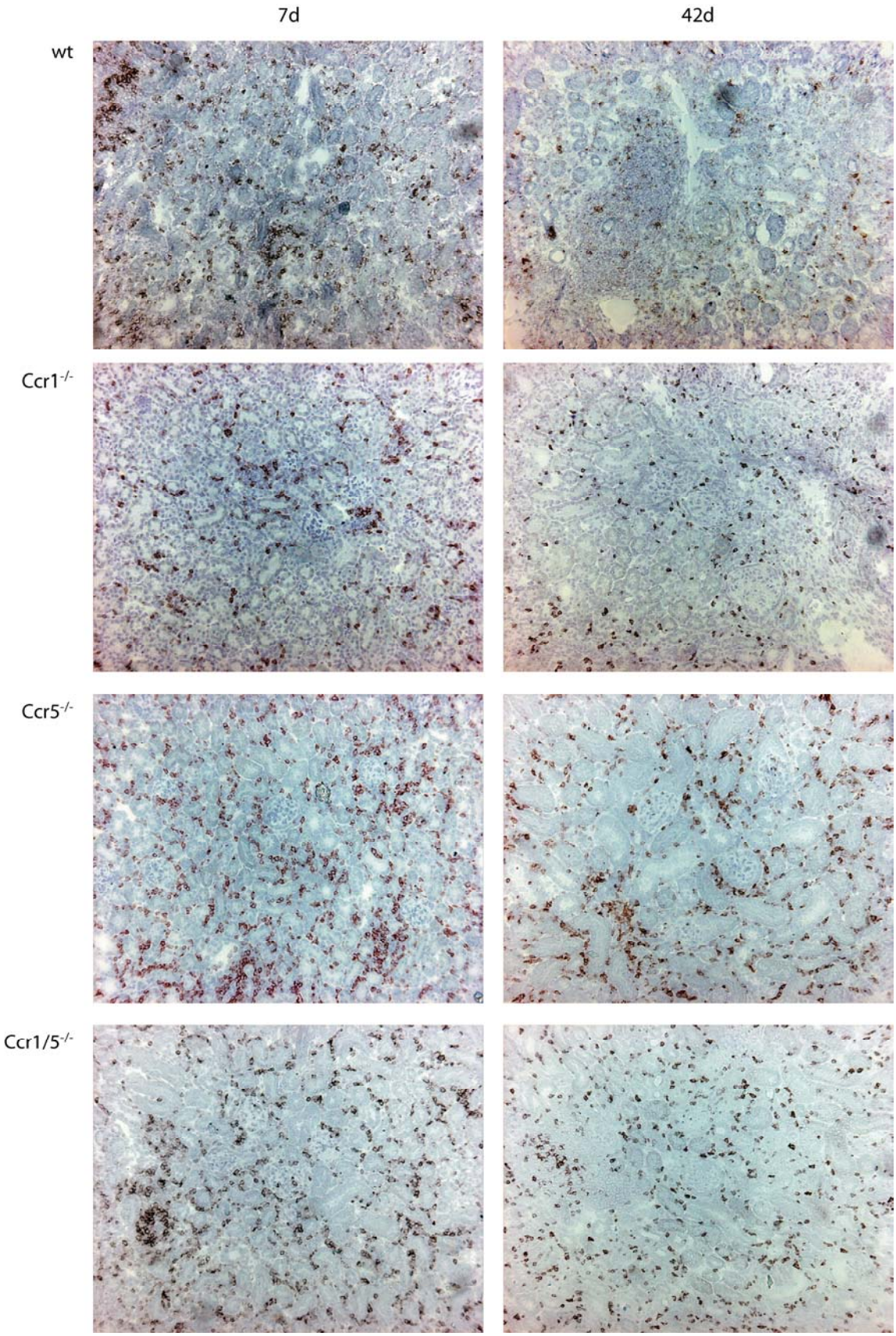

Figure 35. Effect of chemokine receptor deficiency on renal allograft infiltration with CD8$^+$ cells. Representative micrographs of sections from wt, Ccr1$^{-/-}$, Ccr5$^{-/-}$ and Ccr1/Ccr5$^{-/-}$ renal allograft recipients stained for CD8$^+$ cells after 7d and 42d post transplantation are shown (100x).

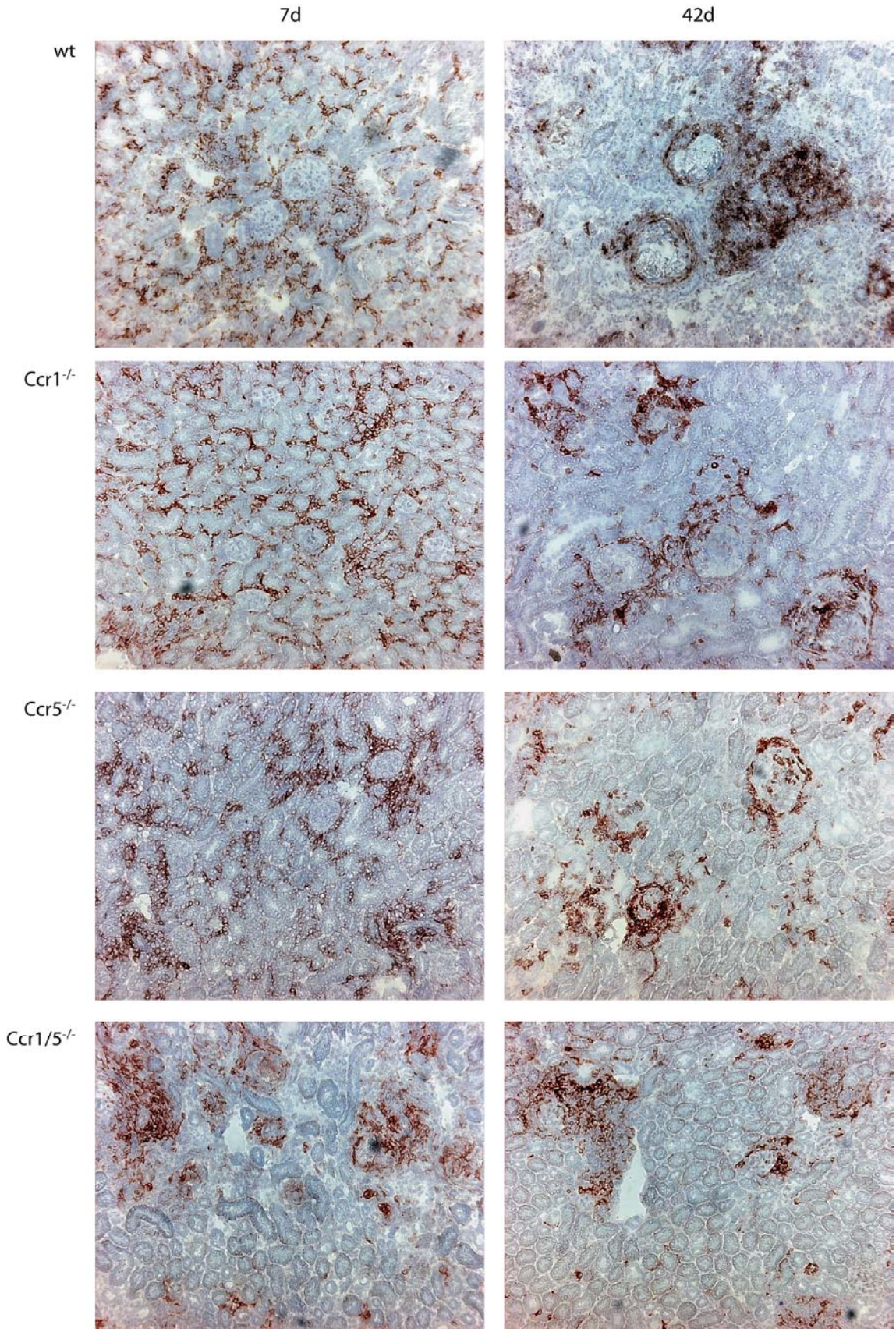

Figure 36. Effect of chemokine receptor deficiency on renal allograft infiltration with CD11c$^+$ cells. Representative micrographs of sections from wt, Ccr1$^{-/-}$, Ccr5$^{-/-}$ and Ccr1/Ccr5$^{-/-}$ renal allograft recipients stained for CD11c$^+$ cells after 7d and 42d post transplantation are shown (100x).

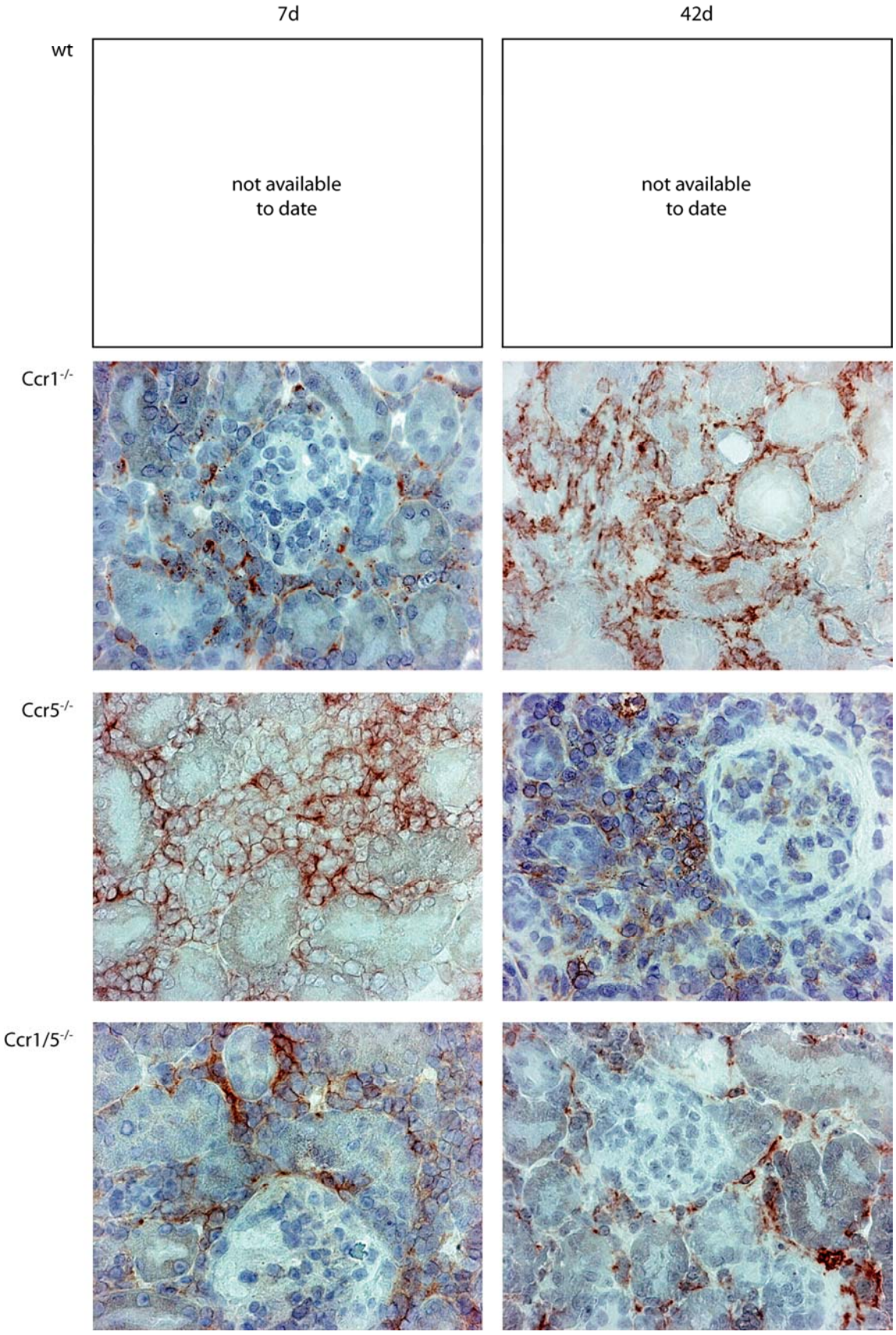

Figure 37. Effect of chemokine receptor deficiency on renal allograft infiltration with F4/80$^+$ cells. Representative micrographs of sections from Ccr1$^{-/-}$, Ccr5$^{-/-}$ and Ccr1/Ccr5$^{-/-}$ renal allograft recipients stained for F4/80$^+$ cells after 7d and 42d post transplantation are shown (400x).

7.3 Publications and collaborations

Original manuscripts

Dehmel S, Wang S, Schmidt C, Kiss E, Loewe RP, Chilla S, Schlöndorff D, Gröne HJ, Luckow B. (2008) „Chemokine receptor Ccr5 deficiency induces alternative macrophage activation and improves long-term renal allograft outcome“ (submitted) (equal contribution)

Luckow B, Hänggli A, Maier H, Chilla S, Loewe RP, **Dehmel S**, Schlöndorff D, Loetscher P, Zerwes HG , Müller M. (2008) „Microinjection of Cre recombinase protein into zygotes enables specific deletion of two eukaryotic selection cassettes and enhances the expression of a DsRed2 reporter gene in Ccr2/Ccr5 double-deficient mice“ (accepted on 21st of January 2009 by *Genesis: The Journal of Genetics and Development*)

Congress talks

Dehmel S (Speaker), Wang S, Schmidt C, Kiss E, Loewe RP, Chilla S, Schlöndorff D, Gröne HJ, Luckow B. „Analyse der Abstoßungsreaktion in Ccr5-defizienten Mäusen nach allogener Nierentransplantation.“ Jahreskongress für Nephrologie, 22.-25. September, 2007, München, Germany.

Dehmel S (Speaker), Wang S, Schmidt C, Kiss E, Loewe RP, Chilla S, Schlöndorff D, Gröne HJ, Luckow B. „ Analysis of renal allograft rejection in chemokine receptor Ccr1- and Ccr5-deficient mice.“ Symposium des DFG Graduiertenkollegs „Vaskuläre Biologie in der Medizin“, 10.-11. November, 2007, Herrsching am Ammersee, Germany.

External events

Practical training „Basic analytical flow cytometry“, May 29-31, 2006, BD Biosciences, Heidelberg, Germany.

Practical training „Mouse immunology and flow cytometry“, March 22-23, 2007, BD Biosciences, Heidelberg, Germany.

Practical training and seminar „Versuchstierkunde“ including certification by GV-SOLAS, September 17-28, 2007, München, Germany.

Collaborations

Prof. Dr. Hermann-Josef Gröne, DKFZ Heidelberg, Abteilung Zelluläre und Molekulare Pathologie, Im Neuenheimer Feld 280, 69120 Heidelberg, Germany, Tel. 06221/42-4351

Dr. Helmut Fuchs, German Mouse Clinic (GMC), Helmholtz Zentrum München, Institut für Experimentelle Genetik, Ingolstädter Landstrasse 1, 85764 München, Germany, Tel. 089/3187-3151

7.4 Curriculum vitae

PERSÖNLICHE ANGABEN

Name:	Stefan Dehmel
Wohnort:	81377 München-Grosshadern
Strasse:	Pelargonienweg 17
Geburtstag und -ort:	07. April 1976 in Altötting
Familienstand:	ledig
Nationalität:	Deutsch

SCHULAUSBILDUNG

09/1982 – 07/1988	Grund- und Hauptschule Töging I
08/1988 – 07/1992	Staatliche Knabenrealschule Altötting, Mittlere Reife
09/1995 – 07/1997	Staatliche Berufsoberschule Altötting, Fachgebundene Hochschulreife

ZIVILDIENST

08/1997 – 09/1998	Hausmeisterliche und administrative Tätigkeiten im Jugendübernachtungshaus "Herrenmühle", einer Einrichtung des Kreisjugendrings Altötting

BERUFSAUSBILDUNG

08/1992 – 06/1995	Ausbildung zum Technischen Zeichner (Maschinenbau) bei der Firma Esterer (Altötting), Abschluss mit Gesellenbrief

BERUFSERFAHRUNG

06/1995 – 09/1995	Anstellung bei der Firma Esterer (Altötting) als Technischer Zeichner

STUDIUM & PROMOTION

10/1998 – 10/2004	Studium der Technischen Biologie an der Universität Stuttgart Abschluss als Diplom-Biologe (t.-o.), Gesamtnote: sehr gut
10/2004 – 04/2005	Promotionsversuch am Genzentrum München, AG Dr. Claudia Petritsch
seit 05/2005	Promotion an der Medizinischen Poliklinik München, AG Klin. Biochemie Betreuer: PD Dr. Bruno Luckow (LMU München) Doktorvater: Prof. Dr. Peter Scheurich (Universität Stuttgart) Hauptberichter: Prof. Dr. Klaus Pfizenmaier (Universität Stuttgart)

8 REFERENCES

1. Abbas, A.T., Lichtman, A.H., Pillai, S., *Cellular and molecular immunology*. 6 ed. 2007, Philadelphia: Saunders Elsevier. 572.
2. Mosser, D.M. and J.P. Edwards, *Exploring the full spectrum of macrophage activation.* Nat Rev Immunol, 2008. **8**(12): p. 958-969.
3. Mellado, M., Rodríguez-Frade, J. M., Mañes, S., Martínez-A., C., *Chemokine Signaling and Functional Responses: The Role of Receptor Dimerization and TK Pathway Activation.* Annual Review of Immunology, 2001. **19**(1): p. 397.
4. Blanpain, C., *et al.*, *CCR5 and HIV infection.* Receptors Channels, 2002. **8**(1): p. 19-31.
5. Luster, A.D., *Chemokines--chemotactic cytokines that mediate inflammation.* N Engl J Med, 1998. **338**(7): p. 436-45.
6. Rot, A. and U.H. von Andrian, *Chemokines in innate and adaptive host defense: basic chemokinese grammar for immune cells.* Annu Rev Immunol, 2004. **22**: p. 891-928.
7. Bronte, V. and P. Zanovello, *Regulation of immune responses by L-arginine metabolism.* Nat Rev Immunol, 2005. **5**(8): p. 641-54.
8. Fischereder, M., *et al.*, *CC chemokine receptor 5 and renal-transplant survival.* Lancet, 2001. **357**(9270): p. 1758-61.
9. Murphy, P.M., *et al.*, *International union of pharmacology. XXII. Nomenclature for chemokine receptors.* Pharmacol Rev, 2000. **52**(1): p. 145-76.
10. Miloslav, N., Jirat, J., Kosata, B., *IUPAC Compendium of Chemical Terminology (Gold Book)*. 2008.
11. Baucke, F., *New IUPAC recommendations on the measurement of pH - background and essentials.* Analytical and Bioanalytical Chemistry, 2002. **374**(5): p. 772-777.
12. Oppenheim, J.J., Feldmann, M., Durum, S. K., Hirano, T., Vilcek, J., Nicola, N. A., *Cytokine Reference: A Compendium of Cytokines and Other Mediators of Host Defense*. Online Database ed. 2000: Academic Press (a Harcourt Science and Technology Company). 2260.
13. Bult, C.J., *et al.*, *The Mouse Genome Database (MGD): mouse biology and model systems.* Nucleic Acids Res, 2008. **36**(Database issue): p. D724-8.
14. Zlotnik, A. and O. Yoshie, *Chemokines: a new classification system and their role in immunity.* Immunity, 2000. **12**(2): p. 121-7.
15. Rossi, D. and A. Zlotnik, *The biology of chemokines and their receptors.* Annu Rev Immunol, 2000. **18**: p. 217-42.
16. Ansel, K.M. and J.G. Cyster, *Chemokines in lymphopoiesis and lymphoid organ development.* Current Opinion in Immunology, 2001. **13**(2): p. 172-179.
17. Fernandez, E.J. and E. Lolis, *Structure, function, and inhibition of chemokines.* Annual Review of Pharmacology and Toxicology, 2002. **42**(1): p. 469-499.
18. Oppermann, M., *Chemokine receptor CCR5: insights into structure, function, and regulation.* Cellular Signalling, 2004. **16**(11): p. 1201-1210.
19. Petkovic, V., *et al.*, *I-TAC/CXCL11 is a natural antagonist for CCR5.* J Leukoc Biol, 2004. **76**(3): p. 701-8.
20. Loetscher, P., *et al.*, *The Ligands of CXC Chemokine Receptor 3, I-TAC, Mig, and IP10, Are Natural Antagonists for CCR3.* J. Biol. Chem., 2001. **276**(5): p. 2986-2991.
21. McQuibban, G.A., *et al.*, *Matrix metalloproteinase processing of monocyte chemoattractant proteins generates CC chemokine receptor antagonists with anti-inflammatory properties in vivo.* Blood, 2002. **100**(4): p. 1160-7.
22. Berahovich, R.D., *et al.*, *Proteolytic activation of alternative CCR1 ligands in inflammation.* J Immunol, 2005. **174**(11): p. 7341-51.

23. Mellado, M., *et al.*, *Chemokine receptor homo- or heterodimerization activates distinct signaling pathways.* EMBO J, 2001. **20**(10): p. 2497-507.
24. El-Asmar, L., *et al.*, *Evidence for negative binding cooperativity within CCR5-CCR2b heterodimers.* Mol Pharmacol, 2005. **67**(2): p. 460-9.
25. Springael, J.Y., E. Urizar, and M. Parmentier, *Dimerization of chemokine receptors and its functional consequences.* Cytokine Growth Factor Rev, 2005. **16**(6): p. 611-23.
26. Springael, J.Y., *et al.*, *Allosteric modulation of binding properties between units of chemokine receptor homo- and hetero-oligomers.* Mol Pharmacol, 2006. **69**(5): p. 1652-61.
27. Yang, D., *et al.*, *Beta-defensins: linking innate and adaptive immunity through dendritic and T cell CCR6.* Science, 1999. **286**(5439): p. 525-8.
28. Yang, D., *et al.*, *Multiple roles of antimicrobial defensins, cathelicidins, and eosinophil-derived neurotoxin in host defense.* Annu Rev Immunol, 2004. **22**: p. 181-215.
29. Nakayama, T., *et al.*, *Liver-expressed chemokine/CC chemokine ligand 16 attracts eosinophils by interacting with histamine H4 receptor.* J Immunol, 2004. **173**(3): p. 2078-83.
30. Chen, C., *et al.*, *Heterodimerization and cross-desensitization between the [mu]-opioid receptor and the chemokine CCR5 receptor.* European Journal of Pharmacology, 2004. **483**(2-3): p. 175-186.
31. AbdAlla, S., H. Lother, and U. Quitterer, *AT1-receptor heterodimers show enhanced G-protein activation and altered receptor sequestration.* Nature, 2000. **407**(6800): p. 94-8.
32. Isik, N., D. Hereld, and T. Jin, *Fluorescence resonance energy transfer imaging reveals that chemokine-binding modulates heterodimers of CXCR4 and CCR5 receptors.* PLoS ONE, 2008. **3**(10): p. e3424.
33. Springael, J.-Y., *et al.*, *Allosteric Modulation of Binding Properties between Units of Chemokine Receptor Homo- and Hetero-Oligomers.* Mol Pharmacol, 2006. **69**(5): p. 1652-1661.
34. Gao, J.L., *et al.*, *Structure and functional expression of the human macrophage inflammatory protein 1 alpha/RANTES receptor.* J Exp Med, 1993. **177**(5): p. 1421-7.
35. Gao, J.L. and P.M. Murphy, *Human cytomegalovirus open reading frame US28 encodes a functional beta chemokine receptor.* J Biol Chem, 1994. **269**(46): p. 28539-42.
36. Billstrom, M.A., *et al.*, *Intracellular Signaling by the Chemokine Receptor US28 during Human Cytomegalovirus Infection.* J. Virol., 1998. **72**(7): p. 5535-5544.
37. O'Dowd, B.F., *et al.*, *Palmitoylation of the human beta 2-adrenergic receptor. Mutation of Cys341 in the carboxyl tail leads to an uncoupled nonpalmitoylated form of the receptor.* J Biol Chem, 1989. **264**(13): p. 7564-9.
38. Murdoch, C. and A. Finn, *Chemokine receptors and their role in inflammation and infectious diseases.* Blood, 2000. **95**(10): p. 3032-3043.
39. Gao, J.-L., *et al.*, *Impaired Host Defense, Hematopoiesis, Granulomatous Inflammation and Type 1-Type 2 Cytokine Balance in Mice Lacking CC Chemokine Receptor 1.* J. Exp. Med., 1997. **185**(11): p. 1959-1968.
40. Baggiolini, M., *Chemokines and leukocyte traffic.* Nature, 1998. **392**(6676): p. 565-8.
41. Amin, K., *et al.*, *CC chemokine receptors CCR1 and CCR4 are expressed on airway mast cells in allergic asthma.* J Allergy Clin Immunol, 2005. **116**(6): p. 1383-6.
42. Maghazachi, A.A., *G protein-coupled receptors in natural killer cells.* J Leukoc Biol, 2003. **74**(1): p. 16-24.
43. Shang, X., *et al.*, *Chemokine receptor 1 knockout abrogates natural killer cell recruitment and impairs type-1 cytokines in lymphoid tissue during pulmonary granuloma formation.* Am J Pathol, 2000. **157**(6): p. 2055-63.
44. Furuichi, K., *et al.*, *Chemokine Receptor CCR1 Regulates Inflammatory Cell Infiltration after Renal Ischemia-Reperfusion Injury.* J Immunol, 2008. **181**(12): p. 8670-8676.

45. Kaufmann, A., *et al.*, *Increase of CCR1 and CCR5 expression and enhanced functional response to MIP-1 alpha during differentiation of human monocytes to macrophages.* J Leukoc Biol, 2001. **69**(2): p. 248-52.
46. Varani, S., *et al.*, *Human cytomegalovirus inhibits the migration of immature dendritic cells by down-regulating cell-surface CCR1 and CCR5.* J Leukoc Biol, 2005. **77**(2): p. 219-228.
47. Sato, K., *et al.*, *CC Chemokine Receptors, CCR-1 and CCR-3, Are Potentially Involved in Antigen-Presenting Cell Function of Human Peripheral Blood Monocyte-Derived Dendritic Cells.* Blood, 1999. **93**(1): p. 34-42.
48. Jugdé, F., *et al.*, *Regulation by allergens of chemokine receptor expression on in vitro-generated dendritic cells.* Toxicology, 2005. **212**(2-3): p. 227-238.
49. Caux, C., *et al.*, *Dendritic cell biology and regulation of dendritic cell trafficking by chemokines.* Springer Semin Immunopathol, 2000. **22**(4): p. 345-69.
50. Su, S.-b., *et al.*, *Inhibition of Immature Erythroid Progenitor Cell Proliferation by Macrophage Inflammatory Protein-1alpha by Interacting Mainly With a C-C Chemokine Receptor, CCR1.* Blood, 1997. **90**(2): p. 605-611.
51. Clemetson, K.J., *et al.*, *Functional expression of CCR1, CCR3, CCR4, and CXCR4 chemokine receptors on human platelets.* Blood, 2000. **96**(13): p. 4046-54.
52. Ribeiro, S. and R. Horuk, *The clinical potential of chemokine receptor antagonists.* Pharmacol Ther, 2005. **107**(1): p. 44-58.
53. Wells, T.N., *et al.*, *Chemokine blockers--therapeutics in the making?* Trends Pharmacol Sci, 2006. **27**(1): p. 41-7.
54. Reichel, C.A., *et al.*, *Chemokine receptors Ccr1, Ccr2, and Ccr5 mediate neutrophil migration to postischemic tissue.* J Leukoc Biol, 2006. **79**(1): p. 114-22.
55. Broxmeyer, H.E., *et al.*, *Dominant myelopoietic effector functions mediated by chemokine receptor CCR1.* J Exp Med, 1999. **189**(12): p. 1987-92.
56. Rodriguez-Sosa, M., *et al.*, *CC chemokine receptor 1 enhances susceptibility to Leishmania major during early phase of infection.* Immunol Cell Biol, 2003. **81**(2): p. 114-20.
57. Topham, P.S., *et al.*, *Lack of chemokine receptor CCR1 enhances Th1 responses and glomerular injury during nephrotoxic nephritis.* J Clin Invest, 1999. **104**(11): p. 1549-57.
58. Zernecke, A., *et al.*, *Deficiency in CCR5 but not CCR1 protects against neointima formation in atherosclerosis-prone mice: involvement of IL-10.* Blood, 2006. **107**(11): p. 4240-3.
59. Atchison, R.E., *et al.*, *Multiple Extracellular Elements of CCR5 and HIV-1 Entry: Dissociation from Response to Chemokines.* Science, 1996. **274**(5294): p. 1924-1926.
60. Khan, I.A., *et al.*, *CCR5 is essential for NK cell trafficking and host survival following Toxoplasma gondii infection.* PLoS Pathog, 2006. **2**(6): p. e49.
61. Loetscher, P., *et al.*, *CCR5 is characteristic of Th1 lymphocytes.* Nature, 1998. **391**(6665): p. 344-345.
62. N. Ødum, S.B., K.W. Eriksen, S. Skov, L.P. Ryder, K. Bendtzen, R.J.J. Van Neerven , A. Svejgaard, P. Garred,, *The CC-chemokine receptor 5 (CCR5) is a marker of, but not essential for the development of human Th1 cells.* Tissue Antigens, 1999. **54**(6): p. 572-577.
63. Barbonetti, A., *et al.*, *RANTES and human sperm fertilizing ability: effect on acrosome reaction and sperm/oocyte fusion.* Mol. Hum. Reprod., 2008. **14**(7): p. 387-391.
64. Isobe, T., *et al.*, *The effect of RANTES on human sperm chemotaxis.* Hum. Reprod., 2002. **17**(6): p. 1441-1446.
65. Muciaccia, B., *et al.*, *Beta-chemokine receptors 5 and 3 are expressed on the head region of human spermatozoon.* FASEB J, 2005. **19**(14): p. 2048-50.
66. Choudhary, S.K., *et al.*, *R5 Human Immunodeficiency Virus Type 1 Infection of Fetal Thymic Organ Culture Induces Cytokine and CCR5 Expression.* J. Virol., 2005. **79**(1): p. 458-471.

67. Houle, M., *et al.*, *IL-10 up-regulates CCR5 gene expression in human monocytes.* Inflammation, 1999. **23**(3): p. 241-51.
68. Sato, K., *et al.*, *TGF-{beta}1 Reciprocally Controls Chemotaxis of Human Peripheral Blood Monocyte-Derived Dendritic Cells Via Chemokine Receptors.* J Immunol, 2000. **164**(5): p. 2285-2295.
69. Hill, S.J., *G-protein-coupled receptors: past, present and future.* Br J Pharmacol, 2006. **147 Suppl 1**: p. S27-37.
70. Gulick, R.M., *et al.*, *Maraviroc for Previously Treated Patients with R5 HIV-1 Infection.* N Engl J Med, 2008. **359**(14): p. 1429-1441.
71. Sax, P.E., *FDA approval: maraviroc.* AIDS Clin Care, 2007. **19**(9): p. 75.
72. Horuk, R., *Chemokine receptor antagonists: overcoming developmental hurdles.* Nat Rev Drug Discov, 2009. **8**(1): p. 23-33.
73. Huffnagle, G.B., *et al.*, *Cutting edge: Role of C-C chemokine receptor 5 in organ-specific and innate immunity to Cryptococcus neoformans.* J Immunol, 1999. **163**(9): p. 4642-6.
74. Luangsay, S., *et al.*, *CCR5 mediates specific migration of Toxoplasma gondii-primed CD8 lymphocytes to inflammatory intestinal epithelial cells.* Gastroenterology, 2003. **125**(2): p. 491-500.
75. Machado, F.S., *et al.*, *CCR5 plays a critical role in the development of myocarditis and host protection in mice infected with Trypanosoma cruzi.* J Infect Dis, 2005. **191**(4): p. 627-36.
76. Yurchenko, E., *et al.*, *CCR5-dependent homing of naturally occurring CD4+ regulatory T cells to sites of Leishmania major infection favors pathogen persistence.* J Exp Med, 2006. **203**(11): p. 2451-60.
77. Glass, W.G., *et al.*, *Reduced macrophage infiltration and demyelination in mice lacking the chemokine receptor CCR5 following infection with a neurotropic coronavirus.* Virology, 2001. **288**(1): p. 8-17.
78. Glass, W.G. and T.E. Lane, *Functional analysis of the CC chemokine receptor 5 (CCR5) on virus-specific CD8+ T cells following coronavirus infection of the central nervous system.* Virology, 2003. **312**(2): p. 407-14.
79. Glass, W.G., *et al.*, *Chemokine receptor CCR5 promotes leukocyte trafficking to the brain and survival in West Nile virus infection.* J Exp Med, 2005. **202**(8): p. 1087-98.
80. Tyner, J.W., *et al.*, *CCL5-CCR5 interaction provides antiapoptotic signals for macrophage survival during viral infection.* Nat Med, 2005. **11**(11): p. 1180-7.
81. Ma, B., *et al.*, *Role of CCR5 in IFN-gamma-induced and cigarette smoke-induced emphysema.* J Clin Invest, 2005. **115**(12): p. 3460-72.
82. Alkhatib, G., *et al.*, *CC CKR5: A RANTES, MIP-1alpha , MIP-1beta Receptor as a Fusion Cofactor for Macrophage-Tropic HIV-1.* Science, 1996. **272**(5270): p. 1955-1958.
83. Choe, H., *et al.*, *The [beta]-Chemokine Receptors CCR3 and CCR5 Facilitate Infection by Primary HIV-1 Isolates.* Cell, 1996. **85**(7): p. 1135-1148.
84. Deng, H., *et al.*, *Identification of a major co-receptor for primary isolates of HIV-1.* Nature, 1996. **381**(6584): p. 661-666.
85. Doranz, B.J., *et al.*, *A Dual-Tropic Primary HIV-1 Isolate That Uses Fusin and the [beta]-Chemokine Receptors CKR-5, CKR-3, and CKR-2b as Fusion Cofactors.* Cell, 1996. **85**(7): p. 1149-1158.
86. Dragic, T., *et al.*, *HIV-1 entry into CD4+ cells is mediated by the chemokine receptor CC-CKR-5.* Nature, 1996. **381**(6584): p. 667-673.
87. Feng, Y., *et al.*, *HIV-1 Entry Cofactor: Functional cDNA Cloning of a Seven-Transmembrane, G Protein-Coupled Receptor.* Science, 1996. **272**(5263): p. 872-877.
88. Deng, H., *et al.*, *Expression cloning of new receptors used by simian and human immunodeficiency viruses.* Nature, 1997. **388**(6639): p. 296-300.

89. Liao, F., *et al.*, *STRL33, A Novel Chemokine Receptor-like Protein, Functions as a Fusion Cofactor for Both Macrophage-tropic and T Cell Line-tropic HIV-1.* J. Exp. Med., 1997. **185**(11): p. 2015-2023.
90. Pleskoff, O., *et al.*, *Identification of a Chemokine Receptor Encoded by Human Cytomegalovirus as a Cofactor for HIV-1 Entry.* Science, 1997. **276**(5320): p. 1874-1878.
91. Weissman, D., *et al.*, *Macrophage-tropic HIV and SIV envelope proteins induce a signal through the CCR5 chemokine receptor.* Nature, 1997. **389**(6654): p. 981-5.
92. Xiao, X., *et al.*, *Constitutive cell surface association between CD4 and CCR5.* Proc Natl Acad Sci U S A, 1999. **96**(13): p. 7496-501.
93. Lynch, E.A., *et al.*, *Cutting Edge: IL-16/CD4 Preferentially Induces Th1 Cell Migration: Requirement of CCR5.* J Immunol, 2003. **171**(10): p. 4965-4968.
94. Staudinger, R., *et al.*, *Evidence for CD4-enchanced signaling through the chemokine receptor CCR5.* J Biol Chem, 2003. **278**(12): p. 10389-92.
95. Cocchi, F., *et al.*, *Identification of RANTES, MIP-1alpha, and MIP-1beta as the Major HIV-Suppressive Factors Produced by CD8+ T Cells.* Science, 1995. **270**(5243): p. 1811-1815.
96. Garred, P. and J. Eugen-Olsen, *Dual effect of CCR5 Delta 32 gene deletion in HIV-1 infected patients.* Lancet, 1997. **349**(9069): p. 1884.
97. Hall, I.P., *et al.*, *Association of CCR5 delta32 with reduced risk of asthma.* Lancet, 1999. **354**(9186): p. 1264-5.
98. Zimmerman, P.A., *et al.*, *Inherited resistance to HIV-1 conferred by an inactivating mutation in CC chemokine receptor 5: studies in populations with contrasting clinical phenotypes, defined racial background, and quantified risk.* Mol Med, 1997. **3**(1): p. 23-36.
99. Faure, E. and M. Royer-Carenzi, *Is the European spatial distribution of the HIV-1-resistant CCR5-[Delta]32 allele formed by a breakdown of the pathocenosis due to the historical Roman expansion?* Infection, Genetics and Evolution, 2008. **8**(6): p. 864-874.
100. Sabeti, P.C., *et al.*, *The Case for Selection at CCR5delta32.* PLoS Biology, 2005. **3**(11): p. e378.
101. Nelson, P.J. and A.M. Krensky, *Chemokines, chemokine receptors, and allograft rejection.* Immunity, 2001. **14**(4): p. 377-86.
102. Gao, W., *et al.*, *Targeting of the chemokine receptor CCR1 suppresses development of acute and chronic cardiac allograft rejection.* J Clin Invest, 2000. **105**(1): p. 35-44.
103. Hamrah, P., *et al.*, *Deletion of the Chemokine Receptor CCR1 Prolongs Corneal Allograft Survival.* Invest. Ophthalmol. Vis. Sci., 2007. **48**(3): p. 1228-1236.
104. J. Bedke, E.K., L. Schaefer, C.-L. Behnes, M. Bonrouhi, N. Gretz, R. Horuk, M. Diedrichs-Moehring, G. Wildner, P. J. Nelson, H.J. Gröne,, *Beneficial Effects of CCR1 Blockade on the Progression of Chronic Renal Allograft Damage.* American Journal of Transplantation, 2007. **7**(3): p. 527-537.
105. Horuk, R., *et al.*, *CCR1-specific non-peptide antagonist: efficacy in a rabbit allograft rejection model.* Immunology Letters, 2001. **76**(3): p. 193-201.
106. Proudfoot, A.E., *et al.*, *Extension of recombinant human RANTES by the retention of the initiating methionine produces a potent antagonist.* J Biol Chem, 1996. **271**(5): p. 2599-603.
107. Yun, J.J., *et al.*, *Combined Blockade of the Chemokine Receptors CCR1 and CCR5 Attenuates Chronic Rejection.* Circulation, 2004. **109**(7): p. 932-937.
108. Gröne, H.J., *et al.*, *Met-RANTES reduces vascular and tubular damage during acute renal transplant rejection: blocking monocyte arrest and recruitment.* FASEB J, 1999. **13**(11): p. 1371-83.
109. Akashi, S., *et al.*, *A novel small-molecule compound targeting CCR5 and CXCR3 prevents acute and chronic allograft rejection.* Transplantation, 2005. **80**(3): p. 378-84.
110. Xu, H., *et al.*, *Effects of blocking the chemokine receptors, CCR5 and CXCR3, With TAK-779 in a rat small intestinal transplantation model.* Transplantation, 2008. **86**(12): p. 1810-7.

111. Gao, W., *et al.*, *Beneficial effects of targeting CCR5 in allograft recipients.* Transplantation, 2001. **72**(7): p. 1199-205.
112. Luckow, B., *et al.*, *Reduced intragraft mRNA expression of matrix metalloproteinases Mmp3, Mmp12, Mmp13 and Adam8, and diminished transplant arteriosclerosis in Ccr5-deficient mice.* Eur J Immunol, 2004. **34**(9): p. 2568-78.
113. Amano, H., *et al.*, *Absence of recipient CCR5 promotes early and increased allospecific antibody responses to cardiac allografts.* J Immunol, 2005. **174**(10): p. 6499-508.
114. Bickerstaff, A., *et al.*, *Acute humoral rejection of renal allografts in CCR5(-/-) recipients.* Am J Transplant, 2008. **8**(3): p. 557-66.
115. Schnickel, G.T., *et al.*, *Role of CXCR3 and CCR5 in Allograft Rejection.* Transplantation Proceedings, 2006. **38**(10): p. 3221-3224.
116. Schroppel, B., *et al.*, *Differential expression of chemokines and chemokine receptors in murine islet allografts: the role of CCR2 and CCR5 signaling pathways.* J Am Soc Nephrol, 2004. **15**(7): p. 1853-61.
117. Abdi, R., *et al.*, *The Role of CC Chemokine Receptor 5 (CCR5) in Islet Allograft Rejection.* Diabetes, 2002. **51**(8): p. 2489-2495.
118. Yi, S., *et al.*, *Involvement of CCR5 signaling in macrophage recruitment to porcine islet xenografts.* Transplantation, 2005. **80**(10): p. 1468-75.
119. Murai, M., *et al.*, *Peyer's patch is the essential site in initiating murine acute and lethal graft-versus-host reaction.* Nat Immunol, 2003. **4**(2): p. 154-60.
120. Welniak, L.A., *et al.*, *An absence of CCR5 on donor cells results in acceleration of acute graft-vs-host disease.* Exp Hematol, 2004. **32**(3): p. 318-24.
121. Wysocki, C.A., *et al.*, *Differential roles for CCR5 expression on donor T cells during graft-versus-host disease based on pretransplant conditioning.* J Immunol, 2004. **173**(2): p. 845-54.
122. Wysocki, C.A., *et al.*, *Critical role for CCR5 in the function of donor CD4+CD25+ regulatory T cells during acute graft-versus-host disease.* Blood, 2005. **106**(9): p. 3300-7.
123. Kallikourdis, M., *et al.*, *Alloantigen-enhanced accumulation of CCR5+ 'effector' regulatory T cells in the gravid uterus.* Proc Natl Acad Sci U S A, 2007. **104**(2): p. 594-9.
124. Jones, D.B., *Glomerulonephritis.* Am J Pathol, 1953. **29**(1): p. 33-51.
125. Segerer, S., *et al.*, *Expression of chemokines and chemokine receptors during human renal transplant rejection.* Am J Kidney Dis, 2001. **37**(3): p. 518-31.
126. Syrbe, U., J. Siveke, and A. Hamann, *Th1/Th2 subsets: distinct differences in homing and chemokine receptor expression?* Springer Semin Immunopathol, 1999. **21**(3): p. 263-85.
127. Segerer, S., P.J. Nelson, and D. Schlondorff, *Chemokines, chemokine receptors, and renal disease: from basic science to pathophysiologic and therapeutic studies.* J Am Soc Nephrol, 2000. **11**(1): p. 152-76.
128. Yun, J.J., *et al.*, *Early and late chemokine production correlates with cellular recruitment in cardiac allograft vasculopathy.* Transplantation, 2000. **69**(12): p. 2515-24.
129. Shimizu, K. and R.N. Mitchell, *The Role of Chemokines in Transplant Graft Arterial Disease.* Arterioscler Thromb Vasc Biol, 2008. **28**(11): p. 1937-1949.
130. Pattison, J., *et al.*, *RANTES chemokine expression in cell-mediated transplant rejection of the kidney.* Lancet, 1994. **343**(8891): p. 209-11.
131. Ode-Hakim, S., *et al.*, *Delayed-type hypersensitivity-like mechanisms dominate late acute rejection episodes in renal allograft recipients.* Transplantation, 1996. **61**(8): p. 1233-40.
132. D'Elios, M.M., *et al.*, *Predominant Th1 cell infiltration in acute rejection episodes of human kidney grafts.* Kidney Int, 1997. **51**(6): p. 1876-84.
133. Oliveira, G., *et al.*, *Cytokine analysis of human renal allograft aspiration biopsy cultures supernatants predicts acute rejection.* Nephrol Dial Transplant, 1998. **13**(2): p. 417-22.

134. Ruster, M., *et al.*, *Differential expression of beta-chemokines MCP-1 and RANTES and their receptors CCR1, CCR2, CCR5 in acute rejection and chronic allograft nephropathy of human renal allografts.* Clin Nephrol, 2004. **61**(1): p. 30-9.
135. Mayer, V., *et al.*, *Expression of the chemokine receptor CCR1 in human renal allografts.* Nephrol. Dial. Transplant., 2007. **22**(6): p. 1720-1729.
136. Tauber, A., Chernyak, L, *Metchnikoff and the origins of immunology: from metaphor to theory.* Monographs on the history and philosophy of biology. 1991 New York: Oxford University Press.
137. Gordon, S., *Elie Metchnikoff: Father of natural immunity.* European Journal of Immunology, 2008. **38**(12): p. 3257-3264.
138. van Furth, R., *et al.*, *The mononuclear phagocyte system: a new classification of macrophages, monocytes, and their precursor cells.* Bull World Health Organ, 1972. **46**(6): p. 845-52.
139. Fogg, D.K., *et al.*, *A clonogenic bone marrow progenitor specific for macrophages and dendritic cells.* Science, 2006. **311**(5757): p. 83-7.
140. Ziegler-Heitbrock, H., *Definition of human blood monocytes.* J Leukoc Biol, 2000. **67**(5): p. 603-606.
141. Gordon, S. and P.R. Taylor, *Monocyte and macrophage heterogeneity.* Nat Rev Immunol, 2005. **5**(12): p. 953-64.
142. Tacke, F. and G.J. Randolph, *Migratory fate and differentiation of blood monocyte subsets.* Immunobiology, 2006. **211**(6-8): p. 609-618.
143. Varol, C., S. Yona, and S. Jung, *Origins and tissue-context-dependent fates of blood monocytes.* Immunol Cell Biol, 2008. **87**(1): p. 30-38.
144. Hume, D.A., *Macrophages as APC and the Dendritic Cell Myth.* J Immunol, 2008. **181**(9): p. 5829-5835.
145. Rabinovitch, M., *Professional and non-professional phagocytes: an introduction.* Trends Cell Biol, 1995. **5**(3): p. 85-7.
146. Aderem, A. and D.M. Underhill, *Mechanisms of phagocytosis in macrophages.* Annual Review of Immunology, 1999. **17**(1): p. 593.
147. Indik, Z.K., *et al.*, *The molecular dissection of Fc gamma receptor mediated phagocytosis.* Blood, 1995. **86**(12): p. 4389-99.
148. Janeway, C.A., Jr., *The immune system evolved to discriminate infectious nonself from noninfectious self.* Immunol Today, 1992. **13**(1): p. 11-6.
149. Meylan, E., J.r. Tschopp, and M. Karin, *Intracellular pattern recognition receptors in the host response.* Nature, 2006. **442**(7098): p. 39-44.
150. Gordon, S., *The macrophage: past, present and future.* Eur J Immunol, 2007. **37 Suppl 1**: p. S9-17.
151. Martinez, F.O., *et al.*, *Transcriptional profiling of the human monocyte-to-macrophage differentiation and polarization: new molecules and patterns of gene expression.* J Immunol, 2006. **177**(10): p. 7303-11.
152. Mosmann, T.R., *et al.*, *Two types of murine helper T cell clone. I. Definition according to profiles of lymphokine activities and secreted proteins.* J Immunol, 1986. **136**(7): p. 2348-57.
153. Mosmann, T.R. and R.L. Coffman, *TH1 and TH2 cells: different patterns of lymphokine secretion lead to different functional properties.* Annu Rev Immunol, 1989. **7**: p. 145-73.
154. Romagnani, S., *Th1/Th2 cells.* Inflamm Bowel Dis, 1999. **5**(4): p. 285-94.
155. Martinez, F.O., *et al.*, *Macrophage activation and polarization.* Front Biosci, 2008. **13**: p. 453-61.
156. Gordon, S., *Alternative activation of macrophages.* Nat Rev Immunol, 2003. **3**(1): p. 23-35.
157. Mantovani, A., *et al.*, *The chemokine system in diverse forms of macrophage activation and polarization.* Trends in Immunology, 2004. **25**(12): p. 677-686.
158. Klimp, A.H., *et al.*, *A potential role of macrophage activation in the treatment of cancer.* Critical Reviews in Oncology/Hematology, 2002. **44**(2): p. 143-161.

159. Stein, M., *et al.*, *Interleukin 4 potently enhances murine macrophage mannose receptor activity: a marker of alternative immunologic macrophage activation.* J Exp Med, 1992. **176**(1): p. 287-92.
160. Martinez, F.O., L. Helming, and S. Gordon, *Alternative Activation of Macrophages: An Immunologic Functional Perspective.* Annu Rev Immunol, 2008.
161. Maggi, E., *The TH1/TH2 paradigm in allergy.* Immunotechnology, 1998. **3**(4): p. 233-44.
162. Brandt, E., *et al.*, *IL-4 production by human polymorphonuclear neutrophils.* J Leukoc Biol, 2000. **68**(1): p. 125-30.
163. Mosser, D.M. and J.P. Edwards, *Exploring the full spectrum of macrophage activation.* Nat Rev Immunol, 2008. **8**(12): p. 958-69.
164. Porcheray, F., *et al.*, *Macrophage activation switching: an asset for the resolution of inflammation.* Clin Exp Immunol, 2005. **142**(3): p. 481-9.
165. Gratchev, A., *et al.*, *M[phi]1 and M[phi]2 can be re-polarized by Th2 or Th1 cytokines, respectively, and respond to exogenous danger signals.* Immunobiology, 2006. **211**(6-8): p. 473-486.
166. Stout, R.D., *et al.*, *Macrophages sequentially change their functional phenotype in response to changes in microenvironmental influences.* J Immunol, 2005. **175**(1): p. 342-9.
167. Yardimci, N., *et al.*, *Neurologic complications after renal transplant.* Exp Clin Transplant, 2008. **6**(3): p. 224-8.
168. Tejani, A. and L. Emmett, *Acute and chronic rejection.* Semin Nephrol, 2001. **21**(5): p. 498-507.
169. Knoll, G., *Trends in kidney transplantation over the past decade.* Drugs, 2008. **68 Suppl 1**: p. 3-10.
170. O. Cheng, R.T., E. Sampson, G. Schultz, P. Ruiz, X. Zhang, P.S.T. Yuen, R.B. Mannon,, *Connective Tissue Growth Factor is a Biomarker and Mediator of Kidney Allograft Fibrosis.* American Journal of Transplantation, 2006. **6**(10): p. 2292-2306.
171. Niimi, M., *The technique for heterotopic cardiac transplantation in mice: experience of 3000 operations by one surgeon.* J Heart Lung Transplant, 2001. **20**(10): p. 1123-8.
172. Zhang, Z., *et al.*, *Pattern of liver, kidney, heart, and intestine allograft rejection in different mouse strain combinations.* Transplantation, 1996. **62**(9): p. 1267-72.
173. Abdi, R., *et al.*, *Differential Role of CCR2 in Islet and Heart Allograft Rejection: Tissue Specificity of Chemokine/Chemokine Receptor Function In Vivo.* J Immunol, 2004. **172**(2): p. 767-775.
174. Haskova, Z., *et al.*, *Organ-specific differences in the function of MCP-1 and CXCR3 during cardiac and skin allograft rejection.* Transplantation, 2007. **83**(12): p. 1595-601.
175. Stasikowska, O. and M. Wagrowska-Danilewicz, *Chemokines and chemokine receptors in glomerulonephritis and renal allograft rejection.* Med Sci Monit, 2007. **13**(2): p. RA31-6.
176. Wong, M.M. and E.N. Fish, *Chemokines: attractive mediators of the immune response.* Semin Immunol, 2003. **15**(1): p. 5-14.
177. Luther, S.A. and J.G. Cyster, *Chemokines as regulators of T cell differentiation.* Nat Immunol, 2001. **2**(2): p. 102-7.
178. Lee, C., *et al.*, *Macrophage activation through CCR5- and CXCR4-mediated gp120-elicited signaling pathways.* J Leukoc Biol, 2003. **74**(5): p. 676-682.
179. Gao, J.L., *et al.*, *Impaired host defense, hematopoiesis, granulomatous inflammation and type 1-type 2 cytokine balance in mice lacking CC chemokine receptor 1.* J Exp Med, 1997. **185**(11): p. 1959-68.
180. Senger, M., *et al.*, *X-HUSAR, an X-based graphical interface for the analysis of genomic sequences.* Comput Methods Programs Biomed, 1995. **46**(2): p. 131-41.
181. Rozen, S. and H. Skaletsky, *Primer3 on the WWW for general users and for biologist programmers.* Methods Mol Biol, 2000. **132**: p. 365-86.
182. Cui, W., D.D. Taub, and K. Gardner, *qPrimerDepot: a primer database for quantitative real time PCR.* Nucleic Acids Res, 2007. **35**(Database issue): p. D805-9.

183. Zhang, Z., *et al.*, *Improved techniques for kidney transplantation in mice.* Microsurgery, 1995. **16**(2): p. 103-9.
184. Kiss, E., *et al.*, *Isotretinoin ameliorates renal damage in experimental acute renal allograft rejection.* Transplantation, 2003. **76**(3): p. 480-9.
185. Adams, J., *et al.*, *13-cis retinoic acid inhibits development and progression of chronic allograft nephropathy.* Am J Pathol, 2005. **167**(1): p. 285-98.
186. Ward, J.M., *et al.*, *Hyalinosis and Ym1/Ym2 gene expression in the stomach and respiratory tract of 129S4/SvJae and wild-type and CYP1A2-null B6, 129 mice.* Am J Pathol, 2001. **158**(1): p. 323-32.
187. Pfaffl, M.W., *A new mathematical model for relative quantification in real-time RT-PCR.* Nucleic Acids Res, 2001. **29**(9): p. e45.
188. Hopken, U.E., *et al.*, *The chemokine receptor CCR7 controls lymph node-dependent cytotoxic T cell priming in alloimmune responses.* Eur J Immunol, 2004. **34**(2): p. 461-70.
189. Gillies, S.D., *et al.*, *A tissue-specific transcription enhancer element is located in the major intron of a rearranged immunoglobulin heavy chain gene.* Cell, 1983. **33**(3): p. 717-28.
190. Corraliza, I.M., *et al.*, *Determination of arginase activity in macrophages: a micromethod.* J Immunol Methods, 1994. **174**(1-2): p. 231-5.
191. Munder, M., *et al.*, *Th1/Th2-regulated expression of arginase isoforms in murine macrophages and dendritic cells.* J Immunol, 1999. **163**(7): p. 3771-7.
192. Doschko, G.U.M., *Untersuchungen zur Regulation des Enzyms Arginase in humanen Granulozyten*, in *Arbeitsgruppe Immunologie der Tierärztlichen Hochschule Hannover und dem Deutschen Krebsforschungszentrum Heidelberg (Kooperationseinheit Molekulare Hämatologie und Onkologie, Medizinische Klinik und Poliklinik V der Universität Heidelberg)*. 2004, Tierärztliche Hochschule Hannover: Hannover. p. 183.
193. Gersuk, G.M., L.W. Razai, and K.A. Marr, *Methods of in vitro macrophage maturation confer variable inflammatory responses in association with altered expression of cell surface dectin-1.* Journal of Immunological Methods, 2008. **329**(1-2): p. 157-166.
194. Ladner, M.B., *et al.*, *cDNA cloning and expression of murine macrophage colony-stimulating factor from L929 cells.* Proc Natl Acad Sci U S A, 1988. **85**(18): p. 6706-10.
195. Boltz-Nitulescu, G., *et al.*, *Differentiation of rat bone marrow cells into macrophages under the influence of mouse L929 cell supernatant.* J Leukoc Biol, 1987. **41**(1): p. 83-91.
196. Cowden, R.R. and S.K. Curtis, *Microfluorometric investigations of chromatin structure. I. Evaluation of nine DNA-specific fluorochromes as probes of chromatin organization.* Histochemistry, 1981. **72**(1): p. 11-23.
197. Schmid, I., *et al.*, *Dead cell discrimination with 7-amino-actinomycin D in combination with dual color immunofluorescence in single laser flow cytometry.* Cytometry, 1992. **13**(2): p. 204-8.
198. Daeron, M., *Fc receptor biology.* Annu Rev Immunol, 1997. **15**: p. 203-34.
199. Deka, C., *et al.*, *Analysis of fluorescence lifetime and quenching of FITC-conjugated antibodies on cells by phase-sensitive flow cytometry.* Cytometry, 1996. **25**(3): p. 271-9.
200. Silbernagl, S., Despopoulos, A., *Taschenatlas der Physiologie*. 4., überarbeitete Auflage ed. 1991: Georg Thieme Verlag. 371.
201. Luster, A.D., *The role of chemokines in linking innate and adaptive immunity.* Curr Opin Immunol, 2002. **14**(1): p. 129-35.
202. Serbina, N.V. and *E.G.* Pamer, *Monocyte emigration from bone marrow during bacterial infection requires signals mediated by chemokine receptor CCR2.* Nat Immunol, 2006. **7**(3): p. 311-7.
203. Gaffen, S.L. and K.D. Liu, *Overview of interleukin-2 function, production and clinical applications.* Cytokine, 2004. **28**(3): p. 109-123.
204. Mathan, A., S. Kuruvilla, and G. Abraham, *Interleukin 2 receptor expression in renal biopsies and the diagnosis of acute allograft rejection*. Vol. 49. 2006. 12-6.

205. Siveke, J.T. and A. Hamann, *T helper 1 and T helper 2 cells respond differentially to chemokines.* J Immunol, 1998. **160**(2): p. 550-4.
206. Sundrud, M.S., *et al.*, *Genetic reprogramming of primary human T cells reveals functional plasticity in Th cell differentiation.* J Immunol, 2003. **171**(7): p. 3542-9.
207. Hebenstreit, D., *et al.*, *Signaling mechanisms, interaction partners, and target genes of STAT6.* Cytokine Growth Factor Rev, 2006. **17**(3): p. 173-88.
208. Afzali, B., *et al.*, *The role of T helper 17 (Th17) and regulatory T cells (Treg) in human organ transplantation and autoimmune disease.* Clin Exp Immunol, 2007. **148**(1): p. 32-46.
209. Chen, Y. and K.J. Wood, *Interleukin-23 and TH17 cells in transplantation immunity: does 23+17 equal rejection?* Transplantation, 2007. **84**(9): p. 1071-4.
210. Iwakura, Y. and H. Ishigame, *The IL-23/IL-17 axis in inflammation.* J Clin Invest, 2006. **116**(5): p. 1218-22.
211. Veldhoen, M. and B. Stockinger, *TGFbeta1, a "Jack of all trades": the link with pro-inflammatory IL-17-producing T cells.* Trends Immunol, 2006. **27**(8): p. 358-61.
212. Ensminger, S.M., *et al.*, *Increased transplant arteriosclerosis in the absence of CCR7 is associated with reduced expression of Foxp3.* Transplantation, 2008. **86**(4): p. 590-600.
213. Forster, R., A.C. Davalos-Misslitz, and A. Rot, *CCR7 and its ligands: balancing immunity and tolerance.* Nat Rev Immunol, 2008. **8**(5): p. 362-71.
214. Lee, I., *et al.*, *Recruitment of Foxp3+ T regulatory cells mediating allograft tolerance depends on the CCR4 chemokine receptor.* J Exp Med, 2005. **201**(7): p. 1037-44.
215. Kahnert, A., *et al.*, *Alternative activation deprives macrophages of a coordinated defense program to Mycobacterium tuberculosis.* Eur J Immunol, 2006. **36**(3): p. 631-47.
216. Mantovani, A., *et al.*, *Macrophage polarization: tumor-associated macrophages as a paradigm for polarized M2 mononuclear phagocytes.* Trends Immunol, 2002. **23**(11): p. 549-55.
217. Potter, P.K., *et al.*, *Lupus-Prone Mice Have an Abnormal Response to Thioglycolate and an Impaired Clearance of Apoptotic Cells.* J Immunol, 2003. **170**(6): p. 3223-3232.
218. Cook, A.D., E.L. Braine, and J.A. Hamilton, *The phenotype of inflammatory macrophages is stimulus dependent: implications for the nature of the inflammatory response.* J Immunol, 2003. **171**(9): p. 4816-23.
219. Munder, M., K. Eichmann, and M. Modolell, *Alternative metabolic states in murine macrophages reflected by the nitric oxide synthase/arginase balance: competitive regulation by CD4+ T cells correlates with Th1/Th2 phenotype.* J Immunol, 1998. **160**(11): p. 5347-54.
220. Munder, P.G., M. Modolell, and D.F.H. Wallach, *Cell propagation on films of polymeric fluorocarbon as a means to regulate pericellular pH and pO_2 in cultured monolayers.* Febs Letters, 1971. **15**(3): p. 191-&.
221. van der Meer, J.W.M., *et al.*, *Suspension cultures of mononuclear phagocytes in the Teflon culture bag.* Cellular Immunology, 1979. **42**(1): p. 208-212.
222. Modolell, M., *et al.*, *Killing of Borrelia burgdorferi by macrophages is dependent on oxygen radicals and nitric oxide and can be enhanced by antibodies to outer surface proteins of the spirochete.* Immunology Letters, 1994. **40**(2): p. 139-146.
223. Zou, W., *et al.*, *Macrophage-derived dendritic cells have strong Th1-polarizing potential mediated by beta-chemokines rather than IL-12.* J Immunol, 2000. **165**(8): p. 4388-96.
224. Russell, P.S., *et al.*, *Induced immune destruction of long-surviving, H-2 incompatible kidney transplants in mice.* J Exp Med, 1978. **147**(5): p. 1469-86.
225. Fischereder, M., *Chemokines and chemokine receptors in renal transplantation--from bench to bedside.* Acta Physiol Hung, 2007. **94**(1-2): p. 67-81.
226. Calo, L., *et al.*, *Oxidative stress and nitric oxide system in post-transplant hypertension.* Clin Nephrol, 2000. **53**(4): p. suppl 6-7.

227. Matthias Mack, J.P., Christian Weber, Kim S.C. Weber, Peter J. Nelson, Tamara Rupp, Konstantin Maletz, Hilke Brühl, Detlef Schlöndorff,, *Chondroitin sulfate A released from platelets blocks RANTES presentation on cell surfaces and RANTES-dependent firm adhesion of leukocytes.* European Journal of Immunology, 2002. **32**(4): p. 1012-1020.
228. Weber, C., *et al.*, *Specialized roles of the chemokine receptors CCR1 and CCR5 in the recruitment of monocytes and T(H)1-like/CD45RO(+) T cells.* Blood, 2001. **97**(4): p. 1144-6.
229. Moser, B., *et al.*, *Chemokines: multiple levels of leukocyte migration control.* Trends Immunol, 2004. **25**(2): p. 75-84.
230. Lakkis, F.G., *et al.*, *Immunologic 'ignorance' of vascularized organ transplants in the absence of secondary lymphoid tissue.* Nat Med, 2000. **6**(6): p. 686-8.
231. Sallusto, F. and A. Lanzavecchia, *Understanding dendritic cell and T-lymphocyte traffic through the analysis of chemokine receptor expression.* Immunol Rev, 2000. **177**: p. 134-40.
232. Cools, N., *et al.*, *Balancing between immunity and tolerance: an interplay between dendritic cells, regulatory T cells, and effector T cells.* J Leukoc Biol, 2007. **82**(6): p. 1365-1374.
233. Cook, C.H., *et al.*, *Spontaneous Renal Allograft Acceptance Associated with "Regulatory" Dendritic Cells and IDO.* J Immunol, 2008. **180**(5): p. 3103-3112.
234. Turner, J.E., *et al.*, *Targeting of Th1-associated chemokine receptors CXCR3 and CCR5 as therapeutic strategy for inflammatory diseases.* Mini Rev Med Chem, 2007. **7**(11): p. 1089-96.
235. Bromley, S.K., T.R. Mempel, and A.D. Luster, *Orchestrating the orchestrators: chemokines in control of T cell traffic.* Nat Immunol, 2008. **9**(9): p. 970-80.
236. Geissmann, F., S. Jung, and D.R. Littman, *Blood monocytes consist of two principal subsets with distinct migratory properties.* Immunity, 2003. **19**(1): p. 71-82.
237. Fantuzzi, L., *et al.*, *Loss of CCR2 expression and functional response to monocyte chemotactic protein (MCP-1) during the differentiation of human monocytes: role of secreted MCP-1 in the regulation of the chemotactic response.* Blood, 1999. **94**(3): p. 875-83.
238. Wang, J., *et al.*, *Cytokine Regulation of Human Immunodeficiency Virus Type 1 Entry and Replication in Human Monocytes/Macrophages through Modulation of CCR5 Expression.* J. Virol., 1998. **72**(9): p. 7642-7647.
239. Sozzani, S., *et al.*, *Interleukin 10 increases CCR5 expression and HIV infection in human monocytes.* J Exp Med, 1998. **187**(3): p. 439-44.
240. Shurin, M.R., *et al.*, *Th1/Th2 balance in cancer, transplantation and pregnancy.* Springer Semin Immunopathol, 1999. **21**(3): p. 339-59.
241. Benghiat, F.S., *et al.*, *Interleukin 17-producing T helper cells in alloimmunity.* Transplantation Reviews, 2009. **23**(1): p. 11-18.
242. Piccotti, J.R., *et al.*, *Are Th2 helper T lymphocytes beneficial, deleterious, or irrelevant in promoting allograft survival?* Transplantation, 1997. **63**(5): p. 619-24.
243. Le Moine, A. and M. Goldman, *Non-classical pathways of cell-mediated allograft rejection: new challenges for tolerance induction?* Am J Transplant, 2003. **3**(2): p. 101-6.
244. Chan, S.Y., *et al.*, *In vivo depletion of CD8+ T cells results in Th2 cytokine production and alternate mechanisms of allograft rejection.* Transplantation, 1995. **59**(8): p. 1155-61.
245. Guillonneau, C., *et al.*, *CD40Ig treatment results in allograft acceptance mediated by CD8CD45RC T cells, IFN-gamma, and indoleamine 2,3-dioxygenase.* J Clin Invest, 2007. **117**(4): p. 1096-106.
246. Sawitzki, B., *et al.*, *IFN-gamma production by alloantigen-reactive regulatory T cells is important for their regulatory function in vivo.* J Exp Med, 2005. **201**(12): p. 1925-35.
247. Thebault, P., *et al.*, *Role of IFNgamma in allograft tolerance mediated by CD4+CD25+ regulatory T cells by induction of IDO in endothelial cells.* Am J Transplant, 2007. **7**(11): p. 2472-82.
248. Wood, K.J., *et al.*, *Interferon gamma: friend or foe?* Transplantation, 2007. **84**(1 Suppl): p. S4-5.
249. Chen, L., *et al.*, *TLR engagement prevents transplantation tolerance.* Am J Transplant, 2006. **6**(10): p. 2282-91.

250. David M. Miller, T.T., Todd Pearson, Masahiro Yamazaki, Michael A. Brehm, Aldo A. Rossini, Dale L. Greiner,, *TLR Agonists Abrogate Co-stimulation Blockade-Induced Mixed Chimerism and Transplantation Tolerance.* Annals of the New York Academy of Sciences, 2008. **1150**(Immunology of Diabetes V From Bench to Bedside): p. 149-151.
251. Porrett, P.M., *et al.*, *Mechanisms Underlying Blockade of Allograft Acceptance by TLR Ligands.* J Immunol, 2008. **181**(3): p. 1692-1699.
252. Miura, M., T. El-Sawy, and R.L. Fairchild, *Neutrophils mediate parenchymal tissue necrosis and accelerate the rejection of complete major histocompatibility complex-disparate cardiac allografts in the absence of interferon-gamma.* Am J Pathol, 2003. **162**(2): p. 509-19.
253. Li, J., *et al.*, *Gene transfer of soluble interleukin-17 receptor prolongs cardiac allograft survival in a rat model.* Eur J Cardiothorac Surg, 2006. **29**(5): p. 779-83.
254. Antonysamy, M.A., *et al.*, *Evidence for a role of IL-17 in organ allograft rejection: IL-17 promotes the functional differentiation of dendritic cell progenitors.* J Immunol, 1999. **162**(1): p. 577-84.
255. Antonysamy, M.A., *et al.*, *Evidence for a role of IL-17 in alloimmunity: a novel IL-17 antagonist promotes heart graft survival.* Transplant Proc, 1999. **31**(1-2): p. 93.
256. Bettelli, E., *et al.*, *Reciprocal developmental pathways for the generation of pathogenic effector TH17 and regulatory T cells.* Nature, 2006. **441**(7090): p. 235-8.
257. Russell, P.S., *et al.*, *Kidney transplants in mice. An analysis of the immune status of mice bearing long-term, H-2 incompatible transplants.* J Exp Med, 1978. **147**(5): p. 1449-68.
258. Bickerstaff, A.A., *et al.*, *The graft helps to define the character of the alloimmune response.* Transpl Immunol, 2002. **9**(2-4): p. 137-41.
259. Schneider, M.A., *et al.*, *CCR7 is required for the in vivo function of CD4+ CD25+ regulatory T cells.* J Exp Med, 2007. **204**(4): p. 735-45.
260. Lohr, J., *et al.*, *Role of IL-17 and regulatory T lymphocytes in a systemic autoimmune disease.* J Exp Med, 2006. **203**(13): p. 2785-91.
261. Veldhoen, M., *et al.*, *TGFbeta in the context of an inflammatory cytokine milieu supports de novo differentiation of IL-17-producing T cells.* Immunity, 2006. **24**(2): p. 179-89.
262. Xu, L., *et al.*, *Cutting edge: regulatory T cells induce CD4+CD25-Foxp3- T cells or are self-induced to become Th17 cells in the absence of exogenous TGF-beta.* J Immunol, 2007. **178**(11): p. 6725-9.
263. Eis, V., *et al.*, *Chemokine receptor CCR1 but not CCR5 mediates leukocyte recruitment and subsequent renal fibrosis after unilateral ureteral obstruction.* J Am Soc Nephrol, 2004. **15**(2): p. 337-47.
264. Ramos, C.D.L., *et al.*, *MIP-1{alpha}[CCL3] acting on the CCR1 receptor mediates neutrophil migration in immune inflammation via sequential release of TNF-{alpha} and LTB4.* J Leukoc Biol, 2005. **78**(1): p. 167-177.
265. Gladue, R.P., *et al.*, *The Human Specific CCR1 Antagonist CP-481,715 Inhibits Cell Infiltration and Inflammatory Responses in Human CCR1 Transgenic Mice.* J Immunol, 2006. **176**(5): p. 3141-3148.
266. O'Garra, A. and P. Vieira, *T(H)1 cells control themselves by producing interleukin-10.* Nat Rev Immunol, 2007. **7**(6): p. 425-8.
267. Andres, P.G., *et al.*, *Mice with a selective deletion of the CC chemokine receptors 5 or 2 are protected from dextran sodium sulfate-mediated colitis: lack of CC chemokine receptor 5 expression results in a NK1.1+ lymphocyte-associated Th2-type immune response in the intestine.* J Immunol, 2000. **164**(12): p. 6303-12.
268. Famulski, K.S., Sis, B., Billesberger, L., Halloran, P. F., *Interferon-gamma and Donor MHC Class I Control Alternative Macrophage Activation and Activin Expression in Rejecting Kidney Allografts: A Shift in the Th1-Th2 Paradigm.* American Journal of Transplantation, 2008. **8**(3): p. 547-556.

269. Grau, V., B. Herbst, and B. Steiniger, *Dynamics of monocytes/macrophages and T lymphocytes in acutely rejecting rat renal allografts.* Cell Tissue Res, 1998. **291**(1): p. 117-26.
270. Wyburn, K.R., *et al.*, *The role of macrophages in allograft rejection.* Transplantation, 2005. **80**(12): p. 1641-7.
271. Le Meur, Y., *et al.*, *Macrophage accumulation at a site of renal inflammation is dependent on the M-CSF/c-fms pathway.* J Leukoc Biol, 2002. **72**(3): p. 530-7.
272. Le Meur, Y., *et al.*, *Macrophage colony-stimulating factor expression and macrophage accumulation in renal allograft rejection.* Transplantation, 2002. **73**(8): p. 1318-24.
273. Surquin, M., *et al.*, *Skin graft rejection elicited by beta 2-microglobulin as a minor transplantation antigen involves multiple effector pathways: role of Fas-Fas ligand interactions and Th2-dependent graft eosinophil infiltrates.* J Immunol, 2002. **169**(1): p. 500-6.
274. Surquin, M., *et al.*, *IL-4 deficiency prevents eosinophilic rejection and uncovers a role for neutrophils in the rejection of MHC class II disparate skin grafts.* Transplantation, 2005. **80**(10): p. 1485-92.
275. Goldman, M., *et al.*, *A role for eosinophils in transplant rejection.* Trends in Immunology, 2001. **22**(5): p. 247-251.
276. Hogan, S., Rosenberg, H., Moqbel, R., Phipps, S., Foster, P., Lacy, P., Kay, A., Rothenberg, M., *Eosinophils: Biological Properties and Role in Health and Disease.* Clinical & Experimental Allergy, 2008. **38**(5): p. 709-750.
277. Luckow, B., *et al.*, *Reduced intragraft mRNA expression of matrix metalloproteinases Mmp3, Mmp12, Mmp13 and Adam8, and diminished transplant arteriosclerosis in Ccr5-deficient mice.* Eur J Immunol, 2004. **34**(9): p. 2568-78.
278. Hansson, G.K. and P. Libby, *The immune response in atherosclerosis: a double-edged sword.* Nat Rev Immunol, 2006. **6**(7): p. 508-19.
279. Braunersreuther, V., *et al.*, *Ccr5 but not Ccr1 deficiency reduces development of diet-induced atherosclerosis in mice.* Arterioscler Thromb Vasc Biol, 2007. **27**(2): p. 373-9.
280. Cornell, L.D., R.N. Smith, and R.B. Colvin, *Kidney Transplantation: Mechanisms of Rejection and Acceptance.* Annual Review of Pathology: Mechanisms of Disease, 2008. **3**(1): p. 189.
281. Kunkel, S.L. and N. Godessart, *Chemokines in autoimmunity: from pathology to therapeutics.* Autoimmun Rev, 2002. **1**(6): p. 313-20.
282. Proudfoot A., P.C., Wells T.,, *The strategy of blocking the chemokine system to combat disease.* Immunological Reviews, 2000. **177**(1): p. 246-256.
283. Haringman, J.J. and P.P. Tak, *Chemokine blockade: a new era in the treatment of rheumatoid arthritis?* Arthritis Res Ther, 2004. **6**(3): p. 93-7.
284. Proudfoot, A.E.I., *Chemokine receptors: multifaceted therapeutic targets.* Nat Rev Immunol, 2002. **2**(2): p. 106-115.
285. Lloyd, C.M., *et al.*, *Three-colour fluorescence immunohistochemistry reveals the diversity of cells staining for macrophage markers in murine spleen and liver.* Journal of Immunological Methods, 2008. **334**(1-2): p. 70-81.
286. Taylor, P.R., *et al.*, *Macrophage receptors and immune recognition.* Annual Review of Immunology, 2005. **23**(1): p. 901.
287. Fadok, V.A., *et al.*, *Macrophages that have ingested apoptotic cells in vitro inhibit proinflammatory cytokine production through autocrine/paracrine mechanisms involving TGF-beta, PGE2, and PAF.* J Clin Invest, 1998. **101**(4): p. 890-8.
288. Raes, G., *et al.*, *Differential expression of FIZZ1 and Ym1 in alternatively versus classically activated macrophages.* J Leukoc Biol, 2002. **71**(4): p. 597-602.
289. Raes, G., *et al.*, *FIZZ1 and Ym as tools to discriminate between differentially activated macrophages.* Dev Immunol, 2002. **9**(3): p. 151-9.

290. Loke, P., *et al.*, *Alternative activation is an innate response to injury that requires CD4+ T cells to be sustained during chronic infection.* J Immunol, 2007. **179**(6): p. 3926-36.
291. Schroder, C., *et al.*, *CCR5 blockade modulates inflammation and alloimmunity in primates.* J Immunol, 2007. **179**(4): p. 2289-99.
292. Heinzel, F.P., *et al.*, *Reciprocal expression of interferon gamma or interleukin 4 during the resolution or progression of murine leishmaniasis. Evidence for expansion of distinct helper T cell subsets.* J Exp Med, 1989. **169**(1): p. 59-72.
293. Mills, C.D., *et al.*, *M-1/M-2 macrophages and the Th1/Th2 paradigm.* J Immunol, 2000. **164**(12): p. 6166-73.
294. Brake, D.K., *et al.*, *ICAM-1 expression in adipose tissue: effects of diet-induced obesity in mice.* Am J Physiol Cell Physiol, 2006. **291**(6): p. C1232-1239.
295. Montecino-Rodriguez, E., H. Leathers, and K. Dorshkind, *Bipotential B-macrophage progenitors are present in adult bone marrow.* Nat Immunol, 2001. **2**(1): p. 83-88.
296. Tiemessen, M.M., *et al.*, *CD4+CD25+Foxp3+ regulatory T cells induce alternative activation of human monocytes/macrophages.* Proc Natl Acad Sci U S A, 2007. **104**(49): p. 19446-51.
297. Fang, F.C. and C.F. Nathan, *Man is not a mouse: reply.* J Leukoc Biol, 2007. **81**(3): p. 580.
298. Munder, M., *et al.*, *Arginase I is constitutively expressed in human granulocytes and participates in fungicidal activity.* Blood, 2005. **105**(6): p. 2549-56.
299. Loong, C.C., *et al.*, *Evidence for the early involvement of interleukin 17 in human and experimental renal allograft rejection.* J Pathol, 2002. **197**(3): p. 322-32.
300. Van Kooten, C., *et al.*, *Interleukin-17 activates human renal epithelial cells in vitro and is expressed during renal allograft rejection.* J Am Soc Nephrol, 1998. **9**(8): p. 1526-34.
301. B. M. Vanaudenaerde, S.I.D.V., R. Vos, I. Meyts, D. M. Bullens, V. Reynders, W. A. Wuyts, D. E. Van Raemdonck, L. J. Dupont, G. M. Verleden,, *The Role of the IL23/IL17 Axis in Bronchiolitis Obliterans Syndrome After Lung Transplantation.* American Journal of Transplantation, 2008. **8**(9): p. 1911-1920.
302. Di Marzio, P., *et al.*, *Role of Rho family GTPases in CCR1- and CCR5-induced actin reorganization in macrophages.* Biochemical and Biophysical Research Communications, 2005. **331**(4): p. 909-916.